Regulation of pancreatic β-cell death and cancer cell migration by TRPM2 channels

Fangfang Li

Submitted in accordance with the requirements for the degree of Doctor of Philosophy

The University of Leeds

School of Biomedical Sciences

June 2016

The candidate confirms that the work submitted is their own and that appropriate credit has been given where reference has been made to the work of others

Acknowledgements

First and foremost I would like to thank my supervisor Professor Asipu Sivaprasadarao for his guidance and support throughout my time here. I came to his lab with plant science background and had difficult time in learning mammalian and human biology at the beginning of my PhD study. It is my supervisor's patience and encouragement that helped me to go through the hard time.

I would like to thank Dr. Nada Aruarab, Dr. Melanie Ludlow, Mrs. Hong-lin Rong, Mr. Tim Munsey, Mr. Gareth Howell, Mrs. Sally Boxall and Mr. Brian Jackson for all their valuable advice and technical assistance during my time here. Additionally, I am grateful to the people here for making the last few years such an enjoyable time.

My PhD would not have been possible without the generous scholarship from China Scholarship Council and University of Leeds.

Finally, I wish to thank my family for their continuing love and support throughout the last few years. My gratitude is written in Chinese.

壬辰年，别至亲而远赴英邦。

春秋轮回已三载有余，求学之苦似浮尘云烟。

吾上不得侍双亲以尽孝，下不能携君而养子女。

然天下事，多成于取舍之间。

唯借片纸之言以谢至亲之谅解与支持。

小女 芳芳

丙申年春于英格兰利兹

2

Publications

Manna, Paul T., Munsey, Tim S., Abuarab, N., **Li, F.,** Asipu, A., Howell, G., Sedo, A., Yang, W., Naylor, J., Beech, David J. et al. (2015). TRPM2-mediated intracellular Zn^{2+} release triggers pancreatic β-cell death. *Biochem J* **466**, 537-546.

Li, F., Abuarab, N., Sivaprasadarao, A. (2016) Reciprocal regulation of actin cytoskeleton remodelling and cell migration by calcium and zinc: role of TRPM2 channels. *J Cell Sci.* (accepted)

Abstract

Chronic elevation of circulating glucose and free fatty acids leads to the dysfunction and death of pancreatic β-cells. These effects, often termed as 'glucolipotoxicity', are a characteristic feature of diabetes mellitus. In addition to affecting β-cells, glucolipotoxicity impacts a number of other cellular processes, including cell migration, by increasing the production of reactive oxygen species (ROS). Recent studies have reported that diabetic patients are at an increasing risk of cancer. The aim of this study was to investigate the role of the ROS sensitive transient receptor potential melastatin 2 (TRPM2) channels in pancreatic β-cell death and cancer cell migration.

TRPM2 channel is capable of elevating the intracellular levels of two cytotoxic ions, Ca^{2+} and Zn^{2+}. Chapter 3 of the thesis investigated the role of TRPM2 channels in palmitate induced pancreatic β-cell death using the INS1 β-cell line and islets isolated from wild-type and TRPM2 knock-out mice. Palmitate caused an increase in the intracellular levels of ROS (required for TRPM2 activation) by activating NADPH oxidase-2 (NOX-2), and induced breakdown of the mitochondrial network. Chemical or siRNA inhibition of TRPM2 channels prevented mitochondrial fragmentation by preventing the distribution of free Zn^{2+} into mitochondria. Palmitate induced, TRPM2 mediated rise in mitochondrial Zn^{2+} caused loss of mitochondrial membrane potential and recruitment of cytoplasmic Drp-1 (a dynamin related GTPase that catalyses mitochondrial fission) to mitochondria. Palmitate induced β-cell death could be prevented by TRPM2 inhibition and by Zn^{2+} chelation alone. Taken together, Chapter 3 provides evidence for a novel mechanism for palmitate induced β-cell death: it involves TRPM2 dependent mobilisation of Zn^{2+} to mitochondria and the consequent increase in mitochondrial fragmentation and β-cell death.

Chapters 4 and 5 tested the hypothesis that TRPM2 channels mediate H_2O_2 induced migration of HeLa and PC (prostate cancer)-3 cancer cells by regulating the actin and focal adhesion dynamics. H_2O_2 caused loss of actin stress fibres, and induced formation of stress fibres and disassembly of focal adhesions; these changes contribute to H_2O_2 induced cell migration. These effects could be prevented by the inhibition of TRPM2 channels and chelation of Zn^{2+}. Elevation of intracellular Zn^{2+} with a zinc ionophore reproduced the effects of H_2O_2, whereas elevation of Ca^{2+} showed the opposite effects. The results thus revealed reciprocal roles for Ca^{2+} and Zn^{2+} on the actin and focal adhesion dynamics.

In summary, this thesis reveals two new roles for TRPM2 channels, firstly in mitochondrial fragmentation in pancreatic β-cells, and secondly in actin cytoskeleton remodelling in migrating cancer cells.

Table of Contents

Chapter 3 Nutrient stress induced cell death is mediated by TRPM2 stimulated mitochondrial ROS production and fragmentation

List of Figures

Chapter 4

Chapter 5

Chapter 6

List of Abbreviation

ROS	Reactive oxygen species
SODs	Superoxide dismutases
AD	Alzheimer's disease
PD	Parkinson's disease
T2DM	Type 2 diabetes mellitus
NF-κB	Nuclear factor-kappa B
FFAs	Free fatty acids
Aβ	Amyloid-β peptide
APP	Amyloid precursor protein
MAPK	mitogen-activated protein kinase
EMT	Epithelial-mesenchymal transition
MET	Mesenchymal-epithelial transition
MMPs	Matrix metallo-proteinases
ECM	Extracellular matrix
VEGF	Vascular endothelial growth factor
NOXs	Nicotinamide adenine dinucleotide phosphate oxidases
TTFA	Thenoyltrifluoroacetone
mROS	Mitochondrial ROS
ETC	Electron transport chain
HRECs	Human retinal endothelial cells
RIRR	ROS-induced ROS release
mPTP	Mitochondrial permeability transition pore
IMAC	Inner membrane anion channels
PTPs	Protein tyrosine phosphatases
PI-3Ks	Phosphoinositide 3-kinases

Erk1/2	Extracellular signal-related kinases
JNK	c-Jun N-terminal kinases
BMK1/Erk5	Big MAP kinase 1
DAG	Diacylglycerol
GAPDH	Glyceraldehyde-3-phosphate dehydrogenase
RTKs	Receptor tyrosine kinases
EGF	Epidermal growth factor
PIP3	Phosphatidylinositol 3,4,5 triphosphate
PIP2	Phosphatidylinositol 4,5 bisphosphate
CRAC	Ca^{2+}-release-activated channels
Ca_v	Voltage-gated Ca^{2+} channel
TRP	Transient receptor potential channel
STIM	Stromal interaction molecule
SOCE	Store-operated Ca^{2+} channels
ADPR	Adenosine diphosphate ribose
NUDT9-H	Nudix-type motif 9 homology domain
cADPR	Cyclic adenosine diphosphate-ribose
NADase	NAD^+ nucleosidase
PARP1	Poly (ADP-ribose) Polymerase 1
PARG	*Poly (ADP-ribose) glycohydrolase*
2-APB	2-aminoethoxydiphenyl borate
ACA	N-(p-amylcinnamoyl) anthranilic acid
FFA	Flufenamic acid
OMM	Outer mitochondrial membrane
IMM	Inner mitochondrial membrane
Drp1	Dynamin-related protein 1
Fis1	Fission protein 1
Mff	Mitochondrial fission factor

Mfn	Mitofusin
OPA1	Optic atrophy1
POMC	Pro-opiomelanocortin
IBMX	3-isobutyl-1-methylxanthine
$\Delta\Psi m$	Mitochondrial membrane potential
Apaf-1	Apoptotic protease activating factor I
AIF	Apoptosis-inducing factor
OGD	Oxygen and glucose deprivation
DISC	Death-inducing signalling complex
FADD	Fas-associated death domain
AMF	Autocrine motility factor
IGF-1	Insulin-like growth factor 1
FAK	Focal adhesion kinase
Ena, MENA	Ena proteins related to actin polymerisation, in mice named MENA
VASP	Vasodilator-stimulated phosphoprotein
WASP	Wiskott-Aldrich syndrome family protein
ARP2/3	Actin-related protein2 and protein3
GEFs	Guanine-nucleotide-exchange factors
GAPs	GTPase-activating proteins
IRSp53	insulin-receptor substrate p53
Cdc42	Cell division control protein homologue 42
RIF	Rho in filopodia
mDia2	Diaphanous-related formin-2
CaMKII	Ca^{2+}/calmodulin dependent protein kinase
MDCK	Madin-Darby Canine Kidney Epithelial Cells
PTP-PEST	Protein tyrosine phosphatase non-receptor type 12
DMSO	Dimethyl sulphoxide
HEK	Human embryonic kidney

EGTA	Ethylene glycol tetraacetic acid
EDTA	Ethylenediamine tetraacetic acid
H_2DCFDA	2', 7'-dichlorodihydrofluorescein diacetate
dUTP	Deoxyudine triphosphate
TdT	Terminal deoxynucleotidyl transferase
SBS	Standard buffer solution
PFA	Paraformaldehyde
PMSF	phenylmethanesulfonyl fluoride or phenylmethylsulfonyl fluoride
NAC	N-acetyl cysteine
Apocynin	4'-hydroxy-3'-methoxyacetophenone
TPEN	N, N, N' N'-tetrakin (-)[2-pyridylmethyl]-ethylenediamine
CCCP	Carbonyl cyanide m-chlorophenyl hydrazine
PI	Propidium iodide
PS	Phosphatidylserine
TGF-β	Transforming growth factor β
SERCA	Sarco/endoplasmic reticulum Ca^{2+} ATPase

Chapter 1 Introduction

Diabetes and cancer are the two major diseases that cause high mortality worldwide. Diabetes is a group of metabolic diseases characterized by high blood glucose levels. Loss of insulin-producing pancreatic β-cells due to immune destruction is the main cause of type 1 diabetes. Type 2 diabetes, on the other hand, is caused by insulin resistance, but as the disease progresses, β-cell death also occurs due to prolonged exposure to high blood glucose, free fatty acids and cytokines (Cnop et al., 2005). Thus, β-cell death plays an essential role in both forms of diabetes. Cancer is characterized by the decreased rate of cell death, uncontrolled proliferation and metastasis. Among these, metastasis, whereby tumour cells migrate and invade other tissues from original site of tumour is the main reason for cancer mortality (Mehlen and Puisieux, 2006). Significant progress has been made in our understanding of how β-cells die and cancer cells migrate, but the roles of ion channels in these processes are not fully understood. There is some evidence that diabetes can increase the risk of cancer, but the underlying molecular mechanisms are unclear (Legros et al., 2002). A common feature of both these diseases is disruption of the homeostasis of reactive oxygen species (ROS) (Houstis et al., 2006; Liou and Storz, 2010). The aim of this study is to investigate how ROS can affect the ROS sensitive TRPM2 channels and how the resultant changes in ion homeostasis influence pancreatic β-cell death and cancer cell migration. This section of the thesis will review the literatures on ROS homeostasis, TRPM2 channels, mitochondrial dynamics, and mechanisms of β-cell death and cancer cell migration.

1. 1 ROS in human diseases

ROS are oxygen-derived small molecules, that include oxygen radicals [superoxide anion (O_2-), hydroxyl radical ($\bullet HO$), peroxyl radical ($RO_2\bullet$), and alkoxyl ($RO\bullet$)] and non-radicals, such as hydrogen peroxide (H_2O_2). ROS generation generally starts with the production of superoxide, and superoxide then rapidly undergoes dismutation to H_2O_2 by the action of superoxide dismutases (SODs). Excess ROS is harmful to most proteins, lipids and nucleic acids, but can be detoxified by scavenging enzymes, such as glutathione peroxidase. For example, following the conversion of superoxide to H_2O_2 by SOD, glutathione peroxidase can reduce H_2O_2 to water, thereby normalizing the intracellular ROS level (D'Autréaux and Toledano, 2007). However, when the cytosolic ROS levels exceed the capacity of antioxidant systems to detoxify ROS, cells and tissues undergo pathological changes leading to ROS-related diseases. Human diseases induced by excessive ROS production have been extensively studied in the last few decades. These include diabetes,

cardiovascular diseases and neurodegenerative diseases which include Alzheimer's disease (AD) (Multhaup et al., 1997) and Parkinson's disease (PD) (Tieu et al., 2003).

1. 1. 1 ROS in diabetes

The development of insulin resistance and consequent type 2 diabetes mellitus (T2DM) is one area where ROS have been consistently implicated in disease pathogenesis. T2DM is a metabolic disease characterized by the elevation of blood glucose levels (hyperglycaemia), lipid abnormalities and vascular complications (Kaneto et al., 2010). Studies have shown that insulin resistance occurs prior to the development of hyperglycaemia and is a major feature in the progression of T2DM (Houstis et al., 2006; Martin et al., 1992) (Figure 1.1). Insulin resistance means that pancreatic β-cells are able to secrete sufficient insulin but this insulin fails to act on the insulin-sensitive cells to exert normal functions, such as removal of excess glucose from blood stream and maintenance of sufficient fatty acid metabolism (Saltiel and Kahn, 2001). The causal role of ROS in multiple forms of insulin resistance has been observed both in animal models and cell lines (Houstis et al., 2006). The link between ROS and insulin resistance has been ascribed to alterations in several intracellular signalling pathways. There is direct evidence showing that H_2O_2 can inhibit insulin-stimulated tyrosine phosphorylation of insulin receptor to induce insulin resistance (Hansen et al., 1999). Moreover, it has been demonstrated that ROS can regulate the activity of nuclear factor-kappa B (NF-κB) transcription factors (Kamata et al., 2002; Morgan and Liu, 2011). The contribution of NF-κB signalling to insulin resistance has been demonstrated in many studies (Arkan et al., 2005; Cai et al., 2005). Furthermore, these transcription factors are essential for the transcription of pro-inflammatory molecules, such as cytokines, thereby contributing to the pathogenesis of diabetes (Patel and Santani, 2009).

Although these data suggest that ROS contributes to insulin resistance, it has been suggested that insulin resistance can conversely induce excessive ROS production (Kroemer and Reed, 2000). With the progression of insulin resistance, the levels of glucose and fatty acids in blood stream increase beyond normal levels, leading to the glucolipotoxicity. A large amount of experimental evidence indicates that endogenous ROS level is largely increased by glucolipotoxicity both in cell lines and in pancreatic islets. For example, in cultured vascular cells, high glucose and free fatty acids (FFAs) stimulate ROS generation (Inoguchi et al., 2000). In isolated rat pancreatic islets, ROS is largely induced by the combination of glucose and FFA (Morgan et al., 2007). It has been demonstrated that the increased ROS level is a key trigger for apoptosis in many types of cells, including endothelial cells, podocytes and β-cells (Piconi et al., 2006; Robertson et al., 2004; Susztak

et al., 2006). Thus, elevated ROS level contributes to the pathogenesis of diabetes and other abnormalities by impairing cellular function.

Compared to other cell types, pancreatic β-cell are more vulnerable to oxidative damage with increased susceptibility for apoptosis. This high risk is likely due to the relatively low levels of free radical detoxifying and redox-regulating enzymes, such as SOD, catalase and glutathione peroxidase (Lenzen et al., 1996; Tiedge et al., 1997). Therefore, ROS homeostasis of pancreatic β-cells is easily to be disrupted under nutrient overload conditions. The source of this dys-regulated ROS is mainly mitochondria (Robertson, 2004; Robertson et al., 2004). Studies have shown that pharmacological strategies that increase mitochondrial antioxidant levels could partially reverse the cellular dysfunctions caused by ROS (Green et al., 2004). In addition to mitochondrial source, plasma membrane NADPH oxidase (NOX) generates ROS (Newsholme et al., 2009) and inhibition of NOX activity markedly improves the survival of β-cells exposed to high concentrations of palmitate (C16 fatty acid) (Yuan et al., 2010). These findings suggest that multiple ROS generation systems could contribute to the pathogenesis of diabetes.
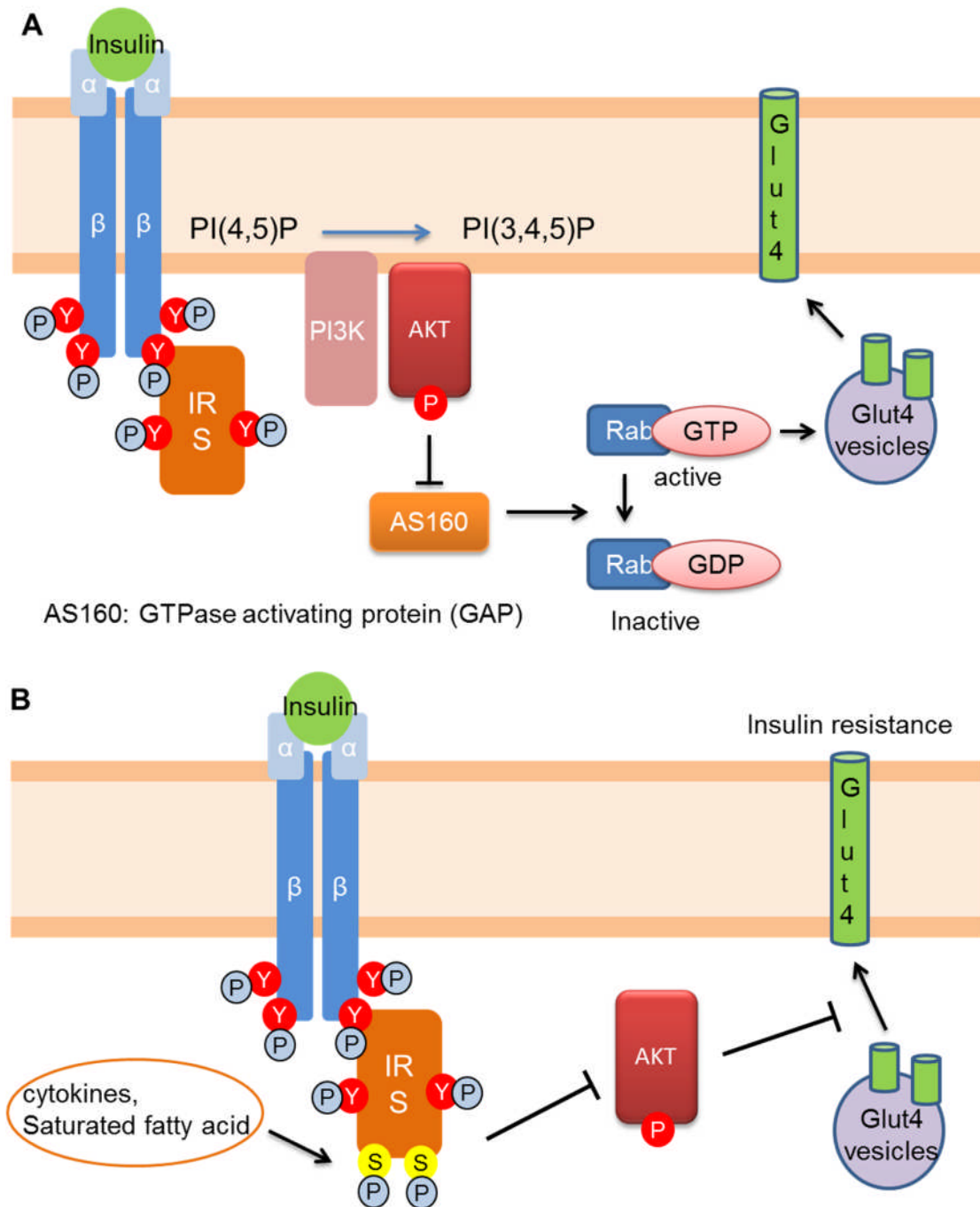
Figure 1. 1 Schematic showing insulin-stimulated GLUT4 translocation and insulin resistance (**A**) Binding of insulin (green circle) to its tetrameric receptor (2 α- and 2 β-subunits) leads to tyrosine phosphorylation of insulin receptor substrate (IRS) proteins and the recruitment of phosphatidylinositol 3 kinase (PI3-kinase), which catalyzes the conversion of PI(4,5)P2 to PI(3,4,5)P3. PI(3,4,5)P3 generation results in the phosphorylation of AKT. AKT phosphorylates AS160 suppressing its GAP activity and resulting in active GTP-bound Rab proteins that promote glucose transporter 4 (GLUT4) vesicle translocation. (**B**) Serine phosphorylation of IRS by cytokines or saturated fatty acid inhibits Akt phosphorylation, thereby preventing GLUT4 translocation which leads to insulin resistance.

1. 1. 2 ROS in neurodegenerative diseases

Neurodegenerative diseases represent another area where ROS play a key role (Barnham et al., 2004). In AD, ROS has been shown to induce cell death by inducing mitochondrial DNA (mtDNA) mutations and impairing the energy production (Eckert et al., 2003). AD is characterized clinically by the progressive cognitive decline and pathologically by the accumulation of senile brain plagues composed mainly of amyloid-β peptide (Aβ) and dys-regulated microtubules made up of hyper-phosphorylated tau. Aβ can be produced from amyloid precursor protein (APP) by β- and γ-secretases within cells. There are extensive studies demonstrating a role for ROS in the pathogenesis of AD. For instance, ROS can activate p38 mitogen-activated protein kinase (MAPK) to induce neuronal cell death (Hashimoto et al., 2003; Zhu et al., 2002) or increase the expression of β- secretase, thereby producing Aβ (Tamagno et al., 2005) to accelerate the progression of AD. ROS can increase aberrant tau phosphorylation by activation of glycogen synthase kinase 3 (Lovell et al., 2004). The ability of antioxidant treatment to improve the median survival time in an AD trial further supports a role for ROS in AD progression (Sano et al., 1997).

The essential role of ROS in triggering PD progression was also supported by a large body of evidence. PD is characterized clinically by progressive bradykinesia and tremor, and pathologically by the loss of pigmented neurons of the substantia nigra (Lin and Beal, 2006). It has been reported that deficiency of complex I of the respiratory chain accounts for neural apoptosis in PD (Zuo and Motherwell, 2013). Deficiency of complex I in mitochondria results in insufficient ATP production and increased ROS generation, thereby inhibiting synapses from receiving adequate amount of energy; these changes eventually lead to neuron cell death in PD (Braun, 2012; Correia et al., 2012). It is now widely accepted that mitochondria-derived ROS production plays a primary role in neurodegenerative diseases (Beal, 2004; Onyango, 2008) and more and more clinical trials are being carried out to explore the protective effects of antioxidant drugs (Dumont and Beal, 2011; Uttara et al., 2009).

1. 1. 3 Linking diabetes to cancer via ROS

It is known for a long time that type 2 diabetic patients have higher risk of developing cancer compared to the non-diabetic people (Marble, 1934). However, the incidence of prostate cancer appears to be reduced in men with diabetes (Orrenius et al., 2003). The relative risks imparted by diabetes are greatest (approximately 2-fold or higher) for cancers of the liver, pancreas, and endometrium, and less (approximately 1.2-fold to 1.5- fold) for cancers of the colon/rectum, breast, and bladder (Legros et al., 2002). The molecular association between diabetes and cancer, however, is unclear. Due to the dependence of many cancers on

glycolysis for energy (Vander Heiden et al., 2009), cancers might favour the environment with high glucose, such as hyperglycaemia in T2D. Consistent with this, many cancers have highly effective up-regulated glucose uptake mechanisms (Vander Heiden et al., 2009). A recent study reported that high glucose promotes migration of breast cancer cells (Takatani-Nakase et al., 2014); this finding that supports the link between diabetes and cancer. Apart from hyperglycaemia, in T2D, inflammatory cytokines (Pickup et al., 2000) and free fatty acids released from adipose tissues may also play a role in cancer progression. Previous studies have shown that cytokines, such as interleukin-6, can enhance cancer growth (Lou et al., 2000) and invasion (Obata et al., 1996). Moreover, the saturated fatty acid, palmitate, is reported to induce breast cancer cell migration (Nomura et al., 2010). All these findings implicate that there is a crosstalk between diabetes and cancer although the underlying mechanisms are far from clear. One common effect of hyperglycaemia, inflammatory cytokines and fatty acids is elevation of intracellular ROS level (Inoguchi et al., 2000; Yang et al., 2007; Yu et al., 2006). The damaging effect of ROS has already been described above. However, 'non-damaging' levels of ROS promote signal transduction to mediate multiple physiological processes, such as actin remodelling and cell migration (see later), rather than causing a deleterious effect. Actin remodelling and cell migration are essential for cancer metastasis (Gupta and Massagué, 2006; Rao and Li, 2004). Therefore, ROS may represent the key factor linking diabetes to cancer.

1. 1. 4 ROS and cancer metastasis

Cancer is a leading cause of death worldwide. Uncontrolled proliferation, reduced apoptosis and metastasis are hallmarks of cancer (Hanahan and Weinberg, 2011). Mutation of genes that control cell proliferation leads to abnormal proliferation of tumour cells (Evan and Vousden, 2001). Dys-regulated apoptotic pathways result in the suppression of apoptosis of tumour cells. Cancer metastasis is responsible for approximately 90% of all cancer mortality (Gupta and Massagué, 2006). Thus, metastasis is a key target for anti-cancer strategies. Metastasis consists of a series of sequential steps: epithelial-mesenchymal transition (EMT), dissociation and intravasation of cells from a primary tumour into the circulation, survival of the cells in the circulation, arrest in small vessels in the down-stream organs, adhesion to endothelial cells, extravasation into surrounding tissues, mesenchymal-epithelial transition (MET), proliferation, and vascularization of tumour tissues (Mehlen and Puisieux, 2006) (Figure 1. 2).

ROS are implicated in cancer metastasis (Nishikawa, 2008). Although high levels of ROS can kill cancer cells (López-Lázaro, 2007), at sub-lethal concentrations, ROS works as a second messenger to mediate signal transduction, up-regulating the expression of various

molecules (Liou and Storz, 2010). It has been demonstrated that expression of the antioxidant enzyme SOD is reduced in many types of cancer, such as pancreatic cancer (Lewis et al., 2005) and breast cancer (Hitchler et al., 2008). Moreover, direct H_2O_2 treatment enhances metastasis in mice (Kundu et al., 1995). These studies indicate that the intracellular redox state governs crucial steps in the metastatic process. To undergo intravasation into the circulation, cancer cells need to migrate close to blood or lymphatic vessels (Reymond et al., 2013). To enable this, primary tumour cells undergo EMT. Studies have shown that ROS generation induced by growth factors plays an important role in triggering EMT (Fukawa et al., 2012; Hiraga et al., 2013; Kim and Cho, 2014). Following EMT, cells disseminated from the primary tumours undergo migration which is facilitated by the activation of matrix metallo-proteinases (MMPs) to degrade the extracellular matrix (ECM) (Nabeshima et al., 2002; Xu et al., 2005). It has been demonstrated that H_2O_2 causes increased expression of MMPs in gastric cancer cells (Gencer et al., 2013). In addition to the effect on intravasation, ROS can also affect proliferation. Various signalling pathways are activated by ROS, including MAPK and Akt/protein kinase B signalling pathways (Liou and Storz, 2010). Both MAPK and Akt are involved in cancer proliferation (Kumar et al., 2008; Park et al., 2009b; Reddy and Glaros, 2007). Abnormal proliferation increases the demand for oxygen and nutrients. This requirement can be met by the expansion of the vascular network, whereby new blood vessels are formed by a process known as angiogenesis (Folkman, 1995). It has been shown that ROS can trigger angiogenesis either by regulating transcriptional factors, such as NF-κB (Ushio-Fukai and Nakamura, 2008) or by inducing expression of the genes such as vascular endothelial growth factor (VEGF) closely associated with angiogenesis (Xia et al., 2007).
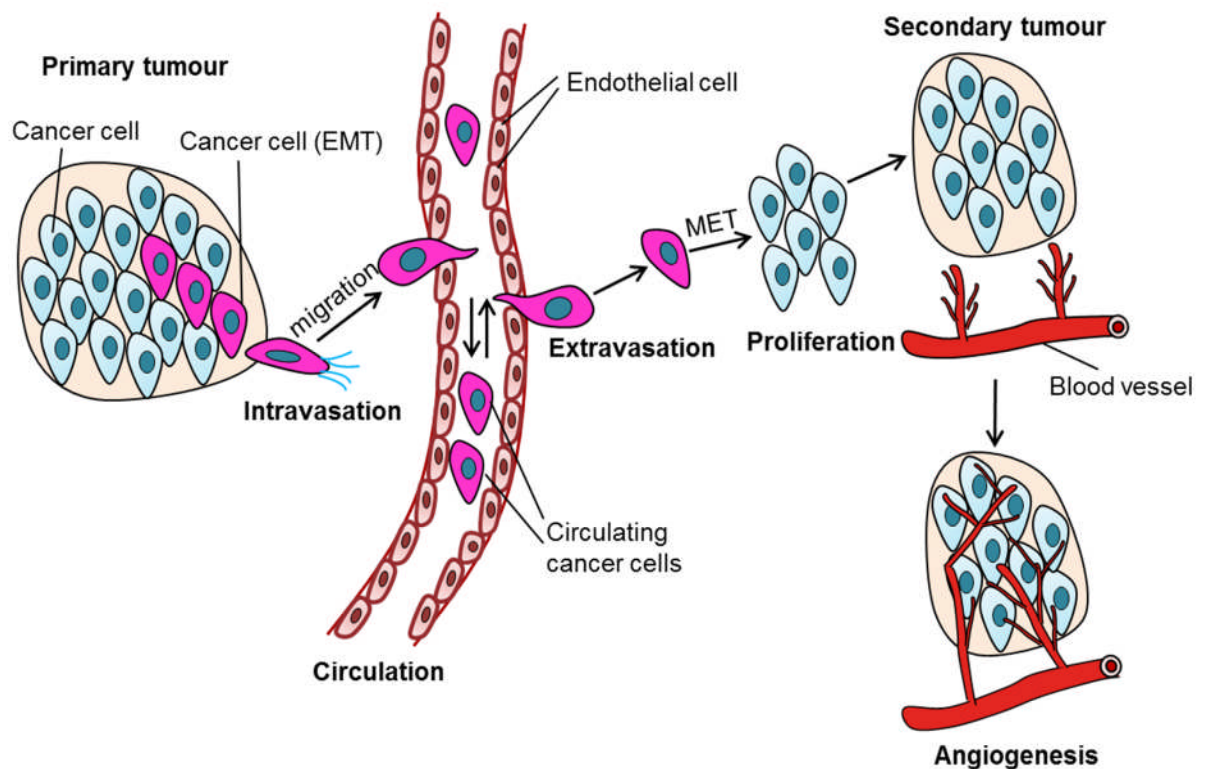
Figure 1. 2 Schematic representation of cancer metastasis When tumour cells are growing, a small population of tumour cells (**fuchsia cells**) can undergo EMT. EMT enables tumour cells to assume a mesenchymal cell phenotype which includes enhanced migratory capacity and invasiveness. These cells form protrusions and undergo migration, entering into circulation by a process known as intravasation. When the cells reach their destination, extravasation occurs. The tumour cells undergo MET and proliferation until a secondary tumour is formed at the distant site. With the development of secondary tumour, more nutrient and oxygen supply is required. To enable this, new blood vessels are formed to supply nutrient and oxygen to the growing tumour. This process is termed angiogenesis. Figure reproduced from Buddihini Samarasinghe (Hallmarks of cancer 6: Tissue invasion and metastasis. 2013).

1. 2 ROS production in cells

1. 2. 1 NADPH oxidases (NOXs)

1. 2. 1. 1 Structure and activation of NOXs

NOXs are initially reported in phagocytic cells of the immune system, including granulocytes (Segal and JONES, 1978) and neutrophils (Dinauer et al., 1987). NOXs are a family of plasma membrane-bound enzymes (NOX1, NOX2, NOX3, NOX4, NOX5, DUOX1 and DUOX2 in phagocyte), which share the capability to transfer electrons across the plasma membrane to generate superoxide and other downstream ROS. During phagocytosis, NOXs are required to elevate intracellular ROS level to damage or kill pathogenic organisms (Lambeth, 2004). NOXs are not restricted to the immune system but are expressed in other cell types, such as endothelial cells (Lassegue and Clempus, 2003) and pancreatic β-cells (Newsholme et al., 2009). Thus, NOXs may represent an essential component of redox signalling mechanisms in these cells (see below for details). NOX is a protein complex, composed of six subunits: a Rho GTPase (generally Rac1 and Rac2), NOX2, p22^{phox}, p67^{phox}, p40^{phox} and p47^{phox}. In the inactive state, NOX2 and p22^{phox} located in the plasma membrane constitute the catalytic core of the "classical" enzyme, while the other subunits are located in the cytosol. Upon activation, such as when stimulated by protein kinase C, the cytosolic subunits are trans-located to the plasma membrane to initiate the enzyme activation (Abramov et al., 2005) (Figure 1.3). Thus, activation of NADPH oxidase is spatiotemporally regulated by the assembly of spatially separated subunits.

1. 2. 1. 2 Regulation of NOX

A number of factors have been implicated in the activation of NOX, including glucose, saturated fatty acids and inflammatory cytokines. In cardiomyocytes, high glucose stimulates ROS production through NOX2 by activating Rac1 and mediating p47^{phox} translocation to the plasma membrane. The resultant increase in ROS subsequently induces cell death (Balteau et al., 2011). In addition to glucose, high levels of palmitate have been demonstrated to activate NOX2 and mediate ROS production both in pancreatic islets and pancreatic β-cells (Morgan et al., 2007). In diabetic conditions, apart from high glucose and fatty acids, inflammatory responses also occur; activation of NOX by cytokines has also been reported previously. In human retinal epithelial cells, it was found that both IL-1β and IFN-γ are able to induce ROS production through NOX (Yang et al., 2007). The authors of this study found that IFN-γ induced ROS production is partially derived from mitochondria as thenoyltrifluoroacetone (TTFA), one of the mitochondrial respiratory chain inhibitors, partially

blocked this ROS generation (Yang et al., 2007). Thus, cytokines can induce ROS production via two mechanisms: that is via NOX and via mitochondria.

It has been demonstrated in cultured cortical neurons and astrocytes that Zn^{2+} overload induces translocation of NOX subunits (p47^{phox} and p67^{phox}) to plasma membrane to activate NOX (Noh and Koh, 2000). Although the impact of such translocation on cytosolic ROS levels has not been investigated, the inhibitory effect of ROS scavengers on zinc overload-induced cell death was observed (Noh and Koh, 2000). This observation indicates a close relationship between Zn^{2+} and NOX-derived ROS. Other studies have shown that direct Zn^{2+} exposure induces ROS production in cortical neurons (Kim et al., 1999; Sensi et al., 2000). In non-neuronal cells, such as adipocytes, Zn^{2+} has been shown to induce formation of superoxide and H_2O_2 (May and Contoreggi, 1982). As for the underlying mechanism for Zn^{2+} induced ROS generation, little information is available. Mize and Langdon suggest that Zn^{2+} induces ROS generation via inhibition of glutathione reductase and peroxidase, the major enzymes for cellular antioxidant defence system (Mize and Langdon, 1962). As cytosolic free Zn^{2+} functions as a second messenger (Yamasaki et al., 2007), the mechanism of Zn^{2+} induced ROS generation might be more complex and needs further investigation.
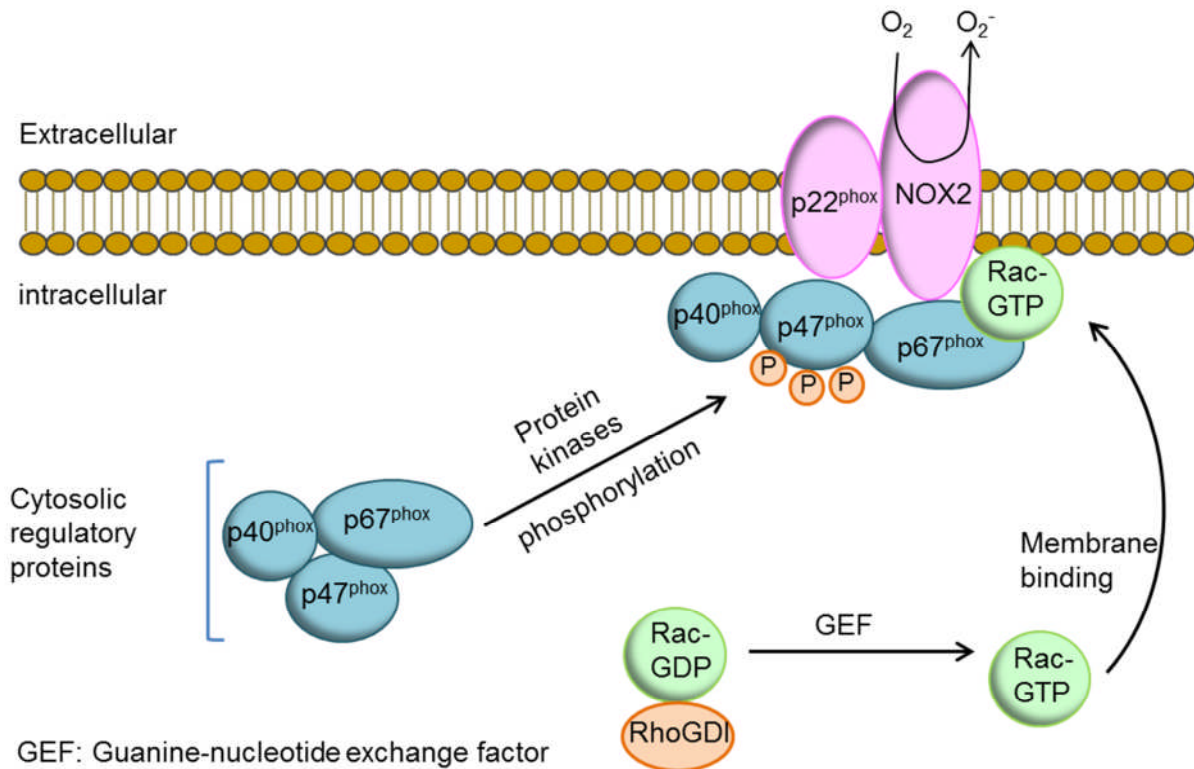
Figure 1. 3 Schematic showing the activation mechanism of NADPH oxidase (NOX) Activation of NOX is dependent on the assembly of cytosolic regulatory proteins (p40^{phox}, p67^{phox} and p47^{phox}) with the plasma membrane-anchored p22^{phox} and NOX2. p47^{phox} binds to p67^{phox} and p40^{phox} in the cytosol. Protein kinases, such as PKC, induce phosphorylation of p47^{phox}, allowing p47^{phox} to bind to p22^{phox}. Rac-GDP is maintained in the cytosol by the inhibitory protein RhoGDP-dissociation inhibitor (RhoGDI). Activation of GEF triggers GTP binding, resulting in conformation changes in Rac that promote dissociation from RhoGDI. The conformation change also promotes Rac binding to p67^{phox}, leading to the assembly of the active complex. Figure adapted from (Lambeth, 2004)

1. 2. 2 Mitochondrial ROS (mROS)

Mitochondria generate ATP by transferring electrons from the donors (e.g., NADH and FADH2) to acceptors (O_2) via the electron transport chain (ETC). During this process, electrons can leak out and generate ROS (Murphy, 2009). Under normal conditions, in the inner mitochondrial membrane, electron transfer through complexes I, III, and IV extrudes protons outward into the intermembrane space, generating a proton gradient that drives ATP synthesis by ATP synthase (complex V) as protons pass back through the inner membrane into the matrix. However, under pathological conditions, such as diabetic conditions, supply of substrates to the TCA cycle increases; these include glucose-derived pyruvate and fatty acid-derived acetyl-CoA (Sivitz and Yorek, 2010). The increased substrates increase the production of electron donors (NADH and FADH2), which is leaked to molecular oxygen, thereby generating superoxide.

1. 2. 2. 1 Production of mROS in diabetes

Superoxide is the initial oxygen free radical formed by the mitochondria, which is then converted to other more reactive species that can damage cells in numerous ways (Zorov et al., 2014). Excessive mROS can be triggered by many factors, such as high glucose (Piconi et al., 2006), high fatty acid level (Newsholme et al., 2007) as well as increased cytokine release. There are extensive studies indicating that high glucose induces mROS overproduction. For instance, in primary arterial endothelial cells *in vitro*, high glucose increases the voltage across the mitochondrial membrane above the critical threshold to increase superoxide formation (Korshunov et al., 1997). However, there are some studies indicating that the induction of mROS generation by glucose is not a direct effect, but through glucose-induced cytokine release in endothelial cells. For example, in cultured human retinal endothelial cells (HRECs), high glucose failed to induce mROS generation, but increased the IL-1β release which induces marked increase in mROS production (Busik et al., 2008). Thus, whether the effect of glucose on ROS production is direct, or indirect through cytokines, remains to be established. Alternatively, different cells may use different mechanisms. In isolated pancreatic islets from a rat model of T2D, direct measurement of mitochondrial superoxide revealed ROS generation is coupled with perturbed mitochondrial function (Bindokas et al., 2003). In addition to hyperglycaemia, in type 2 diabetic state, the pancreatic β-cells are also confronted with increased plasma levels of triacylglycerols and non-esterified fatty acids, specifically, palmitate. Studies have shown that excessive levels of palmitate induce apoptosis of pancreatic islets and β-cells by producing excessive mitochondrial ROS (Carlsson et al., 1999; Piro et al., 2002; Shimabukuro et al., 1998).

1. 2. 2. 2 mROS production in Diabetes

31

The central role for mROS production in the development of diabetic complications has been suggested by a number of studies. However, the detailed molecular mechanism about how high glucose and saturated fatty acids elevate mROS production is less well understood. Besides, apart from the inter-conversion between different ROS types, multiple lines of evidence indicate that there is a functional connectivity between different sources of ROS. This view is termed ROS-induced ROS release (RIRR). It was suggested that excessive mROS production can activate mitochondrial permeability transition pore (mPTP) and inner membrane anion channels (IMAC) which can result in mROS release to cytosol (Zorov et al., 2014). Although this ROS release might cause destruction of nearby mitochondria, it can also function as signalling molecules to activate ROS-sensitive proteins, such as protein kinase C (PKC) that has been demonstrated to increase NOX activity (Inoguchi et al., 2000). Therefore, the mROS signal can be amplified by NOX-derived ROS generation.

1. 2. 2. 3 Relationship between NOX-derived ROS and mROS

NOX-derived ROS generation and mROS production play an important role in redox signalling in cells and the cross-talk between the two has been reported previously (Lee et al., 2006; Pinton et al., 2008). In human 293T cells, serum withdrawal can induce mROS generation that in turn leads to NOX1 activation. NOX1 activation in turn leads to cell death, indicating a role for NOX in amplifying the deleterious effect of mROS (Lee et al., 2006). In another study, it has been reported that hypoxia-induced mROS generation subsequently induces NOX activation through PKCε in mouse pulmonary arteries (Rathore et al., 2008). Conversely, it has been reported that NOX-derived superoxide can induce mROS release by acting on ATP-sensitive K^+ channels in the inner mitochondrial membrane in rat myocardium: opening of mitochondrial K_{ATP} channels results in mitochondrial depolarization and release of mROS to cytosol (Kimura et al., 2005). These findings indicate an intriguing interplay between NOX-derived ROS and mitochondria-generated ROS.

1. 3 ROS mediated signalling pathways

ROS plays an important part both in physiological conditions and pathological processes. Under physiological conditions such as wound healing (Kanta, 2011) and angiogenesis (Ushio-Fukai and Alexander, 2004), ROS mediate essential signal transduction. However, when ROS are accumulated beyond the threshold, they can lead to pathological conditions such as diabetes. Although there is ample evidence demonstrating the role of ROS in regulating cellular signalling pathways, the question of how ROS mediates various signalling pathways is less well understood. It is believed that ROS alters protein functions mainly through the redox regulation of redox-reactive cysteine (Cys) residues on proteins (Ray et al., 2012). These oxidative modifications result in changes in structures or functions of proteins.

Due to the reversible nature of these modifications by ROS scavengers (Denu and Tanner, 1998; Roos and Messens, 2011), ROS are thought to play a signalling role in a range of cellular functions.

1. 3. 1 Inhibition of phosphatases

Protein tyrosine phosphatases (PTPs) control the phosphorylation state of numerous signal-transducing proteins and are therefore involved in the regulation of multiple cellular functions, such as cell survival (Santin et al., 2011), metabolism (Gurzov et al., 2015) and migration (Li et al., 2014; Zheng and Lu, 2013). The catalytic region of PTPs includes cysteines (Salmeen and Barford, 2005), which are susceptible to oxidative inactivation (Denu and Tanner, 1998). Thus ROS can decrease phosphatase activity and thereby enhance protein tyrosine phosphorylation leading to activation of multiple signalling pathways, such as MAPK (Lee and Esselman, 2002) and PI3-Ks (Nakanishi et al., 2014).

1. 3. 2 Activation of kinases

MAPKs regulate diverse cellular programmes including embryogenesis (Corson et al., 2003), proliferation (Zhang and Liu, 2002) and apoptosis (Wada and Penninger, 2004) based on the different cues from the environment of the cells. The MAPK cascades consist of four major MAPKs: the extracellular signal-related kinases (Erk1/2), the c-Jun N-terminal kinases (JNK), the p38 kinase (p38), and the big MAP kinase 1 (BMK1/Erk5). There is abundant evidence for regulation of MAPKs by ROS. For example, treatment of endothelial cells with H_2O_2 leads to phosphorylation and activation of p38 MAP kinase (Djordjevic et al., 2005). It was suggested that regulation of MAP kinase by ROS is dependent on the activation of signalling pathways upstream of Erk1/2. On the other hand, activation of MAPK pathways might be due to the direct inhibition of MAPK phosphatases by ROS (Robinson et al., 1999). The authors of this study demonstrated that ROS induced p38 activation occurs concurrently with inhibition of protein phosphatases in cultured astrocytes (Robinson et al., 1999). In addition to the MAPK cascades, PKC is an important target of ROS. PKCs are a family of more than 11 isoforms that are widely distributed in mammalian cells. The activity of PKCs is greatly enhanced by diacylglycerol (DAG) (Geraldes and King, 2010). Activation of PKC isoforms by ROS under diabetic conditions can mediate tissue injury. Elevated ROS is able to inhibit the activity of glycolytic enzyme glyceraldehyde-3-phosphate dehydrogenase (GAPDH) (Hwang et al., 2009), thereby raising the intracellular DAG precursor triose phosphate and DAG, which in turn enhances PKC activity (Du et al., 2003). Another signalling pathway that can be regulated by ROS is the PI3-K pathway. The PI3-K is tightly coupled with receptor tyrosine kinases (RTKs) activated by various growth factors, such as

epidermal growth factor (EGF) (Shah et al., 2006) and insulin (Niswender et al., 2003). PI3-K catalyses the synthesis of the second messenger phosphatidylinositol 3,4,5 triphosphate (PIP3) from phosphatidylinositol 4,5 bisphosphate (PIP2), wherein the membrane bound PIP3 serves as a signalling molecule to recruit proteins and mediate further downstream signalling events, such as proliferation (Hemmings and Restuccia, 2012). The synthesis of PIP3 is negatively regulated primarily by the phosphatase and tensin homologue (PTEN), which dephosphorylates PIP3 back to PIP2 (Stambolic et al., 1998). H_2O_2 has been demonstrated to oxidise and inactivate PTEN (Lee et al., 2002; Leslie et al., 2003), thereby affecting PI3-K-related cellular functions.

1. 3. 3 Regulation of ion channels

Ca^{2+} ions are essential second messengers involved in many cellular functions, such as apoptosis (Pinton et al., 2008) and cell migration (Minton, 2014). Therefore, Ca^{2+} homeostasis is essential for cells and is tightly regulated by distinct Ca^{2+} channels (Bose et al., 2015) and pumps (Marín et al., 1998). It has been demonstrated that ROS can regulate many intracellular and plasma membrane Ca^{2+} channels, including Ca^{2+}-release-activated channels (CRAC), voltage-gated Ca^{2+} channels (Ca_V) as well as the transient receptor potential (TRP) channels (Bogeski et al., 2011). CRAC channels are composed of two components: plasma membrane protein Orai (Orai1 and Orai2) forms the pore of the CRAC channel (DeHaven et al., 2007; Prakriya et al., 2006) and stromal interaction molecule (STIM) functions as the regulatory subunit (Park et al., 2009a). Upon depletion of intracellular Ca^{2+}-store (primarily ER), as a sensor for Ca^{2+} level in ER, STIM is activated and translocated to sites near plasma membrane where STIM interacts with and activates store-operated Ca^{2+} channels (SOCE) to cause Ca^{2+} influx (Smyth et al., 2010). Oxidizing agents such as H_2O_2 have been reported to induce activation of CRAC channels by depleting the ER Ca^{2+} stores (Grupe et al., 2010). However, the effects of ROS on CRAC channels are debatable because several other studies have shown that higher level of H_2O_2 (>1 mM) can inhibit CRAC channel (Florea and Blatter, 2008; Tintinger et al., 2007). Apart from Ca^{2+}-store depletion, ROS has been demonstrated to directly modify STIM to regulate the activity of CRAC channels. It has been shown that ROS can activate CRAC channels by oxidizing cysteine residues in STIM1 (Hawkins et al., 2010). Thus, by modifying the different components of CRAC activation pathways, ROS can regulate the Ca^{2+} homeostasis either leading to deleterious effects or supporting essential cellular functions. Ca_V channels are one of the first Ca^{2+} channels to be identified as ROS sensitive (Todorovic and Jevtovic-Todorovic, 2014). They consist of five major subgroups including L-Type (L for "long-lasting"), N-Type (N for "Neural"), P/Q-Type, R-Type and T-Type (T for "Transient"). These channels

are formed as a complex of several subunits, of which the α1 forms the ion conducting pore (Lacinova, 2005). The reactive cysteine in α1 is the main molecular target of ROS (Hudasek et al., 2004). A number of studies have reported regulation of Ca_V channel activity by ROS (Bogeski et al., 2011). TRP channels are also tightly regulated by ROS. Mammalian TRP channels include six subgroups (TRPC, TRPM, TRPV, TRPA, TRPP and TRPML) according to amino acid sequence homologies and protein domains (Venkatachalam and Montell, 2007). Previous studies have indicated that ROS can activate TRPC5, TRPM2, TRPM4 and TRPA1 in different cell types (Bessac et al., 2008; Cao et al., 2010; Simon et al., 2010; Yamamoto et al., 2010). However, H_2O_2 has been shown to inhibit TRPM6 channel activity (Cao et al., 2010). As TRP channels are involved in cell death (Miller, 2006), inflammation responses (Schumacher, 2010), cell migration (Pla and Gkika, 2013) and many other functions (Clapham, 2003), the role of ROS in these cellular functions might be through regulation of TRP channels and Ca^{2+} signals. Apart from mediating Ca^{2+} entry or release, some TRP channels are also permeable to other ions, such as Zn^{2+} (Bouron et al., 2014). Although Zn^{2+} normally exists in a protein-bound form, it has been reported that cytosolic free Zn^{2+} in certain situations can function as a second messenger to mediate signal transduction (Yamasaki et al., 2007). More details will follow below.

1. 4 TRP channels

TRP proteins are the products of *trp* genes, the first of which was discovered in *Drosophila melanogaster* (Montell and Rubin, 1989). All TRP channels are suggested to form tetramers (homo or hetero). The subunits of these channels share common structural features: six transmembrane segments; a pore-forming region between fifth and sixth transmembrane segments; cytoplasmic N- and C-terminal regions (Clapham, 2003). Mammalian TRPs can be divided into six subfamilies: TRPC (1-7), TRPV (1-6), TRPA (1), TRPP (1-3), TRPML (1-3) and TRPM (1-8). The TRP-melastatin subfamily (TRPM) contains eight mammalian members: TRPM1-TRPM8, which are divided into 4 pairs by the degree of homology of their protein sequences. They are TRPM1/TRPM3, TRPM2/TRPM8, TRPM4/TRPM5 and TRPM6 /TRPM7 (Figure 1. 4) (Fleig and Penner, 2004). Similar to the other TRP channels, TRPM proteins comprise a TRP domain within their C-termini. Additionally, the N-terminus of the TRPM subfamily member is characterized by four stretches of residues, termed as the TRPM homology domain or MHD (Perraud et al., 2001).

Even within the major subfamilies, TRP channels exhibit a remarkable diversity in their mechanisms of activation. TRPC channels are receptor-activated ion channels while TRPV1 and TRPM8 channels are responsive to heat (> 48 °C) (Caterina et al., 1997) and cold (< 30°C) respectively (Peier et al., 2002). TRPM4 channels have been shown to be activated

by increased Ca^{2+} (Launay et al., 2002). As mentioned above, some members of TRP channel family are regulated by ROS and control various cellular processes. For example, ROS can activate TRPM2 channels in brain neuronal cells which cause Ca^{2+} overload to induce cell death (Kaneko et al., 2006); ROS can also modulate TRPC5 channels (Yamamoto et al., 2010) which play important roles in growth cone filopodia formation (Greka et al., 2003) and endothelial cell migration (Chaudhuri et al., 2008). Activation of TRP channels in plasma membrane mediates flux of Ca^{2+} or Na$^+$ into the cells, thereby raising intracellular concentrations of these ions and depolarizing the cells to affect cellular functions (Nilius, 2006; Venkatachalam and Montell, 2007). In addition to the plasma membrane, many TRP channels are expressed in intracellular organelles, such as TRPM8 and TRPV1 channels in ER (Thebault et al., 2005; Turner et al., 2003), and TRPML3 and TRPM2 channels in lysosomes (Dong et al., 2010b; Kim et al., 2009a). Therefore, intracellular TRP channels may function as Ca^{2+} release channels and regulate the intracellular Ca^{2+} homeostasis (Lange et al., 2009). However, the functions and regulation of these intracellular membrane TRP channels are poorly defined. Due to the essential role of Ca^{2+} and intracellular organelles in diverse cellular functions, such as waste clearance (Kalwat and Thurmond, 2013) and trafficking (Tsai et al., 2015), it is speculated that intracellular-membrane-residing TRP channels play essential roles in these functions (Samie et al., 2013). TRP channels are widely expressed in different tissues and cell types, including excitable cells and non-excitable cells (Perraud et al., 2003a). The wide expression profile indicates the diversity of the biological roles that TRP channels play (Dong et al., 2010b).
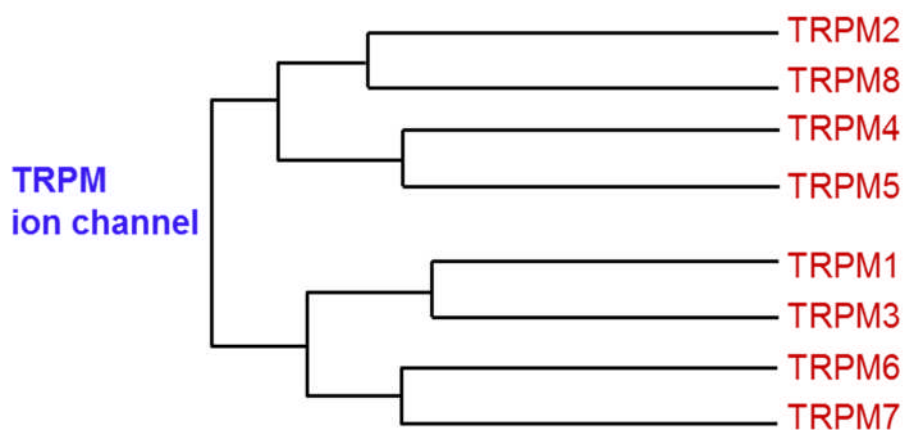
Figure 1. 4 Phylogenetic analysis of TRPM channels Based on homology, TRPM ion channels are divided into 4 pairs: TRPM1/TRPM3; TRPM2/TRPM8; TRPM4/TRPM5; TRPM6/TRPM7.

1. 5 TRPM2 channel

TRPM2 is the first identified ROS-sensitive TRP channel that is activated by H_2O_2 (Hara et al., 2002). Accumulating evidence has demonstrated that TRPM2 channels and TRPM2-mediated Ca^{2+} signalling play essential roles in cell death (Kaneko et al., 2006; Zhang et al., 2006) and the production of pro-inflammatory cytokines (Wehrhahn et al., 2010). Recently, the role of lysosomal TRPM2 channels and TRPM2-mediated Ca^{2+} release in dendritic cell maturation and chemotaxis has been demonstrated (Sumoza-Toledo et al., 2011). This finding indicates that TRPM2 channels can mediate other cellular functions in addition to cell death and immune responses. As the molecular and biophysical properties are closely related to functions, the structure and modulation of TRPM2 channel activity will be introduced below.

1. 5. 1 TRPM2 structure

Like other TRPM channels, TRPM2 protein also has six trans-membrane segments (S1-S6) with N- and C-termini oriented toward the cytoplasm and the pore-forming loop domain is located between S5 and S6 (Figure 1. 5A). Four TRPM2 subunits assemble together to form a functional ion channel. The N-terminal contains four homologous regions (MHR) (Figure 1. 5B) (Tong et al., 2006). The C-terminal contains a TRP box and a coil-coil domain, which has been shown to be critical for the homo-tetrameric assembly of TRPM2 (Jiang, 2007). Additionally, the C-terminus of TRPM2 channels contains a unique C-terminal adenosine diphosphate ribose (ADPR) pyro-phosphatase domain (NUDT9-H domain) (Perraud et al., 2003b) (Figure 1.5B). For this reason, like TRPM6/7, TRPM2 is known as a "chanzyme" because of the protein's dual function as an ion channel and an enzyme. The NUDT9-H domain was suggested to be responsible for ADPR gating for TRPM2 activation (Kühn and Lückhoff, 2004). In addition to this function, the other functions of this enzymatic domain are poorly understood. Recently, the structure of TRPV1 and TRPA1 channels has been identified by electron cryo-microscopy (Liao et al., 2013; Paulsen et al., 2015). Like TRPM2 channels, both TRPV1 and TRPA1 channels are homo-tetramers assembled by four subunits. Each subunit consists of six transmembrane segments (S1-S6) with pore-forming loop located between S5 and S6. Besides, the authors demonstrate that the C-terminal coiled-coil domain of TRPA1 subunit mediates extensive subunit interactions (Paulsen et al., 2015). And this interaction may facility concerted conformational changes of channels. Similar to this, the C-terminal coiled-coil domain of TRPM2 channels has also been demonstrated to engage in subunit interaction and assembly of mature channels (Mei et al., 2006). Therefore, these studies may provide hints to study high-resolution structure of TRPM2 channels.
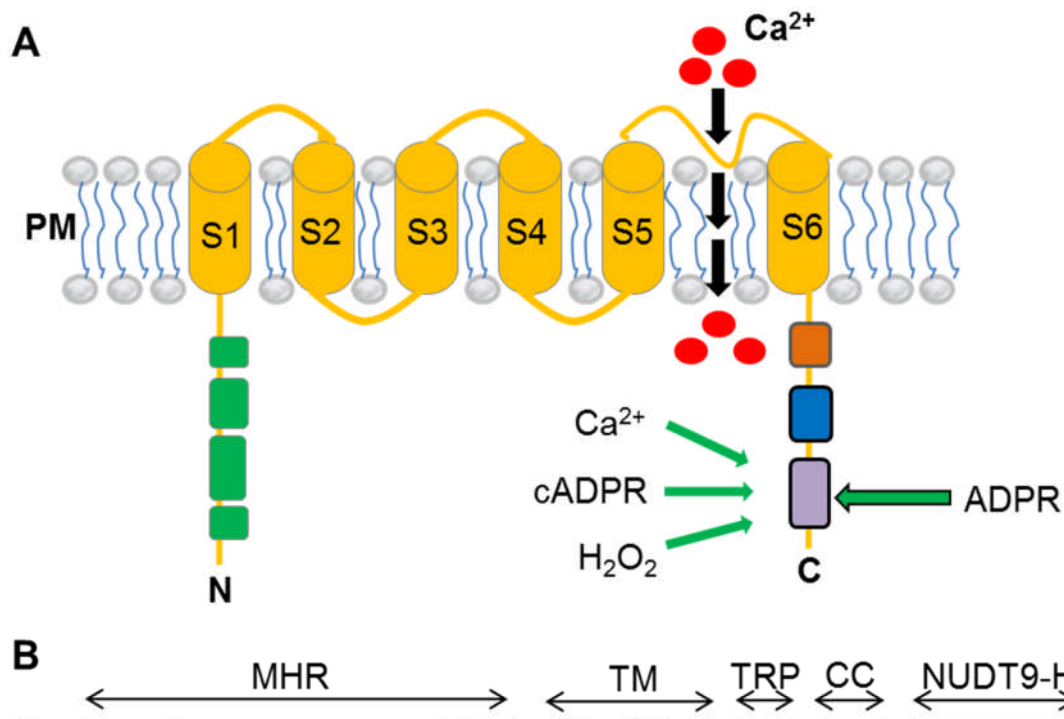
Figure 1.5 Structure and transmembrane topology of TRPM2 channel. (A) The TRPM2 protein subunit comprises six transmembrane segments (S1-S6), flanked by the intracellular N- and C-termini with the pore-forming loop domain being located between S5 and S6. ADPR is considered the primary gating molecule of TRPM2. It binds to the Nudix-like domain (NUDT9-H) in the C-terminus and then causes the channel to open and allow permeation of sodium and calcium ions into the cell. H_2O_2, cADPR and Ca^{2+} also activate TRPM2 channels (see text). (**B**) The TRPM2 N-terminus has four homologous regions (MHR) followed by six TM segments. The C-terminus contains a NUDT9-H domain, a TRP box and a coiled-coil domain (CC), which has been suggested to be critical for the homo-tetrameric assembly of TRPM2. Figure redrawn from (Sumoza‐Toledo and Penner, 2011).

1. 5. 2 TRPM2 activation

TRPM2 is a Ca^{2+}-permeable nonselective channel that can be activated by diverse signals. Notably, TRPM2 channel is activated by H_2O_2 in many types of cells, including pancreatic β-cells (Cooper et al., 2013; Manna et al., 2015), microglial (Kraft et al., 2004) and endothelial cells (Hecquet et al., 2008). In TRPM2-expressing cells, application of H_2O_2 induces TRPM2 current and an increase in cytosolic Ca^{2+} (Hara et al., 2002). Many studies so far have indicated that TRPM2 channels can also be specifically gated by ADPR which can bind to NUDT9-H region. This gating can be facilitated by cyclic adenosine diphosphate-ribose (cADPR) and Ca^{2+} (Figure 1.5A). Upon binding of ADPR, TRPM2 channels open and allow the permeation of extracellular Na^+, K^+ and Ca^{2+} into the cell (Perraud et al., 2001; Sano et al., 2001; Venkatachalam and Montell, 2007). The source of ADPR can be nucleus or mitochondria. Mitochondria, as an important site for ADPR formation, contain 75% of cellular NAD^+ (Di Lisa and Ziegler, 2001). In the mitochondria, ADPR is generated from NAD^+ by the action of NAD^+ nucleosidase (NADase). Within the nucleus, ADPR is generated from NAD^+ through the combined actions of Poly (ADP-ribose) Polymerase 1 (PARP1)/ *Poly (ADP-ribose) glycohydrolase* (PARG) pathway (Fauzee et al., 2010) (Figure 1. 6).

As a PARP inhibitor, PJ34 can indirectly inhibit TRPM2 channels by blocking the generation of ADPR (Fonfria et al., 2004). 2-aminoethoxydiphenyl borate (2-APB) is a non-selective cation channel blocker which can inhibit the current of TRPM2 channels (Togashi et al., 2008). N-(p-amylcinnamoyl) anthranilic acid (ACA) is also used as an inhibitor for TRPM2 channels. Kraft et al have reported that ACA inhibits TRPM2 activity by modulating channel gating. ACA, however, is also nonspecific as it can also inhibit TRPM8 and TRPM6 channels (Kraft et al., 2006). Flufenamic acid (FFA) has been described as an efficient inhibitor for TRPM2 channel. Hill et al reported that FFA could inhibit ADPR-induced current of TRPM2 channels (Hill et al., 2004). However, none of these inhibitors is fully specific for TRPM2 channels. Thus, to examine the role of TRPM2 channels, other methods such as knockdown by siRNA should be combined with pharmacological inhibitors.

More recently, Yu et al reported that TRPM2 can also conduct Zn^{2+} ions in HEK293 and Jurkat cells (Yu et al., 2012). Manna et al found activation of TRPM2 channels by H_2O_2 can increase cytosolic Zn^{2+} level in pancreatic β-cells (Manna et al., 2015). Therefore, both Ca^{2+} and Zn^{2+} should be taken into account when examining the functions of TRPM2 channels.
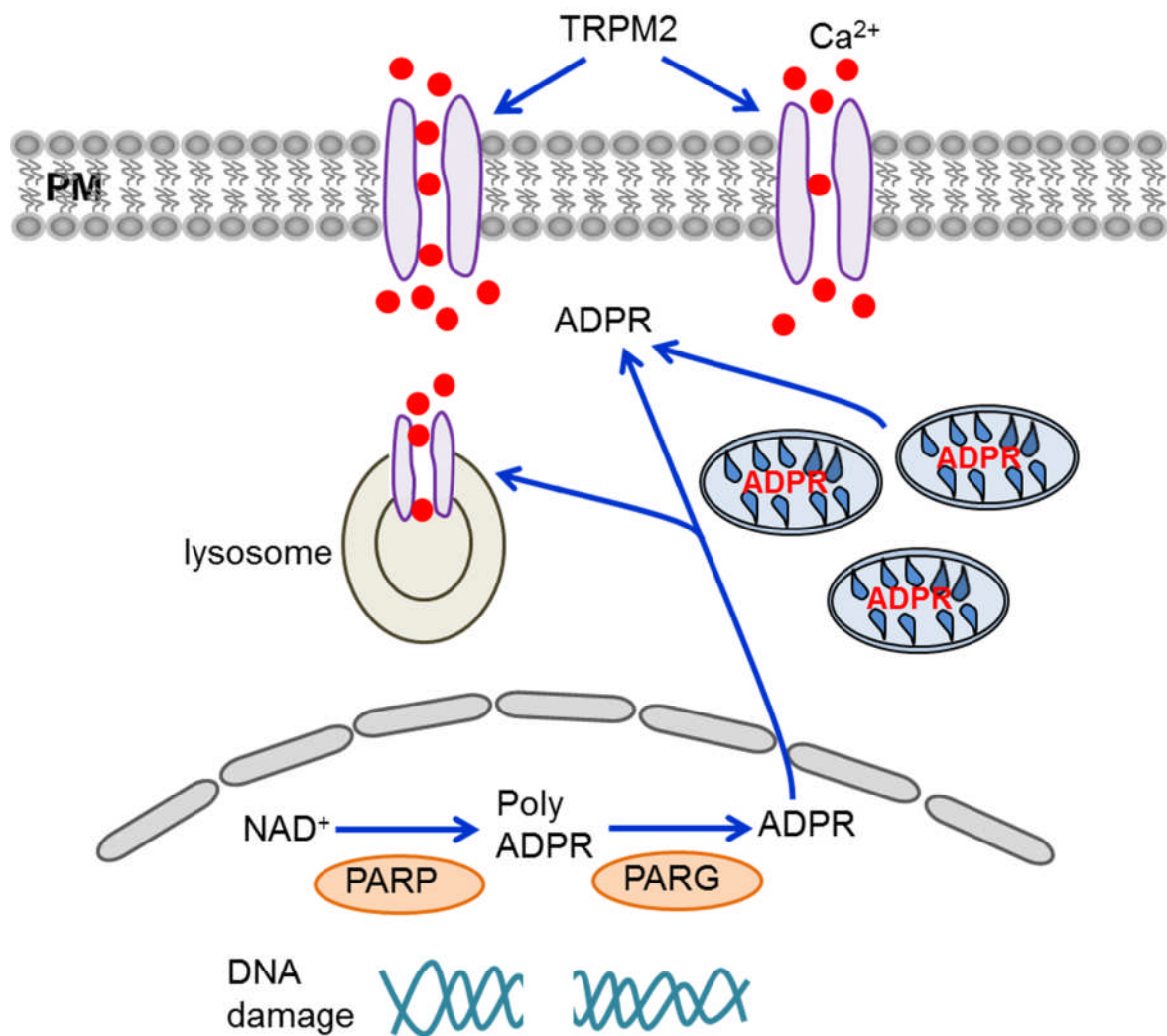
Figure 1. 6 Signalling mechanisms for ADPR generation for TRPM2 activation ADPR generation in the nucleus involves activation of PARP/PARG pathway during oxidative DNA damage. PARP-1 binds to the damaged DNA and catalyzes the cleavage of NAD^+ to ADPR. ADPR is then polymerized onto various nuclear proteins, activating DNA repair mechanisms. Free ADPR is generated following the degradation of ADPR polymers by PARG. Then these free ADPR molecules enter the cytosol and activate plasma membrane or lysosomal TRPM2 channels to mediate Ca^{2+} entry and Ca^{2+} release respectively. Figure redrawn from (Sumoza‐Toledo and Penner, 2011).

1. 5. 3 Tissue distribution and subcellular localization

TRPM2 channels are highly expressed in brain (Jang et al., 2014); it is also expressed in other tissues such as bone marrow, spleen and liver (Sumoza‑Toledo and Penner, 2011). Besides, they are found in different cell types, such as pancreatic β-cells (Lange et al., 2009) and endothelial cells (Hecquet et al., 2008). This widespread expression pattern implies a significant role for TRPM2 channels in physiological and pathological functions. TRPM2 channels are generally located in the plasma membrane and mediate influx of Ca^{2+} upon activation. However, recent studies have shown that TRPM2 channels are also localized to intracellular organelles (Lange et al., 2009; Sumoza-Toledo et al., 2011). For example, Lange et al reported localization of TRPM2 channels in the membrane of lysosome of pancreatic β-cells (Lange et al., 2009). The authors demonstrated that lysosomal TRPM2 channels induce cell death by mediating Ca^{2+} release from lysosomes in response to cADPR. As TRPM2 channels can be activated by Ca^{2+} (Csanády and Törőcsik, 2009), Ca^{2+} influx though the plasma membrane might activate lysosomal TRPM2 channels, thereby inducing Ca^{2+} release. However, this interplay between plasma membrane and lysosomal TRPM2 channels is poorly understood.

1. 5. 4 TRPM2 channels in cell death

A major function of TRPM2 channels is to mediate death of many cell types, such as pancreatic β-cells, neuronal cells and endothelial cells. Due to the involvement of TRPM2 in cell death, TRPM2 channels play essential roles in many human diseases like diabetes (Uchida and Tominaga, 2014), neurodegenerative diseases (Nazıroğlu, 2011) and cardiovascular diseases (Inoue et al., 2006). For example, it has been reported that lack of TRPM2 channels impairs the insulin secretion and glucose metabolism in mice (Uchida et al., 2011). Besides, it has been reported that H_2O_2-activated TRPM2 channels mediates endothelial injury (Hecquet and Malik, 2009). All these studies implicated the intracellular Ca^{2+} overload as the mechanism triggering pathological outcomes. The role of Zn^{2+}, on the other hand, in cell death is less well understood. A recent study has shown a role for Zn^{2+} in H_2O_2-induced death in pancreatic β-cells (Manna et al., 2015). The authors reported that upon activation, TPRM2 channels mediate Zn^{2+} release from the lysosomal stores and the following rise in cytosolic Zn^{2+} triggers the cell death. However, the authors also demonstrated that the Zn^{2+} release mediated by TRPM2 is dependent on Ca^{2+}. Thus, interplay between Ca^{2+} and Zn^{2+} appears to contribute to β-cell death. Interestingly, this study has shown that chelation of Zn^{2+} alone is sufficient to prevent β-cell death, indicating that Zn^{2+} plays a major role in H_2O_2 induced β-cell death.

Consistent with the role of TRPM2 channels in cell death, TRPM2 channels have been shown to regulate caspase signalling. For example, activation of TRPM2 channels induces activation of caspase-8, caspase-9 and caspase-3 in endothelial cells (Sun et al., 2012) and hematopoietic cells (Zhang et al., 2006). These findings indicate the involvement of caspase activation in TRPM2-mediated cell death. Mitochondria play an important role in cell death induced by ROS (Orrenius, 2007). In diabetes, both glucose and fatty acid levels are increased which have been demonstrated to elevate ROS levels, thereby leading to cell death. However, as a ROS-sensitive ion channel, whether TRPM2 channels mediate glucose and fatty acid-induced ROS-dependent cell death is still unknown. Besides, the role of mitochondrial morphology and functions in this process needs to be examined.

1. 6 Mitochondria

1. 6. 1 Mitochondrial structure and dynamics

Mitochondria are at the centre of cellular energy metabolism. They also play essential roles in regulating cell survival and death. They are double membrane, filamentous, tubular organelles that provide energy to cells by mediating oxidation phosphorylation. Besides, they are highly dynamic, constantly changing location and shape in cells (Chen and Chan, 2009). Normally, mitochondria are located in the perinuclear region, however, under some circumstances, mitochondria can translocate to a specific site, such as to the leading edge of migrating cancer cells (Zhao et al., 2013). In addition to location change, mitochondria undergo continuous fusion and fission to sustain a healthy network (Figure 1.7).

The fission of the outer membrane is mediated by dynamin-related protein 1 (Drp1) and its receptors: fission protein 1 (Fis1), mitochondrial fission factor (Mff), mitochondrial dynamics proteins of 49 and 51 kDa (MiD49 and MiD51) (Figure 1.7). Drp1 is a member of the dynamin family of proteins that can constrict cellular membranes that requires the GTPase function of these proteins. Drp1 assembles into a ring-like structure (Smirnova et al., 2001), around mitochondria at a site pre-constricted by the ER tubules (Friedman et al., 2011; Yoon et al., 2011). Drp1 is primarily located in the cytosol with a small proportion being located on mitochondria (Shin et al., 1997). When Drp1 accumulates on the surface of mitochondria, it mediates scission of the mitochondria, resulting in fission of the mitochondrial network via its GTPase activity. However, increasing the levels of Drp1 alone fails to cause mitochondrial fission (Pitts et al., 1999), which suggests the existence of limiting factors or regulatory mechanisms underlying Drp1 induced mitochondrial fission. Fis1 can bind to Drp1 to promote mitochondrial fission. Overexpression of Fis1 could induce mitochondrial fragmentation but requires intact Drp1 function, indicating that Drp1 and Fis1 work

cooperatively to mediate mitochondrial fragmentation (Yoon et al., 2003). Mff, MiD49 and MiD51 promote Drp1 recruitment and form rings surrounding mitochondria (Palmer et al., 2011), which can facilitate mitochondrial membrane constriction. The mechanism by which the inner membrane undergoes fission is less well understood. Whether Drp1 mediated constriction of outer membrane alone is sufficient to drive inner membrane scission remains unclear.

As mitochondria are double membrane organelles, fusion occurs sequentially: fusion of the outer membrane is followed by that of the inner membrane. Mitochondrial fusion is controlled by mitofusins (Mfn1 and Mfn2) and optic atrophy1 (OPA1) (Figure 1.7). The Mfn1 and Mfn2 orchestrate fusion of the outer membrane and are required for the maintenance of a tubular mitochondrial network in cells (Mishra and Chan, 2014). OPA1, anchored in inner membrane, mediates inner membrane fusion. Knockdown of OPA1 could prevent mitochondrial fusion even with intact Mfn protein in the outer membrane (Cipolat et al., 2004). Thus, complete mitochondrial fusion requires both outer and inner membrane fusion.

Mitochondrial morphology is dynamic and sensitive to metabolic alterations (Benard et al., 2007). The balance of fusion and fission can be tipped in either direction by changes in nutrient availability, causing mitochondria to become fragmented or hyper-fused. For example, excess of glucose causes mitochondrial fragmentation and increased ROS production in a Drp1-dependent fashion (Yu et al., 2006), while in response to glucose withdrawal, Mfn1 deacetylation promotes mitochondrial fusion to prevent excess ROS production (Lee et al., 2014). Besides, in patients with T2D, Mfn2 transcript levels are lowered, indicating that nutrient status can regulate mitochondrial dynamics *in vivo* (Bach et al., 2005). Mitochondrial dynamics can regulate metabolism. For example, ablation of OPA1 causes mitochondrial fragmentation and death of pancreatic β-cells, which impairs insulin secretion and systemic glucose homeostasis (Zhang et al., 2011b). Deletion of Mfn2 in pro-opiomelanocortin (POMC) neurons causes severe obesity (Schneeberger et al., 2013).
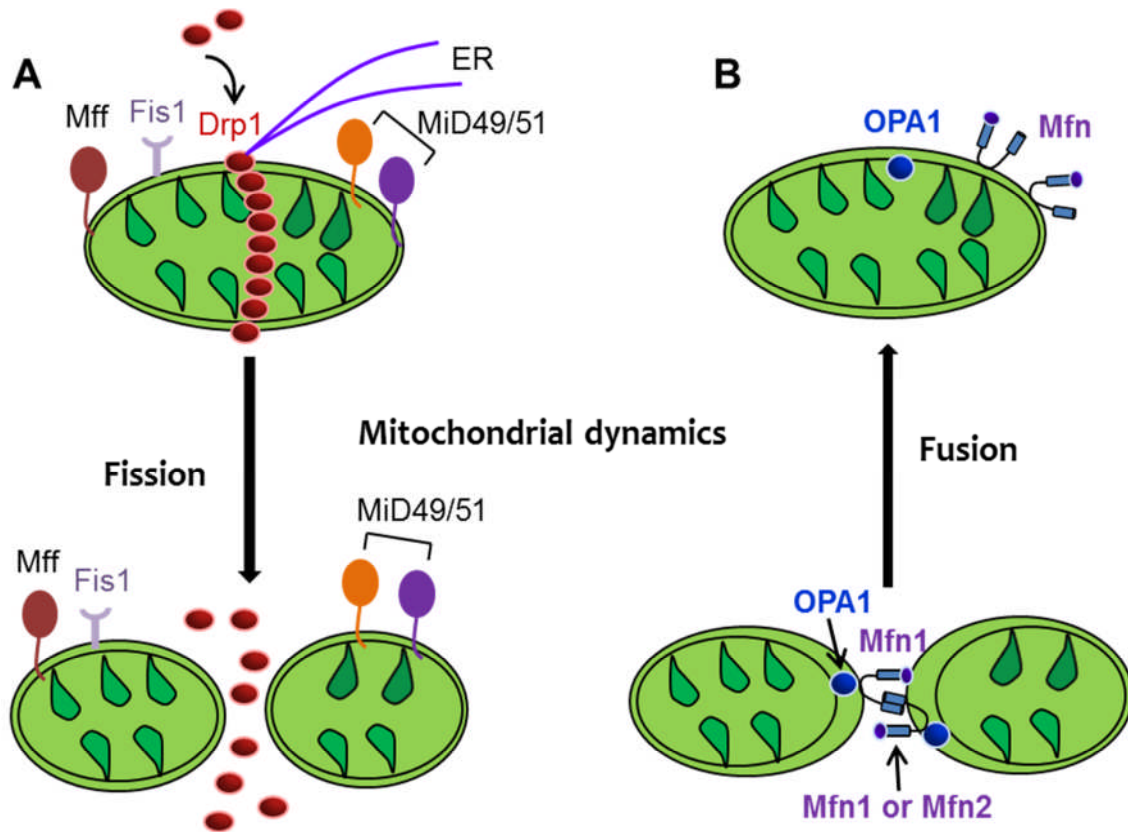
Figure 1. 7 Mitochondrial fusion and fission machinery (**A**) Fission machinery. Fis1 (**light purple block arc**), Mff (**red oval**) and MiD49/51 (**orange and dark purple oval**) are localized uniformly to the mitochondrial membrane, whereas Drp1 (**red oval**) is localized to the cytosol as well as mitochondria. In response to a stimulus such as stress, Drp1 is recruited to constriction sites pre-constricted by ER (**purple curve**) that leads to mitochondrial fission. (**B**) Fusion mechanism. Mfn is a mitochondrial outer membrane protein with a cytosolic GTPase domain (**purple oval**) and two coiled coil regions (**light blue magnetic disk**). The C-terminal coiled coil mediates oligomerization (homo- and heterotypic) between Mfn molecules on adjacent mitochondria. OPA1 (**blue oval**) is a GTPase in the intermembrane space. Mfns and OPA1 coordinate mitochondrial fusion. Figure redrawn from (Mandemakers et al., 2007).

1. 6. 2 Regulation of mitochondrial morphology by Ca^{2+} and Zn^{2+}

As an essential intracellular second messenger, Ca^{2+} homeostasis is closely related to mitochondria dynamics. Extensive studies have demonstrated that disrupted Ca^{2+} homeostasis leads to mitochondrial fragmentation (Jeyaraju et al., 2009; Kaddour-Djebbar et al., 2010; Rintoul et al., 2003). Though a role for cytosolic Ca^{2+} elevation in triggering mitochondrial fission has been observed (Duncan et al., 1980), recent studies have indicated that excessive mitochondrial Ca^{2+} uptake is more important for mitochondrial fragmentation compared to the global Ca^{2+} increase (Hajnóczky et al., 2006; Rapizzi et al., 2002). For example, when endothelial cells are exposed hyperglycaemic conditions, mitochondrial Ca^{2+} overload and mitochondrial fragmentation occurs (Paltauf-Doburzynska et al., 2004). Further studies indicated that Ca^{2+} induced mitochondrial fragmentation is dependent on Ca^{2+} induced mPTP opening (Vander Heiden et al., 1997) as inhibition of mPTP by cyclosporine A, an agent that desensitizes the PTP opening, could prevent Ca^{2+} induced mitochondrial fragmentation (Cereghetti et al., 2010). Activation of mPTP can result in swelling of mitochondrial matrix and release of the apoptogenic proteins from the intermembrane space (Kokoszka et al., 2004). Mitochondrial protein, 18kDa (MTP18) is an intermembrane space protein anchored to the IMM. Overexpression of MTP18 has been shown to induce mitochondrial fragmentation, suggesting a role for MTP18 in maintaining the integrity of mitochondrial structure (Tondera et al., 2005). MTP18 is also a downstream effector of Ca^{2+}-mediated signalling pathways, such as PI-3K (Danciu et al., 2003; Tondera et al., 2004). Thus, MTP18 could regulate mitochondrial dynamics in response to changes in mitochondrial Ca^{2+} uptake.

There are two sources of Ca^{2+} for mitochondrial uptake: cytosolic Ca^{2+} and intracellular organelle Ca^{2+}. Crosstalk between ER and mitochondria during Ca^{2+}-mediated mitochondrial fission has been reported (Breckenridge et al., 2003; Rizzuto et al., 2009; Romagnoli et al., 2007). As the most important intracellular Ca^{2+} store, ER plays a crucial role in regulating mitochondrial Ca^{2+} level, thereby affecting mitochondrial morphology (Breckenridge et al., 2003). The authors of this study showed that Ca^{2+} release from ER is accompanied by the uptake of Ca^{2+} into mitochondria, recruitment of Drp1 and mitochondrial fragmentation in epithelial and lung carcinoma cancer cells. However, so far, the crosstalk between other organelles and mitochondria has not been reported. Apart from the ER, some acidic organelles, such as lysosomes, have been suggested to serve as intracellular Ca^{2+} stores (Haller et al., 1996; McGuinness et al., 2007). Lysosomes are generally responsible for degradation and recycling of cellular waste (Settembre et al., 2013), however, under certain conditions, lysosomes can contribute to cellular Ca^{2+} signals. For example, it has been

shown that neutralisation of lysosomes can induce Ca^{2+} release from lysosomes to cytosol, thereby increasing intracellular Ca^{2+} level (Christensen et al., 2002). Besides, the crosstalk between ER and lysosomes in regulating intracellular Ca^{2+} signal has been demonstrated (López-Sanjurjo et al., 2013). However, mitochondrial Ca^{2+} uptake from lysosomes has not been demonstrated so far. In mammalian cells, very little Zn^{2+} exists in free form in the cytosol. It is stored in at least three pools. First, Zn^{2+} binds tightly to metalloproteins as a structural component. Second, Zn^{2+} is bound to metallothioneins. Third, Zn^{2+} can accumulate in the lumen of cytoplasmic vesicles, secretory granules and intracellular organelles (Kambe et al., 2004). Lysosome is one of these organelles that accumulate Zn^{2+} (Kukic et al., 2014). Cytosolic Zn^{2+} homeostasis is regulated by Zn^{2+} transporters, including two families: ZnT and IRT-like protein (ZIP) (Kambe et al., 2004). It has been demonstrated that Zn^{2+} can be transported from cytosol to lysosomes by ZnT2 and ZnT4, thereby leading to accumulation of Zn^{2+} in lysosomes (Falcón-Pérez and Dell'Angelica, 2007; McCormick and Kelleher, 2012). Zn^{2+} dys-homeostasis has been demonstrated to induce mitochondrial fragmentation (Park et al., 2014). The authors of this study reported that a Parkinson's disease-associated human ATPase (ATP13A2) mutant located in the lysosomal membrane results in Zn^{2+} dys-homeostasis, thereby leading to mitochondrial dysfunction. 3-isobutyl-1-methylxanthine (IBMX), which can prevent Drp1 accumulation in mitochondria, rescued the Zn^{2+} induced mitochondrial fragmentation, implying the role of Drp1 in Zn^{2+} induced mitochondrial fragmentation. However, the relationship between Zn^{2+} and Drp1 is unclear.

1. 6. 3 Mitochondrial membrane potential (ΔΨm)

The reducing equivalents (NADH and FADH2) that are produced from the TCA cycle are re-oxidized via a process that involves transfer of electrons through the electron transport chain (ETC) and translocation of protons across the mitochondrial inner membrane, creating an electrochemical gradient termed ΔΨm. ΔΨm is critical for maintaining the physiological function of the respiratory chain, that is to generate ATP. The ΔΨm value needs to be maintained in an appropriate range. Low ΔΨm impairs the ATP production while high ΔΨm could generate significant amount of ROS (Finkel, 2012). Therefore, both reduction of ΔΨm or increase of ΔΨm can result in mitochondrial dysfunction, release of apoptogenic factors, and cell death (Ly et al., 2003). The involvement of ΔΨm in cytochrome *c* release has been demonstrated in a number of apoptotic systems (De Giorgi et al., 2002), including in palmitate induced β cell apoptosis (Peng et al., 2012).Dissipation of ΔΨm also precedes cytokine-induced apoptosis (Barbu et al., 2002).

A relationship between mitochondrial morphology and ΔΨm has been reported. Mitochondrial fission generally produces two uneven daughter organelles, one with higher

ΔΨm and another with lower ΔΨm. It has been shown that the daughter mitochondria with low ΔΨm have reduced level of OPA1 and re-fusion activity (Westermann, 2012), indicating the essential role of ΔΨm in mitochondrial dynamics. There is evidence that mitochondrial fusion is strongly inhibited by dissipation of ΔΨm (Ishihara et al., 2003; Legros et al., 2002) and the reduced mitochondrial fusion could lead to cell death (Westermann, 2010). Therefore, ΔΨm and mitochondrial dynamics, play an important role in cell death.

1. 6. 4 Regulation of ΔΨm by Ca^{2+} and Zn^{2+}

It has been reported that elevated mitochondrial Ca^{2+} uptake could induce loss of ΔΨm which is accompanied by ROS production in mitochondria (Baumgartner et al., 2009). Sudden Ca^{2+} increase induces a transient decrease in ΔΨm in isolated mitochondria (Brustovetsky and Dubinsky, 2000). Further studies indicated that dissipation of ΔΨm is dependent on Ca^{2+}-induced mPTP opening (Basso et al., 2005; Starkov et al., 2004). However, there are other studies that suggest that Ca^{2+} signalling does not affect ΔΨm (Chalmers and McCarron, 2008; Collins et al., 2001). For example, in muscle cells, Ca^{2+} oscillations failed to induce ΔΨm change (Chalmers and McCarron, 2008). Therefore, the impact of Ca^{2+} signals on ΔΨm could depend on the cell type and the characteristics of the Ca^{2+} signal.

A role for Zn^{2+} in mPTP opening (Jiang et al., 2001) and loss of ΔΨm (Sensi et al., 2003) has also been reported. However, the underlying molecular mechanism is unclear.

1. 6. 5 Mitochondria and intrinsic apoptosis pathway

Multicellular organisms have evolved a self-demise mechanism to remove damaged, infected and unwanted cells. This programmed cell death is called apoptosis. It is characterized by shrinkage of the cell, chromatin condensation and nuclear fragmentation (Ly et al., 2003). A critical part of apoptosis is the activation of caspases that cleave many cellular substrates to result in cell suicide (Earnshaw et al., 1999). Caspases exists as inactive proenzymes and are divided into two groups: initiator caspases and effector caspases (Salvesen and Riedl, 2008). The initiator caspases include caspases 2, 8, 9 and 10 that can activate effector caspases. The effector caspases, such as caspase 3, 6 and 7 can cleave other protein substrates to elicit apoptosis (Lakhani et al., 2006; McIlwain et al., 2013). There are two major apoptotic pathways: intrinsic and extrinsic pathways (Figure 1. 8). Both pathways converge on the activation of effector caspase cascade (Elmore, 2007).The intrinsic pathway is also called the mitochondria pathway in which mitochondria are the central decision makers. Mitochondria are not only the site where the anti-apoptotic and pro-apoptotic proteins interact and determine the cell fate, but also the site where signals

initiating the caspases activation, such as cytochrome *c*, are generated (Wang and Youle, 2009). Cytochrome *c* is an essential component of the ETC, but also plays essential roles in apoptosis (Hüttemann et al., 2012). Under apoptotic stimuli, such as excessive ROS (Atlante et al., 2000), cytochrome *c* is released from IMM and then forms a complex with Apoptotic Peptidase Activating Factor 1 (Apaf-1) which then binds pro-caspase 9 to form a protein complex known as apoptosome. The apoptosome then cleaves pro-caspase 9 to active form, caspase 9, that in turn activates caspase 3 to induce apoptosis (Bao and Shi, 2007). Intact mitochondrial structure and function is essential for cells to survive while disruption of mitochondrial network by excessive mitochondrial fission or impaired fusion is a common feature of apoptosis (Arnoult, 2007; Karbowski and Youle, 2003; Knott et al., 2008). For example, alteration of mitochondrial structure caused by depletion of OPA1 is associated with the release of cytochrome *c* into the cytosol and subsequent induction of apoptotic cell death (Olichon et al., 2003). Inhibition of mitochondrial fragmentation by dominant-negative Drp1 mutant could prevent stimuli-induced nuclear DNA fragmentation as well as the decrease of $\Delta\Psi m$, suggesting a close relationship between mitochondrial structure and $\Delta\Psi m$ (Landes et al., 2010). Bax is an important pro-apoptotic protein in apoptotic pathway (Wei et al., 2001). Studies have revealed that Bax can translocate to the OMM from cytosol upon induction of apoptosis (Rahman et al., 2000; Wolter et al., 1997) and concentrate to the sub-mitochondrial punctate foci (Nechushtan et al., 2001) associated with mitochondrial fragmentation (Capano and Crompton, 2002; Karbowski et al., 2002). Besides, overexpression of Bax induces mitochondrial fragmentation (Ashktorab et al., 2004).

The loss of $\Delta\Psi m$ is also an essential marker for apoptosis. Apoptosis-inducing factor (AIF) is a pro-apoptotic protease located in the mitochondrial intermembrane space. Upon induction of apoptosis, AIF is released to the cytosol and translocate to the nucleus to induce chromatin condensation (Susin et al., 1999). A number of studies have correlated AIF translocation with $\Delta\Psi m$ alteration (Jeong et al., 2011; Pardo et al., 2001). For example, in SH-SY5Y cells, oxygen and glucose deprivation (OGD) induced loss of $\Delta\Psi m$ is accompanied with AIF translocation and subsequent apoptosis (Zhang et al., 2011a). However, the molecular mechanism by which dissipation of $\Delta\Psi m$ causes AIF release is less clear.

1. 6. 6 Role of Ca^{2+} and Zn^{2+} in intrinsic apoptosis

Studies have shown that Ca^{2+} plays a pivotal role in mitochondrial apoptosis pathway. It has been demonstrated that Ca^{2+} release from the ER can induce a marked release of cytochrome *c* from IMM and thereby increase apoptosis (Szalai et al., 1999). Furthermore, remodelling of mitochondrial cristae has been implicated in apoptosis which is dependent on

Ca^{2+}-induced mPTP opening (Webster, 2012). Calpain is a Ca^{2+}-dependent cysteine protease. It has two isoforms: μ-calpain and m-calpain, which differ in terms of their Ca^{2+} requirements. Calpain has been shown to activate tBid (Mandic et al., 2002), a pro-apoptotic protein which induces cytochrome c release (Korsmeyer et al., 2000). In addition to calpain, overexpression of calcineurin, a Ca^{2+}-dependent protein phosphatase, has been demonstrated to potentiate procaspase-3 activation in HEK293 cells (Saeki et al., 2007).

Zn^{2+} overload can lead to irreversible inactivation of matrix enzymes in mitochondrial respiration (Gazaryan et al., 2007). Moreover, Zn^{2+} can induce mPTP opening and subsequent cytochrome c release (Bossy-Wetzel et al., 2004; Jiang et al., 2001). A recent study has demonstrated that cytosolic Zn^{2+} level is progressively increased in hippocampal slices during oxygen glucose deprivation (OGD). Rise in cytosolic Zn^{2+} was rapidly followed by the uptake of Zn^{2+} into mitochondria, which then led to depolarization of mitochondrial membrane and cell death. Removal of Zn^{2+} with chelators facilitated the recovery of ΔΨm and tolerance to OGD (Medvedeva et al., 2009).

1. 6. 7 Extrinsic apoptosis pathway

The extrinsic apoptosis pathway is activated from the outside of the cell by pro-apoptotic ligands that interact with specialized cell surface death receptors (Elmore, 2007). Upon activation by certain ligands, such as tumor necrosis factor-related apoptosis-inducing ligand (TRAIL), receptors can form the death-inducing signalling complex (DISC) by recruiting the adaptor Fas-associated death domain (FADD) and procaspases 8 and 10, leading to activation of these initiator caspases. Activation of caspases 8 and 10 leads to activation of executioner caspases 3, 6 and 7, which ultimately cause apoptosis (Figure 1. 8). Although mitochondria are less important for extrinsic apoptosis compared to intrinsic pathway, a role of mitochondria-mediated intrinsic pathway in amplifying extrinsic apoptosis has been suggested (Degli Esposti et al., 2001; Kuwana et al., 1998). For example, in a cell with low level of DISC formation, the intrinsic pathway can be recruited by caspase 8. Upon activation, caspase 8 can activate tBid which then translocate to mitochondria and induce cytochrome c release to amplify extrinsic apoptosis (Li et al., 1998). Moreover, it has been shown that activation of cell surface death receptors can cause Ca^{2+} release from ER and lead to Drp1-mediated mitochondrial fission, thereby leading to cytochrome c release and apoptosis (Breckenridge et al., 2003). These studies provide evidence for the crosstalk between intrinsic and extrinsic apoptotic pathway.

1. 6. 8 Role of Ca^{2+} in extrinsic apoptosis

Although Ca^{2+} plays a critical role in the intrinsic apoptosis, it has been demonstrated that Ca^{2+} could induce mitochondria-independent apoptosis through calpain (NakagawaT, 2000). The authors of this study reported that activation of calpain by Ca^{2+} activates caspase 12 and the subsequent caspase 3 activation. Caspase 12, predominantly localized to the ER, has been shown to mediate an ER-specific apoptosis pathway independently of mitochondria (Nakagawa et al., 2000). This pathway allows execution of apoptosis to proceed without recruitment of mitochondria.
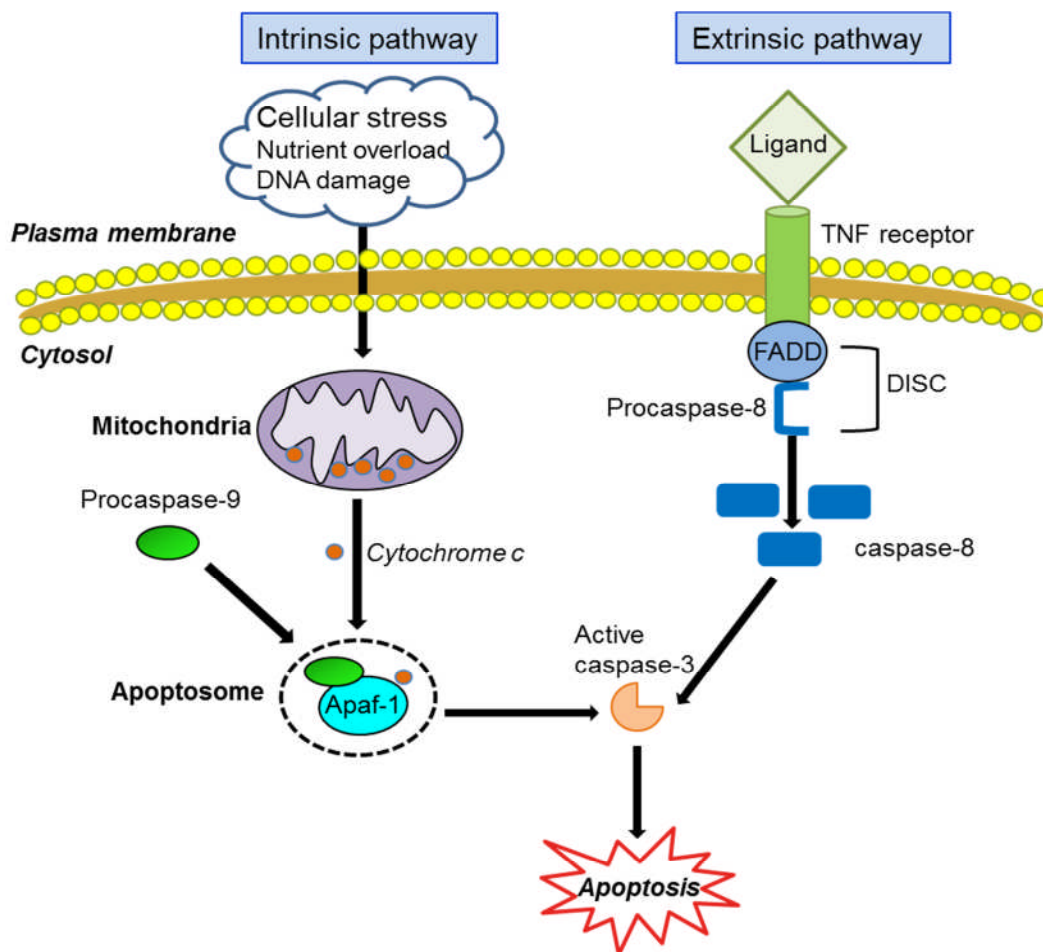
Figure 1. 8 Schematic representation of the main molecular pathways leading to apoptosis In the intrinsic pathway, in response to cellular stresses, such as nutrient overload and DNA damage, cytochrome *c* (**orange**) is released from the mitochondria leading to the formation of the apoptosome (dashed black oval) and activation of caspase 9. In the extrinsic pathway, upon ligand binding to specific receptors, such as TNF receptor, the DISC complex is formed and caspase 8 (**blue rounded rectangle**) is activated. Both Caspase 9 and 8 then activate downstream caspases such as caspase 3 leading to apoptosis. Figure redrawn from (Favaloro et al., 2012).

1. 7 Cell migration

As mentioned above, cancer cell migration and invasion into adjacent tissues and intravasation into circulation is a critical step in cancer metastasis (Friedl and Wolf, 2003; Reymond et al., 2013). Previous *in vitro* and *in vivo* observations have shown that tumour cells infiltrate neighbouring tissues via diverse mechanisms. They can disseminate from primary tumours as individual cells, referred to as 'single cell migration' or spread as groups, called 'collective cell migration' (Friedl and Wolf, 2003). In many tumours, both single cell migration and collective migration are simultaneously present while epithelial tumours commonly use collective migration mechanisms; examples include prostate cancer (Cui and Yamada, 2013) and breast cancer (Friedl and Gilmour, 2009). In principle, the lower the differentiation stage, the more likely the tumour is to disseminate via individual cells (Thiery, 2002). To migrate, the cell body must modify its shape to adjust with the surrounding environment. Cell migration results from a continuous cycle of interdependent steps: polarization of migrating cells, formation of leading edge and protrusions, assembly of new focal adhesions, contraction of cell body and disassembly of focal adhesions at the rear of migrating cells (Sheetz et al., 1998). Studies have shown that certain cytokines and growth factors contribute to cancer migration by affecting distinct steps. For example, autocrine motility factor (AMF) is a tumour-secreted cytokine that can induce melanoma cell migration by regulating protrusion formation (Tsutsumi et al., 2002); insulin-like growth factor-1 (IGF1) can induce breast cancer cell migration through regulation of focal complex dynamics (Guvakova and Surmacz, 1999). Since regulation of cancer cell migration is complex and involves a large number of molecules, a better understanding of how individual steps in cell migration are regulated is required.

1. 7. 1 ROS in cell migration

EGF is a chemo-attractant that mediate migration of breast cancer and cervical cancer (Chen et al., 2011; Wang et al., 2004). Studies have reported that EGF induced cancer cell migration is dependent on ROS production (Binker et al., 2009; Cho et al., 2014). ROS can regulate MMP expression, thereby affecting cancer cell migration (Zhang et al., 2002). Adhesions are dynamic structures that must be assembled at the leading edge and disassembled at the cell rear for efficient migration. The effects of ROS on focal adhesion dynamics have been described in numerous studies (Chiarugi and Fiaschi, 2007; Mahdi et al., 2000). For instance, ROS can induce tyrosine phosphorylation of focal adhesion kinases (FAK) (Mahdi et al., 2000) thereby inducing focal adhesion formation (Chiarugi et al., 2003). In addition to focal adhesions, several reports have implicated ROS in cytoskeleton

remodelling in carcinoma cells (Diaz et al., 2009; Kim et al., 2009b). For example, NOX-mediated ROS generation has been shown to be necessary for the formation of invadopodia that are required for cancer cell invasion (Diaz et al., 2009); Direct H_2O_2 application induces disruption of actin cytoskeleton in L929 fibrosacoma cells (Préville et al., 1998). In summary, regulation of cell migration by ROS is attributed to the effects on different aspects, not a single stage in moving cells.

1. 7. 2 Role of Ca^{2+}, Zn^{2+} and TRP channels in cell migration

Ca^{2+} signalling is important for cell migration but the effects on cell migration are dependent on microenvironments and physiology of different cells. For example, in breast cancer cells, Ca^{2+} elevation increases turnover of focal adhesions, thereby inducing cell migration (Yang et al., 2009a), while in prostate cancer cells, Ca^{2+} elevation decreases cell migration by inactivating FAK (Yang et al., 2009b). Besides, recent studies demonstrated that Ca^{2+} gradient is more important for cell migration compared to global Ca^{2+} increase (Fabian et al., 2008; Tsai et al., 2014). In renal epithelial cells, Ca^{2+} gradient appears to mediate polarity formation and cell migration as increase of global Ca^{2+} by Ca^{2+} ionophore failed to induce cell migration (Fabian et al., 2008). Nevertheless, it is still unclear whether cancer cells develop a Ca^{2+} gradient to mediate cell migration.

Zn^{2+} also plays an important role in cell migration (Jin et al., 2015; Kagara et al., 2007). For example, it has been demonstrated that Zn^{2+} and its transporter mediates breast cancer cell invasion (Kagara et al., 2007). Consistent with a role for Zn^{2+} in cancer, elevated concentrations of Zn^{2+} have been observed in numerous cancers such as liver carcinomas (Costello et al., 2004). However, the function of the elevated Zn^{2+} in tumour progression is poorly understood.

As TRP channels are important Ca^{2+}-entry pathways, the role of several TRP channels in cell migration has been demonstrated. According to a recent study (Pla et al., 2011), TRPV4 expression is significantly up-regulated in human breast cancer endothelial cells compared to that of normal endothelial cells. Activation of TRPV4 mediates Ca^{2+} entry and induces carcinoma endothelial cell migration, but not normal endothelial cells. Besides, the authors of the study observed that actin remodelling occurs upon TRPV4 activation. TRPM7 mediated Ca^{2+} flickers in migrating fibroblast cells have also been demonstrated (Wei et al., 2009). TPRC5 and TRPC6 are also involved in cell migration (Tian et al., 2010). By mediating Ca^{2+} entry into fibroblasts, TRPC5 induces Rac1 activation and TRPC6 induces RhoA activation. Rac1 promotes cell migration whereas RhoA has an opposite effect. Thus, there is antagonistic regulation of cell motility by TRPC5 and TRPC6 channels. In addition to Ca^{2+}, some TRP channels associated with cell migration are also permeable to Zn^{2+}; these include

TRPM7, TRPC6 and TRPM2 (Nilius and Szallasi, 2014). Whether Zn^{2+} plays a role in cell migration mediated by these TRP channels is yet to be investigated.

1. 7. 3 Actin remodelling and focal adhesion dynamics in cell migration

Cell migration requires cyclical changes in actin cytoskeleton and focal adhesions. During cell migration, actin protrusions are formed at the leading edge: filopodia are responsible for sensing extracellular signals and lamellipodia allow the cells to migrate forward and form new focal adhesions. At the rear of migrating cells, stress fibres mediate focal adhesion disassembly and consequent rear release. Continuous remodelling of actin cytoskeleton and focal adhesions is required for directional cells migration (Figure 1.9). The characteristics and regulation of actin remodelling and focal adhesion dynamics will be discussed below.
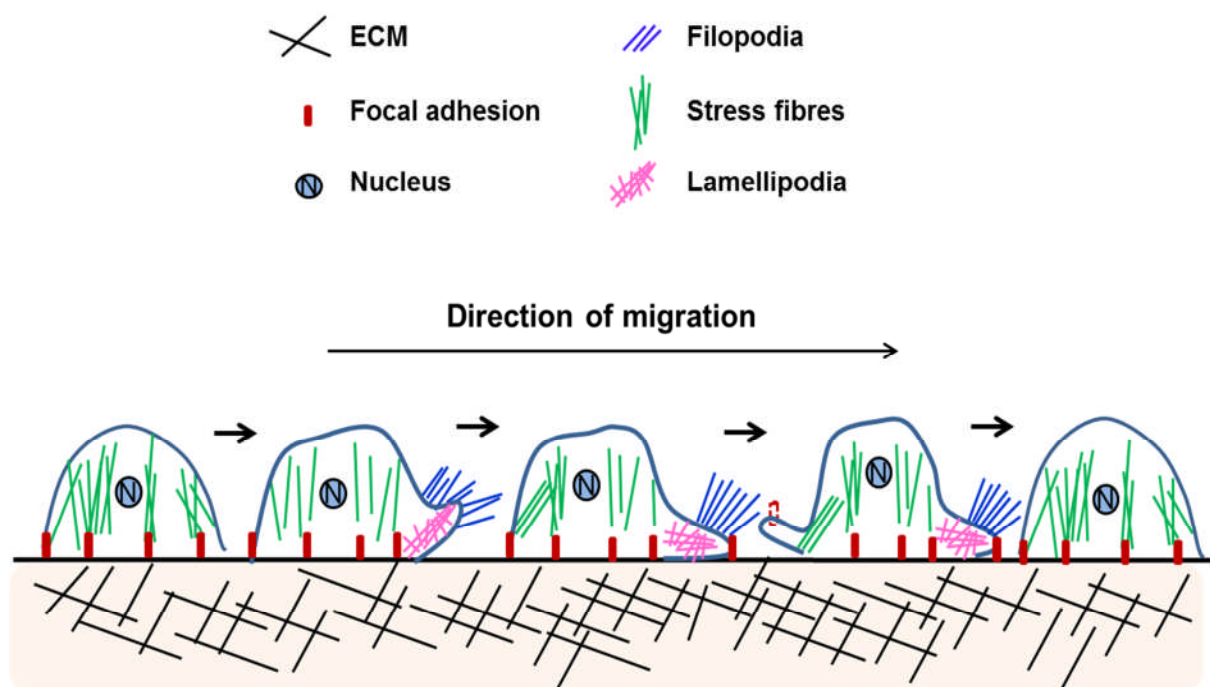
Figure 1. 9 Schematic representation of cell migration Cell migration can be divided in 4 steps along the direction of migration. (i) filopodia and lamellipodia are formed at the leading edge of migrating cells to sense the motile stimuli and induce cellular extension respectively; (ii) lamellipodia mediate new focal adhesion formation at the leading edge; (iii) stress fibres mediate focal adhesion disassembly and rear release allowing forward progression; (iv) recycling of the actin cytoskeleton and focal adhesion remodelling.

1. 8 Actin remodelling

The cytoskeleton helps cells maintain cell shape and internal organization. It is composed of three major filament systems: F-actin microfilaments, microtubules and intermediate filaments. Of these three structures, the actin cytoskeleton has been well studied during the last several decades. Actin cytoskeleton is a highly dynamic structure and undergoes assembly and disassembly constantly by a process termed as actin remodelling. Actin remodelling plays an important role in cell migration, macrophage phagocytosis, lipoprotein degradation and protein trafficking (Hölttä-Vuori et al., 2012; Johnson et al., 2012; Sander et al., 1999; Yokoyama et al., 2011). Thus, the regulation of actin remodelling is essential for maintaining multiple cellular functions.

1. 8. 1 Actin polymerization and de-polymerization

Actin remodelling involves actin polymerisation and depolymerisation (Figure 1. 10). During actin polymerisation, G-actin, which is an Mg^{2+}/ATP-bound subunit, is assembled into the growing filaments at the positive (+) end. There are three main promoters contributing to this process which comprise formin families, Ena/VASP and 54rofiling families. However, in contrast to formin and 54rofiling which directly bind to G-actin and then push G-actin to the extending filaments, the Ena/VASP exerts its function by keeping the positive end out of inhibitory cap-proteins (Defilippi et al., 1999; Huber et al., 2003; Pollard and Borisy, 2003). Proteins from the WASP-ARP2/3 family promote generation of F-actin branches. These branches subsequently generate mesh works which are important for lamellipodia formation. Actin de-polymerization involves shedding of G-actin from the existing fibres. Proteins of the cofilin family could sever filaments and promote G-actin dissociation from the negative (-) ends. It has been shown that calcium influx regulates functions of actin-regulating proteins, such as 54rofiling and cofilin in conjunction with PI-3K and inositol phosphates (Rousseau et al., 2000). PI-3K lies downstream of RhoA which is a main regulator of stress fibre formation.

1. 8. 2 Stress fibres, filopodia, lamellipodia and relevant Rho GTPases

By rapidly switching between actin polymerization and de-polymerization, actin cytoskeleton could form three different structures: stress fibres, filopodia and lamellipodia (Figure 1. 9). Formation of these three types of actin is regulated by RhoA, Cdc42 and Rac which belong to the Rho GTPase family (Nobes and Hall, 1995). Stress fibres are long actin filaments spanning across the whole cell. Formation of stress fibres is mediated by RhoA. Filopodia are spike-like membrane projections arranged into tight bundles which are mainly regulated by Cdc42. Lamellipodia are brush-like cytoplasmic protrusions in the proximity of the plasma

membrane which is regulated by Rac. Lamellipodia contributes to focal contact point formation. All these three structures are crucial to the actin-based cell motility.
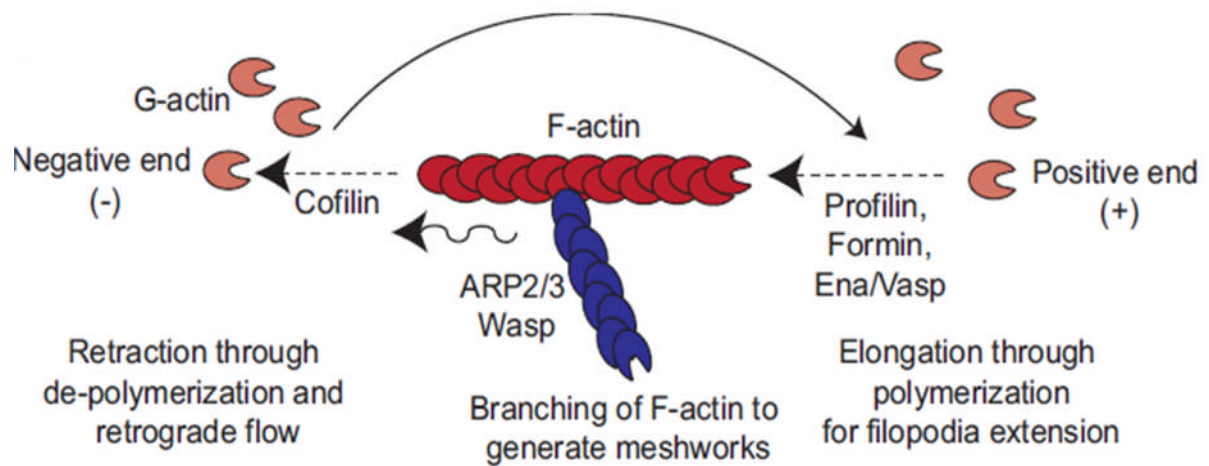
Figure 1. 10 Schematic representation of regulation of actin assembly and disassembly F-actin fibres are elongated at their positive end by proteins of the 55rofiling, Ena/VASP, and formin families, which promote polymerization of G-actin into long F-actin strings. At the negative end of the actin-filament, cofilin depolymerizes and shortens the actin string. Branching of F-actin filaments is mediated by ARP2/3 complex and WASP family. Figure reproduced from (De Smet et al., 2009).

1. 8. 3 Role of Ca^{2+} and TRP channels in actin remodelling

The regulation of actin filaments by Ca^{2+} has been extensively studied. It has been shown that Ca^{2+} oscillation induces cortical actin oscillations that in turn efficiently regulate exocytosis in mast cells (Wollman and Meyer, 2012). In this study, the authors demonstrated that Ca^{2+} induces cortical actin change by recruiting N-WASP. In primary neurons, Ca^{2+} influx could induce 56rofiling targeting to dendritic spines thereby stabilizing the actin structures (Ackermann and Matus, 2003). The authors of this study demonstrated that the effect of 56rofiling on actin is dependent on the interaction with VASP/MENA family. It was suggested that Ca^{2+} can affect actin cytoskeleton through activating various actin regulatory proteins (Oertner and Matus, 2005). TRP channels have been reported to regulate actin remodelling by mediating Ca^{2+} influx. For instance, Ca^{2+} influx through TRPC1 activates the phosphatase calcineurin, which relays the signal to Slingshot (Wen et al., 2007). Slingshot dephosphorylates cofilin, which thereby promotes actin filament severing (Huang et al., 2006). TRPM7 has also been shown to promote cytoskeletal remodelling by inducing phosphorylation of myosin II heavy chains. However, the authors suggested that these cytoskeletal effects were largely TRPM7 associated kinase dependent, as a catalytically inactive mutant of TRPM7 maintained normal channel function but failed to induce actin remodelling. Since the interaction between the kinase and its substrate is facilitated by Ca^{2+} influx (Clark et al., 2006), it remains unclear whether channel activity is completely dispensable. A recent study indicated that TRPC5 and TRPC6 regulate different actin types by mediating Ca^{2+} influx. It was demonstrated that TRPC5-mediated Ca^{2+} induces stress fibre formation while TRPC6-mediated Ca^{2+} has an opposite effect (Tian et al., 2010). The authors suggested that different levels and durations of intracellular Ca^{2+} signals can produce different impacts on actin cytoskeleton.

1. 8. 4 Role of filopodia in cellular function

Filopodia are finger-like protrusions generally protruding from the lamellipodial actin network (Lewis and Bridgman, 1992). Filopodia are described as 'antennae' that are used to probe the extracellular signals from the environment (Mattila and Lappalainen, 2008). In addition, filopodia have been implicated in other cellular processes, such as cell-cell adhesions (Arjonen et al., 2011) and neuron growth (Chien et al., 1993). However, the role of filopodia in directional cell migration (Jones, 2000) is perhaps the best characterized.

1. 8. 4. 1 Probing the extracellular signal

Filopodia are closely linked to the directional cell migration because filopodia are responsible to sense extracellular signals, such as chemo-attractants (Ridley et al., 2003). Filopodia

contain receptors for diverse signalling pathways, therefore, they act as sites for signal transduction. A number of studies have demonstrated that invasive cancer cells are enriched in filopodia (Machesky, 2008; Vignjevic et al., 2007). In addition to the role in cell migration, filopodia formation also plays an essential role in immune cell phagocytosis. Macrophages form filopodia to bind to pathogen and then pull the bound pathogen towards the macrophage cell body. Therefore, inhibition of filopodia formation reduces the rate of phagocytosis (Niedergang and Chavrier, 2004; Vonna et al., 2007).

1. 8. 4. 2 Cell-cell adhesion

Filopodia are also central to the proper alignment and attachment of cells during embryonic development. In a sheet of epithelial cells, filopodia, protruding from the opposing cells, help the cells to align and adhere to each other (Jacinto et al., 2000). This function is also essential in wound healing. During wound healing, studies have shown that filopodia operate as "knitting" to help the epithelial cells form adhesion at the end of repair (Abreu-Blanco et al., 2012; Redd et al., 2004).

1. 8. 4. 3 Filopodia in neuron

Filopodia in neurons help the growth cones to navigate their environments and sense cues as to the direction of migration and destination (Gallo and Letourneau, 2004). Growth cone filopodia orient toward a gradient of guidance cues, an event that precedes the extension (Dent et al., 2007), turning, or branching of the growth cone–tipped neurite toward chemo-attractants (Zheng et al., 1996). Furthermore, it has been shown that filopodia that protrude from the lengths of the dendrites might be the initiating events in the formation of post-synaptic structures, which specialize in conveying responsiveness to neurotransmitter release (Cingolani and Goda, 2008; Jontes et al., 2000).

1. 8. 5 Role of small Rho GTPases in filopodia formation

Members of the Rho family of GTPases function as molecular switches by cycling between an inactive (GDP-bound) and active (GTP-bound) state. Cycling is controlled by a large group of guanine-nucleotide-exchange factors (GEFs), which catalyse the exchange of GDP for GTP, and by GTPase-activating proteins (GAPs), which promote the hydrolysis of GTP to GDP (Bos et al., 2007). Rho GTPases regulate multiple cellular functions, such as cell polarity (Iden and Collard, 2008), vesicle trafficking (Symons and Rusk, 2003) as well as cell migration (Raftopoulou and Hall, 2004; Ridley, 2001), among which the regulation of actin cytoskeleton is a prominent one (Ridley, 2006). There are two Rho GTPases that are involved in filopodia formation: Cdc42 and Rif.

1. 8. 5. 1 Cdc42

The Rho GTPase Cdc42 is a key mediator of filopodia formation. Cdc42 interacts with multiple proteins to mediate filopodia formation. The two main pathways regulated by Cdc42 that contribute to filopodia formation are insulin-receptor substrate p53 (IRSp53) pathway and WASP-ARP2/3 pathway. Cdc42 binds and activates IRSp53 to recruit its effector MENA to the filopodia tip and protects filopodia from capping (Krugmann et al., 2001). In addition to IRSp53 signalling pathway, Cdc42 regulates WASP-ARP2/3 pathway to trigger filopodia formation. Because ARP2/3 complex binds to pre-existing actin filaments and nucleates actin polymerization, it is essential for actin filament nucleation and branch formation. Cdc42 can activate WASP family, thereby inducing activation of ARP2/3 (Rohatgi et al., 1999). Thus, by inducing ARP2/3 complex, Cdc42 regulates the formation of filopodia.

1. 8. 5. 2 RIF

More recently, another small GTPase, termed Rho in filopodia (RIF), was reported to mediate filopodia formation (Pellegrin and Mellor, 2005). Rif mediated filopodia formation pathway does not require Cdc42 activation. Besides, filopodia produced by Rif are distinct from those triggered by Cdc42. Cdc42 triggers short filopodia, generally arising from lamellipodia at the periphery of the cells (Svitkina et al., 2003). On the contrary, Rif induced filopodia are longer, generally associated with the apical surface of the cells and do not arise from lamellipodia (Pellegrin and Mellor, 2005). Further work from the same group demonstrated that Rif triggers filopodia formation through Diaphanous-related formin-2 (mDia2), which promotes nucleation and elongation of linear F-actin that are essential for filopodia formation.

1. 8. 6 Ca^{2+} and Zn^{2+} in regulation of filopodia dynamics

Ca^{2+} in regulation of filopodia dynamics has been extensively investigated. However, most of these studies focused on neurons. For example, increase in cytosolic Ca^{2+} regulates elongation of neuronal growth cone filopodia, thereby affecting the territory of growth cones (Rehder and Kater, 1992). Another study showed that local Ca^{2+} transients affect dendritic filopodia dynamics. The authors of this study found low levels of local Ca^{2+} transients facilitate filopodia outgrowth while high levels inhibit the formation of filopodia (Lohmann et al., 2005). In other cell types, Ca^{2+} can affect multiple actin-related proteins to regulate filopodia formation, such as cofilin and myosin (Taylor et al., 1989; Wang et al., 2005). Cofilin is an F-actin severing protein (Huang et al., 2006) and myosin is a main regulator of filopodia formation (Bohil et al., 2006). In prostate cancer cells, it has been shown that inhibition of Ca^{2+}/calmodulin dependent protein kinase (CaMKII) increases the frequency and length of filopodia, indirectly supporting the inhibitory role of Ca^{2+} on filopodia formation (Wang et al., 2010). So far, the effect of Zn^{2+} on filopodia formation has not been

demonstrated. As Zn^{2+} mediates diverse signalling pathways, it is possible that Zn^{2+} could affect filopodia formation. Zn^{2+}, however, has been shown to affect actin cytoskeleton. In Madin-Darby canine kidney (MDCK) cells, application of Zn^{2+} disrupts stress fibres (Mills et al., 1992). Moreover, it has been demonstrated that Zn^{2+} can induce PKC translocation from cytosol to actin cytoskeleton (Zalewski et al., 1991). Since PKC can affect actin cytoskeleton (Ren et al., 2009), Zn^{2+} might affect actin cytoskeleton through regulation of PKC activity. Further studies are required to explore the role of Zn^{2+} in actin cytoskeleton dynamics. TRPM2 channels are permeable to both Ca^{2+} and Zn^{2+} which are important actin regulators. Thus it is likely that TRPM2 channels might play a role in the dynamics of actin cytoskeleton by affecting the homeostasis of Ca^{2+} and Zn^{2+}.

1. 9 Cell adhesions

During cell migration, in addition to generating filopodia, cells also establish new cell adhesions to ECM at the leading edge. These cell adhesions are termed focal complex, focal adhesions and 3-D matrix adhesions, depending on their size, cellular localization and composition (Wozniak et al., 2004). Focal complexes are regulated by Rac and Cdc42 and are generally found at the cell periphery of migrating cells (Nobes and Hall, 1995). Focal adhesions are found both at periphery and centrally, and are associated with the end of stress fibres (Zamir and Geiger, 2001), while 3-D matrix adhesions are formed in cells adhering to 3-D fibronectin (Cukierman et al., 2001) or collagen gel (Tamariz and Grinnell, 2002; Wozniak et al., 2003). Cell adhesions not only provide a physical contact between ECM and cells, but also mediate signal transduction to trigger different cell behaviours, such as cell death, migration and cell proliferation (Caltagarone et al., 2007; Nagano et al., 2012; Provenzano and Keely, 2011). Therefore, understanding the composition and dynamics of focal adhesions will provide useful information for therapy development.

1. 9. 1 Composition of focal adhesions

Focal adhesions are composed of multiple proteins, such as scaffolding molecules, kinases and phosphatases (Figure 1. 11). The scaffolding molecules include p130Cas, paxillin and Crk. These scaffolding molecules are responsible for recruitment and activation of small GTPases for focal adhesion turnover and actin remodelling. For example, Crk phosphorylation is essential for Rac activation and subsequent enhanced cell migration (Lamorte et al., 2003). Kinases are important components of focal adhesions which include FAK and Src. These kinases can induce tyrosine phosphorylation of focal adhesion components, thereby regulating focal adhesion dynamics and cell behaviour. For example, Src activation can cause a reduction of focal adhesions by interacting with β integrin

subunits (Frame et al., 2002). Tyrosine de-phosphorylation is as important as tyrosine phosphorylation for focal adhesion dynamics, which is mediated by phosphatases. PTP-PEST is the most important phosphatases in focal adhesions. It has been shown that knockdown of PTP-PEST increases focal adhesions but decrease cell migration (Angers-Loustau et al., 1999). Thus, diverse components determine the dynamics of focal adhesions which is important for diverse cell behaviours.

1. 9. 2 Dynamics of focal adhesion in cell migration

Focal adhesion dynamics is critical for effective cell migration. Generally, in a migrating cell, assembly of focal adhesion occurs at the leading edge and disassembly happens at the rear (Webb et al., 2002). Focal adhesion formation is initiated upon the binding of adhesion receptors to ECM. Among these receptors, integrin is a major one. Activation of integrin allows functional connection between focal adhesions and actin cytoskeleton that is required for cell migration (Geiger et al., 2001). In addition to this, integrin can activate migration-related signalling molecules, such as Rac (Price et al., 1998). It has been shown that the size of focal adhesions is inversely related to migration speed. In rapidly migrating cells, few visible integrin and small adhesions are observed at the leading edge. On the other hand, cells with large integrin clusters are tightly adherent and move slowly (Ridley et al., 2003). Turnover of focal adhesions is regulated by Rho GTPases. Rac and Cdc42 are activated at the leading edge of migrating cells where they trigger protrusion formation and induce small adhesion formation, while Rho is generally activated at the rear and mediates disassembly of focal adhesions (Lamalice et al., 2007). Since activation of Rac inhibits RhoA in the lamellipodia (Hall, 1998), activated RhoA is confined to the rear of migrating cells where it induces rear detachment (Lamalice et al., 2007). By spatiotemporally regulating focal adhesion formation, cells can undergo rapid or slow migration under different conditions.

1. 9. 3 Paxillin

Paxillin is a multi-domain scaffold protein that localizes to focal adhesion complex. It is a 68-70 kDa protein that contains a number of motifs mediating protein-protein interactions. Phosphorylation of paxillin is dependent on FAK/Src complex and is essential for the interaction with Crk, one of the other adaptor proteins in FA (Schaller and Parsons, 1995). It has been shown that the interaction with Crk is necessary for the localization of paxillin to FA and for effects on cell migration (Lamorte et al., 2003). Thus, paxillin serves as a platform for the recruitment of numerous regulatory and structural proteins that together control the dynamic changes of focal adhesions and cell migration. PTP-PEST (protein tyrosine phosphatase non-receptor type 12), a phosphatase that plays an essential role in FA

turnover and cell migration, can be recruited to FA by binding to paxillin (Côté et al., 1999). Apart from the role in focal adhesions, paxillin has also been shown to interact with tubulin, where it regulates the microtubule network (Herreros et al., 2000).

1. 9. 4 Ca^{2+} and Zn^{2+} in regulation of focal adhesions

Ca^{2+} signalling is a prominent factor that regulates focal adhesions in different cell types. However, the effect seems cell type dependent. In astrocytoma cells, local Ca^{2+} increase induces FA disassembly and enhances the localisation of FAK to FA (Giannone et al., 2004). In breast cancer cells, it has been demonstrated that global Ca^{2+} increase is required for FA turnover (Yang et al., 2009a). Besides, the authors of this study demonstrated that inhibition of global Ca^{2+} influx impairs both assembly and disassembly of FAs, thereby inhibiting cell migration (Yang et al., 2009a). Other studies reported that the effect of Ca^{2+} on focal adhesions is through calpain, which is an important protease for FA turnover (Cortesio et al., 2011; Franco et al., 2004). As calpain can cleave several focal adhesion components, such as FAK (Chan et al., 2010), it affects focal adhesion turnover.

To date, the role of Zn^{2+} in focal adhesion dynamics has not been reported. Since Zn^{2+} can inhibit multiple PTPs, such as PTP-PEST, which is a major component of focal adhesions, the possibility of regulation of focal adhesion turnover by Zn^{2+} needs to be investigated.
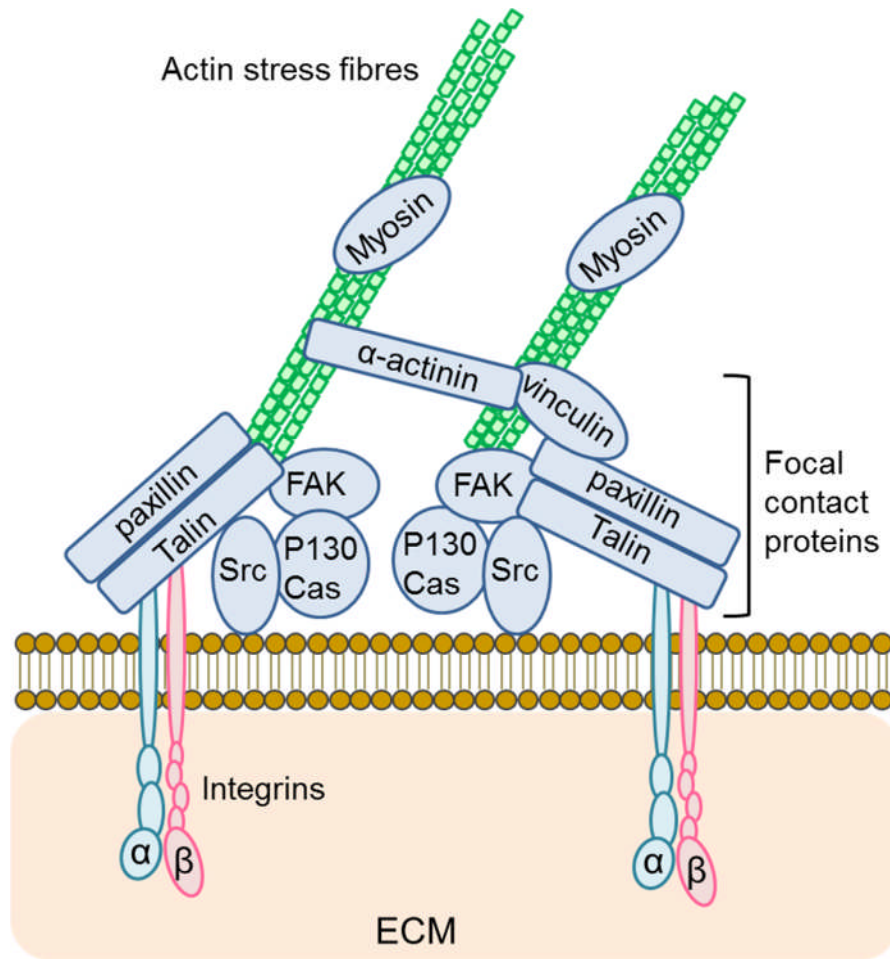
Figure 1. 11 Schematic representation of focal adhesion components The ECM, integrins (α- and β-transmembrane heterodimeric proteins) and the actin cytoskeleton interact at sites called focal contacts. Focal contacts are made up by multiple focal contact proteins. Adaptor protein paxillin recruits focal FAK and vinculin to focal contacts. A-actinin is an actin cytoskeleton protein that binds to vinculin and links actin stress fibres with focal contacts. Myosin is a component of stress fibres. Integrin clustering induces Src and adaptor protein P130Cas recruitment to focal contacts. Depending on the cell behaviour, composition of focal contacts constantly changes. Figure redrawn from (Mitra et al., 2005).

1. 10 Hypothesis and aims of the current study

The effects of hyperlipidaemia on cell death are largely mediated through an increase in oxidative stress. As a ROS-sensitive ion channel, the role of TRPM2 in FFA induced cell death is unclear. As major targets of oxidative stress in almost all cells, including β-cells, mitochondria are closely related to cell death. Besides, FFA has been demonstrated to induce disruption of the mitochondrial network. Based on these previous findings, it was hypothesised that TRPM2 channels mediate FFA-induced mitochondrial fragmentation, thereby leading the death of pancreatic β-cells. To test this hypothesis, a combination of immunofluorescence staining, flow cytometry and gene silencing techniques will be used. The overall aim of this part of the thesis was to understand the role of the ROS-sensitive TRPM2 channel, and the ions it conducts (viz. Ca^{2+} and Zn^{2+}), on mitochondrial dynamics and the death of pancreatic β-cells.

As an important mitogenic signal, H_2O_2 has been demonstrated to induce cell migration; however, the underlying mechanism is not fully understood. H_2O_2 is known to affect Ca^{2+} signalling, which is associated with cell migration through spatial and temporal regulation of the actin cytoskeleton and focal adhesions. Since TRPM2 channels are robustly activated by H_2O_2 and affect Ca^{2+} signalling, it was hypothesised that TRPM2 channels play a role in actin and focal adhesion dynamics, and thus in cell migration. Thus, the second aim of this study was to investigate the role of TRPM2 channels, and the relative roles of Ca^{2+} and Zn^{2+}, in remodelling of actin cytoskeleton and focal adhesions in the context of cell migration.

The results are expected to have implications for our understanding of type 2 diabetes where free fatty acid levels are elevated in the bloodstream and for cancer metastasis where cells migrate to unwanted locations.

Chapter 2 Materials and Methods

2. 1 Materials

2. 1. 1 Chemicals and solutions

All chemicals were obtained from Sigma-Aldrich or Calbiochem unless stated otherwise. Goat serum was bought from EMD Millipore. Stock solutions of compounds were prepared in dimethylsupphoxide (DMSO) or water or ethanol. The stock chemicals were stored as aliquots at -20°C.

2. 1. 2 Antibodies

For immune-staining experiments, Rat monoclonal anti-HA (clone 3F10) antibodies (100 ng/ml, Roche-applied-science, 11867423001), mouse monoclonal anti-paxillin antibodies (1:500, BD Transduction Laboratories™, 610569), mouse monoclonal anti-CD63 antibodies (1:500, abcam®), and mouse monoclonal anti-cMyc antibodies (1:500, Roche) were used as primary antibodies. Alexa-Fluor[488]- conjugated anti-rat (1:500, Life technologies) and Cy3-conjugated anti-mouse (1:500, Jackson Immunoresearch) were used as corresponding secondary antibodies. For western blotting, Rat anti-HA-Peroxidase high affinity antibodies (Roche life science, 12013819001), mouse anti-Lamp1 antibodies (1:5000, BD Transduction Laboratories™, 611043) and rabbit anti-calnexin antibodies (1: 5000, abcam®, ab22595) were used as primary antibodies. Goat anti-Mouse IgG (H+L)-HRP-conjugated antibody (BIO-RAD, 1721011) and Goat anti-Rabbit IgG antibody, (H+L) HRP conjugate (Chemicon®, AP307P) were used as corresponding secondary antibodies.

2. 1. 3 Molecular probes and reagents

Fluozin3™-AM, Fluo4-AM, LysoTracker® Red, MitoTracker® Red, ER-tracker™ Red, Acridine Orange, MitoSOX™ Red and SuperScript® II Reverse Transcriptase were purchased from Life Technologie™. AlexFluor® 488 Phalloidin, AlexFluor® 633 Phalloidin, Lipofectamine®2000 Transfection Reagent and Pluronic®F127 were obtained from Invitrogen™. FuGENE®HD Transfection Reagent and Taq DNA polymerase was obtained from Promega. DAPI-Fluoromount-G™ was purchased from SouthernBiotech. H2DCF-DA was purchased from Biotium. JC-10 was from ATT Bioquest ®. Gp91ds-tat peptide was purchased from AnaSpec, Inc (USA). In Situ Cell death Detection Kit (for TUNEL assay) was purchased from Sigma-Aldrich. IL-1-β and IFN-γ were purchased from PEPROTECH.

2. 1. 4 Oligonucleotides

SiRNA (5'- CUGUCUAAGAUCAAUUACAACCU-3') against the Rat TRPM2 channel was designed using siDirect (Naito et al., 2004) and custom made by Dharmacon™. Control SiRNA was from Ambion. SiRNA-1 (ON-TARGETplus Human TRPM2 (7226)) was from Thermo Scientific. SiRNA-2 (5'- GAAAGAAUGCGUGUAUUUUGUAA-3') against the human TRPM2 channel was designed using siDirect and custom-made by Dharmacon.

2. 1. 5 cDNA clones

EGFP-Cdc42-Q61L and Cdc42-T17N were provided by Dr. Sreenivasan Ponnambalam (University of Leeds). Rif cDNA clones (myc-tagged Rif-Q61L and Rif-T17N) were provided by Prof. Harry mellor (University of Bristol). pActin-tdTomato was kindly provided by Dr. Wolfgang Wagner, University Medical Center, Hamburg, Germany. TRPM2-HA plasmid was made in this lab. pLAMP1-GFP was kindly provided by Dr P.Boquet, Institut National de la Sante et la Recherché Medicale, Nice. Drp1-GFP was a kind gift from Dr. Stefan Strack (University of Iowa, US). Annexin V-GFP is a kind gift from Prof. Christoph Borner (Institute of Molecular Medicine and Cell Research, University of Freiburg, Germany).

2. 1. 6 Medium used for cDNA clone

LB medium (+agar)	1.6 g Bacto-tryptone; 1 g Bacto-yeast extract; 0.5g NaCl; water to 100 ml, 1.5 g Agar was added and then autoclaved.
LB medium (-agar)	1.6 g Bacto-tryptone; 1 g Bacto-yeast extract; 0.5 g NaCl; water to 100 ml and then autoclaved.

2. 1. 7 Animals

C57BL/6 (wild-type) and TRPM2 knock-out mice (TRPM2$^{-/-}$) were used in these studies. Generation of TRPM2$^{-/-}$ mice is as described previously (Palmer et al., 2011). These mice express a non- functional TRPM2 channel lacking the transmembrane domains 3 and 4 (encoded by exons 17 and 18). Mice were bred, maintained and all procedures were performed under UK Home Office licence and ethical procedure.

2. 1. 8 Cell culture

HeLa cervical carcinoma cells were maintained in DMEM/F12 medium (Gibco®) supplemented with 10% fetal calf serum and penicillin (100 U/ml) and streptomycin (100 µg/

ml). A HEK293 cell line conditionally expressing TRPM2 under the control of tetracycline was provided by Dr A.M. Scharenberg (University of Washington, Seattle, WA). This cell line was maintained in DMEM F12 (Invitrogen) supplemented with 10% heat-inactivated fetal calf serum, penicillin (100 U/ml), streptomycin (100 µg/ml), blasticidin (5 µg /ml; Invitrogen) and zeocin (400 µg/ml; Invitrogen). Expression of TRPM2 was induced by overnight exposure to tetracycline (1 µg/ml). The HEK293-MSRII cell line was provided by Glaxo-Smith Kline. PC-3 cells were provided by Michelle Peckham (University of Leeds) and cultured in RPMI 1640 + GlutaMAX^{TM} medium (Invitrogen) supplemented with 10% heat-inactivated fetal calf serum, penicillin (100 U/ml), streptomycin (100 µg/ml), 1 mM sodium pyruvate, 50 µM 2-mercaptoethanol, 10 mM HEPES). INS832/13 rat pancreatic β-cells were cultured as for the PC-3 cell line. Cells cultured in growth media were replaced every 3 days and cells were passaged at 80% confluence. Cells were grown in 25 or 75 cm^2 flasks (Sarstedt) at 37°C in a humidified atmosphere containing 5% CO_2. For passage, cells were first rinsed with Dulbecco's phosphate buffered saline (DPBS) without Ca^{2+} and Mg^{2+}. Then the cells were detached from culture flasks using 1 ml of 0.05% trypsin-EDTA solution (Sigma). Subsequently, detached cells were re-suspended in 5 ml or 8 ml fresh culture media depending on which flask was used. Finally, appropriate volume of suspended cells was transferred to a new flask containing appropriate volume of pre warmed fresh medium. Cells were typically passaged to 20% confluence.

Mouse islets isolated from 8-10 week old wild-type (C57BL/6) or TRPM2 knock-out mice were used in the study. Mouse islets were maintained as for the INS832/13 cells medium. The mouse islets were cultured in dishes at 37°C/5% CO_2.

2. 2 Methods

2. 2. 1 Transformation of competent cells

DH5α competent cells were used for amplification of plasmid DNA. 50 µl aliquots of competent cells were thawed slowly on ice and DNA (~ 100 ng) in 1 µl was added. Cells were subsequently incubated on ice for 30 minutes prior to heat shock at 42 °C for 60 seconds. Following 2 minute incubation on ice, 450 µl pre-warmed LB media was added and cells were incubated at 37°C in a shaking incubator (200 rpm) for 1 hour. 200 µl of cultures were then spread onto LB- Agar plate (media + 1% w/v bacteriological agar) containing the appropriate selection antibiotic (e. g, ampicillin 50 µg/ ml) using a sterile glass spreader. Plates were incubated overnight at 37°C to allow formation of individual colonies.

2. 2. 2 Isolation of plasmid DNA

After overnight incubation at 37°C, colonies were formed. A single bacterial colony transformed with the appropriate desired plasmid DNA was selected and then inoculated into 5 ml LB medium (-agar) supplemented with the appropriate selection antibiotic. Inoculates were then incubated overnight at 37°C and 200 rpm in a shaking incubator. For large scale plasmid isolation, 200 ml LB medium containing the appropriate selection antibiotic was inoculated with 5 ml overnight culture and incubated overnight at 37°C and 200 rpm in a shaking incubator. Plasmid DNA was purified from 100 ml of culture using the plasmid Midi Kit (Qiagen). The concentration of plasmid DNA was assessed using NanoDrop™2000 Spectrophotometer (Thermo Scientific).

2. 2. 3 Agarose gel electrophoresis

TAE Buffer: 40 mM Tris base, 1.14% v/v glacial acetic acid, 0.1 mM ethylenediaminetetraacetic acid (EDTA), pH 8.0

Agarose gel: 1% w/v electrophoresis grade Agarose was prepared in TAE buffer. The mixture was heated in a microwave until well dissolved and allowed to cool to ~60°C. 0.5 μg/ml ethidium bromide was then added and the gel poured into an appropriate mould fitted with a gel comb

Analysis of DNA samples by size was carried out by agarose gel electrophoresis (Sambrook and Russell, 2001). DNA samples were diluted as required in Milli-Q water and 6× loading buffer added to a final concentration of 1×. A pre-cast agarose gel was placed in an electrophoresis apparatus and submerged in TAE buffer. Sample DNA was loaded alongside a size marker for comparison. Samples were electrophoresed at 100 V for 45 minutes or until adequately resolved. Gels were imaged using a Gel Doc trans-illuminator (BioRad).

2. 2. 4 RT-PCR

RNA was extracted from the HeLa, PC-3 and INS832/13 cells using TRI Reagent® (Sigma-Aldrich®.). According to the protocol provided by the Wellcome Trust Sanger Institute, before performing the RT reaction, 5 μg of total RNA was heated in a 10 μl volume at 65°C for 10 minutes and then quenched on ice. To the heated denatured RNA, 3.0 μl of 10× PCR buffer, 2.5 μl of 10 mM dNTPs, 6.0 μl of 25 mM $MgCl_2$, 1.0 μl of random primers (1 μg), 0.5

µl SuperScript II reverse transcriptase and 17 µl of water were added and incubated for 10 minutes at 25°C, and then at 42°C for 1 hour. A control without the reverse transcriptase (-RT) was set up in parallel. Then the cDNA or RNA (-RT) were subjected to PCR. TRPM2 primers were used (forward: 5′-ATGCTACCTCGGAAGCTGAA-3′ and reverse: 5′-TTCTGGAGGAGGGTCTTGTG-3′). For PCR, briefly, the cDNA product (6 µl) was mixed with 1.5 µl of 10×PCR buffer, 0.2 µl of Taq polymerase, 0.5 µl of forward primer and 0.5 µl of reverse primer (0.5 µM), and 11.3 µl of water to a total volume of 20 µl. The amplification protocol for PCR was set as follows: 95°C for 5 minutes, followed by 30 cycles of amplification steps (95°C for 30 seconds, 60°C for 45 seconds, 72°C for 30 seconds), and the final extension at 72°C for 5 minutes. The PCR products were analysed using agarose gel (1%) electrophoresis and visualized under UV light after staining with ethidium bromide (1 µg/ml).

2. 2. 5 Transient transfection

Transient transfection of mammalian cells was carried out using FuGENE® HD transfection reagent as per manufacturers' instructions. Briefly, cells were seeded onto glass coverslips and grown to ~30% confluence. Prior to transfection, culture medium was replaced with fresh medium and Opti-MEM® was pre-warmed to room temperature. For transfection in 24 well plates, the ratio of FuGENE® to DNA was 3:1 (µl: µg) For each well, 0.5 µg of plasmid DNA was added to 20 µl Opti-MEM®, then 1.5 µl of FuGENE® was added and mixed immediately. Subsequently, transfection mixtures were incubated at room temperature for 20 minutes before addition to cells. The cells were returned to the incubator, and incubated for 36-48 hours prior to experiment.

2. 2. 6 RNA interference

Cells were cultured in 24-well plates until the confluence reached 70%. Then 0.5 µl of 50 nM small interfering RNA (siRNA) specific to TRPM2 or scrambled siRNA (Ambion) was mixed with 50 µl of pre-warmed Opti-MEM® (mixture 1) and incubated for 5 minutes at room temperature. Meanwhile, 0.5 µl of Lipofectamine™ 2000 was mixed with 50 µl of pre-warmed Opti-MEM® (mixture 2) and incubate for 5 minutes at room temperature. Subsequently, the two mixtures were combined and incubated for 25 minutes at room temperature before adding to the cells. After 48-72 hours incubation, cells are ready for experiment.

2. 2. 7 Treatments

INS832/13 cells were grown on 35 mm FluoroDishes (World Precision Instruments) for live cell imaging and maintained in RPMI 1640 + GlutaMAX^{TM}. Palmitic acid (Sigma-Aldrich) was dissolved in ethanol and then complexed with 10% fatty acid-free bovine serum albumin (BSA, Sigma-Aldrich) at 65°C. The complex was stored at 4° C and warmed to 37 °C prior to use. 1 M stock solution of mannitol and glucose were prepared in milli-Q water. Unless otherwise specified, palmitate and all the compound diluted in Opti-MEM (5.5 mM Glucose) were added to cells to the desired concentration and incubated for the desired length of time prior to experimentation (see figure legends for details). HeLa and PC-3 cells grown on coverslips to ~50% confluence were treated with different drugs at 37 °C for 2 hr in standard buffered saline (SBS, 10 mM HEPES, 130 mM NaCl, 1.2 mM KCl, 8 mM glucose, 1.5 mM CaCl$_2$, 1.2 mM MgCl$_2$, pH 7.4) with or without H$_2$O$_2$ (see figure legends for details).

2. 2. 8 ROS measurement

2. 2. 8. 1 Whole cell ROS measurement

Cytosolic ROS production was measured by using cell-permeant 2', 7'-dichlorodihydrofluorescein diacetate (H$_2$DCF-DA) (Biotium). H$_2$DCF-DA is an indicator for ROS in cells. Upon cleavage of the acetate groups by intracellular esterases and oxidation, the nonfluorescent H$_2$DCF-DA is converted to the highly fluorescent DCF. Briefly, cells were treated with various agents for the desired length of time and then incubated with HBSS containing 10 µM H$_2$DCF-DA for 30 minutes at 37ºC/ 5% CO$_2$. The cells were then washed three times with HBSS (GIBCO®) prior to loading onto the inverted confocal microscopy (LSM700, Carl Zeiss, Jena, Germany) using 40 ×/1.4NA oil objective for imaging (excitation, 488 nm; emission, 515-540 nm).

2. 2. 8. 2 Mitochondrial ROS measurement

Cells were treated with various agents for the desired length of time and then incubated with HBSS containing 10 µM MitoSOX ™ Red for 30 minutes at 37ºC/ 5% CO$_2$. Cells were then washed three times with HBSS (GIBCO®) prior to loading to the inverted confocal microscopy (LSM700, Carl Zeiss, Jena, Germany) using 40 ×/1.4NA oil objective for imaging (excitation, 488 nm; emission, 515-540 nm).

2. 2. 9 Flow Cytometry

2. 2. 9. 1 Mitochondria membrane potential

Mitochondrial membrane potential was measured using the fluorescent probe JC-10. In normal cells, JC-10 concentrates in the mitochondrial matrix where it produces red fluorescent aggregates. When mitochondrial membrane becomes depolarized, JC-10 exists as monomers producing green fluorescence. Therefore, the green emission and red emission can be analysed in fluorescence channel 1 (FL1) and channel 2 (FL2) respectively in flow cytometer. One day before treatment, cells were plated in a 24-well plate to achieve 80% confluence on the following day. The next day, cells were treated with various agents for 12 hours. After treatment, cells were dislodged with 300 µl of trypsin-EDTA followed by centrifugation for 5 minutes at 500 g. Supernatant was discarded and the cell pellet was washed once with HBSS (GIBCO®)followed by centrifugation for 5 minutes at 500 g. Subsequently, cells were suspended in 500 µl of JC-10 solution (5 µM) and incubated for 30 minutes at 37ºC/ 5% CO_2. Cells were loaded into LSRFortessa™ flow cytometer (BD Biosciences). Cytometer settings were optimized for green (FL-1) and red (FL-2) fluorescence, and data were analysed with FACSDiva™ Software (BD Biosciences).

2. 2. 9. 2 Cell death assays

Cells were cultured in a 24-well plate for 24 to 48 hours until the confluence reached 80%. Cells were then treated with various agents for 24 hours. Both floating and attached cells were collected by adding 300 µl of trypsin-EDTA. Cells were centrifuged for 5 minutes at 500 g followed by washing once with 1× Annexin buffer (10 mM HEPES, 140 mM NaCl, 2.5 mM $CaCl_2$, pH 7.4). Subsequently, cells were suspended in 500 µl Annexin buffer and incubated with 5 µl 4 µg/ ml Annexin V-GFP and 5 µl 1 mg/ml PI for 30 minutes in the dark. Samples were analysed in LSRFortessa™ flow cytometer (BD Biosciences). Cytometer settings were optimized for green (FL-1) and red (FL-2) fluorescence, and data were analysed with FACSDiva™ Software (BD Biosciences).

2. 2. 9. 3 Cytosolic Ca^{2+} and Zn^{2+} measurement

HeLa and PC-3 cells were split into 24-well plates and grown to approximately 60% confluence. After desired treatments, cells were incubated with SBS containing 0.01% Pluoronic-F127 and 1 µM Fluo4-AM or Fluozin3-AM at 37°C for 1 hour. After washing with PBS three times, cells (> 5000) were detached by adding 300 µl of trypsin-EDTA into each well followed by centrifugation for 5 minutes at 500 g. Cell pellets were washed once with HBSS followed by centrifugation for 5 minutes at 500 g. After cells were re-suspended in HBSS, the cells were loaded into LSRFortessa™ flow cytometer. Cytometer settings were optimized for green (FL-1) fluorescence, and data were analysed with FACSDiva™ Software (BD Biosciences).

2. 2. 10 Cell death in mouse islets

Islets were isolated from wild-type and TRPM2$^{-/-}$ mice as described previously (Zou et al., 2013). Pancreata were dissected from mice, minced into pieces (~1 mm^3), and digested with collagenase (Type IA; 1 mg/ml in HBSS) for 10 min with gentle agitation at 37ºC. After washing with medium, islets were hand-picked under a dissecting microscope and incubated overnight in the medium prior to drug treatments. For toxicity assays, islets were incubated with freshly prepared palmitate (500 µM) with or without drugs in Opti-MEM® as appropriate for 5 days at 37ºC in a humidified atmosphere containing 5% CO_2/95% air. Islets were stained with Acridine Orange and propidium iodide (PI) before loading to Zeiss LSM700 confocal microscope. Images were taken using 63 x oil objective at 37 ºC.

2. 2. 11 TUNEL assay and insulin staining in human islets

The use of human islets was approved by the local Ethics Committee (Ethics reference number: BIOSCI 14-003). Human islets were purchased from Prodo Laboratories (Irvine, United States). Islets were incubated without or with palmitate (500 µM) in combination with IL-1β (5 ng / ml) and IFN-γ (5 ng/ ml) for 7 days at 37ºC in a humidified atmosphere containing 5% CO_2/95% air. The islets were then fixed with 4% paraformaldehyde overnight, put in paraffin solution and frozen on dry ice. These islets were then sectioned (5 µm) using Leica cryostat microtome 1900. Sections were placed onto slides, washed once with PBS followed by 2 minutes permeabilization (0.1% TritonX-100/ 0.1% sodium citrate/ PBS) on ice. Sections were then washed with PBS and incubated with TUNEL reaction buffer (50 µl TUNEL reaction mix / 450 µl enzyme solution, see Figure 2.1 for mechanism) and anti-insulin first antibody (1:500 in TUNEL reaction mix) for 1 hour at 37 °C followed by PBS washing and 1 hour incubation with Alexa488-conjugated secondary antibody (1:1000 in PBS). Sections were washed with PBS and placed on mounting medium overnight for DAPI staining. Images were taken with LSM700 inverted confocal microscope using a 63x oil objective with excitation (Alexa488, 494 nm; Cy-3, 548 nm) and emission (Alexa488, 519 nm; Cy-3, 562 nm).
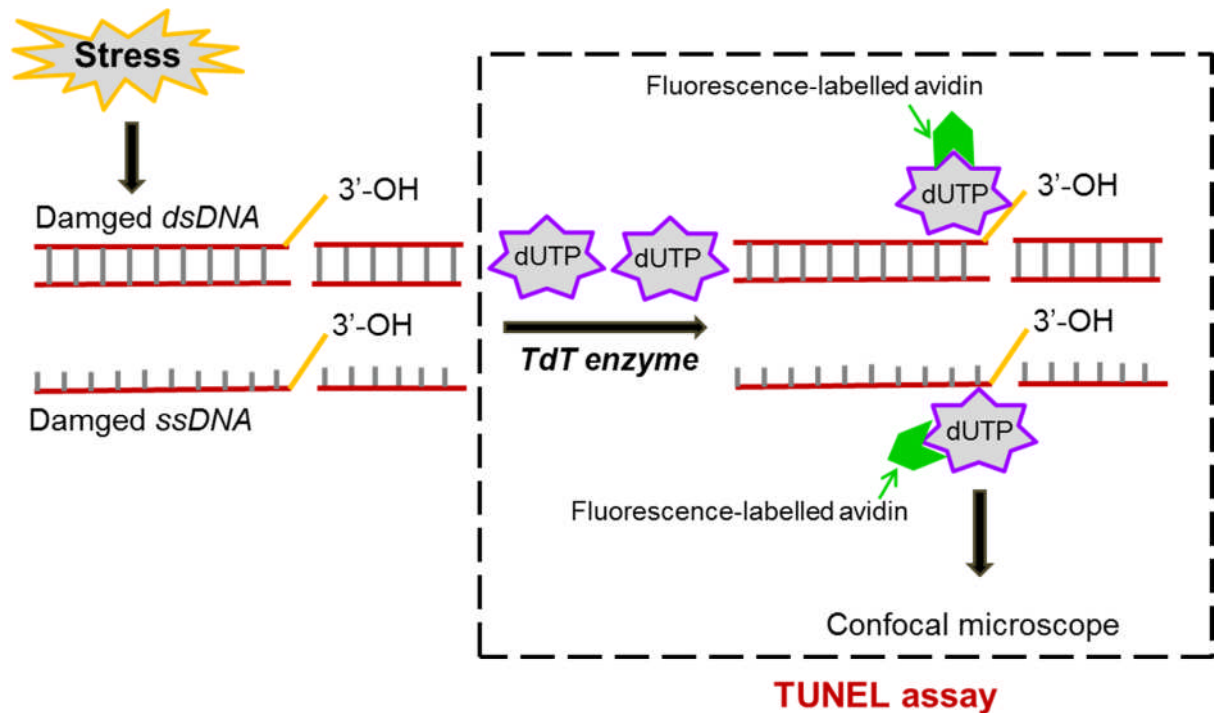
Figure 2. 1 Schematic showing the principle of TUNEL assay Cells subjected to stress, such as exposure to high glucose and fatty acids, undergo DNA fragmentation which results in apoptosis. The 3' OH ends of the DNA fragments are then labelled with biotin tagged deoxyudine triphosphate (dUTP) in a reaction catalysed by terminal deoxynucleotidyl transferase (TdT) (contained in TdT reaction buffer). The biotin tagged DNA ends are secondarily labelled with fluorescent avidin and detected by confocal microscope.

2. 2. 12 Phalloidin staining of the actin cytoskeleton

Cells were cultured on coverslips placed in 24-well plates for 1 day to allow for attachment. The next day, following the desired treatments, cells were fixed with 2% paraformaldehyde (PFA) for 15 minutes, followed by three washes with PBS. Cells were then permeabilised and blocked with 0.2% TritonX-100/ 5% goat serum (Millipore)/PBS for 15 minutes, before adding Alexa Fluor®488 or Alexa Fluor®633 conjugated Phalloidin (1:1000 in 0.2% TritonX-100 and 5% goat serum-contained PBS). After incubation for 1 hour in the dark, cells were washed with PBS three times. Coverslips were mounted with DAPI-Fluoromount-G™ (Southern Biotech) and imaged by confocal microscope (LSM510 Meta, Carl Zeiss, Jena, Germany) using 63 ×/1.4NA oil objective. Images were collected with excitation at 494 nm and emission at 519 nm.

2. 2. 13 Confocal microscopy and immunofluorescence

2. 2. 13. 1 Immunostaining of paxillin

After the desired treatments, Cells were fixed, permeabilized, blocked and stained with phalloidin as described above (phalloidin staining of the actin cytoskeleton). Cells were then incubated with primary anti-paxillin (dilution is 1:500 in goat serum) for 2 hours in the dark followed by three washes with PBS. Cells were then incubated with the anti-mouse Cy-3 (dilution is 1:500 in goat serum) for 1 hour in the dark. After three washes with PBS, cells were mounted and imaged using upright LSM510 Meta confocal microscope (Carl Zeiss, Jena, Germany). Images were collected using 63 ×/1.4NA oil objectives with excitation (Alexa488, 494 nm; Cy-3, 548 nm) and emission (Alexa488, 519 nm; Cy-3, 562 nm).

2. 2. 13. 2 Double staining for TRPM2-HA and CD63

Cells were transfected with TRPM2-HA plasmid and incubated for 48 hours before staining. Cells were fixed, permeabilized and blocked as described above (phalloidin staining of the actin cytoskeleton). Subsequently, cells were treated with anti-CD63 primary antibody (dilution: 1:500 in goat serum) for 2 hours in the dark followed by three PBS washes. Cells were then incubated with anti-HA primary antibody for 2 hours and washed with PBS three times. Cy3 anti-mouse IgG (dilution: 1:500 in goat serum) was used as the secondary antibody for CD63 and incubated in the dark for 1 hour. After three washes with PBS, cells were incubated with Alexa-Fluor 488 anti-rat secondary antibody (dilution: 1:500 in goat serum) in the dark for 1 hour. After three washes with PBS, cells were mounted onto slides as described above. Images were collected using inverted LSM880 Airy scan microscopy

using 63 ×/1.4NA oil objectives with excitation (Alexa488, 494 nm; Cy-3, 548 nm) and emission (Alexa488, 519 nm; Cy-3, 562 nm).

2. 2. 13. 3 Live cell imaging of organelles and intracellular Zn^{2+} redistribution

To monitor intracellular free Zn^{2+}, cells were loaded with 1 µM FluoZin3-AM in the presence of 0.02% Pluoronic-F127 (1 hour, 37° C) and washed twice to remove excess dye. Cells were loaded (30 min, 37° C) with 100 nM LysoTracker ® Red, or MitoTracker® Red or ER-tracker™ Red to stain lysosomes, mitochondria and ER respectively. Images were captured using Zeiss LSM 700 confocal microscope and 63x oil objective at 37°C with excitation (Alexa488, 494 nm; Cy-3, 548 nm) and emission (Alexa488, 519 nm; Cy-3, 562 nm). Images were then analysed for colocalization of Zn^{2+} with organelle markers.

2. 2. 13. 4 Ca^{2+} and Zn^{2+} imaging

Cells were seeded onto 35 mm glass bottomed dishes and grown to approximately 60% confluence. Loading of Fluo4-AM or Fluozin3-AM with or without H_2O_2 (100 µM) was carried out at a concentration of 500 nM in SBS + 0.01% pluronic acid at 37°C for 2 hour. Subsequently cells were washed with PBS once followed by imaging with the inverted confocal microscope (LSM700, Carl Zeiss, Jena, Germany) using 63 ×/1.4NA oil objective. Fluo4-AM and Fluozin3-AM were excited at 488 nm and emission was collected at 510 nm.

2. 2. 14 Agarose spot assay

0.1 g of low-melting point Ultra-Pure agarose (Invitrogen) was placed into a 50-mL Falcon tube and diluted into 20 ml PBS to get a 0.5% agarose suspension. This was heated by microwave until boiling, swirled to facilitate complete dissolution. The solution was cooled to 40°C. 90 µL of agarose solution was pipetted into 1.5-ml Eppendorf tubes containing 10 µl PBS with or without desired substances. Ten-microliter spots of agarose containing PBS alone or PBS with desired substances were pipetted, as rapidly as possible onto 35-mm glass-bottomed dishes (WORLD PRECISION INSTRUMENTS), and allowed to cool for 8 minutes at 4°C. Two spots per dish were pipetted and one containing PBS alone and one containing desired substances. Cells were then plated into these dishes in a complete medium containing 10% FCS and allowed to adhere for 4 h (Figure 2.2). Medium was replaced with fresh medium containing 0.1% FCS, incubated overnight and analysed by microscopy the next morning. Imaging was performed on a EVOS® FL Imaging System inverted microscope with a 10× objective (Life technologies™). For each spot, fields that contained the motile cells penetrating underneath the agarose spot were recorded. More than three independent experiments were carried out. The number of migrating cells from each independent experiment was counted for data quantification.
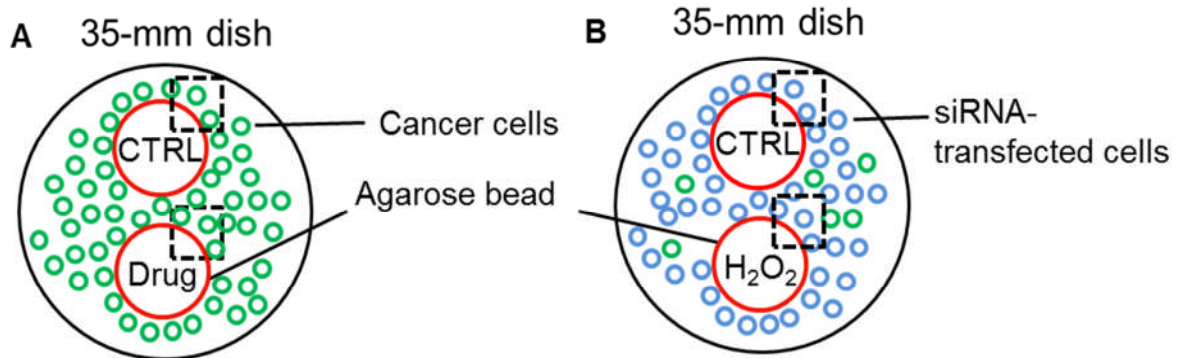
Figure 2. 2 Schematic representation of agarose spot assay (**A**)Two agarose spots were plated onto a 35-mm glass-bottomed dish. One spot contained PBS and the other contained H_2O_2 with or without the desired compounds. Cells (**green circles**) were plated around the agarose spots and incubated at 37°C. (**B**) For siRNA, cells were transfected with TRPM2-siRNA for 48-60 hours before the migration assay. Transfected cells (**blue circles**) were plated into the dish containing two agarose spots prepared as for (A). After the desired length of incubation at 37°C, cell migration into agarose spots was recorded. Boxed regions were presented as representative images.

2. 2. 15 Live cell imaging of actin dynamics and lysosome migration

To examine the actin dynamics and movement of lysosomes in a migrating cell, cells were transfected with Actin-Tdtomato and LAMP1-GFP plasmids. Transfected cells were plated around the agarose spots on a Fluorodish glass-bottomed dish as described above. After 16 hr incubation, cells at the interface of the agarose spot were imaged with an inverted confocal microscope (LSM700, Carl Zeiss, Jena, Germany) using appropriate excitation wavelength (548 nm for Actin-Tdtomato; 488 nm for LAMP1-GFP) and emission wavelength (562 nm for Actin-Tdtomato; 519 nm for LAMP1-GFP) and a 63 ×/1.4NA oil objective.

2. 2. 16 Intracellular Ca^{2+} and Zn^{2+} measurements by Flexstation

Intracellular Ca^{2+} and Zn^{2+} were monitored using Fura-2-AM and FluoZin3-AM respectively and then fluorescence was examined using a Molecular Devices Flexstation (Price and Lummis, 2005). Cells were plated at approximately 40,000 cells per well on clear-bottomed 96-well plates (Costar) and grown overnight. Cells were then incubated in Fura-2-AM (2 µM) or FluoZin3-AM made up in SBS (pH 7.4) containing 0.01% Pluronic F-127 for 1 hr at 37°C. After washing twice with SBS, 200 µl SBS were added. Then the Zn^{2+} fluorescence was monitored directly at 530 nm (excitation wavelength of 490 nm) and the data are expressed as change in F. For Ca^{2+} measurement, the appropriate reagents were prepared and plated onto a round-bottomed 96-well plate. Both plates were loaded onto Flexstation® 3 Multi-Mode Microplate Reader (Molecular Devices, California, USA). Fluorescence was measured for a total 7 min at 10 s intervals using excitation wavelengths of 340 and 380 nm and emission wavelength of 510 nm. At taking control measurements for ~65s, 50 µl of the reagents made up at fivefold the required final concentration were added to wells. The ratio of fluorescence intensities following excitation at 340 and 380 nm was calculated for each measurement point. For statistical comparisons, the mean of the ratios in the last time-point minus baseline was calculated for each treatment and the statistical differences were compared using one-way Anova.

2. 2. 17 Protein chemistry

2. 2. 17. 1 Reagents

Lysis Buffer:

5% (v/v)Tris HCl, pH 7.4; 0.1 M NaCl; 2 mM EDTA; 2 mM EGTA; 1.2% (v/v) Triton × 100

10 ×Transfer Buffer :

1.9 M Glycine; 0.25 M Tris-base

10 × PBS:

1.37 M NaCl; 0.03 M KCl; 0.1 M $Na_2HPO_4{.}7H2O$; 0.02 M KH2PO4

12 % Resolving gel:

12% (v/v) acrylamide mix; 0.375 M Tris (pH 8.8); 0.1% (w/v) SDS; 0.1% (w/v) ammonium persulfate (APS); 0.04% (v/v) TEMED

5% stacking gel:

5% (v/v) acrylamide mix; 0.125 M Tris (pH 6.8); 0.1% (w/v) SDS; 0.1% (w/v) ammonium persulfate; 0.1% (v/v) TEMED

SDS buffer (4×)

0.2 M Tris HCl, pH6.8; 0.28 M SDS; 4.0 ml glycerol; 0.588 M β-mercaptoethanol; 0.05M EDTA; 1.19 mM bromophenol Blue

Homogenization medium:

0.25 M sucrose; 1 mM EDTA; 0.01 M HEPES; pH 7.4

OptiPrep dilution buffer:

0.25 M sucrose; 2 mM EDTA; 0.08 M HEPES; pH to 7.4

OptiPrep™ (Axis-shield)   60% solution

2. 2. 17. 2 Homogenization

To determine the expression of TRPM2 channels in lysosomes of HeLa cells, lysosomes were isolated using Thermo Scientific™ Lysosome Enrichment Kit. Briefly, HeLa cells transfected with TRPM2-HA for 48 hours were collected from two 75 cm^2 flasks by scrapping with ice-cold PBS. Cell suspension was then centrifuged at 500 g/4°C for 10 minutes to get cell pellet. Cell pellet was re-suspended in 0.5 ml of Lysosome Enrichment Reagents A containing 100 µl protease inhibitors (1×) (Roche), 2 µl Pepstatin (1mg/ml) and 2 µl phenylmethanesulfonyl fluoride or phenylmethylsulfonyl fluoride (PMSF) (100 mM). After the cell suspension was incubated on ice for 2 minutes, 0.5 ml Lysosome Enrichment Reagents B was added. Then the cell suspension were homogenized in a cell homogenizer (isobiotec) for 10-15 times using a 16 micron clearance ball followed by centrifugation at 500 g/ 4 ºC for 10 minutes to pellet cell debris, unbroken cells and nuclei. The supernatant was collected, overlaid on the top of an OptiPrep™ density gradient and subjected to ultracentrifugation (Schmidt et al., 2009).

Table 2.1

OptiPrep gradient:

OptiPrep (ml)	Dilution buffer (ml)	OptiPrep final concentration
1.41	3.59	17%
1.67	3.33	20%
1.92	3.08	23%
2.25	2.75	27%
2.5	2.5	30%

2. 2. 17. 3 OptiPrep Density gradient medium

Lysosomes were purified by Optiprep density gradient centrifugation as described previously (Schmidt et al., 2009). The work was carried out at 4°C. Solutions of different OptiPrep concentrations were made up as shown in table 2.1. Desired volume of each concentration was added into a 5 ml clear ultracentrifugation tube carefully to avoid bubbles in the following order: 0.5 ml of 30% at the bottom followed by 1 ml of 27%, 0.5 ml of 23%, 1 ml of 20% and 1ml of 17% at the top (Figure 2.3A). Then 1 ml of the cell homogenate was overlaid on the top of the gradient (Figure 2. 3A). The tubes were centrifuged at 41, 000 rpm for 4 hours in SW Ti 55 rotor in a Beckman ultracentrifuge. After ultracentrifugation, starting from the top, 0.5 ml fractions were collected into Eppendorf tubes. The top layer is enriched in lysosomes (Figure 2.3B). To each fraction, 1 ml PBS was added and centrifuged at 20, 000 *g* for 1 hour. After centrifugation, the pellet (containing lysosomes) was saved for analysis by western blotting.
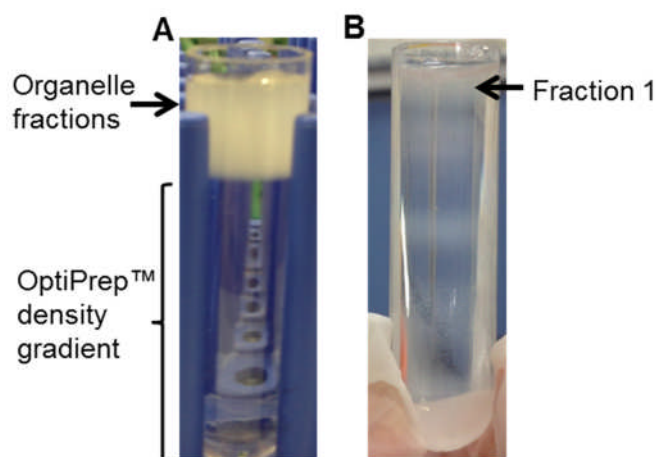
Figure 2. 3 Subcellular fractionation to isolate lysosomes from HeLa cells (**A**) Post-nulear supernatant was loaded onto the top of OptiPrep™ density gradient for ultracentrifugation. (**B**) After 4 hours of ultracentrifugation, lysosomes enriched in fraction 1 were collected, pelleted and used for subsequent analyses.

2. 2. 17. 4 SDS-polyacrylamide gel electrophoresis (SDS-PAGE)

12% resolving gels were poured and topped with ~ 2 cm of 5% stacking gel. Gels were mounted in the gel running apparatus according to the manufacturers' instructions and sufficient SDS-PAGE buffer was added to the gel running tank. Marker (5 µl) and samples (~15 µl) were loaded into preformed wells. Prior to loading, the samples treated with SDS sample buffer were heated at 50°C for 5 minutes and centrifuged at 13000g for 10 minutes. Gels were run at 200 V until the required separation of marker bands was achieved.

2. 2. 17. 5 Western blotting

Following separation of proteins by SDS-PAGE, gels were removed from the tank and placed in ice-cold transfer buffer. Stacking gel was removed and the running gel was placed on a nitrocellulose membrane pre-wetted with the transfer buffer. Blotting papers (pre-wetted with transfer buffer) were then placed with gel on the top of membrane. Proteins were transferred using a semi-dry transfer apparatus (BioRad) with gel on top of membrane at 0.06 A for 1.5 hours. The nitrocellulose membrane was then removed from the stack and washed in chilled PBS (4°C) before blocking in 5% non-fat milk in PBS/Tween20 buffer overnight on a rocking table at 4°C. Milk solution was removed and the membrane was washed thoroughly in chilled 1×PBS/TWEEN20 solution (generally 1hour). Primary antibody was then applied to the membrane overnight in PBS/TWEEN20 containing 5% non-fat milk at 4°C on a rocking platform. Unbound antibody was removed by washing for 1 hour in PBS/TWEEN20 with exchange of the washing solution every 15 minutes. Secondary antibody was then applied for 1 hour at room temperature in PBS/TWEEN20 containing 5%

non-fat milk. Both primary and secondary antibody was used at 1:5000 dilutions. After washing with PBS/TWEEN20, the membrane was treated with PS-ATTO (Lumigen) solution to generate a chemi-luminescent signal visualized using a G:BOX Chemi XX6 imager (Syngene).

2. 3 Quantification and data analysis

2. 3. 1 Analysis of mitochondrial morphology

Mitochondrial fragmentation was detected by staining the cells with MitoTracker Red. For morphological analyses of mitochondria, acquired images were analysed using ImageJ (National Institutes of Health). Briefly, individual cell from digital images was manually selected by enclosing the cell with boundaries as accurately as possible. Then individual cell was cropped. After thresholding, individual particles (mitochondria) were analysed for average size. Mitochondria were considered fragmented when the average size of mitochondria was less than 0.8 μm. Cells with mitochondrial fragmentation were scored when equal or more than 50% of total mitochondria were fragmented.

2. 3. 2 Quantification of filopodia and focal adhesions

Identification and quantification of filopodia was carried out as described previously (Bohil et al., 2006). In present study, all the phalloidin-positive actin bundles that appeared at the boundary of the cell body were counted as filopodia. Filopodia appeared on the dorsal surface were observed but not included into quantification. Filopodium with branches was counted as one. For the quantification of filopodia, filopodia from 5 cells of an individual experiment were counted. Mean and s.e.m of filopodia (from 5 cells) from three individual experiments were presented. For counting the filopodia, images were printed out, and each cell was arbitrarily divided into 4 quadrants of approximately equal area, then each filopodium in a given quadrant was marked with a pen and multiplied the number by 4 to get the total filopodia of each cell. For focal adhesion size and number analysis, 10 cells were chosen from each individual experiment. Focal adhesion numbers were analysed using ImageJ, with size between 0.1~1.0 μm^2.

2. 3. 3 Co-localisation quantification

The co-localisation of Zn^{2+}/Drp1-GFP (green) with mitochondria (red) was assessed using the ImarisColoc module of IMARIS program (Bitplane AG). The co-localization channel (merged of red and green channel) was displayed in yellow colour. The pixel intensities of

yellow channel (Y) and red channel (R) were obtained respectively. $\frac{Y}{R} \cdot 100\%$ was used to show the co-localisation efficiency.

2. 3. 4 Data analysis

Image J was used for analysis of mitochondrial morphology and LAMP1-GFP-positive puncta. Flow cytometry graphs were generated using FlowJo (Tree Star Inc.). All experiments were performed at least 3 times (n) and the values are presented as mean ± SEM. Statistical significance was determined using OriginPro 8.6 (OriginLab®) by Student's *t-test* or one-way Anova, followed by Tukey post-hoc test. Both Student's *t-test* and one-way Anova are parametric methods for means comparison of several groups (N=2 for Student's *t-test* and N≥2 for one-way Anova) (Kanji, 2006). Before performing statistics, the Homogeneity of Variance Test in originPro 8.6 needs to be performed as parametric method requires equal variance among different groups (Kanji, 2006). In current study, the different groups are considered to have equal variance when the *p*-value is greater than 0.01. For statistics, Probability (*p*) is indicated with *, **, *** which correspond to values of 0.05, 0.01 and 0.001 respectively.

Chapter 3 Nutrient stress induced cell death is mediated by TRPM2 stimulated mitochondrial ROS production and fragmentation

3. 1 Introduction

In T2D, it is believed that insulin resistance develops prior to the elevation of blood glucose (Kahn et al., 2006). Obesity is closely associated with insulin resistance. Studies have shown that in obesity, insulin sensitivity of skeletal muscle and adipose tissue is reduced leading to decreased glucose uptake by these tissues (Kahn et al., 2006). Consequently, insulin resistance leads to high blood glucose levels. High caloric intake gradually induces inflammation of adipose tissue, and increases lipolysis (Guilherme et al., 2008). This leads to elevation of free fatty acids in the blood stream. Thus, insulin resistance leads to rise in blood levels of both glucose and fatty acids. To compensate for insulin resistance, β-cells of pancreas start secreting more insulin. However, as the disease progresses, β-cells begin to fail secreting sufficient insulin. This leads to insulin insufficiency and frank diabetes (Cnop et al., 2005). Thus, insulin resistance is the main trigger of type 2 diabetes.

Reactive oxygen species (ROS) have been shown to play important roles in T2D. Increased pancreatic β-cell death has been demonstrated when ROS levels are elevated (Li et al., 2008). Palmitate has been shown to cause β-cell destruction by increasing the cytosolic ROS production (Sato et al., 2014). Previous studies have revealed two sources of palmitate-stimulated ROS: ROS generation through NOX and ROS from the mitochondrial respiratory chain (Mitochondrial ROS). Yuzefovych et al reported a key role for mitochondrial ROS in palmitate induced β-cell death (Yuzefovych et al., 2010). Morgan et al demonstrated that palmitate stimulated ROS production in pancreatic islets and β-cell lines is NOX-dependent (Morgan et al., 2007). However, the mechanism by which palmitate induced ROS production induces β-cell apoptosis is less clear.

Mitochondria play an important role in the death of many cell types including β-cells. They normally exist as a highly branched tubular network. Under physiological conditions, mitochondria undergo efficient fusion and fission (known as mitochondrial dynamics) to eliminate damaged portions of the mitochondria. The fusion and fission events are rigorously regulated by fusion proteins (Mfn1 and 2 and OPA1) and fission proteins (Drp1 and Fis1) respectively (Yoon et al., 2011). Together, they enable the health of the mitochondria to be maintained, which is important for cell function and survival (Maechler and Wollheim, 2001). In T2D (Syed et al., 2011), increased cellular ROS levels affect mitochondrial form and function, often leading to apoptosis (Lin and Beal, 2006). In mitochondria-mediated

apoptosis pathway, loss of ΔΨm occurs and cytochrome *c* is released into cytosol, thereby leading to apoptosis. In this process, prior to, or simultaneous to, cytochrome *c* release, mitochondria fragment into multiple small units (Cereghetti et al., 2010). Some studies suggest that inhibition of mitochondrial fragmentation prevents apoptosis (Brooks et al., 2007; Sugioka et al., 2004). For example, Molina et al reported that palmitate exposure causes mitochondrial fragmentation and apoptosis of β-cells, and when mitochondrial fragmentation was inhibited, the apoptosis was also prevented (Molina et al., 2009). This observation indicates that mitochondrial dynamics is involved in palmitate induced β-cell apoptosis but how palmitate disrupts the balance between fusion and fission events remained unclear.

The TRPM2 channel, a ROS-sensitive Ca^{2+} -permeable cation channel, has been shown to be involved in ROS-dependent pancreatic β-cell death (Manna et al., 2015). However, the signalling mechanism via which TRPM2 channels cause β-cell death is poorly understood. Previous studies have shown that Ca^{2+} overload can mediate mitochondria-dependent apoptosis in other cell types (Chen et al., 2005; Pinton et al., 2008). Since palmitate can increase ROS generation (Nakamura et al., 2009) and Ca^{2+} levels (Gwiazda et al., 2009) and is capable of inducing mitochondrial fragmentation (Molina et al., 2009), it was hypothesized that TRPM2 channels might play a role in palmitate induced pancreatic β-cell death by increasing mitochondrial fragmentation.

This chapter therefore aims to explore the role of TRPM2 channels in palmitate induced β-cell death. The results demonstrate that palmitate activates NOX and the consequent rise in ROS activates TRPM2 channels. Activation of TRPM2 channels stimulates Zn^{2+} distribution to mitochondria, mitochondrial membrane depolarization, mitochondrial ROS overproduction, Drp1 recruitment to mitochondria, mitochondrial fragmentation and apoptosis of INS1 cells. Islets isolated from TRPM2 knockout mice and TRPM2 inhibitor-treated human islets are resistant to palmitate induced apoptosis, which further confirms that TRPM2 deficiency protects palmitate induced mitochondrial fragmentation and apoptosis. Thus, the evidence presented in this chapter provides new insights into the role for TRPM2 channels in the regulation of mitochondrial dynamics under hyperlipidaemic conditions.

3. 2 Results

3. 2. 1 Palmitate induces cytosolic ROS production through NOX2 activation in INS1 cells

A previous study reported that exposure of rat pancreatic islets and clonal beta cell lines to palmitate results in increased ROS production through modulation of NOX activity (Morgan et al., 2007). However, in that study, it was not clear which isoform of NOX mediates palmitate induced ROS production. The effect of chronic palmitate treatment on cytosolic ROS levels of INS1 cells was investigated by staining the cells with H2DCF-DA. The results show that chronic exposure to palmitate causes significant increase in cytosolic ROS and that the antioxidant N-acetyl cysteine (NAC) reverses such increase (Figure 3.1). In order to assess the source of ROS generation, the effect of apocynin, a NOX inhibitor, on palmitate induced ROS production was investigated. Apocynin has been shown to prevent the activation of leukocyte NOX by blocking the assembly of the oxidase (Aldieri et al., 2008). Apocynin completely abolished palmitate induced cytosolic ROS production in INS1 cells (Figure 3. 1). These data suggest that NOX plays a key role in palmitate induced ROS generation in INS1 cells.

The NOX family consists of 7 members (NOX1to NOX5, DUOX1 and 2) (Bedard and Krause, 2007). A previous study demonstrated that NOX2 mediates palmitate induced ROS production in mouse derived NIT-1 cells (Yuan et al., 2010). To test whether NOX2 mediates palmitate induced ROS generation, INS1 cells were treated with Gp91ds-tat, an inhibitory peptide specifically targeted to NOX2 (Walker et al., 2014). By mimicking a sequence of NOX2 that is important for the interaction with p47^{phox}, Gp91ds-tat can specifically inhibit NOX2 (Rey et al., 2001). Here, Gp91ds-tat significantly inhibited palmitate induced rise in cytosolic ROS (Figure 3. 1).

These data indicate that NOX2 plays a major role in palmitate induced cytosolic ROS production in β-cells.
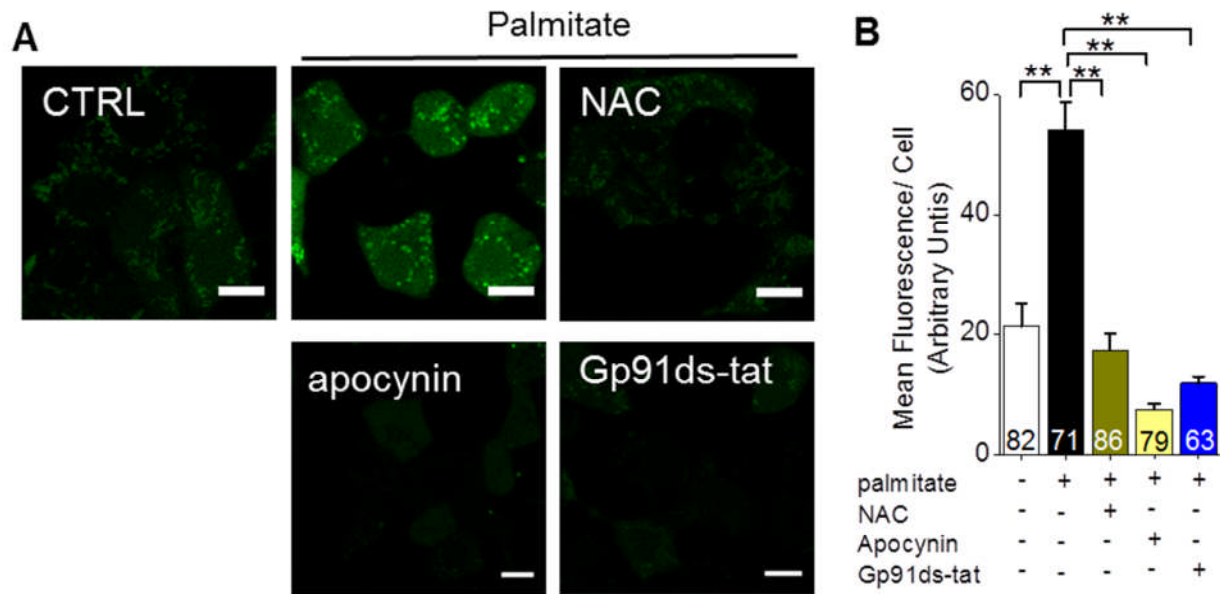
Figure 3. 1 Palmitate induces cytosolic ROS production through NOX2 activation in INS1 cells. (**A**) Live cell fluorescent images of INS1 cells exposed to medium alone (CTRL), medium containing palmitate (500 µM) with or without NAC (10 mM) or NOX inhibitors (20 µM apocynin; 5 µM Gp91ds-tat). Cells were stained for cytosolic ROS (H2DCF-DA). Images show that palmitate exposure increases cytosolic ROS level through NOX2 activation. Scale bars: 10 µm. (**B**) Mean ± SEM of data from (A) expressed as mean fluorescence per cell from the three independent experiments (the number of cells analysed are shown within each bar) following the indicated treatments; ** indicates $p < 0.01$; one-way Anova with post-hoc Tukey test.

3. 2. 2 Palmitate, but not glucose, causes mitochondrial fragmentation in INS1 cells

Previous studies have shown that the mitochondrial network is sensitive to cytosolic ROS in many cell types (Jendrach et al., 2008; Pletjushkina et al., 2006). In Figure 3.1 of this study, ROS staining was prominent in structures that resembled mitochondria. In control cells, ROS staining was faint and was seen in tubular structures (Figure 3. 1A). Following exposure to palmitate, however, the tubular network disappeared and staining was seen in round puncta: ROS staining in these puncta is much stronger compared to the tubular structures. These ROS enriched punctate structures could represent fragmented mitochondria because previous studies have shown that palmitate induces mitochondrial fragmentation (Molina et al., 2009; Wiederkehr and Wollheim, 2009).

Mitochondrial morphology in INS1 cells was next monitored by staining with MitoTracker, a dye used for labelling mitochondria in live cells. Results revealed that cells exposed to medium alone have long, tubular form of mitochondria, while palmitate (500 µM, 4 h) treatment led to the appearance of numerous punctate mitochondria (Figure 3. 2). Combination of high glucose (20 mM) with palmitate produced similar results as palmitate alone. However, in the absence of palmitate, 20 mM glucose failed to affect the mitochondrial architecture discernibly (Figure 3. 2). These data indicate that palmitate, but not high glucose, plays a dominant role in mediating mitochondrial fragmentation in INS1 cells.

Since palmitate triggers marked increase in cytosolic ROS production (Figure 3. 1), the role of cytosolic ROS in palmitate induced mitochondrial fragmentation was next examined. As RPMI1640 medium contains 2-mecaptoethanol that can scavenge ROS to affect the results, the following treatments were carried out in Opti-MEM. Quenching of ROS with the antioxidants (NAC) and inhibition of NOX2 with apocynin and Gp91ds-tat both prevented palmitate-induced mitochondria fragmentation (Figure 3. 3A-C).

Taken together, these results indicate that chronic exposure to palmitate causes mitochondrial fragmentation by activating NOX2 and raising cytosolic ROS.
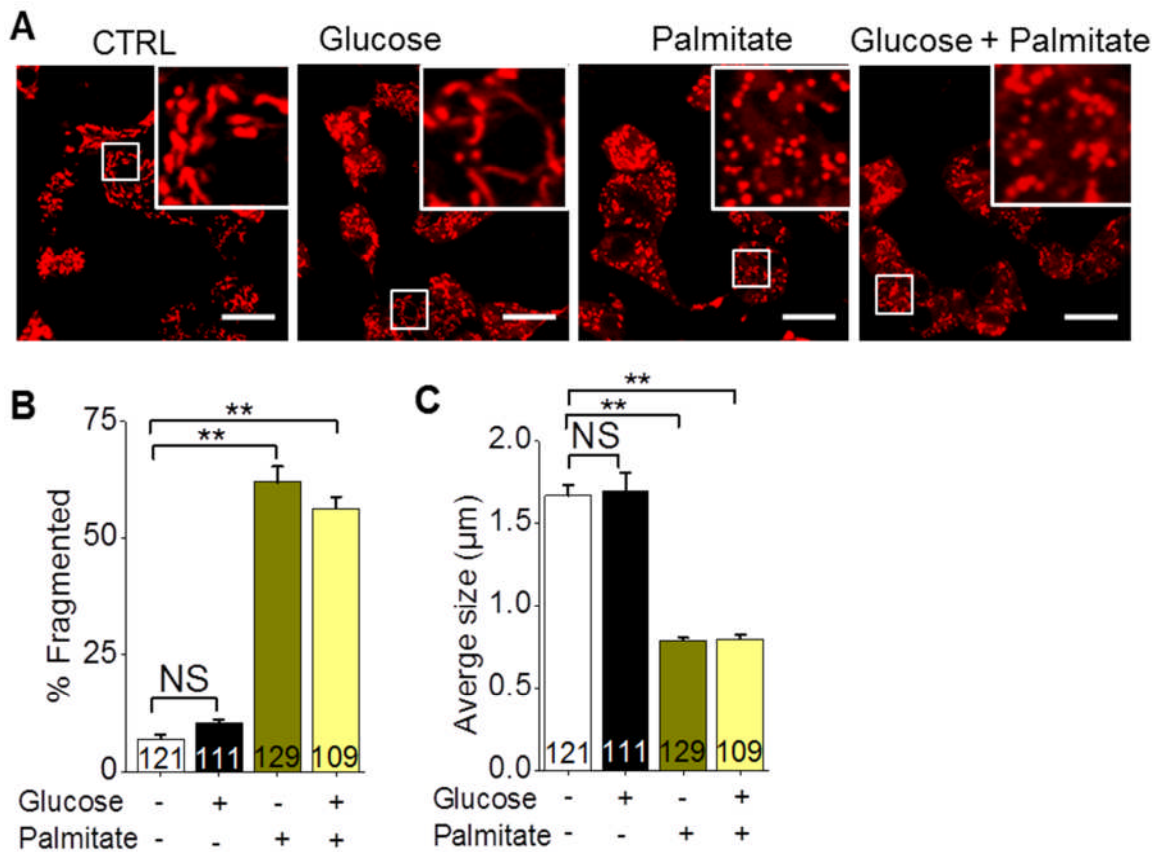
Figure 3. 2 Palmitate, but not glucose, causes mitochondrial fragmentation in INS1 cells. (**A**) INS1 cells were stained for mitochondria (MitoTracker) after 4 hours of different treatments (CTRL: RPMI1640 medium (11 mM Glucose) plus 9 mM mannitol; RPMI1640 medium plus 9 mM glucose (20 mM Glucose final concentration) or 500 µM palmitate; or RPMI1640 medium containing 9 mM glucose and 500 µM palmitate). Live cell fluorescent images show that high palmitate, not glucose causes mitochondrial fragmentation. Boxed regions are magnified in the upper square. Scale bars: 10 µm. (**B-C**) Mean ± SEM of percent of mitochondrial fragmentation (B) and average size of mitochondria (C) from three independent experiments determined from data in (A); ** indicates $p < 0.01$; NS, not significant; one-way Anova with post-hoc Tukey test.
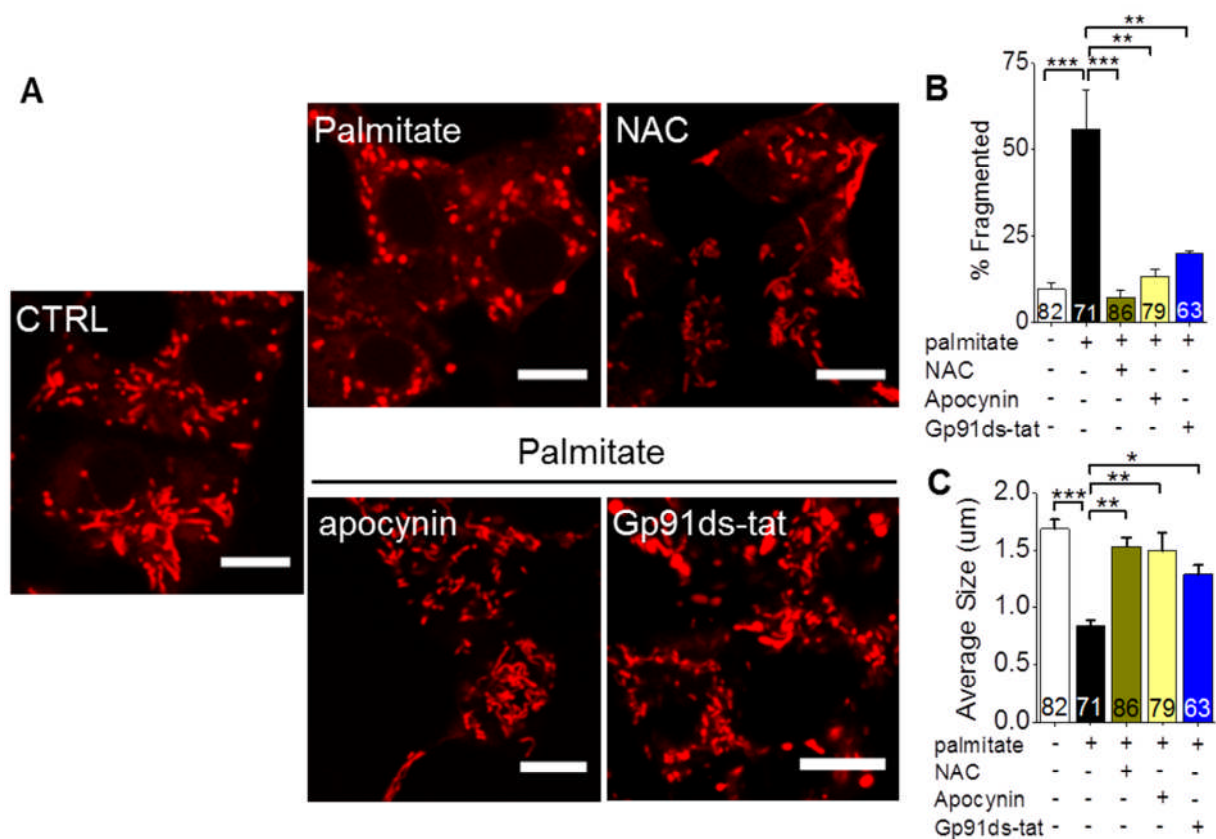
Figure 3. 3 Palmitate induced mitochondrial fragmentation is dependent on NOX2. (**A**) Live cell fluorescent images of INS1 cells exposed to medium alone (CTRL), medium containing palmitate (500 µM) with or without NAC (10 mM) or NOX inhibitors (20 µM apocynin and 5 µM Gp91ds-tat). Cells were stained for mitochondria (MitoTracker). Images show that Inhibition of NOX2 prevents palmitate-induced mitochondrial fragmentation. Scale bars: 10 µm. (**B-C**) Mean ± SEM of percent of mitochondrial fragmentation (B) and average size of mitochondria (C) from three independent experiments were determined from data in (A). ** indicates $p < 0.01$; one-way Anova with post-hoc Tukey test.

3. 2. 3 TRPM2 channels mediate palmitate induced mitochondrial fragmentation

Above data showed that chronic exposure to palmitate elevates cytosolic ROS level that in turn stimulates mitochondrial fragmentation. Since ROS is a potent activator of TRPM2 channels, it was surmised that TRPM2 channels may mediate the effect of palmitate on mitochondrial fragmentation.

Firstly, whether TRPM2 channels are expressed in INS1 cells were examined. Previous study has shown expression of TRPM2 channels in the rat-derived model pancreatic β-cell line, INS1 (Manna et al., 2015). In accordance with the previous finding, RT-PCR results showed TRPM2 messenger RNA expression in INS1 cells (Figure 3.4A). Furthermore, H_2O_2 application induced a rapid rise in cellular Ca^{2+} level that was inhibited by 2-APB, a nonspecific blocker of TRPM2 channels (Figure 3.4B-C). H_2O_2 induced rise in Ca^{2+}, however, gradually declined reaching a plateau phase, indicating desensitization to H_2O_2 over time. In addition to activating TRPM2 channels, H_2O_2 can also activate TRPM7 ion channels. However, the expression of TRPM7 channels in pancreatic β-cells has not yet been found (Uchida and Tominaga, 2011). Therefore, the H_2O_2 induced Ca^{2+} increase in INS1 cells could be attributed partially to the activation of TRPM2 channels.

The role of TRPM2 channels in palmitate-induced mitochondrial fragmentation was next investigated. Inhibition of TRPM2 channels with PJ34 significantly prevented palmitate induced mitochondrial fragmentation (Figure 3. 4D-F). Furthermore, siRNA targeted to TRPM2, also significantly prevented palmitate-induced mitochondrial fragmentation (Figure 3. 4G-I). Reverse transcription reaction (RT) and PCR of transfected cells showed that TRPM2-siRNA is effective in silencing TRPM2 messenger expression in INS1 cells (Figure 3.4J).

To further test the role of TRPM2 channels in palmitate induced mitochondrial fission, effect of palmitate on HEK-293 cells were examined. These cells are known to lack TRPM2 channels (Fonfria et al., 2004) and are therefore expected to be resistant to palmitate induced mitochondrial fragmentation. Consistent with this expectation, palmitate failed to induce mitochondrial fragmentation in HEK-293 cells (labelled -TRPM2 in Figure 3.5). By contrast, cells transfected with pCDNA-3-TRPM2 (+TRPM2) displayed robust mitochondrial fragmentation (Figure 3.5).

Collectively, these data suggest that TRPM2 channels play an important role in mediating palmitate-induced mitochondrial fragmentation.
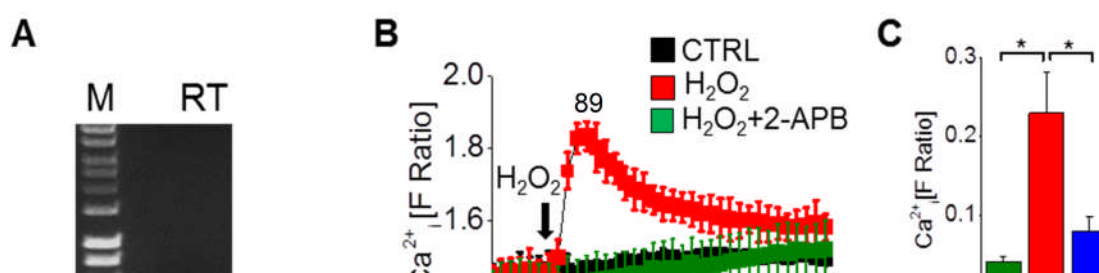
Figure 3. 4 Inhibition of TRPM2 channels prevents palmitate induced mitochondrial fragmentation. (**A**) RNA isolated from INS1 cells was subjected to RT and PCR. (**B**) INS1 cells were loaded with Fura-2-AM and then changes in cytosolic Ca^{2+} were measured using FlexstationII Microplate Reader. Symbols represent mean F ratio (340 nm/380 nm), representing Ca^{2+} levels, at various time points; black, no treatment; red, H_2O_2 applied at the time point shown with an arrow; green, cells were pretreated with 150 μM 2-APB (45 min) prior to H_2O_2 application. (**C**) Mean ± SEM of peak fluorescence from (B); * indicates $p < 0.05$; one-way Anova with post-hoc Tukey test. The data in C are from three independent

experiments. (**D**) Live cell fluorescent images of INS1 cells exposed to medium alone (CTRL), medium containing palmitate (500 µM) with or without PJ34 (10 µM). Cells were stained for mitochondria (MitoTracker). Images show that inhibition of TRPM2 channels with PJ34 inhibits palmitate induced mitochondrial fragmentation. Scale bars: 10 µm. (**E-F**) Mean ± SEM of percent of mitochondrial fragmentation (E) and average size of mitochondria (F) from three independent experiments performed as in (D). ** indicates $p < 0.01$; * indicates $p < 0.05$; one-way Anova with post-hoc Tukey test. (**G**) INS1 cells were exposed to medium alone (CTRL) or medium containing palmitate (500 µM) after transfection with scrambled siRNA or siRNA targeted to TRPM2 channels (siRNA-TRPM2) for 60 hours. Cells were stained with MitoTracker. Images show that inhibition of TRPM2 channels by siRNA prevents palmitate induced mitochondrial fragmentation. (**H-I**) Mean ± SEM of percent of mitochondrial fragmentation (H) and average size of mitochondria (I) from three independent experiments performed as in (G); ** indicates $p < 0.01$; * indicates $p < 0.05$; one-way Anova with post-hoc Tukey test. (**J**) Demonstration of silencing of TRPM2 mRNA expression by RNAi. Lane 1: DNA ladder (HypperLadder I; Bioline). Lane 2: blank. Lanes 3-6: PCR products from TRPM2 plasmid (lane 3) or mRNA without reverse transcription (lane 4) or INS1 cells transfected with scrambled siRNA (lane 5) or siRNA targeted to TRPM2 (lane 6).The results show absence of TRPM2 band (lane 6) in TRPM2 siRNA transfected samples, but not scrambled siRNA control (lane 5).
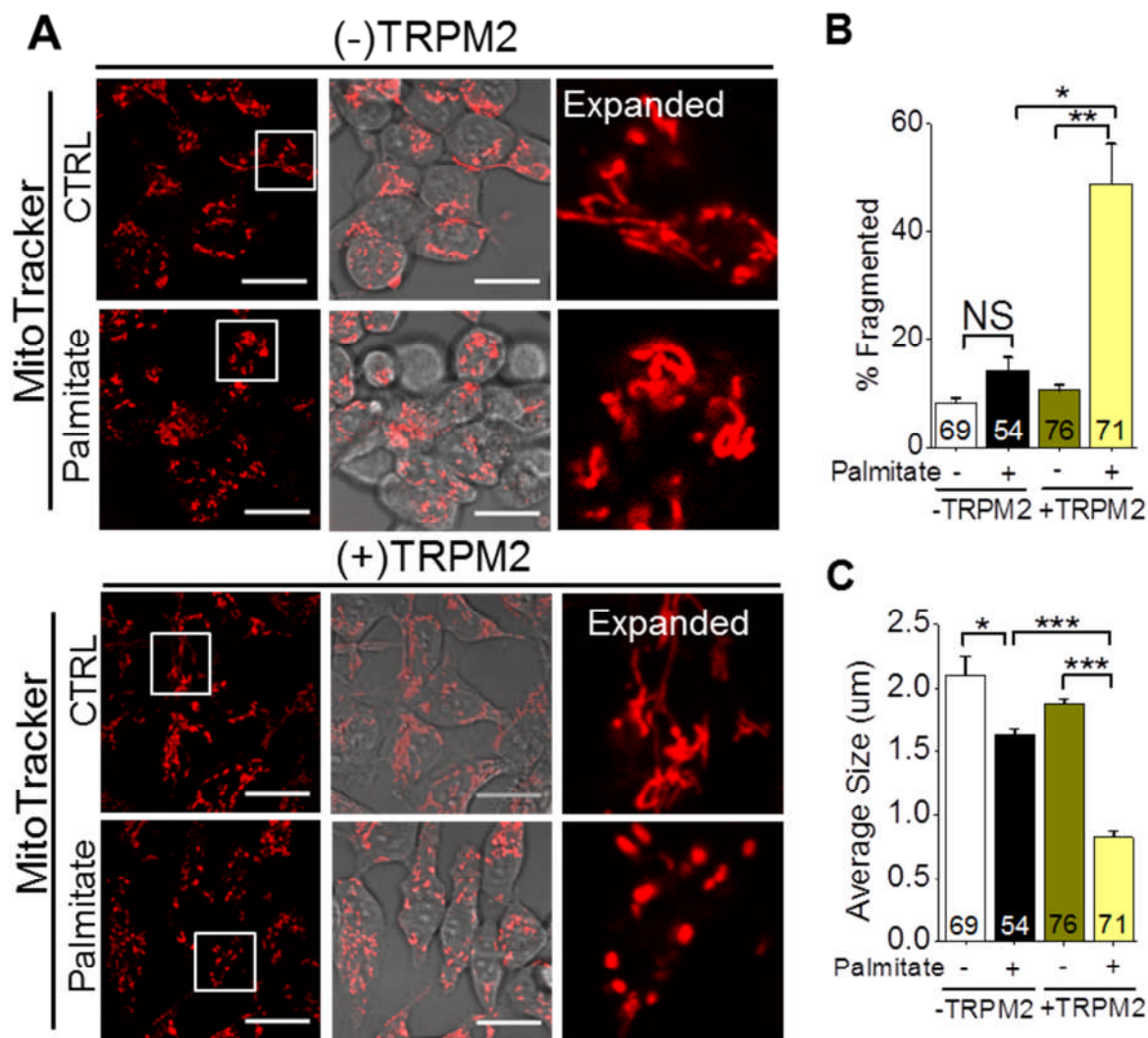
Figure 3. 5 TRPM2 deficient HEK-293 cells are resistant to palmitate induced mitochondrial fragmentation. (**A**) HEK-293 cells (-TRPM2) and HEK-293 cells transfected with pcDNA-3-TRPM2 (+TRPM2) were exposed to medium alone (CTRL) or medium with palmitate (500 µM) for 12 hr at 37 °C. Cells were stained for mitochondria (MitoTracker). Representative confocal data show that HEK-293 cells lacking TRPM2 channels are resistant to palmitate induced mitochondrial fragmentation, but cells transfected with the TRPM2 plasmid construct show extensive mitochondrial fragmentation; scale bars: 10 µm. (**B-C**) Mean ± SEM of percent of mitochondrial fragmentation (B) and average size of mitochondria (C) from three independent experiments performed as in (A); *** indicates $p < 0.001$; ** indicates $p < 0.01$; * indicates $p < 0.05$; NS, not significant; one-way Anova with post-hoc Tukey test.

3. 2. 4 Zn^{2+}, rather than Ca^{2+}, mediates palmitate induced mitochondrial fragmentation

TRPM2 channels have been shown to mediate Ca^{2+} entry from the extracellular medium. A recent study has shown that activation of TRPM2 channels also induces a rise in cytosolic Zn^{2+} (Manna et al., 2015). The role of these two ions in palmitate induced mitochondrial fragmentation was therefore examined using the Ca^{2+} chelator, BAPTA-AM, and the Zn^{2+} chelator, TPEN. Chelation of Ca^{2+} with BAPTA-AM failed to rescue mitochondrial fragmentation while chelation of Zn^{2+} with TPEN rescued palmitate induced mitochondrial fragmentation (Figure 3. 6A-C). These data imply that Zn^{2+} is the main mediator of palmitate induced mitochondrial fragmentation, while Ca^{2+} might play a less important role.

To confirm the role of Ca^{2+} and Zn^{2+} in mitochondrial dynamics, intracellular concentration of Ca^{2+} and Zn^{2+} was individually raised using ionophores: A23187 for Ca^{2+} and pyrithione (PTO) for Zn^{2+}. The results (Figure 3. 6D-F) show that increasing the Ca^{2+} entry via A23187 had no major effect on mitochondrial dynamics, but, interestingly, co-treatment with BAPTA-AM led to mitochondrial fragmentation (Figure 3. 6D-F). Delivery of Zn^{2+} through PTO (using the Zn-PTO complex) caused extensive mitochondrial fragmentation and co-application of TPEN was able to antagonise the effect of Zn-PTO. These results indicate that basal levels of Ca^{2+} are required for healthy mitochondrial dynamics while excess Zn^{2+} promotes mitochondrial fragmentation.

Taken together, these data indicate that Zn^{2+}, rather than Ca^{2+}, plays a major role in mitochondrial fragmentation during palmitate-induced stress on the β-cells.
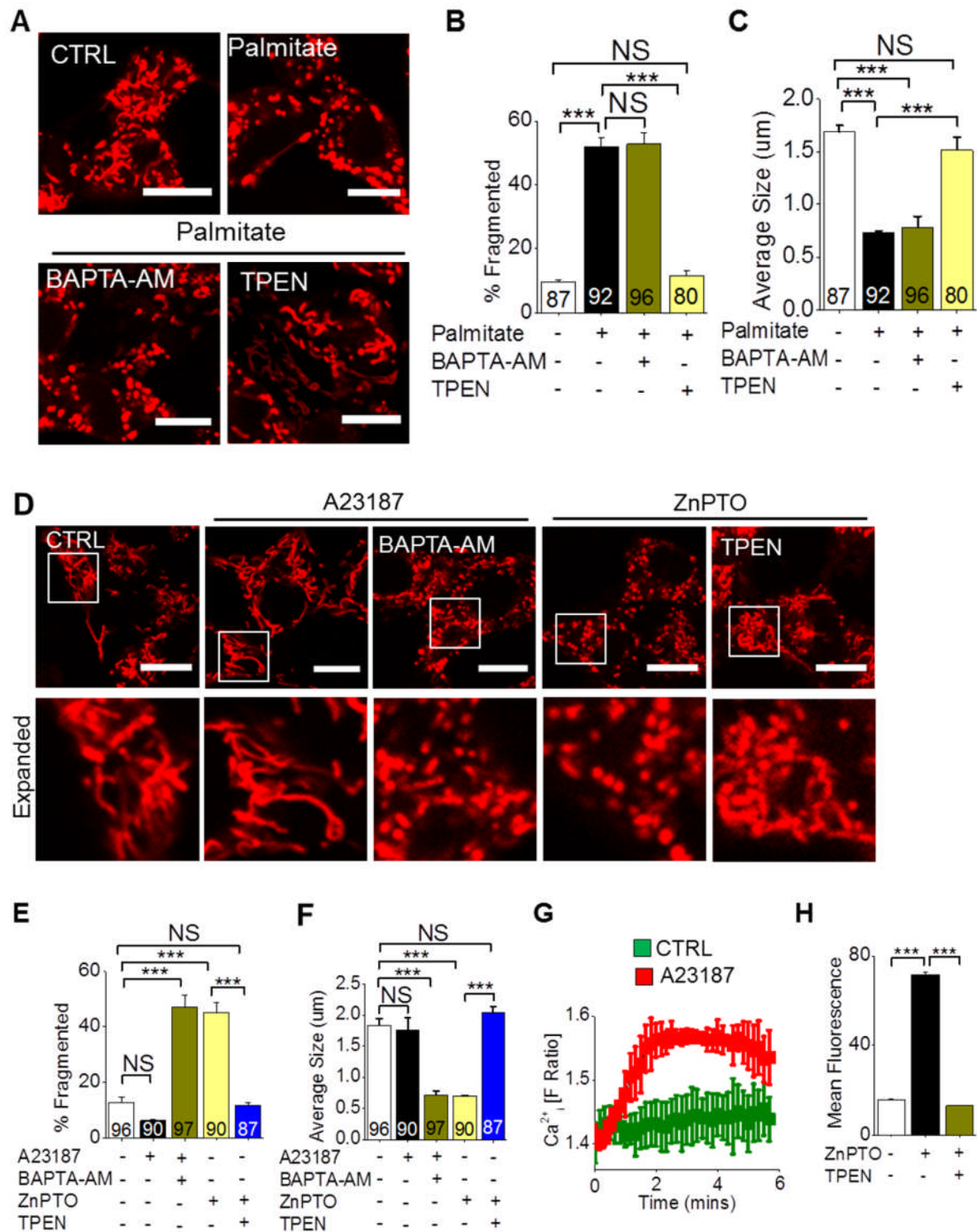
Figure 3. 6 Zn²⁺, rather than Ca²⁺, mediates palmitate induced mitochondrial fragmentation. (**A**) Fluorescent images of INS1 cells exposed to medium alone (CTRL), or medium containing palmitate (500 μM) with or without BAPTA-AM (0.8 μM) or TPEN (0.5 μM) for 12 h. Cells were stained with MitoTracker. Representative images show that chelation of Zn²⁺, but not Ca²⁺, prevents palmitate induced mitochondrial fragmentation. Scale bars: 10 μm. (**B-C**) Mean ± SEM of percent of mitochondrial fragmentation (B) and average size of

mitochondria (C) from three independent experiments performed as in (A). *** indicates $p < 0.001$; ** indicates $p < 0.01$; NS, not significant; one-way Anova with post-hoc Tukey test. (**D**) Cells were treated with medium alone (CTRL), or medium containing A23187 (2 µM) with or without BAPTA-AM (3 µM); Zn-PTO (2 µM) with or without TPEN (3 µM) for 3 hr followed by staining with MitoTracker. Fluorescent images indicate that the rise in cytosolic Ca^{2+} has no effect on mitochondrial structure while Zn^{2+} induces mitochondrial fission. Scale bars: 10 µm. (**E-F**) Mean ± SEM of percent mitochondrial fragmentation (E) and average size of mitochondria (F) from three independent experiments performed as in (D). *** indicates $p < 0.001$; NS, not significant; one-way Anova with post-hoc Tukey test. (**G**) INS1 cells were labelled with Fura-2-AM and then cytosolic Ca^{2+} were measured by FlexstationII Microplate Reader during the application of 2 µM A23187 (red) and under control condition (green). (**H**) INS1 cells were treated with medium alone (CTRL), or medium containing Zn-PTO (2 µM) with or without TPEN (3 µM) for 2 hours. Cells were labelled with FluoZin3-AM and then cytosolic Zn^{2+} was measured by FlexstationII Microplate Reader. Mean ± SEM of fluorescence from at least three independent experiments were shown. *** indicates $p < 0.001$; one-way Anova with post-hoc Tukey test.

3. 2. 5 TRPM2 channels and Zn^{2+} mediate palmitate induced Drp1 recruitment to mitochondria

Mitochondria exist as a dynamic branched network that undergoes fast fusion and fission. Under physiological conditions, the fusion and fission events are rigorously regulated by fusion proteins (Mfn1 and 2 and OPA1) and fission proteins (Drp1 and Fis1) respectively. However, in pathological states, such as T2DM, the balance between fusion and fission is disrupted and more fission occurs due to the dys-regulated fission proteins, such as Drp1 (Jheng et al., 2012). Drp1 is mostly present in the cytoplasm of a cell, but is recruited to mitochondria in response to a fission inducing stimulus (Karbowski et al., 2002). To test whether Drp1 recruitment to mitochondria occurs during palmitate treatment, cells were transfected with GFP-tagged Drp1 and then exposed to palmitate. As expected, palmitate treatment induced significant recruitment of Drp1 to mitochondria (Figure 3.7A-B). This was inhibited in cells treated with PJ34 and siRNA, indicating an essential role for TRPM2 in mediating Drp1 recruitment (Figure 3.7A-D). Chelation of Zn^{2+} with TPEN produced a similar effect as TRPM2 inhibition (Figure 3.7A-B). This suggests that TRPM2 mediated changes in Zn^{2+} dynamics influence Drp1 recruitment.

Collectively, these data indicate that inhibition of TRPM2 channels and chelation of Zn^{2+} prevents palmitate induced Drp1 recruitment to mitochondria and mitochondrial fragmentation.
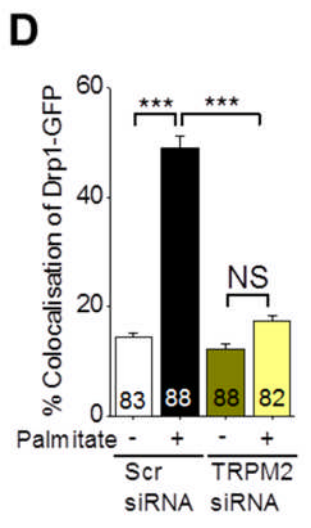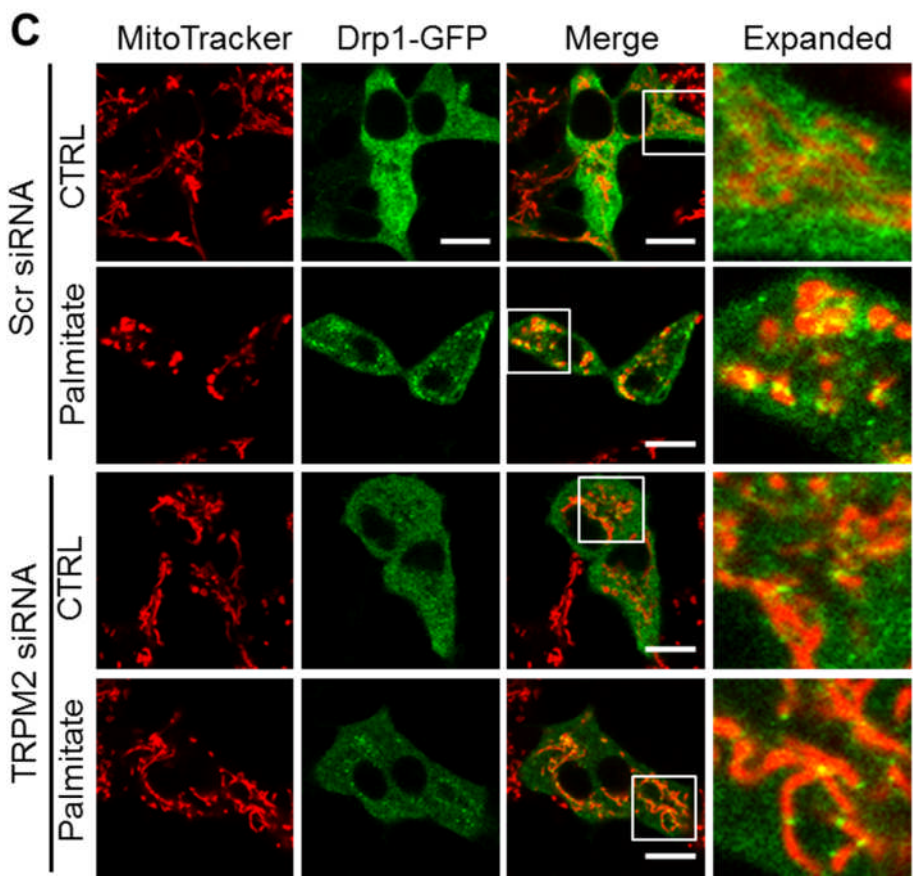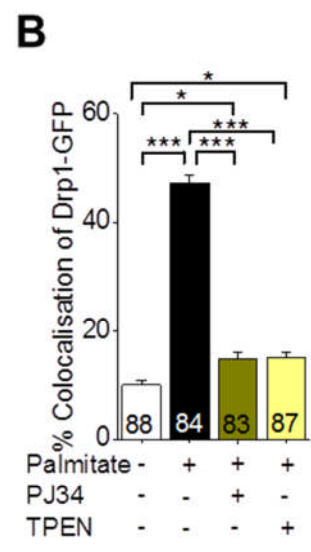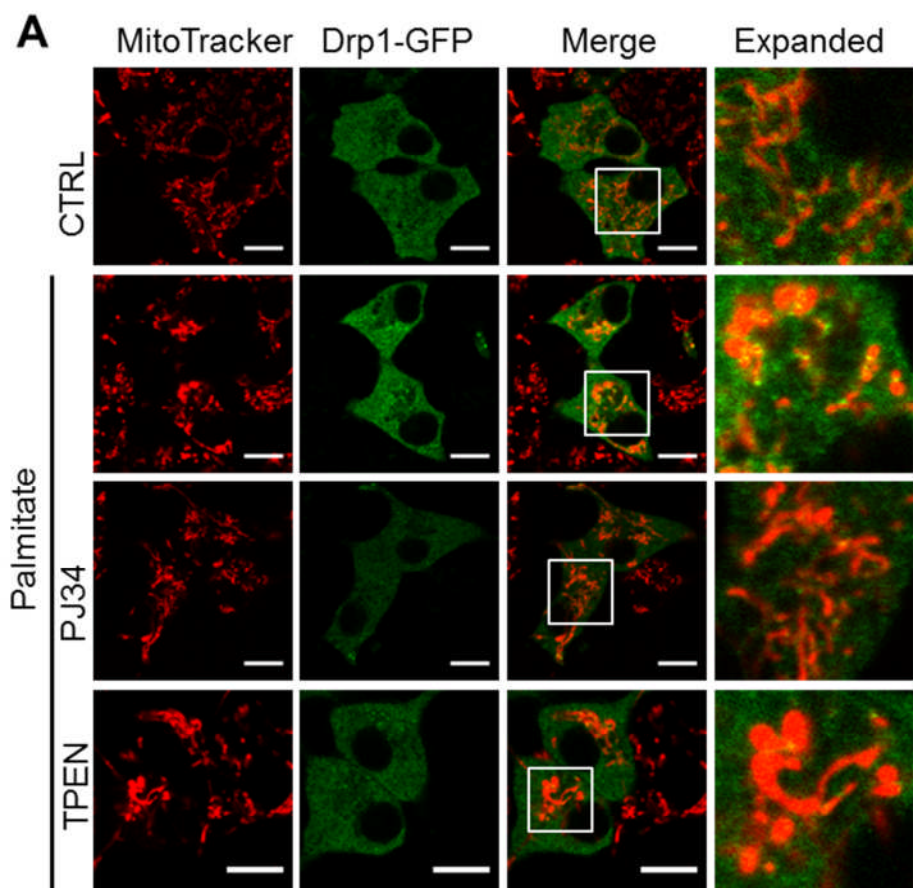
Figure 3. 7 TRPM2 channels and Zn^{2+} mediate palmitate induced Drp1 recruitment to mitochondria. (**A**) INS1 cells were transfected with Drp1-GFP for 48 hours and then exposed to medium alone (CTRL) or medium containing 500 µM palmitate minus or plus PJ34 (10 µM) or TPEN (0.5 µM) for 12 hours. Cells were then stained for mitochondria (MitoTracker). Scale bars: 10 µm. Representative images show that inhibition of TRPM2 channels or chelation of Zn^{2+} blocks palmitate induced Drp1 recruitment to mitochondria and the subsequent mitochondrial fragmentation. (**B**) Percentage co-localization of Drp1-GFP with MitoTracker was calculated from data in (A). Data are presented as mean ± SEM (n = 3); statistical analysis was performed by one-way Anova with post-hoc Tukey test; *** indicates p <0.001; * indicates p <0.05. (**C**) INS1 cells were co-transfected with Drp1-GFP and scrambled siRNA or siRNA targeted to TRPM2 channels (siRNA-TRPM2) for 60 hours and cells were then treated with medium (CTRL) or medium containing palmitate (500 µM) for 12 hours. Cells were stained for mitochondria (MitoTracker). The fluorescent images show that silencing of TRPM2 channels with siRNA prevents palmitate induced Drp1 localisation to mitochondria and subsequent mitochondrial fragmentation. (**D**) Percentage co-localization of Drp1-GFP with MitoTracker was calculated from data in (C). Data are from three independent experiments (number of cells used for quantification are indicated within each bar) as mean ± SEM (n = 3); *** indicates p < 0.001; NS, not significant; one-way Anova with post-hoc Tukey test.

3. 2. 6 Both Ca^{2+} and Zn^{2+} are able to mediate Drp1 recruitment to mitochondria in INS1 cells

The role of Zn^{2+} in mediating Drp1 recruitment to mitochondria has been demonstrated above; however, the role of Ca^{2+} is unclear although previous studies have reported that disrupted Ca^{2+} homeostasis is strongly associated with Drp1 recruitment to mitochondria (Cereghetti et al., 2008; Xu et al., 2013). By treating cells with Ca^{2+} ionophore and Zn^{2+} ionophore, the effects of rise in intracellular Ca^{2+} and Zn^{2+} on Drp1 distribution was tested. In contrast to the lack of effect of A23187 on mitochondrial fragmentation (Figure 3. 6D), A23187 caused an increase in Drp1 recruitment to mitochondria (Figure 3. 8). Despite Drp1 recruitment, mitochondria of A23187 treated cells displayed tubular structures. This finding is consistent with the data in Figure 3. 6D. Zn^{2+} ionophore induced a marked increase in Drp1 recruitment to mitochondria as well as mitochondrial fragmentation (Figure 3.8). Furthermore, Zn-PTO caused significantly greater Drp1 recruitment compared with the Ca^{2+} ionophore.

These results suggest that both Ca^{2+} and Zn^{2+} can mediate Drp1 recruitment to mitochondria but compared to Ca^{2+}, Zn^{2+} plays a dominant role in promoting Drp1 recruitment to mitochondria. Furthermore, it is the rise in cytosolic Zn^{2+}, rather than Ca^{2+}, that induces mitochondrial fragmentation. The reason for why Ca^{2+} induces Drp1 recruitment, but fails to induce mitochondrial fragmentation is unclear.
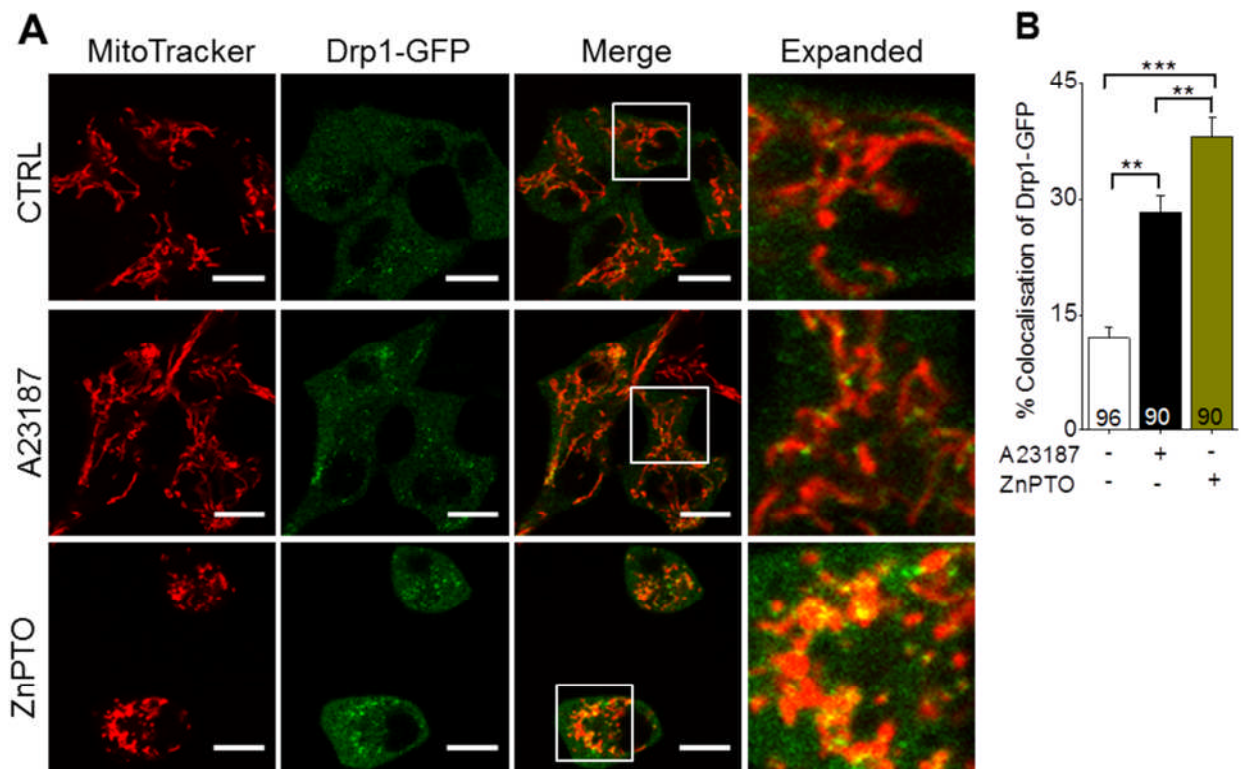
Figure 3. 8 Both Ca^{2+} and Zn^{2+} increase Drp1 recruitment to mitochondria in INS1 cells.
(**A**) INS1 cells were transfected with Drp1-GFP for 48 hours and then exposed to the medium alone (CTRL) or medium containing 2 µM A23187 or 2 µM Zn-PTO for 3 hours. Cells were then stained for mitochondria (MitoTracker). Scale bars: 10 µm. Representative images show that the effect of Zn^{2+} on Drp1 recruitment to mitochondria is greater than that of Ca^{2+}. (**B**) Percentage co-localization of Drp1-GFP with MitoTracker was calculated from three independent experiments (number of cells used for quantification is indicated within each bar) performed as in (A). Data are presented as mean ± SEM; statistical analysis was performed by one-way Anova with post-hoc Tukey test, *** indicates $p < 0.001$; ** indicates $p < 0.01$.

3. 2. 7 Palmitate causes a rise in Zn^{2+} levels of mitochondria

Effect of Zn^{2+} on mitochondria has been demonstrated above. To investigate how Zn^{2+} mediates mitochondrial fragmentation, effect of palmitate on mitochondrial Zn^{2+} levels was examined. INS1 cells were loaded with FluoZin3-AM and MitoTracker. In pancreatic β-cells, it has been demonstrated that two Zn^{2+} ions coordinate six insulin monomers to form hexameric-structure on which matured insulin crystals are based (Li, 2014). Therefore, Zn^{2+} staining by FluoZin3-AM here could, in part, be due to insulin granules. In untreated cells, there was little Zn^{2+} in mitochondria. Following palmitate treatment, there was a significant increase in Zn^{2+} stain in fragmented mitochondria (Figure 3. 9). The effect was rapid and occurred within 4 hours. Longer incubation (12 and 24 hrs) led to the appearance of MitoTrakcer stain in the cytoplasm, presumably caused by the increased permeability of mitochondria.

These results demonstrate that palmitate causes an increase in the levels of free Zn^{2+} in mitochondria. However, the source of Zn^{2+} is unclear.
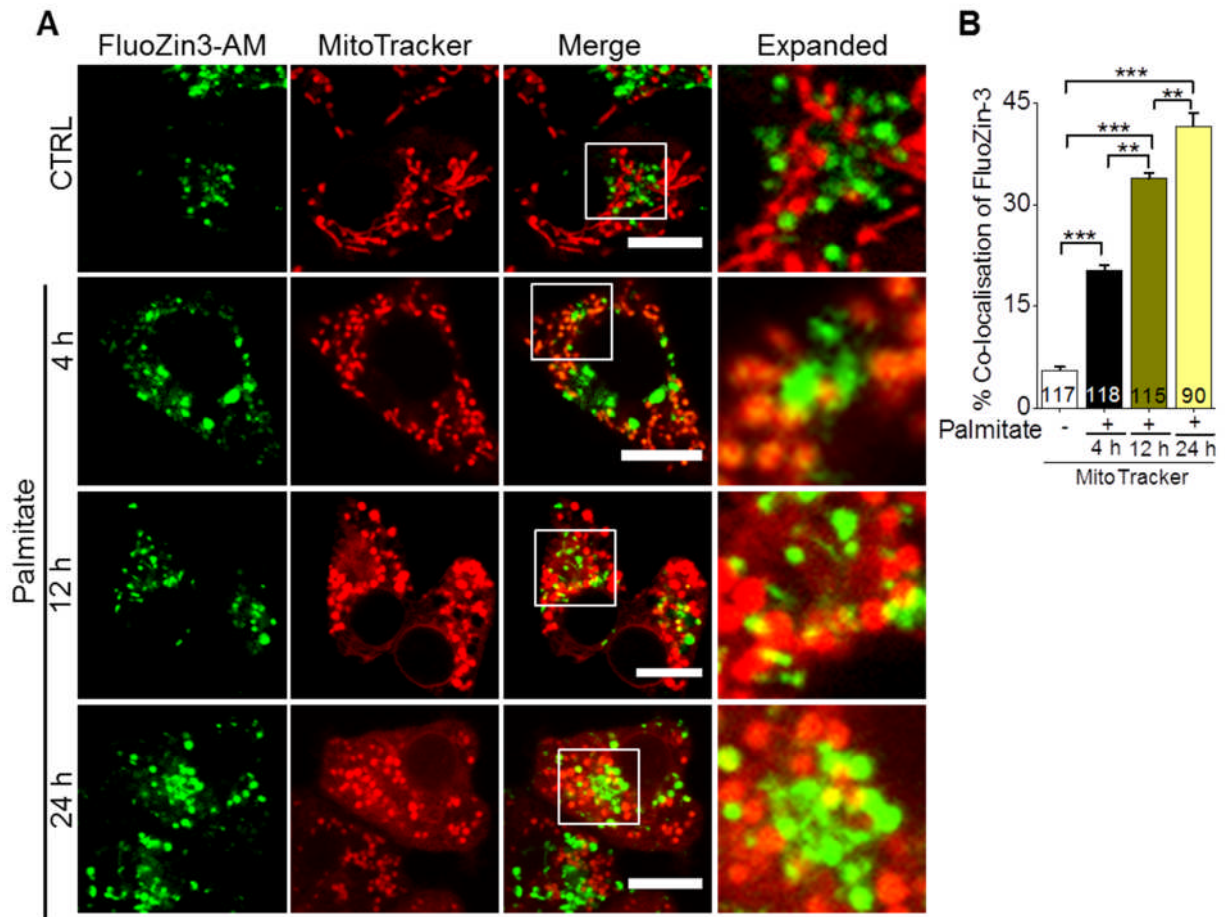
Figure 3. 9 Palmitate causes a rise in Zn^{2+} levels of mitochondria. (**A**) Fluorescent images of INS1 cells co-stained for Zn^{2+} (FluoZin3-AM) and mitochondria (MitoTracker). Images were taken from cells exposed to medium alone (CTRL) or medium containing 500 μM palmitate for 4 hours, 12 hours or 24 hours. Merged and expanded images show that palmitate treatment causes Zn^{2+} accumulation (yellow) in the mitochondria. Scale bars: 10 μm. Boxed regions in the merged images are magnified in the far right panels. (**B**) Data was analysed as in Figure 3. 8.

3. 2. 8 Inhibition of TRPM2 channels or chelation of Zn^{2+} prevents palmitate induced Zn^{2+} distribution to mitochondria

It is shown above that inhibition of TRPM2 channels rescues palmitate induced mitochondrial fragmentation (Figure 3. 4D-I). In addition, there was Zn^{2+} accumulation in the mitochondrial fragments. One possible explanation for this is that TRPM2 channels mediate Zn^{2+} accumulation in mitochondria thereby causing mitochondrial fragmentation. When PJ34 was co-applied with palmitate to INS1 cells, both mitochondrial fragmentation and Zn^{2+} rise in mitochondria were significantly prevented (Figure 3.10A-B). In addition, when TRPM2 expression was silenced with siRNA, palmitate failed to promote Zn^{2+} accumulation in mitochondria (Figure 3.10C-D). These findings indicate that TRPM2 channels might mediate Zn^{2+} accumulation in mitochondria.

When the Zn^{2+} chelator TPEN was co-applied with palmitate to INS1 cells, palmitate failed to induce Zn^{2+} rise in mitochondria and mitochondrial fragmentation (Figure 3.10A-B). Intriguingly, there was significant Zn^{2+} staining in punctate structures. Given the affinity of TPEN is very high for free Zn^{2+}, this finding is hard to explain. It is possible that TPEN was unable to enter these structures or the conditions within these structures are unfavourable for binding of Zn^{2+} to TPEN. These structures, as shown above are likely lysosomes, where the pH is low.

These experiments suggest that palmitate induced mitochondrial fragmentation may be dependent on TRPM2 mediated Zn^{2+} uptake by mitochondria.
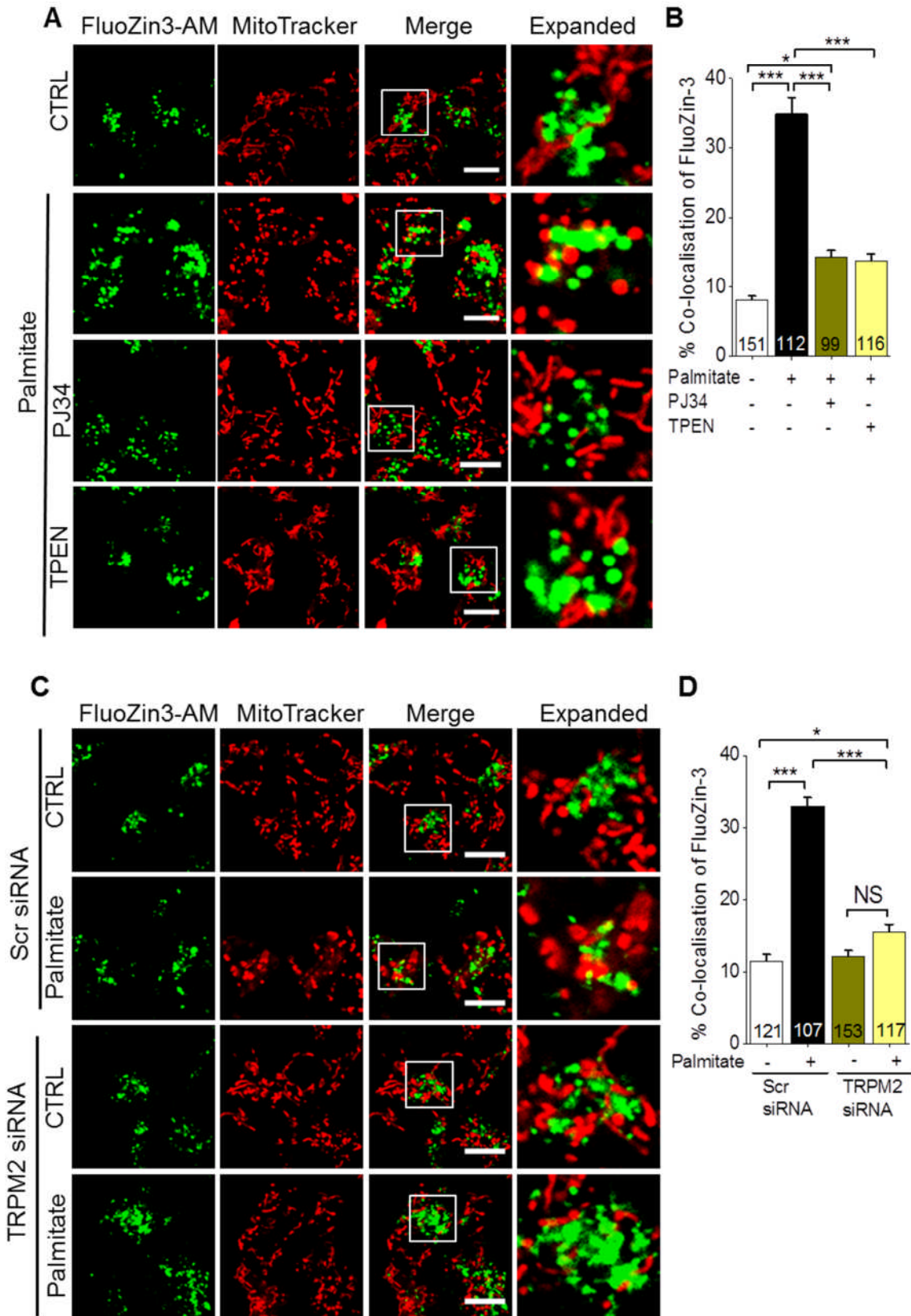
Figure 3. 10 Inhibition of TRPM2 channels or chelation of Zn²⁺ prevents palmitate induced Zn²⁺ distribution to mitochondria. (**A**) Fluorescent images of INS1 cells co-

stained for Zn^{2+} (FluoZin3-AM) and mitochondria (MitoTracker). Images were taken from cells exposed to medium alone (CTRL) or medium containing 500 μM palmitate minus or plus a TRPM2 blocker (10 μM PJ34) or Zn^{2+} chelator (0.5 μM TPEN) for 12 hours. Merged and expanded images show that inhibition of TRPM2 channels by PJ34 or chelation of Zn^{2+} with TPEN prevents Zn^{2+} rise in mitochondria (yellow puncta). (**B**) Percentage co-localization of FluoZin-3 with MitoTracker was calculated from data in (A). Data represent mean ± SEM (n = 3); statistical analysis was performed by one-way Anova with post-hoc Tukey test; *** indicates p <0.001; * indicates p <0.05. (**C**) INS1 cells were transfected with scrambled siRNA or siRNA targeted to TRPM2 channels (siRNA-TRPM2) after 60 hours, cells were treated with or without 500 μM palmitate for 12 hours; Representative fluorescent images of cells co-stained for Zn^{2+} (FluoZin3-AM) and mitochondria (MitoTracker) indicate that silencing of TRPM2 channels prevents palmitate induced rise in mitochondrial Zn^{2+}. (**D**) Data was analysed as in (B). In all the images, scale bars: 10 μm. Boxed regions in the merged images are magnified in the far right panels.

3. 2. 9 Inhibition of TRPM2 channels or chelation of Zn^{2+} rescues palmitate induced dissipation of mitochondrial membrane potential (ΔΨm)

Previous studies have demonstrated a link between the loss of mitochondrial membrane potential (ΔΨm) and mitochondrial network alteration (Bach et al., 2003; Benard et al., 2007). Since palmitate has been shown to cause loss of ΔΨm in pancreatic β-cells, leading to mitochondrial dysfunction (Koshkin et al., 2008), it is possible that palmitate induced mitochondrial fragmentation (Figure 3. 2) is linked to loss of ΔΨm of INS1 cells. Accordingly, the effect of palmitate on ΔΨm was investigated.

INS1 cells were labelled with JC-10, a mitochondrial membrane potential probe, and ΔΨm was assessed by flow cytometry. CCCP, a chemical inhibitor of oxidative phosphorylation in mitochondria, was used as a positive control. The results show that CCCP causes significant loss of ΔΨm (Figure 3. 11) as reported previously (Minamikawa et al., 1999). Exposure of cells to palmitate also caused significant loss of ΔΨm within 6 hours (data not shown), the effect of which was exacerbated after 12 hours (Figure 3.11). Chelation of Zn^{2+} with TPEN prevented ΔΨm loss, indicating a role for Zn^{2+} in palmitate induced ΔΨm loss. Inhibition of TRPM2 channels with PJ34 and TRPM2 siRNA attenuated palmitate induced dissipation of ΔΨm (Figure 3.11).

These findings indicate a key role for TRPM2 channels and Zn^{2+} in palmitate induced ΔΨm loss.
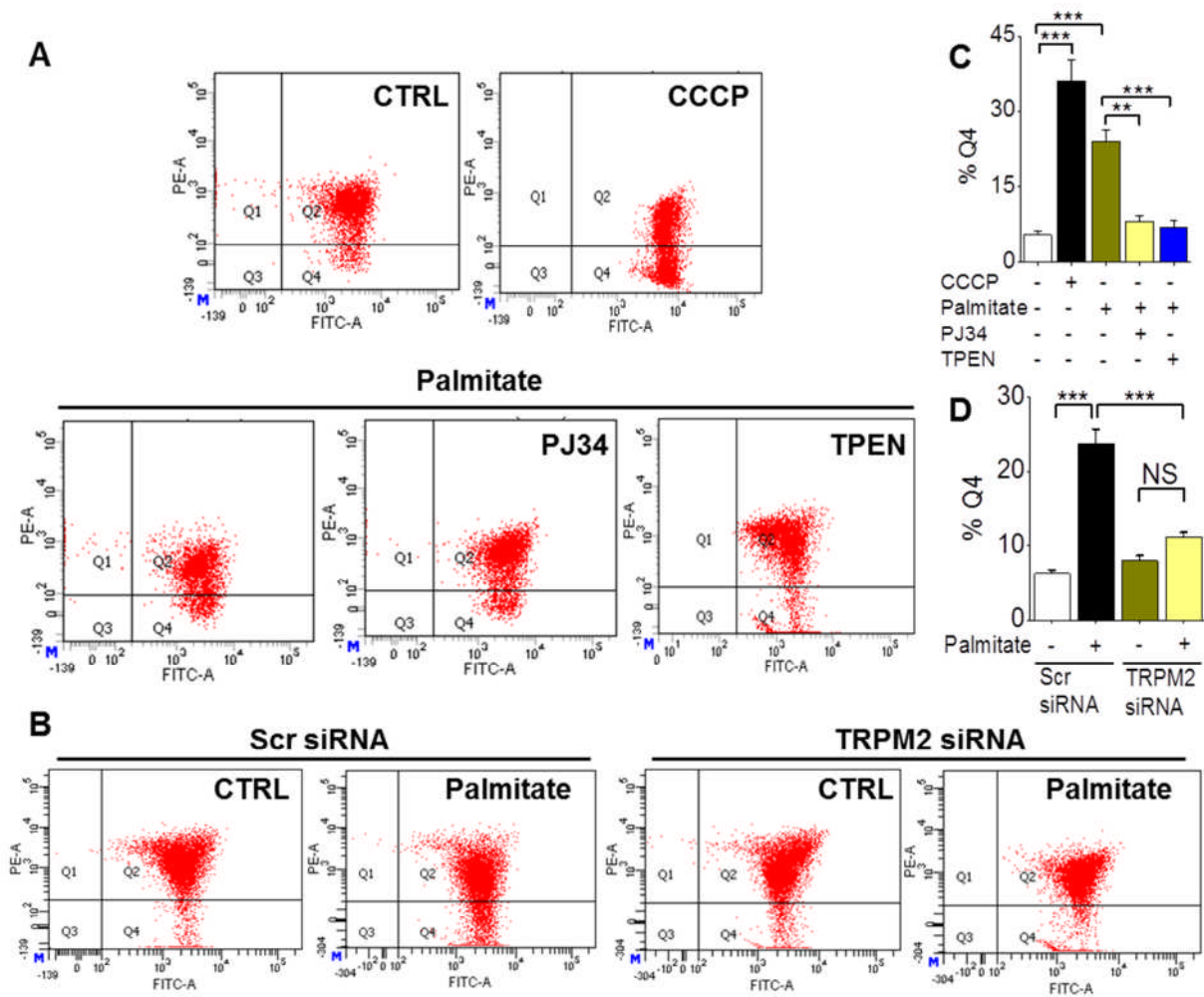
Figure 3. 11 Inhibition of TRPM2 channels or chelation of Zn²⁺ rescues palmitate induced dissipation of mitochondrial membrane potential (ΔΨm). (**A**) INS1 cells were exposed to medium alone (CTRL) or medium containing 0.5 µM protonophore CCCP or 500 µM palmitate minus or plus PJ34 (10 µM) or TPEN (0.5 µM) for 12 hours. Cells were then trypsinised and stained with JC-10 at 37°C for 30 min before loading to LSRFortessa™ flow cytometer (BD Biosciences). The green (FITC) and red (PE-A) fluorescence values from 5000 cells was collected by flow cytometer. The data show that inhibition of TRPM2 channels or chelation of Zn²⁺ prevents palmitate induced dissipation of mitochondrial membrane potential. (**B**) INS1 cells were transfected with scrambled siRNA or siRNA targeted to TRPM2 channels (siRNA-TRPM2) for 60 hours and cells were treated without (CTRL) or with 500 µM palmitate for 12 hours. Cells were subjected to flow cytometry as in (A). The green (FITC) and red (PE-A) fluorescence values from 8000 cells was collected by flow cytometer. The results indicate that silencing TRPM2 channels with siRNA inhibits palmitate induced loss of ΔΨm. (**C-D**) Mean ± SEM of percent of cells from region Q4 (representing loss of ΔΨm) from data in (A) and (B) respectively following the indicated treatments (n=3). *** indicates $p < 0.001$; ** indicates $p < 0.01$; NS, not significant; one-way Anova with post-hoc Tukey test.

3. 2. 10 Zn^{2+}, but not Ca^{2+}, induces dissipation of ΔΨm in INS1 cells

Studies have shown that rise in cytosolic Ca^{2+} and Zn^{2+} is accompanied by the uptake of these ions by mitochondria (Collins et al., 2001; Sensi et al., 2000). Previous studies have reported that Ca^{2+} uptake by mitochondria can dissipate ΔΨm (Lemasters and Nieminen, 1997; Lemasters et al., 1998); the role of Ca^{2+} on ΔΨm was therefore first assessed. Contrary to the previous reports, raising intracellular Ca^{2+} with A23187 failed to induce mitochondrial membrane depolarization (Figure 3.12). This finding, however, is consistent with the above data (Figure 3. 6D-F) where A23187 showed no effect on mitochondrial dynamics (which is known to be dependent on the loss of ΔΨm). In contrast to Ca^{2+}, raising cytosolic Zn^{2+}, with Zn-PTO, caused marked dissipation of ΔΨm (Figure 3.12). Chelation of Zn^{2+} with TPEN prevented palmitate induced ΔΨm loss (Figure 3.12A-B). In addition, inhibition of TRPM2 channels with pharmacological inhibitors (PJ34 and 2-APB) significantly prevented Zn^{2+} induced loss of ΔΨm in INS1 cells.

Taken together with the previous data, these results suggest that TRPM2 channels mediate redistribution of cytosolic Zn^{2+} to mitochondria, and thereby induce ΔΨm loss. The data also suggest that rise in cytosolic Zn^{2+}, rather than Ca^{2+}, has a major impact on the mitochondrial membrane potential of INS1 cells.
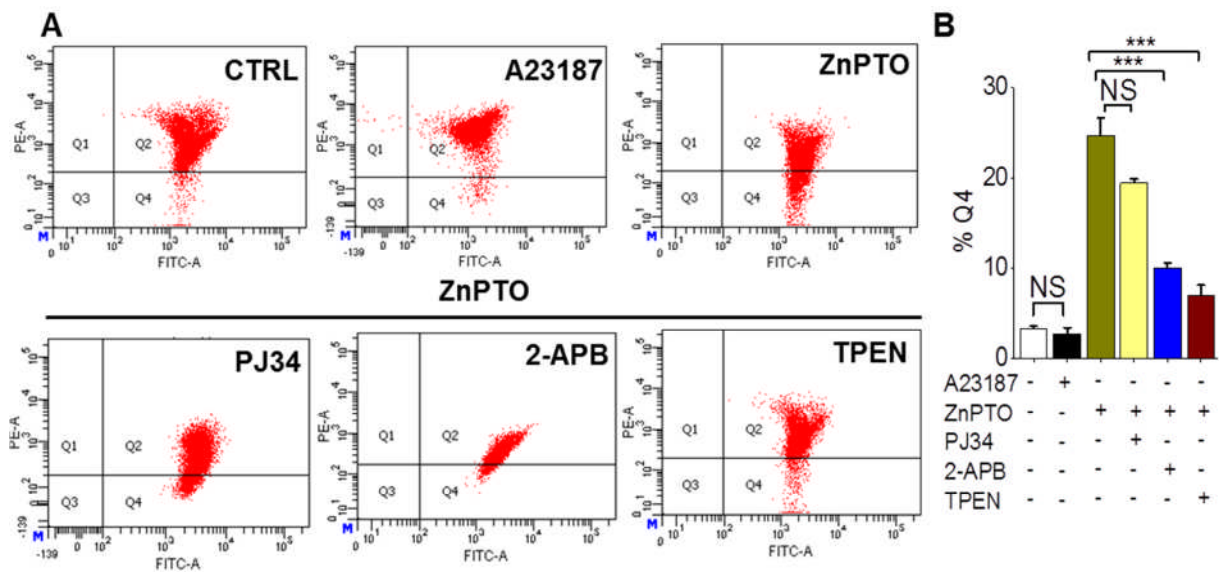
Figure 3. 12 Zn^{2+}, but not Ca^{2+}, induces mitochondrial membrane depolarization in INS1 cells. (**A**) INS1 cells were treated with the medium alone (CTRL), A23187 (2 μM), ZnPTO (2 μM) without or with TRPM2 inhibitors (10 μM PJ34 and 50 μM 2-APB) and TPEN (3 μM) for 3 hours. Cells were trypsinised and stained with JC-10 at 37°C for 30 min before loading to LSRFortessa™ flow cytometer. The green (FITC) and red (PE-A) fluorescence value from 5000 cells was collected by flow cytometer. (**B**) Data was analysed as in Figure 3.11

3. 2. 11 Inhibition of TRPM2 channels or chelation of Zn^{2+} prevents palmitate induced mitochondrial ROS production

Mitochondria generate energy within the cells. Oxidative phosphorylation in the inner mitochondrial membrane produces a large amount of ATP for the different intracellular processes. However, during oxidative phosphorylation, superoxide can be generated due to a small amount of electrons escaping from the ETC and leaking to oxygen directly (Newsholme et al., 2007). In the physiological state, superoxide can be quickly degraded. However, in pathological situations, this superoxide can accumulate within mitochondria to impart ROS-related diseases. Previous data (Figure 3. 1) have shown that palmitate causes an increase in cytosolic ROS through activation of NOX2. The data in Figure 3.1 also revealed marked ROS stain in punctate structures that resembled mitochondria in terms of morphology. Given that chronic exposure of palmitate disrupts mitochondrial network (Figure 3. 2), it was surmised that palmitate might stimulate mitochondrial ROS production, thereby exerting adverse effects on mitochondria. The mitochondrial ROS level was therefore assessed by staining with Mito-SOX, a dye specific for superoxide production in mitochondria. As predicted, palmitate increased the mitochondrial ROS level as displayed by the increased fluorescence both in mitochondria and the cytoplasm (Figure 3.13A-B). Besides, the increase in mitochondrial ROS production was accompanied by the loss of mitochondrial network and appearance of mitochondrial fragments. These results argue that the mitochondrial fragmentation is linked to excess ROS production in mitochondria. Therefore, it was predicted that inhibition of TRPM2 channels may rescue palmitate induced excess mitochondrial ROS production as inhibition of TRPM2 channels significantly reversed mitochondrial fission induced by palmitate. PJ34 treatment indeed prevented palmitate induced mitochondrial ROS production (Figure 3.13A-B). Silencing of TRPM2 channels in INS1 cells produced similar results as PJ34 (Figure 3.13C-D). Taken together, these data indicate that TRPM2 channels mediate mitochondrial ROS production during chronic exposure of INS1 cells to palmitate.

The effect of Zn^{2+} and Ca^{2+} on mitochondrial ROS production was next examined. As shown in Figure 3.13A-B, chelation of Zn^{2+} with TPEN prevented palmitate induced increase in mitochondrial ROS production. When the cytosolic Zn^{2+} level was elevated with Zn-PTO, a marked increase in mitochondrial ROS was observed (Figure 3.13E-F). Raising cytosolic Ca^{2+} with A23187 also caused an increase in mitochondrial ROS production but the effect is significantly less than that of Zn^{2+} (Figure 3.13E-F).

Collectively, these results demonstrate that while both Ca^{2+} and Zn^{2+} contribute to mitochondrial ROS production in INS1 cells, Zn^{2+} appears to play a dominant role.
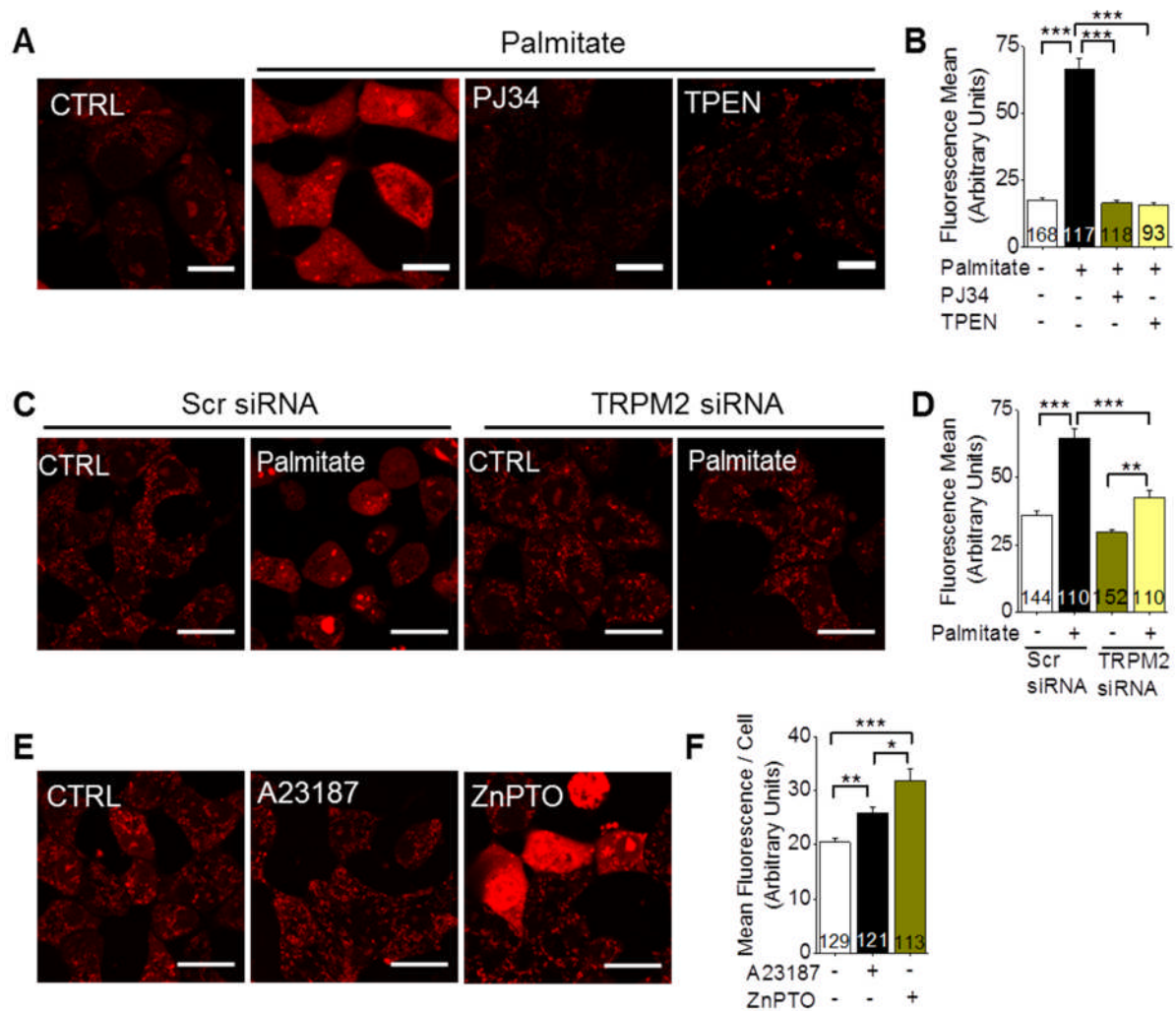
Figure 3. 13 Inhibition of TRPM2 channels or chelation of Zn^{2+} prevents palmitate induced mitochondrial ROS production. (**A**) Fluorescent images of INS1 cells stained for mitochondrial superoxide using Mito-SOX. Images were taken from cells exposed to medium (CTRL) or medium containing 500 µM palmitate minus or plus PJ34 (10 µM) or TPEN (0.5 µM) for 12 hours. The images show that inhibition of TRPM2 channels or chelation of Zn^{2+} prevents palmitate induced mitochondrial ROS production. Scale bars: 20 µm. (**B**) Mean ± SEM of data from (A) expressed as mean fluorescence per cell (number of cells used for quantification are within each bar) following the indicated treatments (n = 4); *** indicates $p <$ 0.001; one-way Anova with post-hoc Tukey test. (**C**) INS1 cells were transfected with scrambled siRNA or siRNA targeted to TRPM2 channels (siRNA-TRPM2) for 60 hours and cells were then treated without (CTRL) or with 500 µM palmitate for 12 hours and stained with Mito-SOX. The images show that silencing of TRPM2 channels inhibits palmitate induced mitochondrial ROS production. Scale bars: 20 µm. (**D**) Data was analysed as in (B); ** indicates $p <$ 0.01. (**E**) INS1 cells were treated without (CTRL), or with A23187 (2 µM) or ZnPTO (2 µM) for 3 hours and stained with Mito-SOX. Representative images show that raising cytosolic Zn^{2+} causes significant mitochondrial ROS production while raising cytosolic Ca^{2+} has less effect. Scale bars: 20 µm. (**F**) Data was analysed as in (B); * indicates $p <$ 0.05.

3. 2. 12 TRPM2 channels and Zn^{2+} mediate palmitate induced apoptosis of INS1 cells

Mitochondrial dysfunction has been linked to apoptosis in many cell types, including β-cells (Maestre et al., 2003). Above findings revealed that palmitate exposure causes mitochondrial fragmentation as well as depolarization of mitochondrial membrane, and these changes are known to be associated with apoptosis (Arnoult, 2007; Ly et al., 2003). Therefore, viability of INS1 cells after palmitate treatment was tested by labelling the treated cells with Annexin V-GFP and propidium iodide (PI) and measuring cell death by flow cytometry. Annexin V-GFP was used to detect the apoptotic cells. Under normal conditions, phosphatidylserine (PS) is located in the inner leaflet of the plasma membrane and is unavailable to Annexin V-GFP. When apoptosis is induced, PS is exposed to the outer leaflet of the membrane and can be labelled with Annexin V-GFP. PI was used to detect dead cells as PI is membrane impermeable and is excluded from live cells. The results show that palmitate induces apoptosis of INS1 cells, as indicated by the increase in Annexin-V and PI-positive cells (Figure 3.14A and C). Furthermore, inhibition of TRPM2 channels with PJ34 and siRNA significantly prevented palmitate induced apoptosis (Figure 3.14A-D).

In addition, chelation of Zn^{2+} significantly rescued palmitate stimulated apoptosis (Figure 3.14A and C), indicating the essential role of Zn^{2+} in palmitate induced apoptosis.

Taken together, these data suggest that TRPM2 channels and Zn^{2+} mediate β-cell apoptosis during palmitate induced oxidative stress.
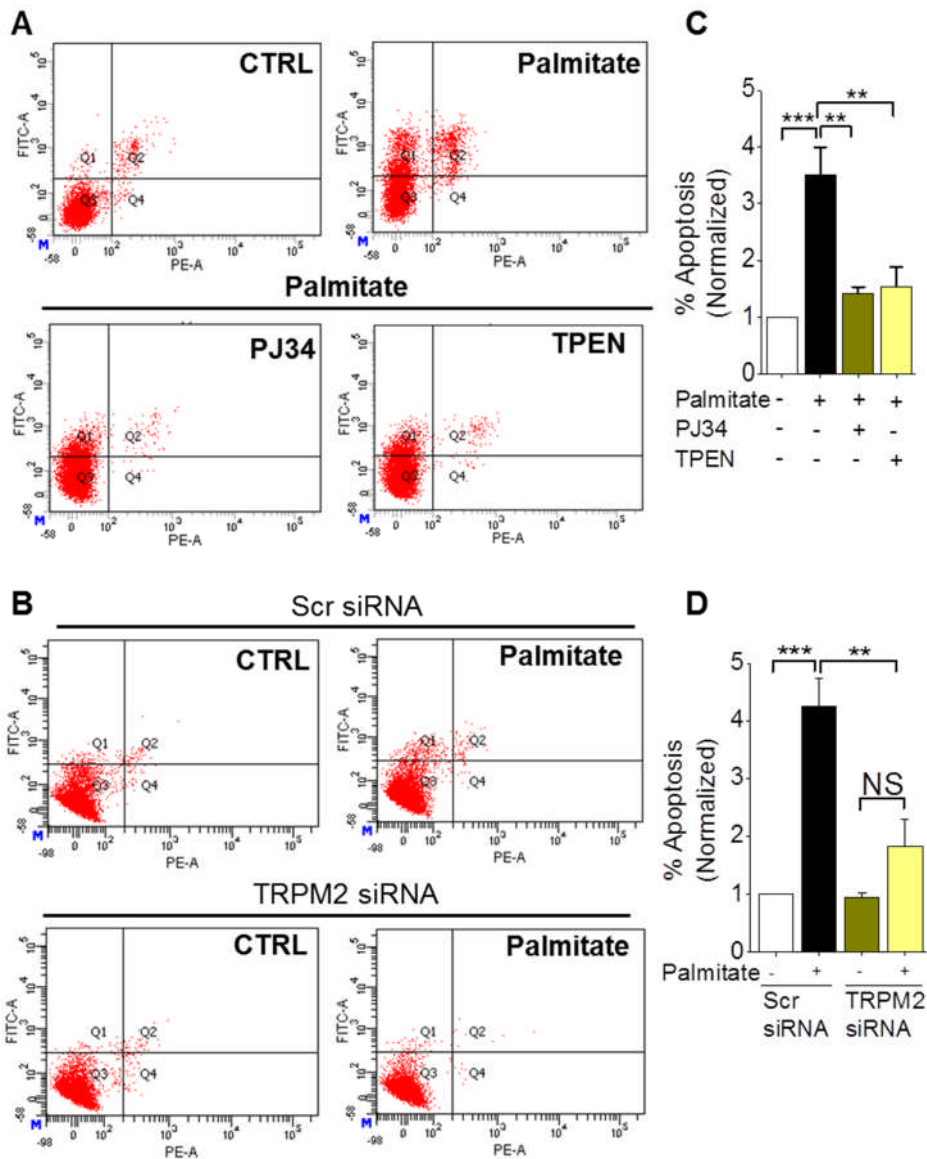
Figure 3. 14 TRPM2 channels and Zn²⁺ mediate palmitate induced apoptosis in INS1 cells. (**A**) INS1 cells were treated with the medium alone (CTRL) or medium containing 500 µM palmitate minus or plus PJ34 (10 µM) or TPEN (0.5 µM) for 12 hrs. Then cells were stained with Annexin V-GFP and PI before loading to LSRFortessa™ flow cytometer. The green (FITC) and red (PE-A) fluorescence value from 8000 cells was collected by flow cytometer. Q1: Live cells undergoing apoptosis; Q2: dead apoptotic cells; Q3: live cells; Q4: dead cells. Representative data show that inhibition of TRPM2 channels with PJ34 and chelation of Zn²⁺ with TPEN prevents palmitate induced apoptosis. (**B**) INS1 cells were transfected with scrambled siRNA or siRNA-TRPM2 for 60 hrs followed by desired treatment. Cells were stained and subjected to flow cytometry as in (A). Representative data from 5000 cells are presented and suggest that TRPM2 channels mediate palmitate induced apoptosis in INS1 cells. (**C-D**) Mean ± SEM of percent apoptotic cells (percentage of cells from Q1 and Q2 regions) are shown from three or four independent experiments performed as in (A) and (B) following the indicated treatments (n=3 for C and n= 4 for D). *** indicates $p < 0.001$; ** indicates $p < 0.01$; NS, not significant; one-way Anova with post-hoc Tukey test.

3. 2. 13 Zn^{2+} and Ca^{2+}-induced apoptosis is dependent on TRPM2 channels and calpain respectively

Since raising the cytosolic Zn^{2+} level directly with zinc ionophore induces mitochondrial fragmentation (Figure 3.6) and loss of ΔΨm (Figure 3.12), it is reasonable to speculate that the increased cytosolic Zn^{2+} might lead to adverse effects on cell viability. To investigate the role of Zn^{2+} on cell viability, INS1 cells were treated with the Zn^{2+} ionophore, Zn-PTO. As predicted, Zn-PTO elicited marked increase in apoptosis after 3 hrs of incubation and TPEN significantly inhibited it (Figure 3. 15). Interestingly, Zn^{2+} simulated apoptosis was largely dependent on TRPM2 activation as both PJ34 and 2-APB prevented Zn-PTO induced apoptosis (Figure 3.15).

Above data demonstrated that raising cytosolic Ca^{2+} level had no effect on mitochondrial dynamics (Figure 3.6) and ΔΨm (Figure 3.12). These findings are inconsistent with the previous studies showing that Ca^{2+} uptake by mitochondria causes mitochondrial dysfunction and subsequent apoptosis of neural cells (Kruman and Mattson, 1999). To address the controversy, effect of Ca^{2+} on β-cell viability was examined. After 3 hrs of incubation, A23187 caused extensive apoptosis similar to that induced by Zn-PTO (compare data in Figure 3.16 with Figure 3.15). This finding is interesting because Ca^{2+} induced apoptosis occurred in the absence of mitochondrial fragmentation and loss of ΔΨm (see above), implying that Ca^{2+} induced apoptosis is likely independent on mitochondria.

Previous studies have shown that Ca^{2+} can activate the protease calpain thereby activating caspase 12 to cause apoptosis (Martinez et al., 2010). Thus A23187 could cause apoptosis via calpain-dependent pathway. Consistent with this idea, calpain inhibitor PD150606 almost completely prevented A23187 induced apoptosis. By contrast, TRPM2 inhibitor PJ34 and Zn^{2+} chelator TPEN partially prevented A23187 induced apoptosis (Figure 3.16). The TPEN inhibition of A23187 induced apoptosis could be explained by the fact that elevated Ca^{2+} can induce release of cytotoxic Zn^{2+} either from cytosolic proteins (Sensi et al., 2003) or lysosomes (Manna et al., 2015). The inhibitory effect of PJ34 can be explained by the fact that Zn^{2+} entry into mitochondria is dependent on TRPM2 activation (see above).

Therefore, it is possible that A23187 induced apoptosis is partially mediated by Zn^{2+}. But this explanation is not persuasive enough as A23187 treatment has no effect on mitochondrial structure and ΔΨm and Zn^{2+} induced apoptosis is dependent on mitochondrial fragmentation and ΔΨm loss. Collectively, these data indicate that Zn^{2+} induced apoptosis is mainly dependent on TRPM2 activation, while Ca^{2+} induced apoptosis appears to be largely mitochondria independent and calpain dependent.
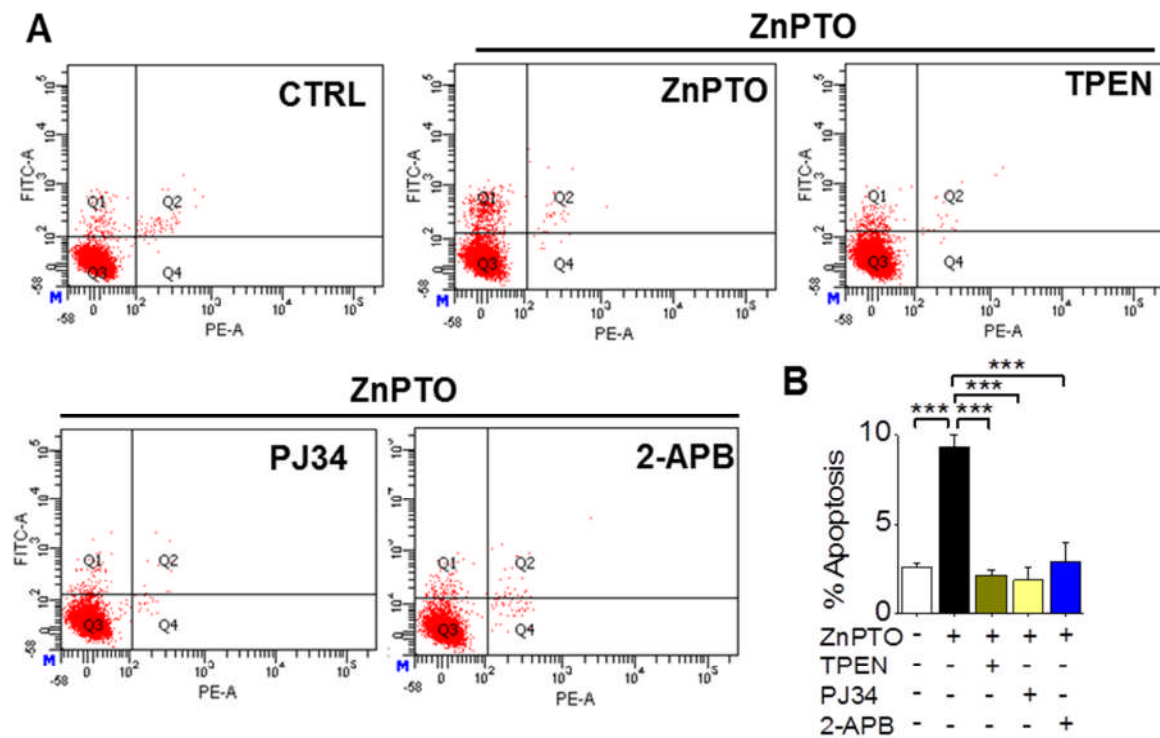
Figure 3. 15 Zn^{2+} induced apoptosis is dependent on TRPM2 channels. (**A**) Cells exposed to medium alone (CTRL), ZnPTO (2 µM) or ZnPTO plus TPEN (3 µM) or TRPM2 inhibitors (10 µM PJ34 and 50 µM 2-APB) were stained with Annexin V-GFP and PI at 37°C for 30 min before loading to LSRFortessa™ flow cytometer. The green (FITC) and red (PE-A) fluorescence values from 8000 cells were collected from the flow cytometer. Representative data show that Zn^{2+} induced apoptosis is dependent on TRPM2 channels. (**B**) Mean ± SEM of percent apoptotic cells (percentage of cells from region Q1 and Q2 region) from three independent experiments performed as in (A). *** indicates $p < 0.001$; one-way Anova with post-hoc Tukey test.
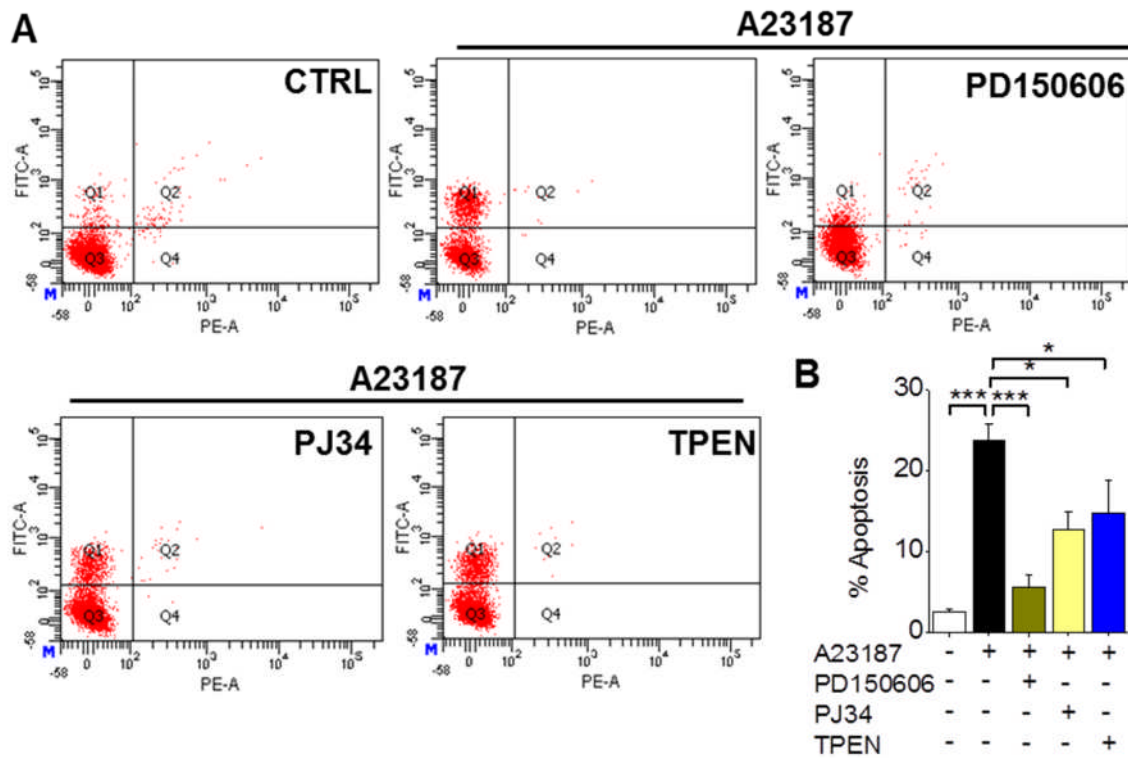
Figure 3. 16 Ca^{2+}-induced cell death is largely calpain dependent and partially dependent on TRPM2 channels. (**A**) Cells exposed to the medium alone (CTRL), A23187 (2 µM), A23187 plus calpain inhibitor (10 µM PD150606) or A23187 plus PJ34 (10 µM) or TPEN (3 µM) were stained with Annexin V-GFP and PI at 37°C for 30 min before loading to LSRFortessa™ flow cytometer. The green (FITC) and red (PE-A) fluorescence values from 8000 cells was collected by flow cytometer. These data show that Ca^{2+} induced apoptosis is largely dependent on calpain activation and partially dependent on TRPM2 channels. (**B**) Mean ± SEM of percent apoptotic cells (percentage of cells from region Q1 and Q2 region) from three independent experiments performed as in (A). *** indicates $p < 0.001$; * indicates $p < 0.05$; one-way Anova with post-hoc Tukey test.

3. 2. 14 TRPM2 inhibition protects mouse and human islets from palmitate induced apoptosis

Since silencing of TRPM2 channels can prevent INS1 cell death induced by palmitate, the role of TRPM2 channels in β-cell death in intact mouse islets was examined using pancreatic islets isolated from TRPM2 deficient mice. Islets isolated from wild-type (WT) mice and TRPM2 knockout (TRPM2$^{-/-}$) mice were stained with Acridine Orange and PI, which stain live cells and dead cells respectively. Chronic exposure of islets to palmitate led to the appearance of a large number of PI stained cells in islets from WT mice (Figure 3.17), while islets from TRPM2$^{-/-}$ mice displayed limited PI-positive staining, indicating the protective role of TRPM2 deficiency against fatty acid induced cell death (Figure 3.17).

In diabetes, in addition to the increase in glucose and fatty acid levels in the blood, cytokines are also increased. It was suggested that cytokines are important factors for development of diabetes (Cnop et al., 2005; Geraldes and King, 2010). Therefore, the effect of palmitate in the absence and presence of cytokines (IL-1β and IFN-γ) on human islets was investigated. The TUNEL assay was used to detect apoptotic cells in islets. As shown in Figure 3.18, the results revealed marked apoptosis when the islets were exposed to a mixture of palmitate and cytokines. Palmitate alone, induced apoptosis, but the effect was modest.

Based on the mouse islets data, the role of TRPM2 channels in palmitate and cytokine induced apoptosis in human islets was examined. Inhibition of TRPM2 channels with PJ34 significantly decreased apoptosis (Figure 3.18). However, PJ34 had no significant effect on apoptosis induced by palmitate alone.

These data are consistent with the INS1 cell data and indicate that TRPM2 inhibition protects mouse islets and human islets from palmitate and cytokines induced cell death.
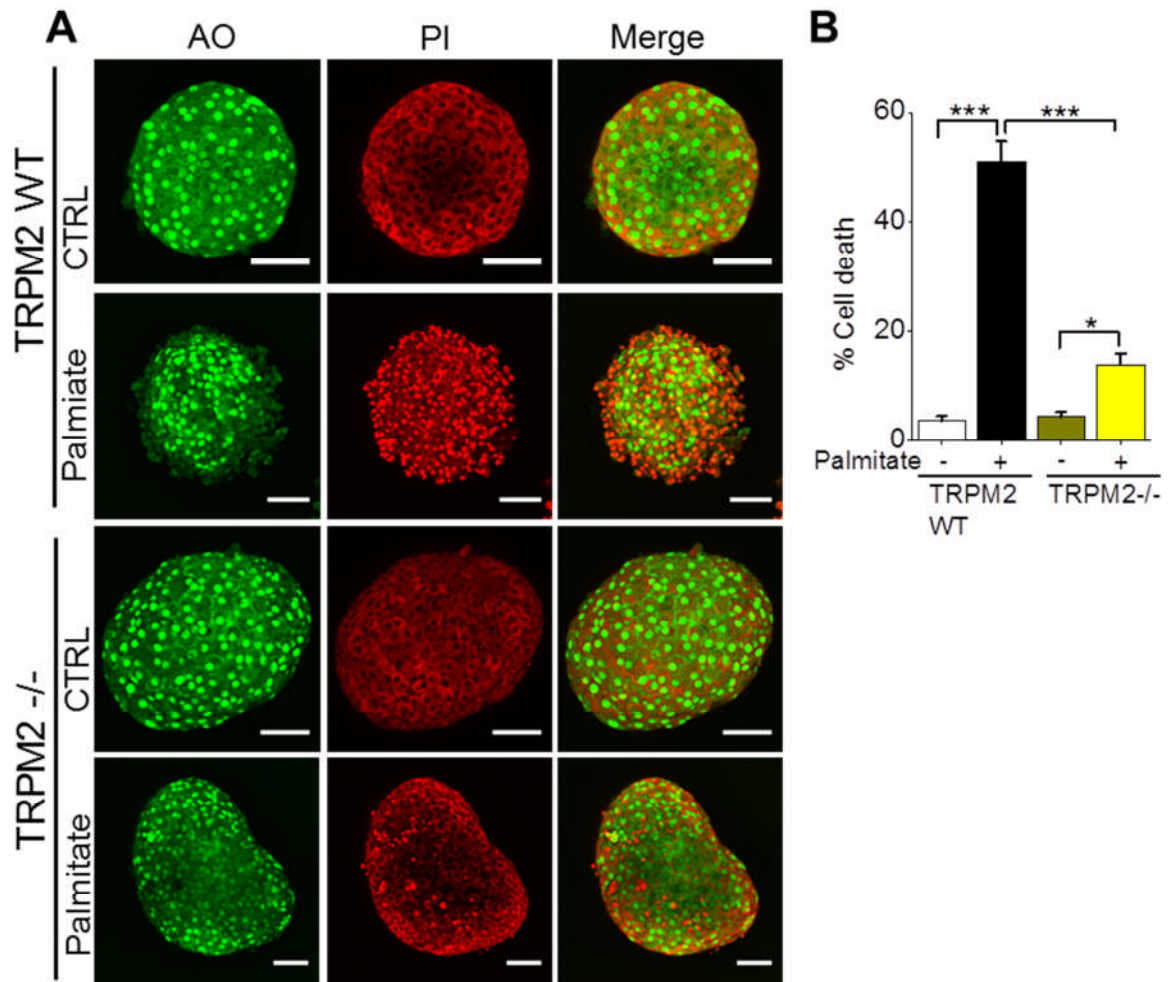
Figure 3. 17 TRPM2 deficiency protects mouse islets from palmitate induced apoptosis. (**A**) Mouse islets isolated from wild type and TRPM2^{-/-} mice were treated with Opti-MEM alone (CTRL) or Opti-MEM containing 500µM palmitate for 5 days before staining with Acridine Orange (green) and PI (red). Representative images show that TRPM2 deficiency prevents palmitate induced cell death in mice. (**B**) Mean ± SEM of percent cell death is shown from three independent experiments performed as in (A); *** indicates $p < 0.001$; ** indicates $p < 0.01$; one-way Anova with post-hoc Tukey test.
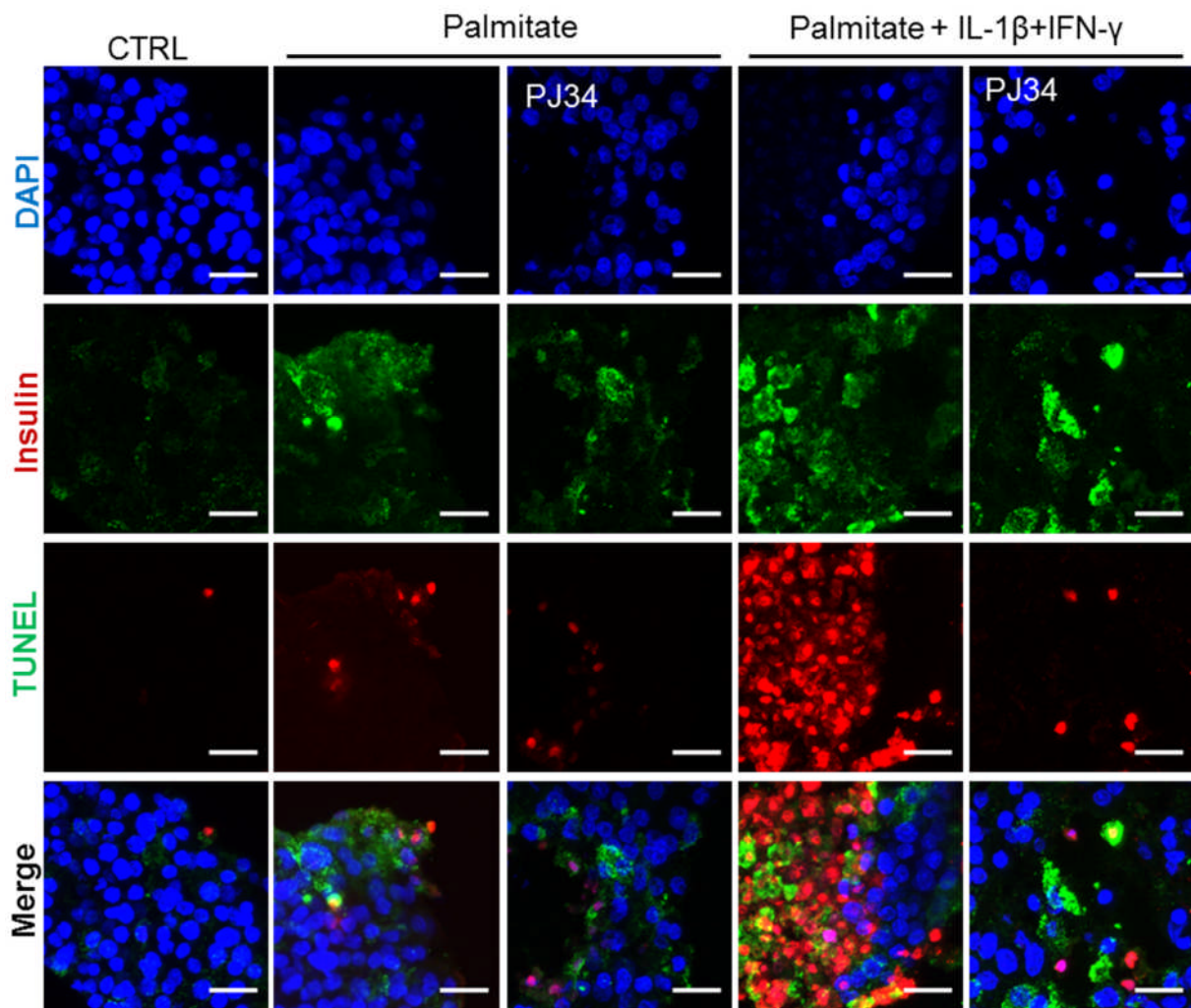
Figure 3. 18 Inhibition of TRPM2 channels protects palmitate and cytokine induced apoptosis in human islets. Human islets purchased from Prodo Labratories (Irvine, United States) were treated with medium (CTRL) or medium containing 500µM palmitate with or without cytokines (IFN-γ, 5 ng/ ml plus IL-1β, 5 ng/ ml) in the absence or presence of PJ34 (15 µM) for 7 days. The treated islets were fixed, frozen and sectioned for TUNEL assay and insulin staining (see material and methods for details). Representative confocal images show that inhibition of TRPM2 channels prevents palmitate and cytokines induced apoptosis and insulin release in human islets.

3. 3 Discussion

In this chapter, how palmitate can affect the structural integrity of mitochondria and cause β-cell death was investigated. The results demonstrate that palmitate activation of NOX2 increases ROS levels in INS1 cells leading to a cascade of events that ultimately results in β-cell apoptosis. The results also demonstrate that by regulating mitochondrial morphology (Figure 3. 4, 3. 5 and 3. 7), ΔΨm (Figure 3. 11) and mitochondrial ROS production (Figure 3. 13), TRPM2 channels mediate palmitate-induced apoptosis of β-cells. Furthermore, the role of Ca^{2+} and Zn^{2+} dynamics in above events was explored. The results provide novel insights into how elevation of FFA could lead to pancreatic β-cell death and contribute to the progression of T2D.

3. 3. 1 Palmitate induced mitochondrial fragmentation is mediated by NOX-derived ROS and activation of TRPM2 channels

In obesity-linked T2D, the expanded adipose tissue releases FFAs, such as palmitate, into the plasma (Guilherme et al., 2008). Studies have shown that rise in FFAs activates NOX2, and NOX2 derived ROS contributes to β-cell dysfunction and apoptosis (Li et al., 2012; Yuan et al., 2010). Molina et al demonstrated that exposure of β-cells to high levels of palmitate causes extensive fragmentation of the mitochondrial network (Molina et al., 2009) which is largely dependent on NOX mediated rise in cytosolic ROS levels (Sato et al., 2014). Moreover, it is generally believed that uncontrolled mitochondrial fragmentation leads to apoptosis (Liot et al., 2009; Yu et al., 2008). Despite the importance, how NOX2 induced ROS production leads to mitochondrial fragmentation remained unclear. The data presented in this chapter (Figure 3. 1, 3. 2, 3. 3 and 3. 4) suggest that NOX2 derived ROS cause mitochondrial fragmentation by activating the TRPM2 channel. Previous studies have shown that deletion of NOX2 (Xiang et al., 2010) and TRPM2 genes (Manna et al., 2015) in mice prevents streptozotocin induced β-cell death and hyperglycaemia. Taken together, these results suggest that NOX2 derived ROS causes β-cell death by promoting TRPM2 mediated mitochondrial fragmentation.

Key evidence comes from the finding that palmitate failed to induce mitochondrial fragmentation in HEK-293 cells, which lack TRPM2 channels; however, ectopic expression of TRPM2 channels led to extensive mitochondrial fragmentation when the cells were exposed to palmitate (Figure 3. 5). Taken together, these data confirm the role of TRPM2 channels in palmitate induced mitochondrial fragmentation.

Interestingly, compared with palmitate, high levels of glucose did not cause detectable fragmentation of mitochondria (Figure 3. 2). Thus although in diabetes, blood levels of both glucose and fatty acids are elevated, it is the increase in the level of fatty acids that play a dominant role in mitochondrial fragmentation of β-cells. These data are consistent with the previous findings with the C2C12 muscle cell line where palmitate, but not glucose, caused extensive fragmentation (Jheng et al., 2012). Given the link between impaired mitochondrial function and diabetes (Sivitz and Yorek, 2010), these cell-based studies highlight the importance of regulating hyperlipidaemia in slowing the progression of the disease.

3. 3. 2 Palmitate induced mitochondrial fragmentation is mediated by TRPM2 dependent changes in Zn^{2+} dynamics and Drp1 translocation

Activation of TRPM2 channels increases the cytosolic levels of free Ca^{2+} as well as Zn^{2+} in β-cells (Manna et al., 2015). Thus the role of both the ions in mitochondrial fragmentation was examined. The data (Figure 3. 6) suggest that Ca^{2+} has little effect on palmitate induced mitochondrial fragmentation. However, basal levels of Ca^{2+} are essential for the maintenance of the mitochondrial network as co-application of BAPTA-AM with A23187 induced marked mitochondrial fragmentation (Figure 3. 6D-F). Similar effects of BAPTA-AM have previously been reported in other cell types (Han et al., 2001).

Excess Zn^{2+} is known to impair mitochondrial function (Jiang et al., 2001; Sensi et al., 2003). However, there are no reports of studies on the effect of Zn^{2+} on mitochondrial dynamics. The results revealed that chelation of Zn^{2+} with TPEN completely inhibited palmitate-induced mitochondrial fission (Figure 3. 6A-C). Direct delivery of Zn^{2+} into cells via the Zn^{2+} ionophore, Zn-PTO, was sufficient to induce mitochondrial fragmentation (Figure 3. 6D-H). Taken together, these data demonstrate that palmitate induced mitochondrial fission is mainly mediated by the TRPM2 mediated changes in intracellular Zn^{2+}.

Under normal physiological conditions, Drp1 is mainly located in the cytosol, but in response to pathological insults, such as hyperlipidaemia, Drp1 is promptly recruited to mitochondria to cause fragmentation (Tsushima et al., 2012). Consistent with the previous studies, the data presented in this chapter show that palmitate induces translocation of Drp1 to mitochondria (Figure 3. 7A-B). Further investigations (Figure 3. 7 and 3. 8) suggested the involvement of TRPM2 channels in Drp1 translocation, which is consistent with the role of TRPM2 channels in mitochondrial fragmentation. Chelation of Zn^{2+} with TPEN also prevented palmitate induced mitochondrial Drp1 recruitment (Figure 3. 7A-B). Conversely, when Zn^{2+} levels were raised with Zn-PTO, there was a marked increase in Drp1 recruitment

to mitochondria (Figure 3. 8). Taken together, these findings demonstrate that TRPM2 mediated changes in intracellular Zn^{2+} induce Drp1 recruitment to mitochondria.

3. 3. 3 TRPM2 mediated increase in mitochondrial Zn^{2+} is responsible for mitochondrial fragmentation

Previous studies with β-cells have shown that oxidative stress causes release of lysosomal Zn^{2+} into the cytoplasm, and that this release is TRPM2 dependent (Manna et al., 2015). Studies have also shown that mitochondria have the ability to sequester cytosolic Zn^{2+} (Colvin et al., 2003; Sensi et al., 2000). These findings raised the possibility that palmitate could induce Zn^{2+} accumulization in mitochondria. Consistent with this possibility, palmitate treatment caused significant accumulation of free Zn^{2+} in mitochondria (Figure 3. 9), with Zn^{2+} staining being largely seen in fragmented mitochondria. Given TPEN was able to inhibit mitochondrial fragmentation, it seems possible that Zn^{2+} entry into mitochondria triggers mitochondrial fission. Most importantly, chemical and siRNA inhibition of TRPM2 channels prevented palmitate induced mitochondrial Zn^{2+} uptake (Figure 3. 10). The mechanism by which TRPM2 channels facilitate uptake of Zn^{2+} by mitochondria remains to be investigated. However, unpublished data from the laboratory found that in HEK cells, transfected TRPM2 channels can be detected in mitochondria. It could therefore be postulated that Zn^{2+} uptake by mitochondria is mediated by TRPM2 channels and the resultant increase in mitochondrial Zn^{2+} triggers fragmentation. .

3. 3. 4 TRPM2 mediated increase in mitochondrial Zn^{2+} induces loss of ΔΨm and mitochondrial ROS production

Previous studies have shown that rise in intracellular Zn^{2+} impairs mitochondrial function (Devinney et al., 2009; Sensi et al., 2003). A number of Zn^{2+} targets have been reported; these include enzymes of the citric acid cycle and multiple sites of the electron transport chain, especially complex I (Sharpley and Hirst, 2006). Binding of Zn^{2+} to complex I inhibits proton translocation (Sharpley and Hirst, 2006) thereby leading to the loss of ΔΨm (Wudarczyk et al., 1999) and ROS production (Lambert and Brand, 2004). Zn^{2+} has also been shown to induce mPTP formation in rat liver mitochondria, which also contributes to loss of ΔΨm (Wudarczyk et al., 1999). Sensi et al have reported that elevation of Zn^{2+} during ischemia increases depolarization of ΔΨm as well as ROS production in cortical neurons (Sensi et al., 2003). Consistent with previous studies and above effects of TRPM2 channels and Zn^{2+} on mitochondria (Figure 3. 4, 3. 5 and 3. 6), the data presented in the current chapter (Figure 3. 11, 3. 12 and 3. 13) suggest that TRPM2 dependent Zn^{2+} influx into

3. 3. 5 Ca^{2+} induced Drp1 recruitment and mitochondrial ROS production, but fails to induce loss of ΔΨm and mitochondrial fragmentation

Studies have shown that loss of ΔΨm is essential for Drp1 mediated mitochondrial fragmentation (Twig et al., 2008; Westermann, 2012). A23187 failed to induce mitochondrial fragmentation, however, caused significant recruitment of Drp1 to mitochondria (Figure 3. 8A-B), which is consistent with the known role of Ca^{2+} in Drp1 recruitment (Pennanen et al., 2014). Drp1 exists in the cytoplasm largely in its phosphorylated state. Rise in Ca^{2+} activates calcineurin, a phosphatase that causes de-phosphorylation of Drp1, leading to its recruitment to mitochondria. Although A23187 induced Drp1 recruitment to mitochondria, it failed to induce loss of ΔΨm (Figure 3. 12). These results suggest that Drp1 recruitment alone is not enough to induce mitochondrial fragmentation, depolarisation of mitochondrial membrane potential is also required.

Drp1 needs to wrap around the mitochondria to cause fission, but normal mitochondria are too wide for Drp1 to wrap around. Studies have shown that ER tubules constrict the mitochondria allowing Drp1 to bind and catalyse mitochondrial fission at the site of constriction (Friedman et al., 2011; Korobova et al., 2013). Current evidence thus suggests that membrane depolarisation is a prerequisite for ER-assisted mitochondrial constriction and that binding of Drp1 to mitochondria in the absence of pre-constriction cannot cause mitochondrial fission. A recent study by Mehta et al has shown Ca^{2+} oscillation (due to activation of ryanodine receptors) and local calcineurin activity near the ER-mitochondria junction in MIN6 β-cells (Mehta et al., 2014). The authors suggested that the ER-mitochondria contact point could represent hotspots for Ca^{2+}/Calcineurin signalling. It therefore seems plausible that the increase in Ca^{2+}/Calcineurin signalling at the ER-constricted mitochondrial sites drives Drp1 recruitment and mitochondrial fission. Thus although A23187 induced Ca^{2+} rise can induce Drp1 recruitment, it failed to cause mitochondrial fission because of its inability to cause depolarisation and ER-assisted mitochondrial constriction.

In contrast to A23187, Zn-PTO not only induces Drp1 recruitment (Figure 3. 8), but also causes loss of ΔΨm (Figure 3. 12) required for ER-assisted mitochondrial constriction. How Zn^{2+} causes Drp1 recruitment, however, is unclear, but likely involves activation of ryanodine receptors and consequent Ca^{2+} /calcineurin signalling. One of the activators of ryanodine receptors is ROS (Cooper et al., 2013) and Zn-PTO is a potent inducer of mitochondrial

ROS production (Figure 3. 13). Given the similarities between the effects of palmitate and Zn-PTO on mitochondria, and the fact that the effects of both these substances could be prevented by TRPM2 inhibition, it is reasonable to speculate that palmitate induced mitochondrial fission is mediated by TRPM2 mediated changes in intracellular Zn^{2+}, rather than Ca^{2+} homeostasis.

3. 3. 6 Role of TRPM2 channels, Zn^{2+} and Ca^{2+} in apoptosis

As mitochondrial dysfunction is closely associated with cell death (Kroemer and Reed, 2000; Lin and Beal, 2006), effect of palmitate on cell viability was examined. The data presented in this chapter (Figure 3. 14, 3. 17 and 3. 18) suggest that TRPM2 channels play an important role in palmitate-induced apoptosis of INS1 cells, mouse islets and human islets. Furthermore, the results indicate that Zn^{2+} plays a key role in palmitate-induced apoptosis of INS1 cells (Figure 3. 14). Delivery of Zn^{2+} to β-cells via Zn-PTO produced the same effect as palmitate (Figure 3. 15), supporting a role for Zn^{2+} in apoptosis. Moreover, Zn–PTO induced apoptosis is dependent on TRPM2 channels (Figure 3. 15), which could be attributed to the possibility that Zn^{2+} induces ROS production and subsequent activation of TRPM2 channels. This possibility, however, remains to be tested in future studies. The role of TRPM2 channels in apoptosis has been widely studied in a variety of cell types (Kaneko et al., 2006; Sun et al., 2012; Zhang et al., 2006). However, these studies focussed on the role of Ca^{2+} and apoptosis-related factors. The present study demonstrates a role for TRPM2 and for Zn^{2+} in the regulation of mitochondrial dynamics suggesting that TRPM2/Zn^{2+} mediated increase in mitochondrial fragmentation may contribute to pathological palmitate induced β-cell death.

The role of Ca^{2+} on apoptosis has been extensively studied (Orrenius et al., 2003; Pinton et al., 2008). It has been suggested that Ca^{2+}-induced apoptosis can occur as a result of activation of two signalling pathways. First, Ca^{2+} elevation triggers mitochondrial permeability transition (Korge and Weiss, 1999), which causes the release of cytochrome *c* from mitochondria (Petronilli et al., 2001). Cytochrome *c* binds to the IMM via cardiolipin. Binding of Ca^{2+} to cardiolipin induces cytochrome *c* release to cause apoptosis (Grijalba et al., 1999). Second, Ca^{2+} can cause apoptosis by inducing ER-stress (Huang et al., 2014). It has been demonstrated that calpain can directly activate caspase-12 which can result in apoptosis in cortical neurons (NakagawaT, 2000). In the present study, A23187 induced rise in cytosolic Ca^{2+} was found to have no effect on the mitochondrial network (Figure 3. 6D-F) and ΔΨm (Figure 3. 12), but induced marked apoptosis (Figure 3. 16). Importantly, the calpain inhibitor, PD150606, prevented A23187 induced apoptosis (Figure 3. 16), indicating that Ca^{2+} induced

apoptosis is likely not dependent on mitochondria-mediated pathway, but dependent on calpain activity.

3. 4 Summary

The current chapter describes findings of the mitochondria-dependent apoptosis pathway during FFA stress on pancreatic β-cells. The data suggest that FFA potentially activate TRPM2 channels by generating ROS, which in turn leads to increased Zn^{2+} uptake by mitochondria and subsequent fragmentation. Excessive fragmentation of mitochondria is likely the cause of apoptosis in pancreatic β-cells. Although activation of TRPM2 channels affects both Ca^{2+} and Zn^{2+} homeostasis, and both ions can cause β-cell death, FFA induced cell death appears to be largely mediated by the Zn^{2+} effects on mitochondria. While Ca^{2+} also causes cell death, the effect is relatively less important. Furthermore, Ca^{2+} effect does not appear to involve mitochondria, but seems to be mediated by calpain. A schematic representation of these findings is presented in figure 3.19. This chapter for the first time provides evidence for the role of TRPM2 channels in palmitate induced apoptosis of mouse and human islets.
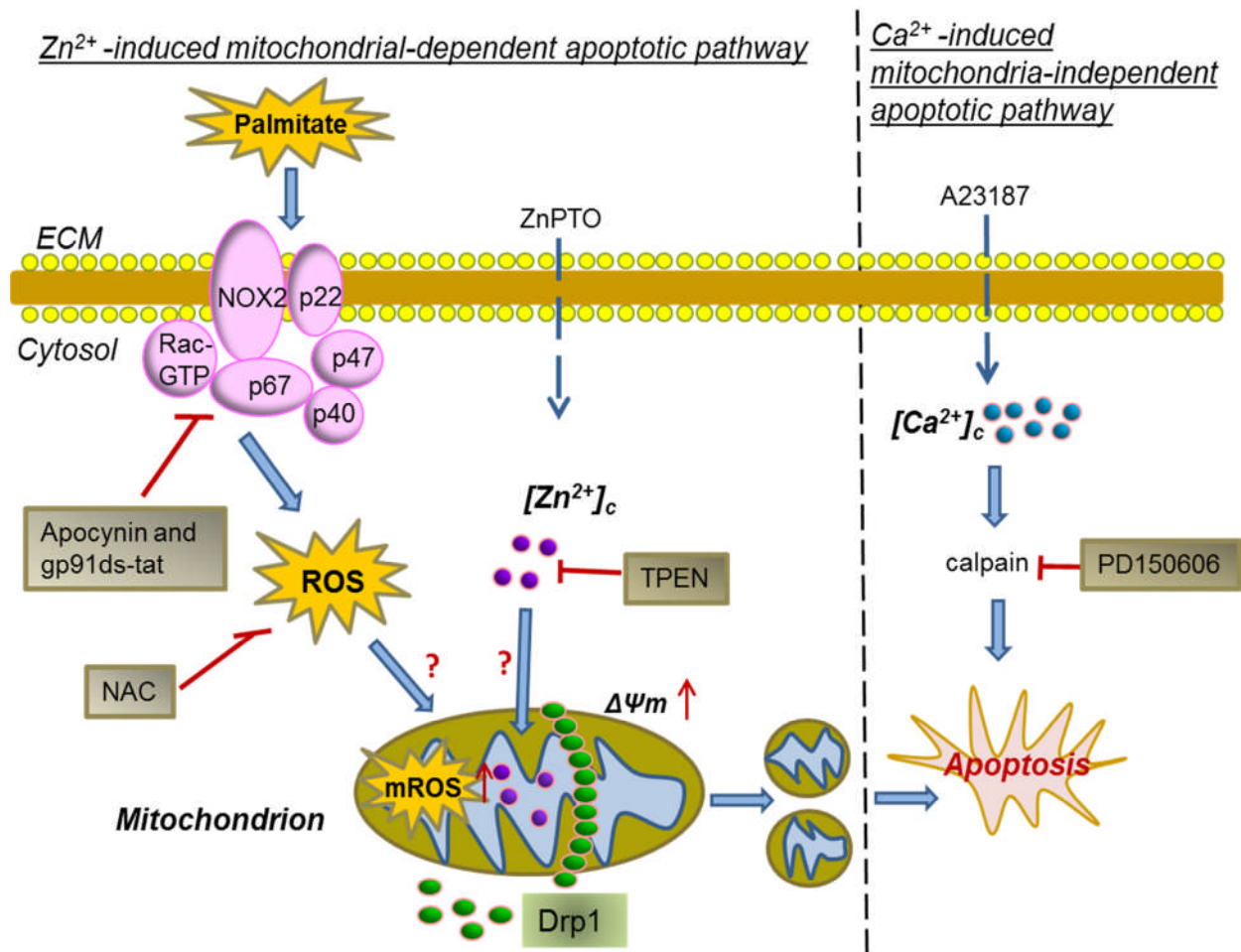
Figure 3.19 Schematic showing the role of ROS, Zn^{2+} and Ca^{2+} dynamics in nutrient stress induced mitochondrial fragmentation and cell death.

Chapter 4 TRPM2 channels regulate remodelling of actin and focal adhesions in cancer cells

4. 1 Introduction

Cell migration is a fundamental feature of multiple processes that includes cancer metastasis. In order to migrate, cells undergo rapid changes in cell morphology, which are driven by the constant remodelling of the actin cytoskeleton into filopodia, lamellipodia and stress fibres. Filopodia are spike-like membrane projections where actin fibres are arranged into tight bundles. Lamellipodia are brush-like protrusions formed at the leading edge of migrating cells, where actin polymerises into a cortical ring. Stress fibres are long actin filaments linked by α-actinin and myosin. Formation of each type of actin cytoskeleton is spatially and temporally regulated by distinct RhoGTPases. RhoA regulates stress fibres, while Cdc42 (and/or Rif) and Rac1 promote filopodia and lamellipodia formation respectively (Nobes and Hall, 1995). Focal adhesions are macromolecular complexes with which cells adhere to their substrate (extracellular matrix). Like the actin cytoskeleton, focal adhesions also undergo cycles of assembly and disassembly. Changes in focal adhesion dynamics enable the cells to attach and detach from their substrate during effective migration. A variety of factors regulating dynamics of actin cytoskeleton and focal adhesions relevant to cell migration have been proposed (Yamaguchi and Condeelis, 2007), of which ROS (Mahdi et al., 2000; Taulet et al., 2012) and Ca^{2+} (Bhatt et al., 2002; Oertner and Matus, 2005) are noteworthy.

Although for a long time, ROS is believed to cause deleterious effects on cell viability, recent evidence suggests that 'non-damaging' levels of ROS play a central role in intracellular signal transduction pathways associated with a variety of cellular processes, including cell migration (Hurd et al., 2012). It has been reported that ROS can affect the dynamics of actin cytoskeleton and focal adhesions (Moldovan et al., 2000; Yang et al., 2003). As a signalling messenger, ROS is able to oxidize critical target molecules such as protein kinase C (PKC)(Wu et al., 2006) and protein tyrosine phosphates (PTPs) (Östman et al., 2011), which are relevant to actin remodelling and focal adhesion reorganization. For example, in vascular smooth muscle cells, PKC activation triggers disassembly of actin stress fibres and appearance of membrane ruffles (Brandt et al., 2002). In endothelial cells, ROS oxidation and inhibition of PTP-PEST, a scaffolding protein tyrosine phosphatase, results in focal adhesion changes and membrane ruffling (Wu et al., 2005). Furthermore, it has been demonstrated that NADPH oxidase-dependent ROS generation is required for transforming growth factor β (TGF-β)-induced actin remodelling in endothelial cells (Hu et al., 2005). However, there is not much information on the role of ROS in actin remodelling and focal

adhesion dynamics in cancer cells except one study where H_2O_2 induced actin remodelling has been demonstrated in L929 fibrosarcoma cells (Préville et al., 1998).

Multiple studies have demonstrated that Ca^{2+} regulates cell migration through spatial and temporal regulation of the actin cytoskeleton and focal adhesions. For example, Tsai et al reported that elevating cytosolic Ca^{2+} level induces focal adhesions and decreases cell migration in both endothelial and lung carcinoma cells (Tsai et al., 2014). Dourdin et al demonstrated that knockdown of Ca^{2+}-dependent protease calpain causes disassembly of both stress fibres and focal adhesions and decreases cell migration of embryonic fibroblasts (Dourdin et al., 2001).

Since TRPM2 channels are highly sensitive to ROS and permeable to Ca^{2+}, it was hypothesised that TRPM2 channels play a role in ROS induced actin remodelling. To address this, the role of TRPM2 channels in ROS-mediated actin remodelling and focal adhesions formation was investigated in this chapter. Two cancer cell lines were chosen: HeLa and PC-3 cells. HeLa is a cell line derived from human cervical cancer and PC-3 is a cell line derived from human prostate cancer. As the causation of these two cancers is different, investigation of these two types of cancer cells might provide a more general insight into the role of TRPM2 channels in ROS-induced actin and focal adhesions remodelling.

This chapter has two main aims. The first aim is to elucidate the effect of elevated ROS level on the dynamics of actin cytoskeleton and focal adhesions in cancer cells; the second aim is to explore the role of TRPM2 channels in the regulation of actin and focal adhesion reorganization.

4. 2 Results

4. 2. 1 H$_2$O$_2$ induces actin remodelling in HeLa and PC-3 cells

A previous study with L929 fibrosarcoma cells reported that H$_2$O$_2$ causes remodelling of the actin cytoskeleton resulting in the loss of stress fibres and appearance of spike-like protrusions (Préville et al., 1998). However, it is not clear whether similar changes occur in other cancer cells. Therefore, the effect of H$_2$O$_2$ on the actin cytoskeleton in HeLa and the PC-3 cell lines was investigated by staining the actin with Alexa[488]-Phalloidin. The results show that application of H$_2$O$_2$ abolishes stress fibres and generates numerous filopodia in both the cell lines (Figure 4.1 A-D). Furthermore, HeLa cells were transfected with tdTomato-F-actin-P and the effect of H$_2$O$_2$ on the actin cytoskeleton was examined by live cell imaging. The results show clear actin stress fibres under control conditions (Figure 4.1E), but disappearance of stress fibres and formation of numerous spike-like filopodia upon H$_2$O$_2$ treatment.

Collectively, these data indicate that H$_2$O$_2$ plays an essential role in inducing filopodia formation and disruption of stress fibres in both HeLa and PC-3 cells.
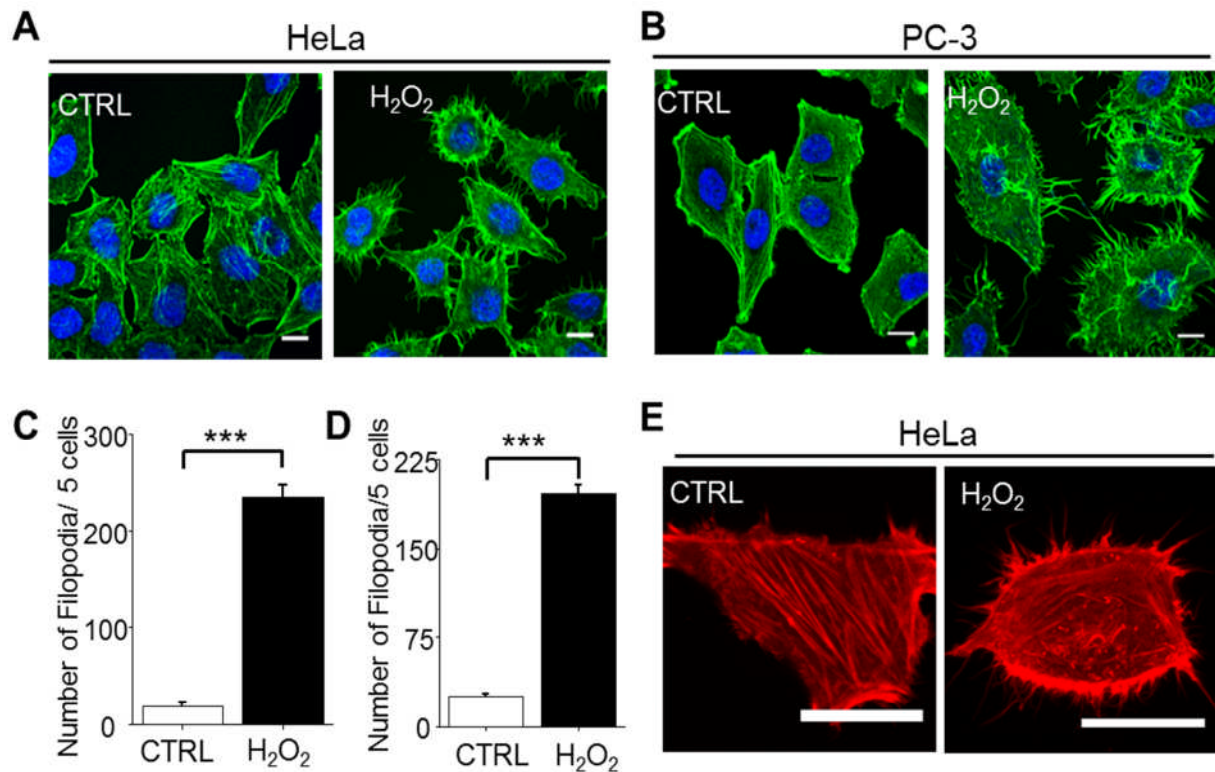
Figure 4. 1 H$_2$O$_2$ induces actin remodelling in HeLa and PC-3 cells. (**A-B**) HeLa (A) and PC-3 (B) cells were stained for F-actin (green) following H$_2$O$_2$ (HeLa, 200 µM; PC-3, 100 µM) treatment for 2 hr at 37ºC; controls (CTRL) were left untreated, representative confocal images show remodelling of the actin cytoskeleton; scale bars: 10 µm. (**C-D**) Mean ± SEM of filopodia number (5 cells) from three independent experiments performed as in (A) and (B) with HeLa (A) and PC-3 (B) cells; *** indicates $p < 0.001$; Student's t test. (**E**) HeLa cells transfected with tdTomato-F-actin-P (ITPKA-9-52) were plated onto glass-bottomed dishes containing PBS (CTRL) or H$_2$O$_2$ (200 µM) and imaged; representative confocal images were shown; scale bars: 20 µm.

4. 2. 2 Functional expression of TRPM2 channels in HeLa and PC-3 cells

Ca^{2+} has been implicated in remodelling of the actin cytoskeleton (Wang et al., 2010). Cytosolic Ca^{2+} dynamics is regulated by multiple ion channels and pumps, located either in the plasma membrane or in intracellular organelles (Brini and Carafoli, 2009; Clapham, 2007) . Among the Ca^{2+}-permeable ion channels, the TRPM2 channel is of special interest as it is highly sensitive to H_2O_2 and thus could play a role in H_2O_2 induced actin remodelling. Furthermore, previous studies have shown that TRPM2 channels are functionally expressed in a variety of different cell types, including cancer cell (Zeng et al., 2010). To determine TRPM2 expression in HeLa and PC-3 cells, reverse transcription (RT)-PCR and Fura-2 based Ca^{2+} assays were employed. RT-PCR data revealed that both HeLa and PC-3 cells express TRPM2 channels (Figure 4.2A); a band of expected size (239 bp) was detected when the PCR products were analysed by agarose gel electrophoresis. Consistent with the RT-PCR data, Ca^{2+} flux assay results indicated that both the cell lines show a rise in Ca^{2+} when the cells were stimulated with H_2O_2. This H_2O_2 induced rise in cytosolic Ca^{2+} was inhibited by 2-APB, an inhibitor for TRP channels (Togashi et al., 2008) (Figure 4.2B-E).

Taken together, these results demonstrate that TRPM2 channels are functionally expressed in HeLa and PC-3 cells.
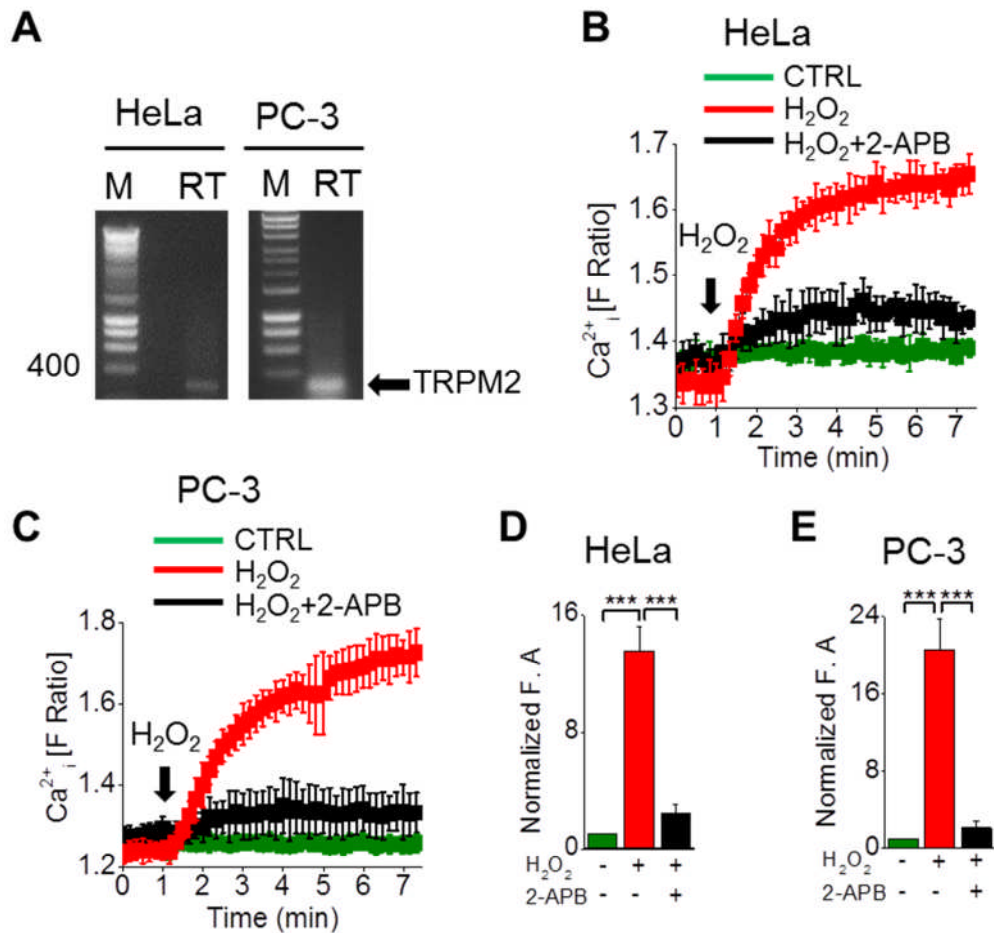
Figure 4. 2 Expression of TRPM2 channels in HeLa and PC-3 cells (**A**) RNA isolated from HeLa and PC-3 cells was subjected to reverse transcription (RT) reaction and PCR and the results were subjected to agarose gel electrophoresis. M: HypperLadder I (Bioline); band size shown on the left. RT: RT-PCR product using TRPM2 primers. The gel shows bands corresponding to the predicted size (293 bp). (**B-C**) H_2O_2 induces a rise in intracellular Ca^{2+} in HeLa (B) and PC-3 (C) cells as determined by Fura-2 mediated rise in fluorescence (F340/380) ratio using FlexStation II; 2-APB (150 µM) inhibits the H_2O_2 effect indicating TRPM2 mediated Ca^{2+} rise. (**D-E**) Normalized mean ± SEM data from three independent experiments performed as in (B) and (C) respectively; Statistical significance was determined using one-way Anova with Tukey post-hoc test *** indicates $p < 0.001$.

4. 2. 3 TRPM2 channels mediate H_2O_2 induced actin remodelling in HeLa and PC-3 cells

Above data have shown that H_2O_2 induces actin remodelling in HeLa and PC-3 cells (Figure 4. 1), and that both the cell lines express TRPM2 channels (Figure 4. 2). As H_2O_2 is an activator of the TRPM2 calcium channel, it was hypothesised that TRPM2 channels play a role in H_2O_2–triggered actin remodelling. Therefore, the role of TRPM2 channels in H_2O_2 induced actin cytoskeleton remodelling was investigated in HeLa and PC-3 cells.

PJ34 and 2-APB were used to test the hypothesis. When co-incubated with PJ34 and 2-APB, H_2O_2 induced filopodia formation was significantly inhibited both in HeLa and PC-3 cells (Figure 4.3A-D). As for stress fibres, 2-APB rescued H_2O_2 induced loss of stress fibres more effectively than PJ34 (Figure 4.3A-B).

To further assess the role of TRPM2 channels in H_2O_2 triggered actin reorganization, siRNAs (siRNA-1 and siRNA-2) specifically targeted to TRPM2 channels were used. Cells were transfected with siRNAs (siRNA-1 and siRNA-2 for HeLa and siRNA-1 for PC-3 cells) targeted to TRPM2 or scrambled control siRNA for 48 hours and then treated with the medium alone or medium containing H_2O_2. F-actin staining showed that knock-down of TRPM2 channels by siRNA, but not by scrambled control siRNA, suppressed H_2O_2 induced filopodia formation; rescue of stress fibres, however, was partial (Figure 4.4A-D). RT-PCR of transfected cells showed that both TRPM2-siRNAs are effective in silencing TRPM2 expression (Figure 4.4E-F).

These data indicate that TRPM2 channels play a significant role in H_2O_2 induced actin cytoskeleton rearrangement.
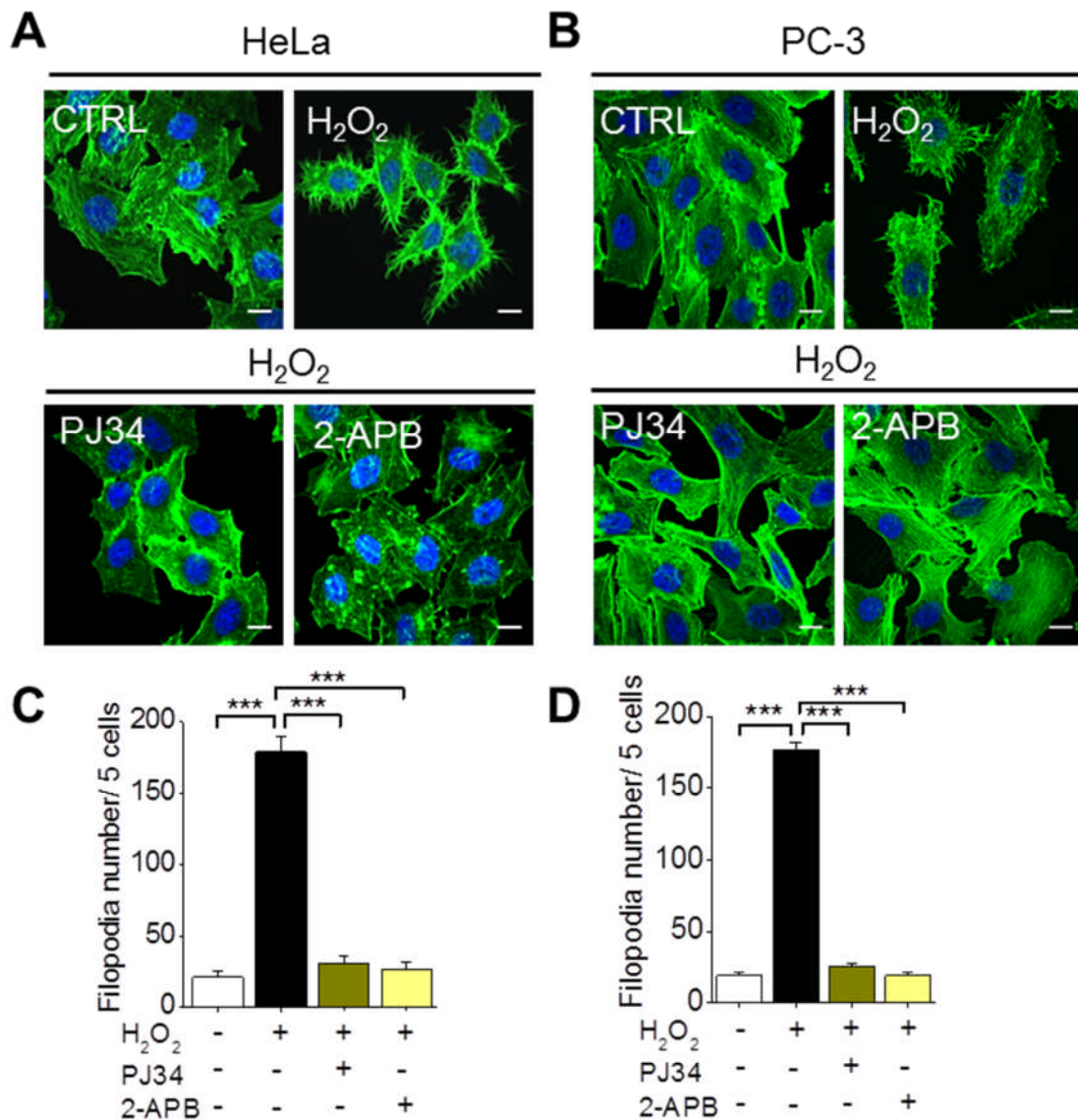
Figure 4. 3 Pharmacological inhibition of TRPM2 channels prevents H₂O₂ induced actin remodelling in HeLa and PC-3 cells. (**A-B**) HeLa (A) and PC-3 (B) cells were either not treated (CTRL) or treated with H₂O₂ in the absence and presence of TRPM2 inhibitors (PJ34, 10 µM; 2-APB, 150 µM) and were then stained for F-actin. Representative confocal images were shown; scale bars = 10 µm. (**C-D**) Mean ± SEM of filopodia number (5 cells) from three independent experiments performed as in (A) and (B) with HeLa and PC-3 cells; *** indicates *p* < 0.001; one-way Anova with Tukey post-hoc test.
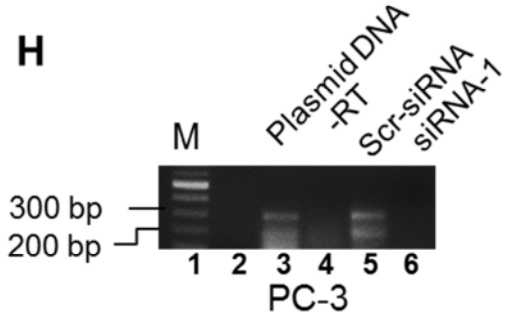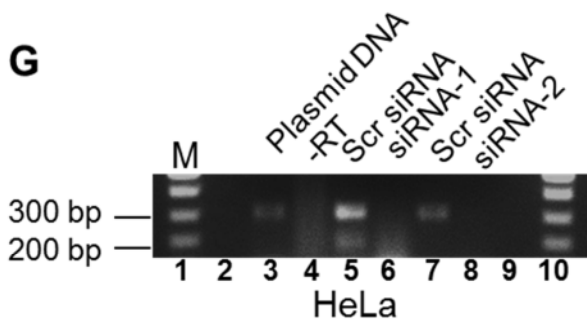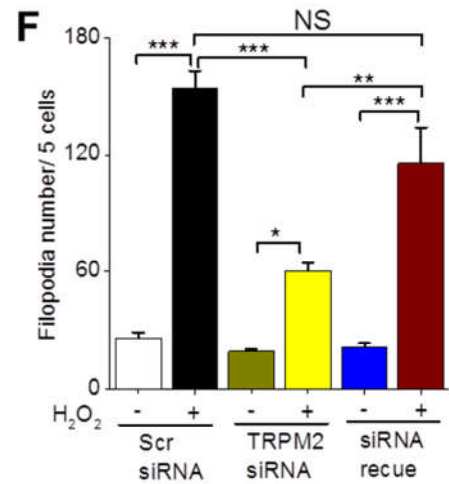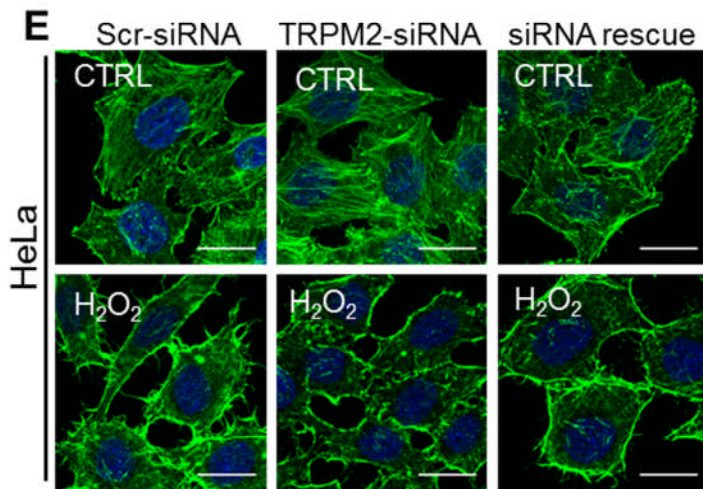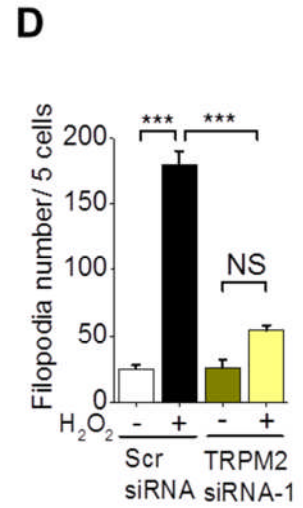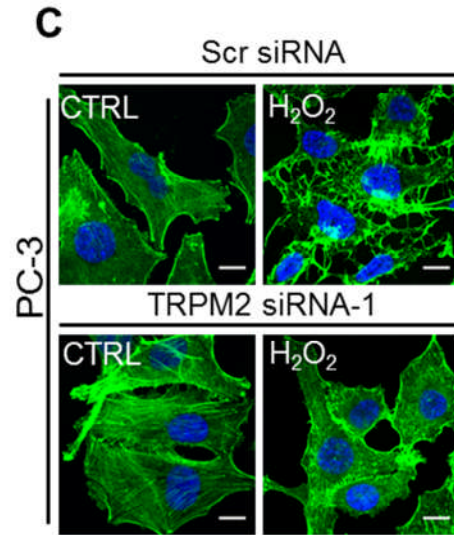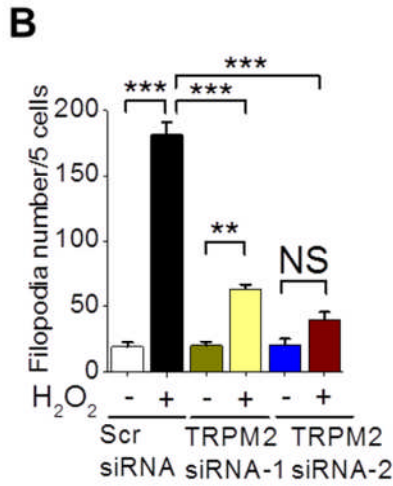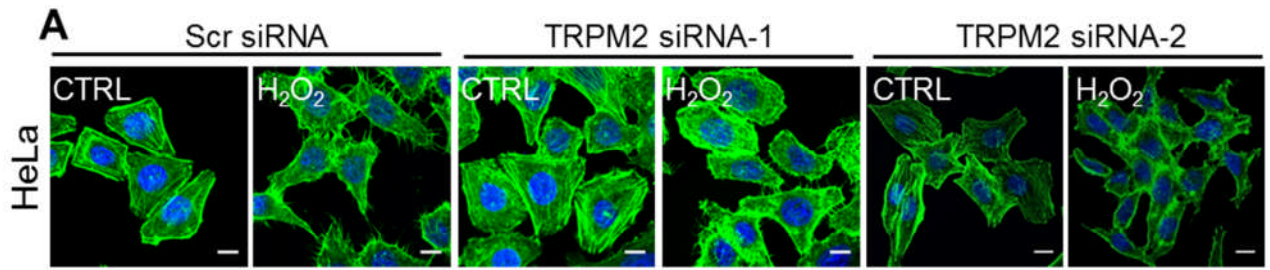
Figure 4. 4 Suppression of TRPM2 expression in HeLa and PC-3 cells with siRNA prevents H$_2$O$_2$ induced actin remodelling. (**A and C**) HeLa (A) and PC-3 (C) cells transfected with scrambled siRNA or siRNAs against TRPM2 were either not treated (CTRL) or treated with H$_2$O$_2$ and stained for F-actin; representative control images are shown; scale bars = 10 μm. (**B and D**) Mean ± SEM of filopodia number (5 cells) were shown from three independent experiments performed as in (A) and (C) with HeLa (B) and PC-3 (D) cells. *** indicates *p* < 0.001; NS, not significant; one-way Anova with Tukey post-hoc test. (**E**) HeLa cells were transfected with scrambled siRNA, or siRNA against TRPM2 in combination with siRNA-resistant plasmid for 48 hour, then cells were either not treated (CTRL) or treated with H$_2$O$_2$ and stained for F-actin; representative confocal images were shown; scale bars = 20 μm. (**F**) Mean ± SEM of filopodia number (5 cells) were shown from three independent experiments performed as in (E). *** indicates *p* < 0.001; ** indicates *p* < 0.01; NS, not significant; one-way Anova with Tukey post-hoc test. (**G**) HeLa cells were transfected with scrambled siRNA or siRNA-1 against TRPM2 for 48 hours. RNA isolated from the transfected cells was subjected to RT-PCR. Lane 1 and lane 10 has DNA ladder (HypperLadder I; Bioline); lane 3: PCR product from TRPM2 plasmid; lanes 4: PCR products from mRNA without reverse transcription reaction; lane 5-8: HeLa cells transfected with scrambled siRNA (lane 5 and lane 7) or siRNA targeted to TRPM2 (lane 6, siRNA-1 and lane 8, siRNA-2).The results show absence of TRPM2 band (lane 6 and 8) in TRPM2 siRNA transfected samples, but not scrambled siRNA controls (lane 5 and 7). (**H**) PC-3 cells were transfected with scrambled siRNA or siRNA-1 against TRPM2 for 48 hours and subjected to RT-PCR. Lane 1 has DNA ladder (HypperLadder I; Bioline); lane 3: PCR product from TRPM2 plasmid; lanes 4: PCR products from mRNA without reverse transcription reaction; lane 5: PC-3 cells transfected with scrambled siRNA; lane 6: siRNA targeted to TRPM2.The results show absence of TRPM2 band (lane 6) in TRPM2 siRNA transfected samples, but not scrambled siRNA controls (lane 5).

4. 2. 4 H_2O_2 activation of TRPM2 channels causes both Ca^{2+} entry and release in HeLa cells

In most cell types, TRPM2 channels are expressed at the plasma membrane of the cell where they promote Ca^{2+} entry from the extracellular medium upon activation by H_2O_2. In some cell types, however, they are also located in the lysosomal membranes where they mediate lysosomal Ca^{2+} release. To examine H_2O_2 induced Ca^{2+} changes, the Fluo-4 Ca^{2+} reporter was introduced into the cells. HeLa cells exposed to H_2O_2 for 2 hours displayed a large increase in intracellular Fluo-4 fluorescence as detected by confocal microscopy (Figure 4.5A-B) and flow cytometry (Figure 4.5C-D). Removal of extracellular Ca^{2+} with EGTA (membrane impermeable chelator) reduced, but failed to abolish the Ca^{2+} signal completely (Figure 4.5A-B), indicating that the fluorescence signal is due to both Ca^{2+} entry and release. When PJ34 and 2-APB were included, the increase in fluorescence was completely abolished (Figure 4.5A-D), indicating a role for TRPM2 channels in H_2O_2 induced Ca^{2+} entry and release. In addition, cells treated with TRPM2 siRNA, but not with scrambled control siRNA, failed to respond to H_2O_2, further revealing the role of TRPM2 channels in mediating H_2O_2 induced Ca^{2+} entry and release (Figure 4.5E-F).

These data illustrate that H_2O_2 induces both Ca^{2+} entry and release in HeLa cells, and that the H_2O_2 effect is mediated by TRPM2 channels.
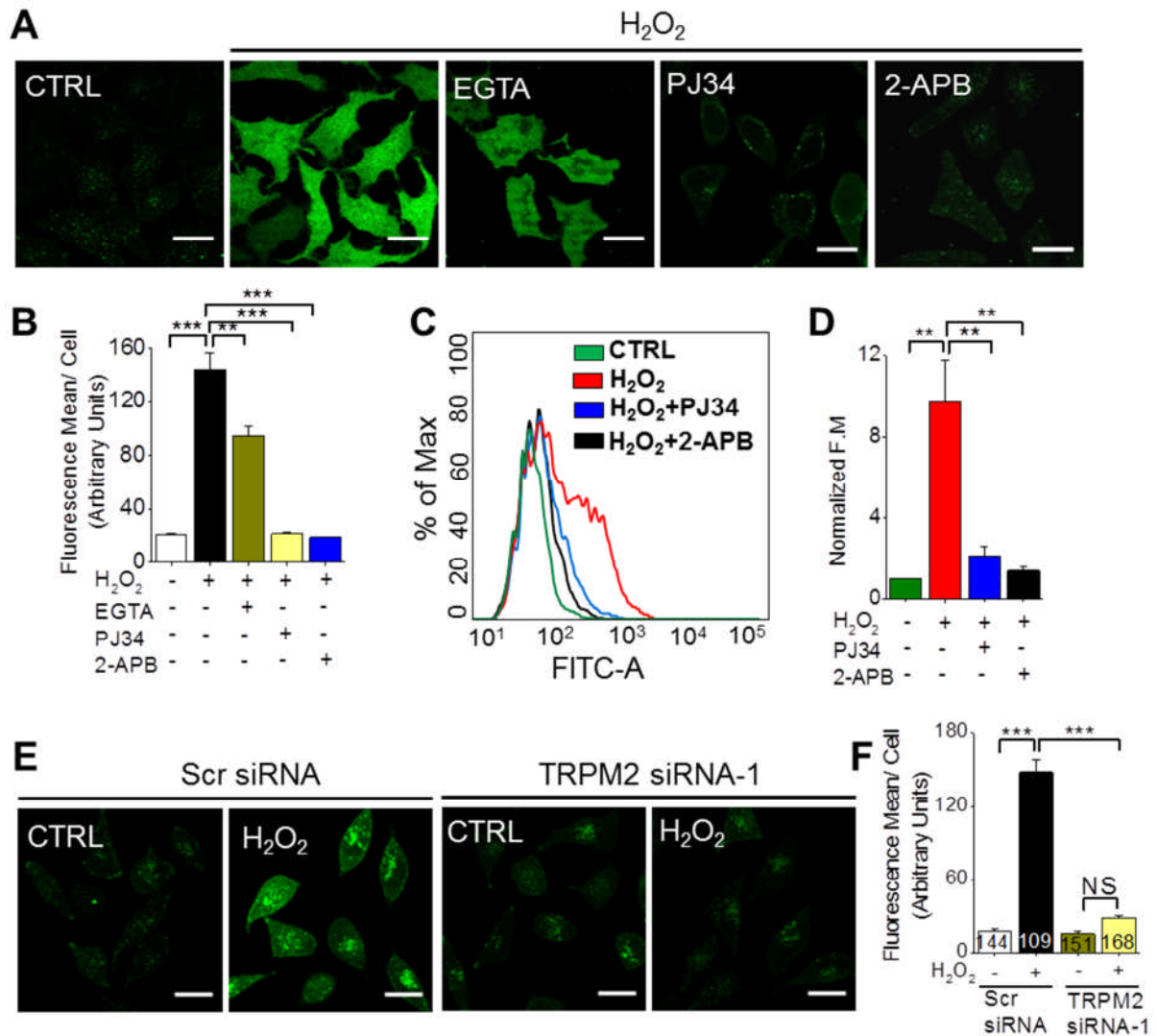
Figure 4. 5 TRPM2 channels mediate H_2O_2 induced Ca^{2+} entry and release in HeLa cells. (**A**) Cytosolic Ca^{2+} in HeLa cells detected with Fluo4-AM; Cells were either not treated (CTRL) or treated with H_2O_2 (200 μM) minus or plus EGTA (5 mM), PJ34 (10 μM) and 2-APB (150 μM); representative control images are shown; scale bars = 20 μm. (**C**) HeLa cells were either not treated (CTRL) or treated with H_2O_2 (200 μM) minus or plus PJ34 (10 μM) and 2-APB (150 μM) followed by loading with Fluo4-AM and were analysed by FACS. Histogram plot of flow cytometry analysis (~ 5000 cells) is shown. Green: CTRL; Red: H_2O_2; Cyan: H_2O_2 plus PJ34; Black: H_2O_2 plus 2-APB. (**D**) Mean ± SEM of Ca^{2+} fluorescence (~5000 cells) from three independent experiments performed as in (C). (**E**) HeLa cells transfected with scrambled siRNA or siRNA against TRPM2 were either not treated (CTRL) or treated with H_2O_2; Ca^{2+} fluorescence was examined by loading the cells with Fluo4-AM; representative control images are shown; scale bars = 20 μm. (**B and F**) Mean ± SEM of average Ca^{2+} fluorescence per cell from three independent experiments performed as in (A) and (E); *** indicates $p < 0.001$; ** indicates $p < 0.01$; NS, not significant; one-way Anova with post-hoc Tukey test.

4. 2. 5 Extracellular Ca^{2+} entry is not essential for actin cytoskeleton remodelling

Previous studies have reported that alteration of Ca^{2+} dynamics influences actin remodelling. Since both Ca^{2+} entry and release were observed in the above experiment, the role of Ca^{2+} entry and release in H$_2$O$_2$ induced actin remodelling was next investigated. Depletion of extracellular Ca^{2+} failed to prevent H$_2$O$_2$ induced filopodia formation (Figure 4.6A-B), indicating extracellular Ca^{2+} entry is not essential for filopodia formation. Interestingly, there was a small, but significant increase in filopodia in the absence of extracellular Ca^{2+}, suggesting that reduced Ca^{2+} might stimulate filopodia formation. Consistent with this interpretation, depletion of intracellular Ca^{2+} with BAPTA-AM, a cell membrane-permeable Ca^{2+} chelator, induced significant increase in filopodia formation in the absence of H$_2$O$_2$ (Figure 4.6C-D). The effect on stress fibres is less discernible as H$_2$O$_2$ treatment in the absence of extracellular Ca^{2+} caused marked cell shrinkage.

Collectively, these results indicate that TRPM2 channels mediate both Ca^{2+} entry and release, and that although Ca^{2+} plays a role in actin remodelling, extracellular Ca^{2+} entry is not essential for this.
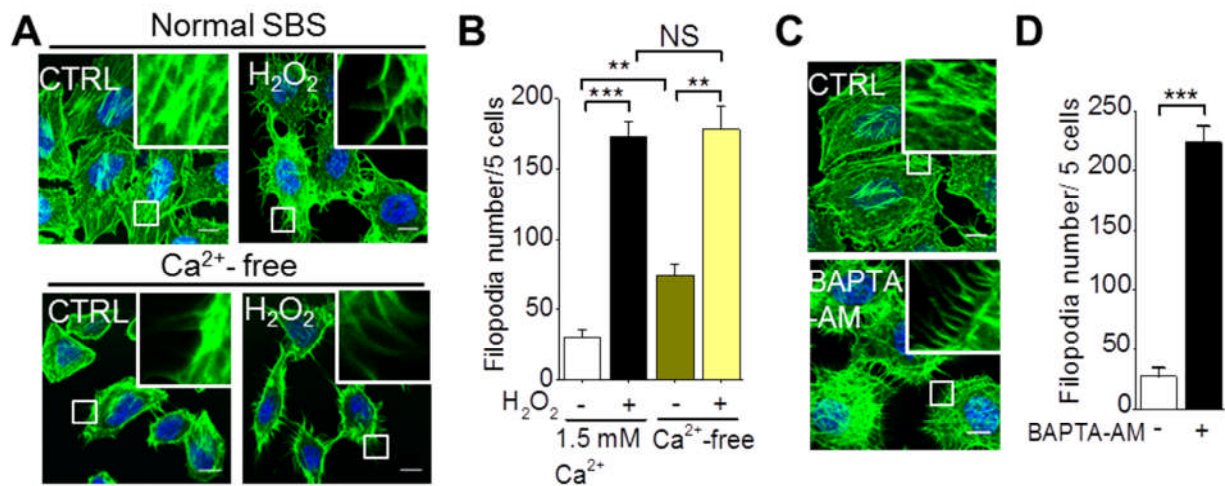
Figure 4. 6 Remodelling of actin cytoskeleton is not dependent on extracellular Ca^{2+} entry. (**A**) HeLa cells were treated without (CTRL) or with H$_2$O$_2$ (200 µM) in the presence (normal SBS) and absence of extracellular Ca^{2+} (Ca^{2+}-free SBS) and were stained for F-actin; representative confocal images are shown; scale bars = 10 µm. (**B**) Mean ± SEM of filopodia number (5 cells) from three independent experiments performed as in (A); *** indicates $P <$ 0.001; ** indicates $p <$ 0.01; NS, not significant; one-way Anova, with post-hoc Tukey test. (**C**) HeLa cells were treated without (CTRL) or with BAPTA-AM (10 µM) and stained for F-actin. Representative confocal images are shown; scale bars = 10 µm. (**D**) Mean ± SEM of filopodia number (5 cells) from three independent experiments performed as in (C); *** indicates $p <$ 0.001; Student's t test. In A and C, boxed regions are expanded in the insets.

4. 2. 6 Inhibition of TRPM2 channels significantly blocked H_2O_2-induced cytosolic Ca^{2+} increase in PC-3 cells

The above data clearly demonstrate that H_2O_2 is capable of inducing marked rise in cytosolic Ca^{2+}, due to Ca^{2+} entry and release in HeLa cells. It was however unclear whether such increase also occurs in PC-3 cells.

To address this question, the Fluo-4 Ca^{2+} reporter was introduced into the PC-3 cells. Consistent with observations in HeLa cells, H_2O_2 treated PC-3 cells showed significant cytosolic Ca^{2+} increase, indicated by the elevated Fluo-4 fluorescence assessed using flow cytometry (Figure 4.7A-B). When PJ34 and 2-APB were included, H_2O_2 induced Ca^{2+} increase was significantly inhibited, indicating a role for TRPM2 channels in the Ca^{2+} increase.

To assess whether this cytosolic Ca^{2+} increase involves both Ca^{2+} entry and release, BAPTA-AM and EGTA were used. Fura-2-AM loaded PC-3 cells showed robust elevation of intracellular Ca^{2+} concentration following the addition of H_2O_2 (Figure 4.7C-D), which is consistent with the flow cytometry data. BAPTA-AM treatment completely prevented H_2O_2 induced Ca^{2+} increase. EGTA, on the other hand, partially decreased H_2O_2 induced Ca^{2+} elevation. These results suggest that H_2O_2 causes a significant Ca^{2+} release from an intracellular source.

Collectively, these data suggest that H_2O_2 induces both Ca^{2+} entry and release in PC-3 cells, which is largely mediated by TRPM2 channels.
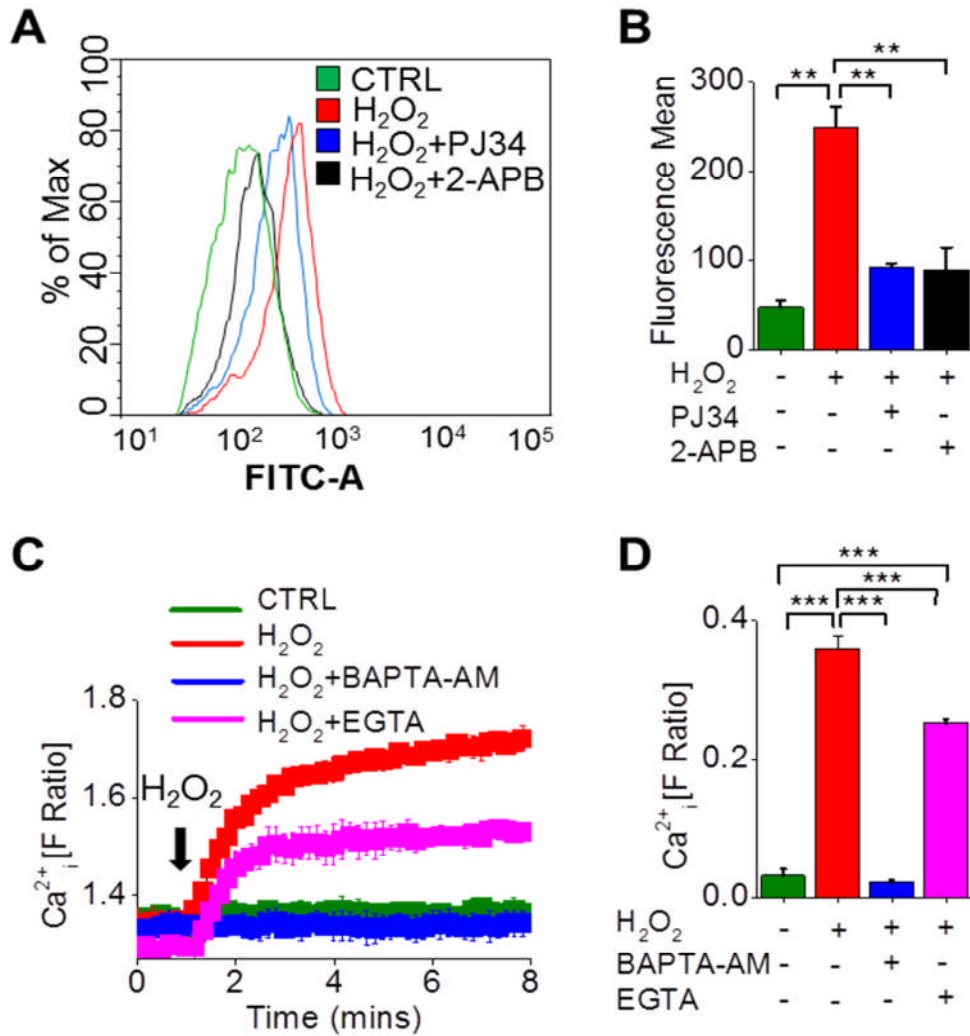
Figure 4. 7 TRPM2 channels mediate H$_2$O$_2$ induced cytosolic Ca^{2+} increase in PC-3 cells. (**A**) PC-3 cells were either not treated (CTRL) or treated with H$_2$O$_2$ (100 µM) minus or plus PJ34 (10 µM) and 2-APB (150 µM). The cells were loaded with Fluo4-AM and analysed by FACS. The results are presented as histogram (~ 5000 cells). Green: CTRL; Red: H$_2$O$_2$; Cyan: H$_2$O$_2$ plus PJ34; Black: H$_2$O$_2$ plus 2-APB. (**B**) Mean ± SEM of Ca^{2+} fluorescence (5000 cells) from three independent experiments performed as in (A); ** indicates $p < 0.01$; one-way Anova with post-hoc Tukey test. (**C**) PC-3 cells were loaded with Fura-2-AM for 1 hour followed with three times washing; cells were then treated as follows: CTRL (SBS alone); H$_2$O$_2$ (SBS alone); BAPTA-AM (SBS containing 10 µM BAPTA-AM); EGTA (SBS containing 1.5 mM EGTA) for 1 hour at 37°C and then cytosolic Ca^{2+} were measured by Flexstation Microplate Reader; at 60 sec, H$_2$O$_2$ was added to H$_2$O$_2$ wells and wells containing BAPTA-AM and EGTA pre-treated cells. The fluorescence ratio of 340/ 380 was recorded. (**D**) Mean ± SEM of fluorescence amplitude from at least three independent experiments performed as in (C). *** indicates $p < 0.001$; one-way Anova with post-hoc Tukey test.

4. 2. 7 H_2O_2 activation of TRPM2 channels causes a rise in cytosolic level of Zn^{2+} in HeLa cells

In addition to raising cytosolic Ca^{2+}, H_2O_2 activation of TRPM2 channels can also increase cytosolic Zn^{2+} in pancreatic β-cells (Manna et al., 2015) and TRPM2 transfected HEK-293 cells (Yu et al., 2012). To examine whether H_2O_2 causes Zn^{2+} rise in HeLa cells, FluoZin-3-AM, was loaded into the cells and H_2O_2 induced changes in fluorescence were measured by confocal microscopy and flow cytometry. The results showed a marked increase in the FluoZin-3 signal induced by H_2O_2 (Figure 4.8A-D). Chemical inhibition of TRPM2 channels by PJ34 and 2-APB fully prevented the H_2O_2 induced increase in Zn^{2+} signal, indicating the role of TRPM2 channels in Zn^{2+} elevation (Figure4.8A-D). Inclusion of EGTA (which can chelate both Ca^{2+} and Zn^{2+}) in the extracellular medium failed to prevent the increase in Zn^{2+} fluorescence indicating that Zn^{2+} is released from an intracellular source. Inhibition of TRPM2 channels by TRPM2 siRNA suppressed the rise in the cytosolic levels of Zn^{2+} (Figure 4.8E-F), further indicating that the changes in Zn^{2+} are TRPM2 mediated.

In combination with Ca^{2+} data in Figure 4.5, these results indicate that H_2O_2 induces marked increase in the intracellular levels of both Ca^{2+} and Zn^{2+} through activation of TRPM2 channels in HeLa cells.
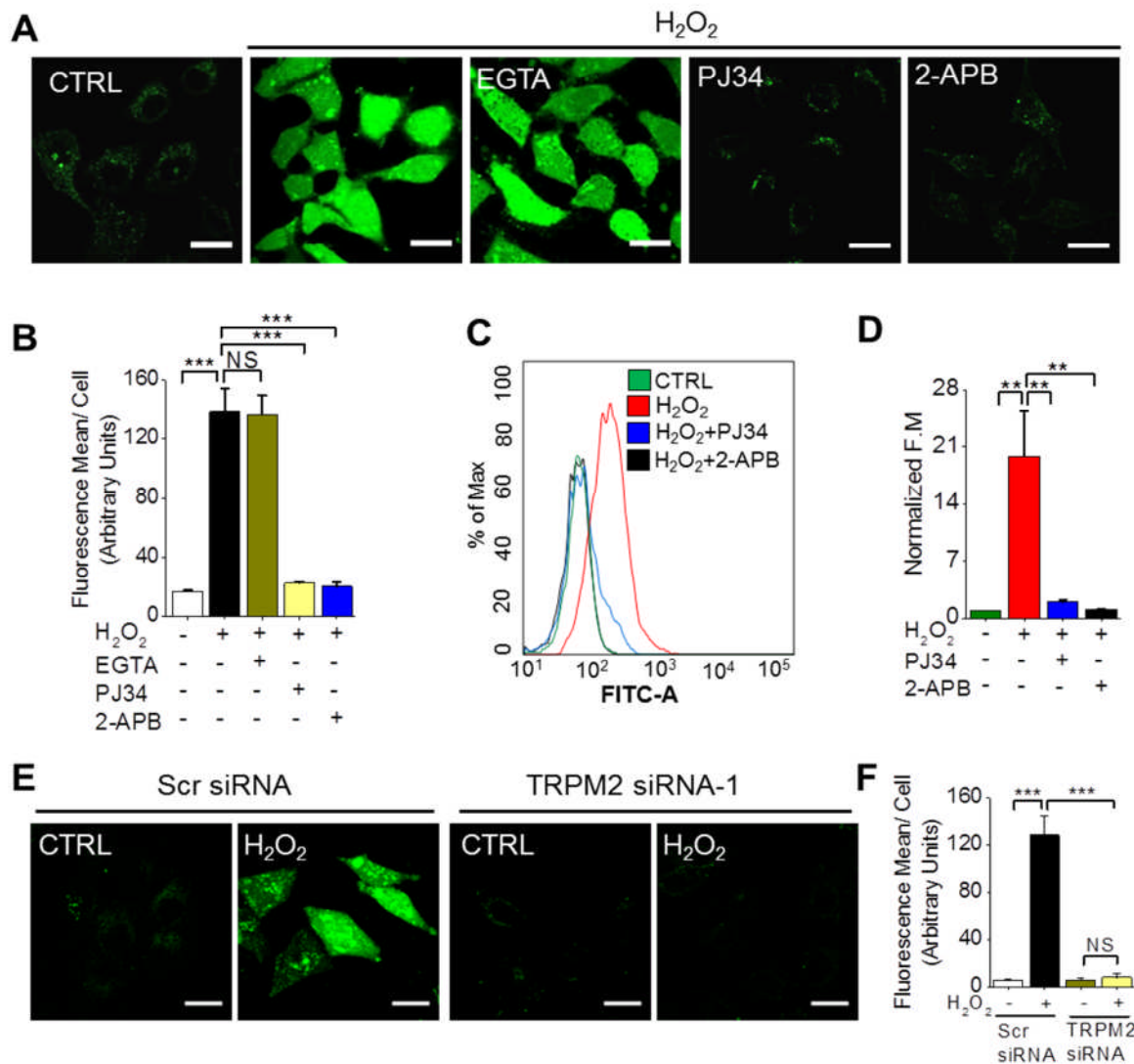
Figure 4. 8 H$_2$O$_2$ activation of TRPM2 channels causes a rise in cytosolic Zn^{2+} in HeLa cells. (**A**) Cytosolic Zn^{2+} in HeLa cells stained with FluoZin3-AM; Cells were either not treated (CTRL) or treated with H$_2$O$_2$ (200 µM) plus or minus EGTA (5 mM), PJ34 (10 µM) and 2-APB (150 µM); representative control images are shown; scale bars = 20 µm. (**B**) Mean ± SEM of average Zn^{2+} fluorescence per cell from three independent experiments performed as in (A); *** indicates $p < 0.001$; NS, not significant; one-way Anova with post-hoc Tukey test. (**C**) HeLa cells were either not treated (CTRL) or treated with H$_2$O$_2$ (200 µM) minus or plus PJ34 (10 µM) and 2-APB (150 µM). Cells were loaded with Fluo4-AM and then analysed by FACS. Histogram plot of flow cytometry analysis (n~ 5000) is shown. Green: CTRL; Red: H$_2$O$_2$; Cyan: H$_2$O$_2$ plus PJ34; Black: H$_2$O$_2$ plus 2-APB. (**D**) Mean ± SEM of Ca^{2+} fluorescence (5000 cell s) from three independent experiments performed as in (C). (**E**) HeLa cells transfected with scrambled siRNA or siRNA against TRPM2 were either not treated or treated with H$_2$O$_2$ (200 µM) and cells were stained with FluoZin3-AM; representative control images are shown; scale bars = 20 µm. (**F**) Mean ± SEM of average Zn^{2+} fluorescence per cell from three independent experiments performed as in (E); *** indicates $p < 0.001$; NS, not significant; one-way Anova with post-hoc Tukey test.

144

4. 2. 8 H_2O_2 activation of TRPM2 channels causes a rise in cytosolic level of Zn^{2+} in PC-3 cells

Having, demonstrated the role of H_2O_2 and TRPM2 channels in induction of cytosolic Zn^{2+} increase in HeLa cells, effect of H_2O_2 on Zn^{2+} dynamics in PC-3 cells was investigated using confocal microscopy and flow cytometry. PC-3 cells were treated with H_2O_2 in the absence or presence of PJ34 and 2-APB and loaded with FluoZin3-AM to monitor changes in cytosolic Zn^{2+}. The results showed a remarkable increase in FluoZin3 fluorescence following H_2O_2 treatment; inclusion of PJ34 and 2-APB completely prevented the H_2O_2 induced Zn^{2+} elevation, indicating that TRPM2 channels are responsible for the changes in Zn^{2+} (Figure 4.9A-B). Consistent with the confocal data, the results of flow cytometry showed strong Zn^{2+} signal induced by H_2O_2 and inhibition of TRPM2 channels with PJ34 and 2-APB rescued the cytosolic Zn^{2+} signal (Figure 4.9C-D). As there is no extracellular Zn^{2+} in the medium, the increase in Zn^{2+} could be attributed to Zn^{2+} release from an intracellular source.

These data indicate that TRPM2 channels mediate H_2O_2 induced Zn^{2+} release in PC-3 cells.
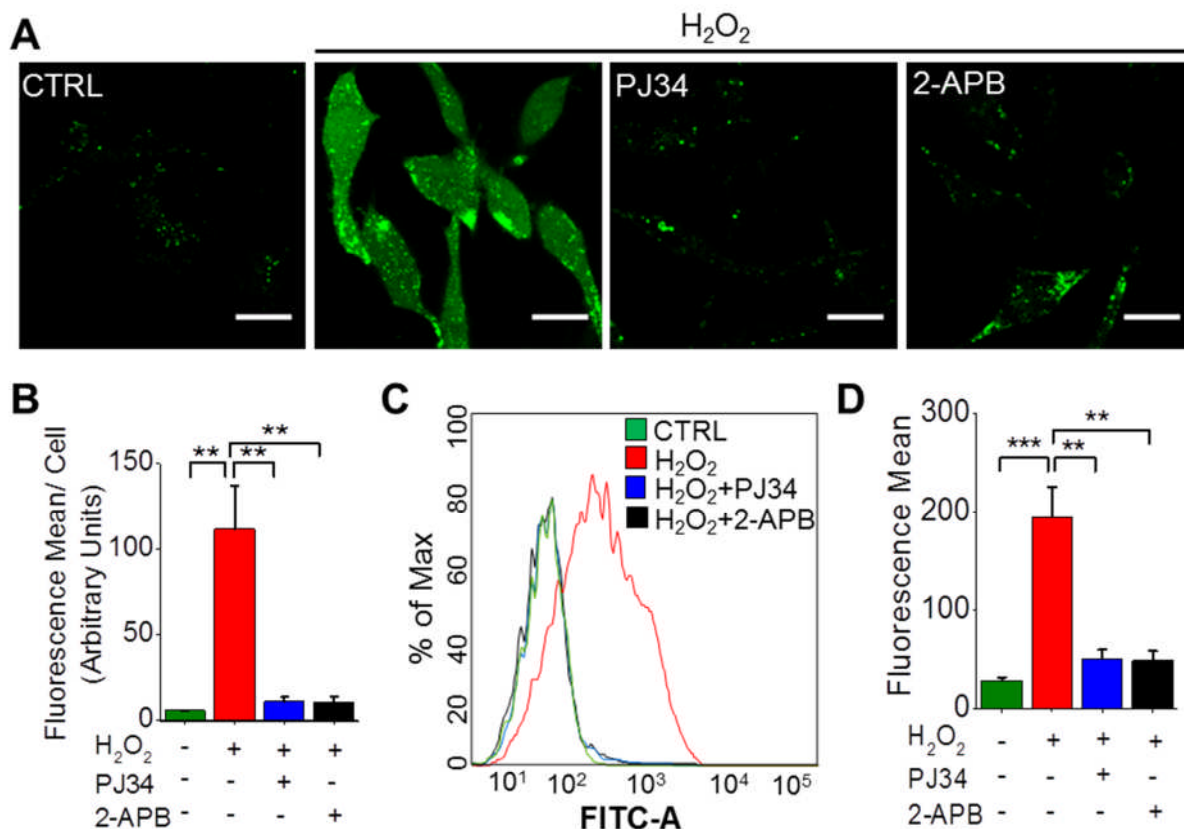
Figure 4. 9 Effect of H$_2$O$_2$ on cytosolic Zn^{2+} in PC-3 cells (**A**) Cells were either not treated (CTRL) or treated with H$_2$O$_2$ (100 µM) plus or minus PJ34 (10 µM) and 2-APB (150 µM); representative control images are shown; scale bars = 20 µm. (**B**) Mean ± SEM of average Zn^{2+} fluorescence per cell (CTRL: 123 cells; H$_2$O$_2$: 126 cells; PJ34: 117 cells; 2-APB: 125 cells) from three independent experiments performed as in (A); ** indicates $p < 0.01$; one-way Anova, with post-hoc Tukey test. (**C**) PC-3 cells were either not treated (CTRL) or treated with H$_2$O$_2$ (100 µM) minus or plus PJ34 (10 µM) and 2-APB (150 µM). Cells were then loaded with FluoZin3-AM and analysed by FACS. Histogram plot of flow cytometry analysis (n ~ 5000) were shown. Green: CTRL; Red: H$_2$O$_2$; Cyan: H$_2$O$_2$ plus PJ34; Black: H$_2$O$_2$ plus 2-APB. (**D**) Mean ± SEM of Zn^{2+} fluorescence (~5000 cells) from three independent experiments performed as in (C). *** indicates $p < 0.001$; ** indicates $p < 0.01$; one-way Anova, with post-hoc Tukey test.

4. 2. 9 Zn^{2+} is enriched in lysosomes of HeLa and PC-3 cells

Since H_2O_2 induced Zn^{2+} release is from an intracellular source, the location of free Zn^{2+} was examined. Previous studies have shown that lysosomes serve as intracellular Zn^{2+} sinks to impact on the net cellular Zn^{2+} distribution (Ira et al., 2013; Kukic et al., 2014). Therefore, to determine the intracellular source of Zn^{2+}, cells were stained with indicators of different organelles. The results show significant co-localisation (yellow in merged images) of Zn^{2+} stain (green) with LysoTracker (red) (Figure 4.10A-B), indicating that the source of the Zn^{2+} is likely lysosomes. Mitochondria and ER stains, on the other hands, showed little co-localisation with the Zn^{2+} stain (Figure 4.10A-B).

Collectively, these data suggest that free Zn^{2+} is largely present in lysosomes of HeLa and PC-3 cells.
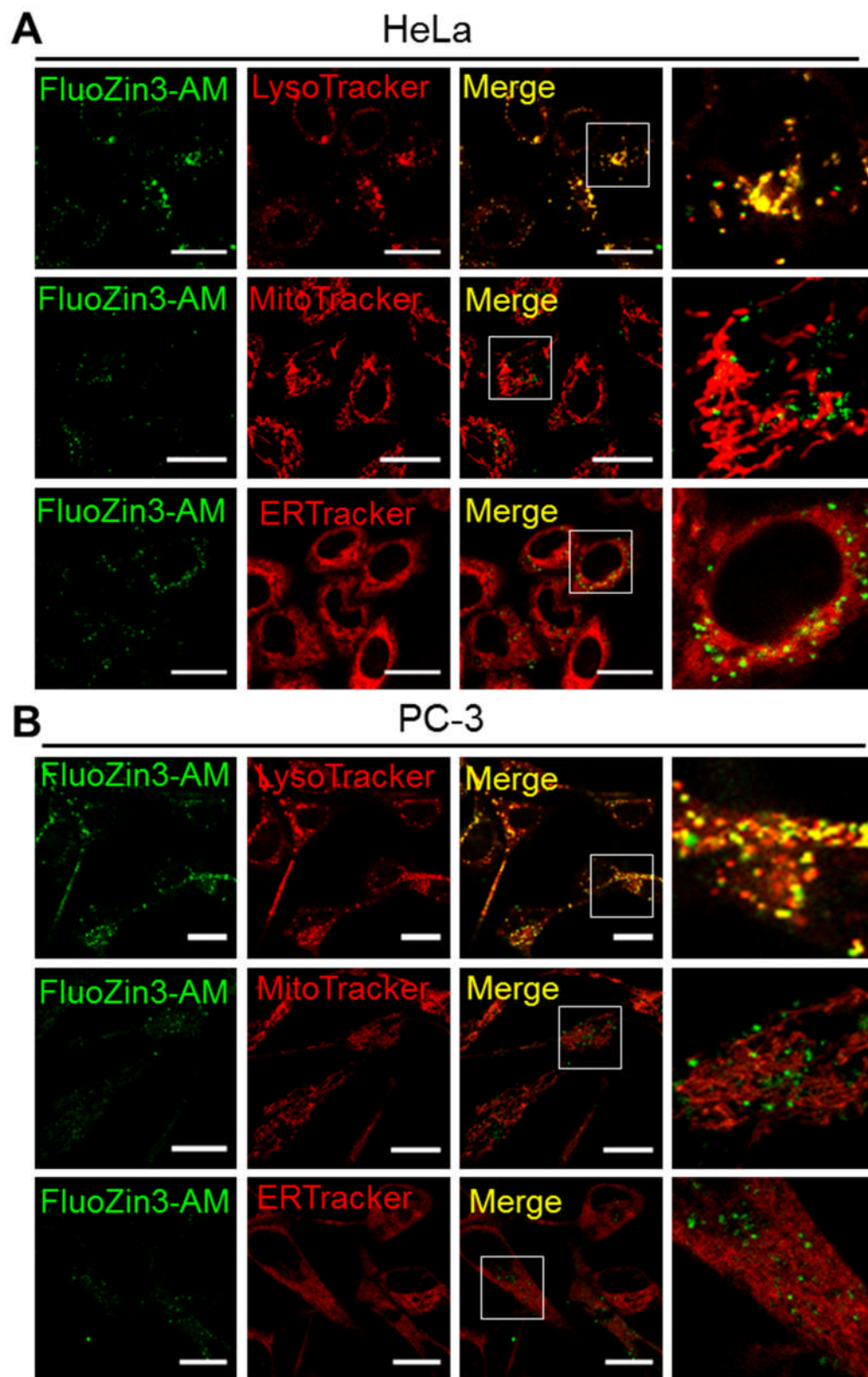
Figure 4. 10 Zn^{2+} is enriched in lysosomes of HeLa and PC-3 cells. (A-B) Staining of HeLa (A) and PC-3 (B) cells with FluoZin3-AM (green) and indicators of organelles (red); representative confocal images are shown; scale bars = 20 μm.

4. 2. 10 TRPM2 expression in lysosomes of HeLa cells

Apart from the plasma membrane, TRPM2 channels have been shown to be expressed in lysosomes of pancreatic β-cells where they mediate Ca^{2+} release (Lange et al., 2009). To test if lysosomes of HeLa cells express TRPM2 channels, two approaches were used: immuno-staining and western blotting.

For immuno-staining, HA-tagged TRPM2 channels were expressed in HeLa cells and stained for HA-TRPM2 using anti-HA antibodies and for lysosomes using anti-LAMP1 antibodies. The Z-stack confocal images (Figure 4. 11A right panel) show clear co-localisation of HA-tagged TRPM2 channels (green) with the lysosomal CD63 protein (red), indicating expression of TRPM2 channels in lysosomes.

To confirm lysosomal expression of TRPM2 channels, lysosomes were isolated by Opti-prep differential centrifugation from HeLa cells transfected with the HA-TRPM2 plasmid construct. Lysosomal fraction was subjected to western blotting using anti-HA, anti-LAMP1 and anti-Calnexin (ER marker) antibodies. The results (Figure 4. 11B) show presence of TRPM2 band (~ 170 KDa) in the lysosomal fraction. Although there is some contamination of the lysosomal fraction with the ER indicated by a band with anti-Calnexin antibodies at (~ 90 KDa), the intensity of calnexin band is relatively weak compared with that for LAMP1 (~ 100 KDa).

Taken together with the imaging data, biochemical results support expression of expressed heterologously TRPM2 channels in lysosomes.
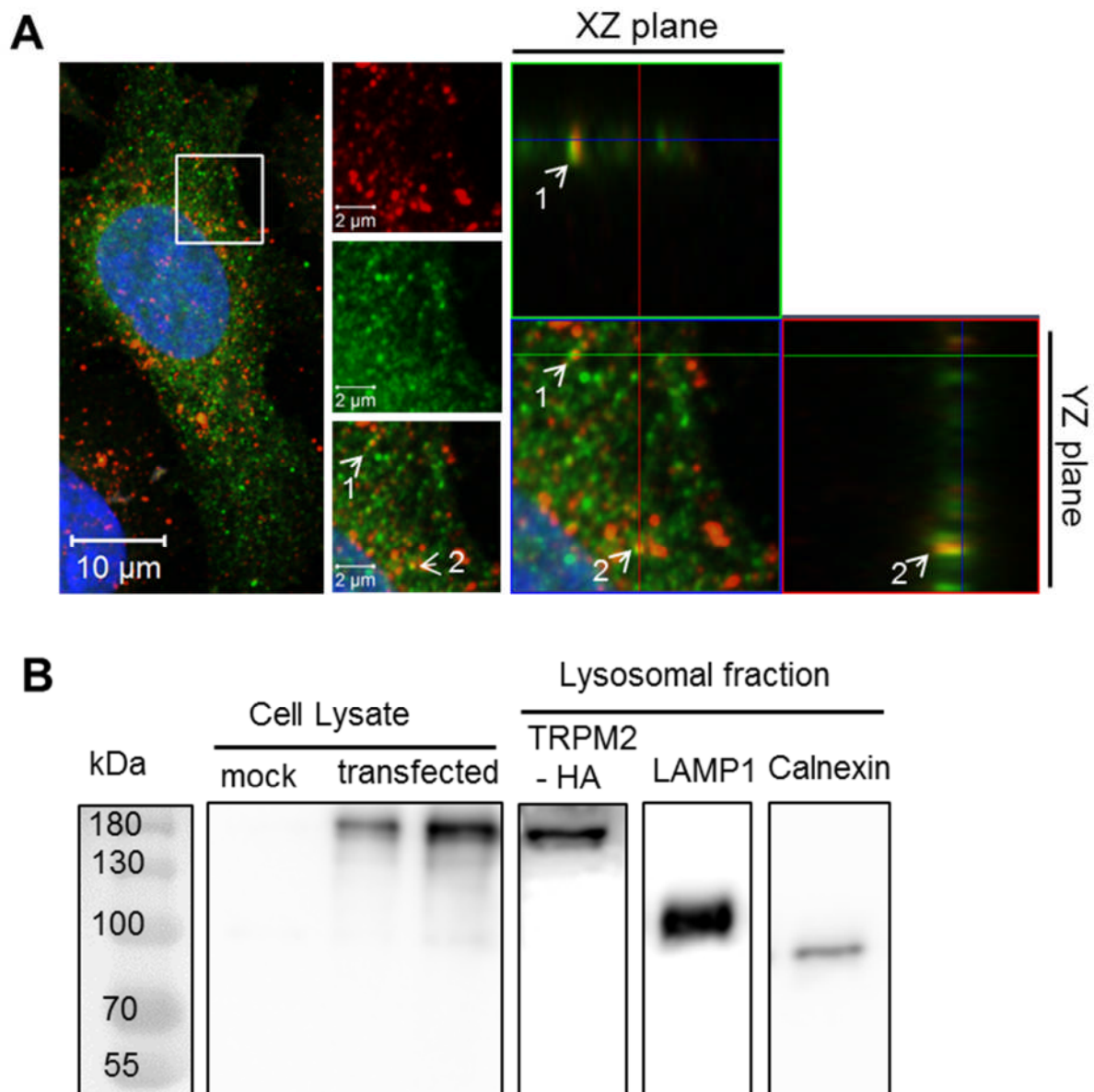
Figure 4. 11 Expression of TRPM2 in lysosomes of HeLa cells (A) HeLa cells were transfected with the HA-tagged TRPM2 plasmid and immunostained for CD63 (red) and the HA epitope (green); white arrows labelled with 1 and 2 indicate representative co-localisation of CD63 and HA-TRPM2 (yellow puncta in right panel). (**B**) Western blot analysis of whole cell lysate and the lysosomal fraction isolated from HeLa cells transfected without (mock) or with (transfected) HA-tagged TRPM2 plasmid. The blots of whole cell lysate were probed with anti-HA antibodies. The blots of lysosomal fraction were probed with antibodies against TRPM2 channels (HA-TRPM2), lysosome marker (LAMP1) and the ER marker (Calnexin).

4. 2. 11 A23187 can be used to selectively induce cytosolic Ca^{2+} rise

Fluo-4 is not specific for Ca^{2+}. It binds Zn^{2+} about 100-fold more avidly than Ca^{2+} (Sensi et al., 2009). Activation of TRPM2 channels was found to cause not only a rise in cytosolic Ca^{2+} (Figure 4. 5), but also Zn^{2+} (Figure 4.8-9). Thus the Fluo-4 signal seen in Figure 4.5, attributed to Ca^{2+}, could, in part, be due to a rise in Zn^{2+}. Consistent with this, the Zn^{2+} selective chelator, TPEN, partially attenuated the H_2O_2 induced Fluo-4 signal, whilst BAPTA-AM, which chelates both Ca^{2+} and Zn^{2+}, was able to fully inhibit the Fluo-4 signal (Figure 4.12A and C).

Since H_2O_2 induces both cytosolic Ca^{2+} and Zn^{2+} increase, it is difficult to distinguish the individual effects of Ca^{2+} and Zn^{2+} on actin remodelling. To examine the individual roles of Ca^{2+} and Zn^{2+}, there is a need for a tool that would selectively increase the levels of Ca^{2+} and Zn^{2+}. A23187, a Ca^{2+} ionophore, is widely used to raise the cytosolic level of Ca^{2+}. However, it is not known if it also increases the cytosolic Zn^{2+} level. When HeLa cells were treated with A23187, intracellular Ca^{2+} level was significantly elevated indicated by the marked increase in Fluo-4 fluorescence. The increase in fluorescence was completely inhibited by BAPTA-AM, but not TPEN (Figure 4.12B and D), indicating that A23187 causes selective rise in intracellular Ca^{2+}.

These data suggest that H_2O_2 induced Fluo4 signal (Figure 4. 12) is partly due to the rise in Zn^{2+} and that A23187 can be used to examine Ca^{2+} specific cellular changes.
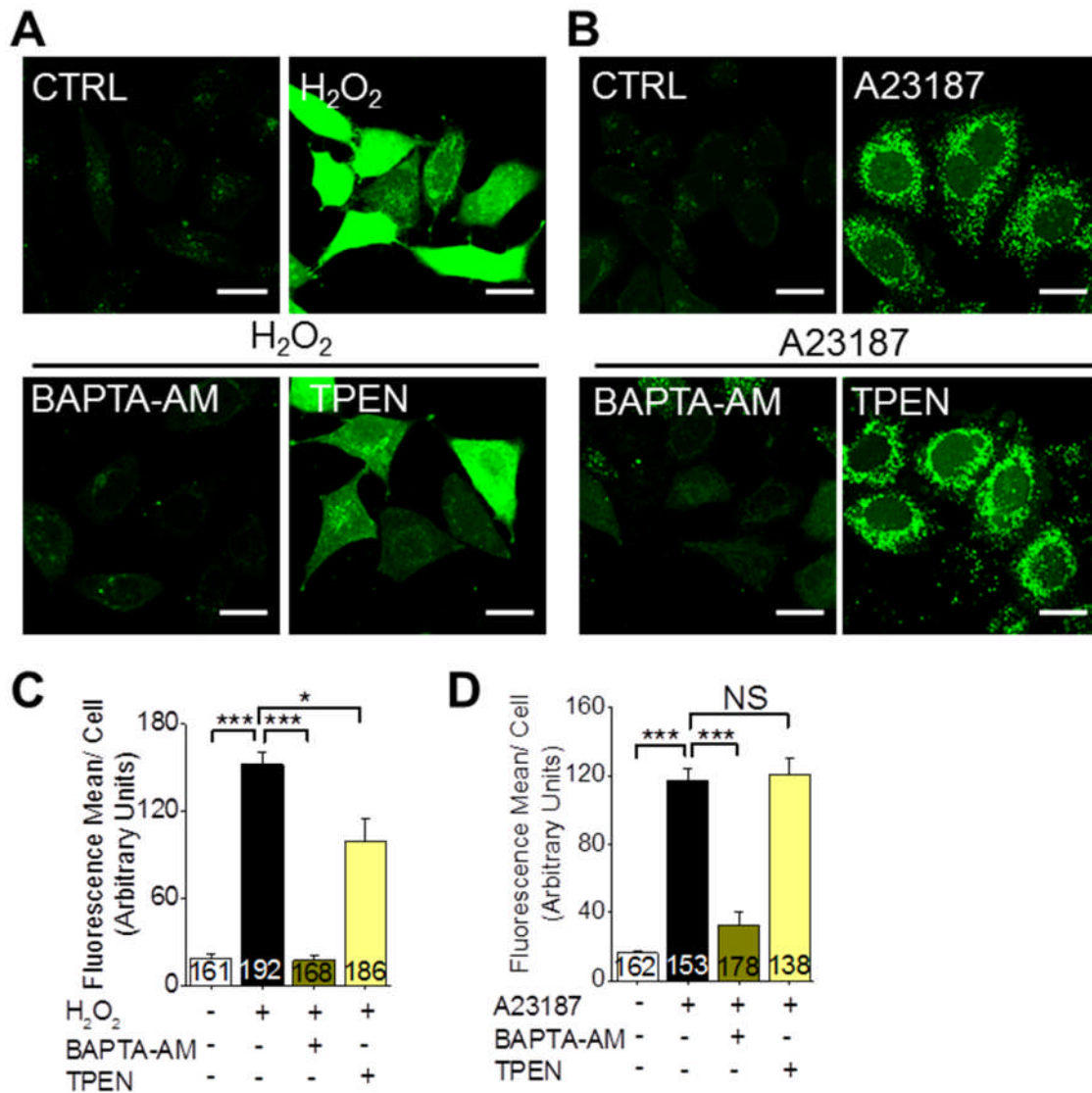
Figure 4. 12 A23187 can be used to induce rise in cytosolic Ca^{2+} selectively. (**A**) H$_2$O$_2$ induced increase in Fluo4 signal can be fully inhibited by BAPTA-AM, and partially by TPEN; HeLa cells were treated without (CTRL) or with H$_2$O$_2$ (200 µM) minus or plus BAPTA-AM (10 µM) and TPEN (5 µM); representative confocal images are shown ; scale bars = 20 µm. (**B**) A23187 raises cytosolic Ca^{2+}, but not Zn^{2+}; Cells were either not treated (CTRL) or treated with A23187 (3 µM) minus or plus BAPTA-AM (10 µM) and TPEN (5 µM); representative confocal images are shown; scale bars = 20 µm. (**C**) Mean ± SEM of average Fluo4 fluorescence per cell (number of cells analysed are shown within each bar) from three independent experiments performed as in (A); *** indicates $p < 0.001$; * indicates $p < 0.05$; one-way Anova with post-hoc Tukey test. (**D**) Mean ± SEM of average Fluo4 fluorescence per cell (number of cells analysed are shown within each bar) from three independent experiments performed as in (B); *** indicates $p < 0.001$; NS, not significant; one-way Anova with post-hoc Tukey test.

4. 2. 12 Zn-pyrithione can be used to selectively elevate cytosolic Zn^{2+} levels

As shown before (Figure 4.8A), after H_2O_2 treatment, intracellular Zn^{2+} was dramatically increased as detected by FluoZin3-AM (Figure 4.13 A and C). H_2O_2 induced Zn^{2+} signal was fully inhibited by TPEN, but partly by BAPTA-AM (Figure 4. 13A and C). Complete inhibition of FluoZin-3 signal by TPEN is consistent with the previous reports (Gyulkhandanyan et al., 2006; Manna et al., 2015) that FluoZin-3 is specific for Zn^{2+}. The partial removal of the FluoZin-3 signal by BAPTA-AM is consistent with its inability to discriminate between Ca^{2+} and Zn^{2+} (Sensi et al., 2009).

The ability of Zn-PTO to selectively elevate cytosolic Zn^{2+} was next examined. For this, cells were treated with Zn-PTO for 2 hours and loaded with FluoZin3-AM. The results show that Zn-PTO causes marked increase in FluoZin-3 fluorescence (Figure 4.13 B and D). TPEN was able to fully abolish the FluoZin-3 signal, whereas BAPTA-AM partially attenuated the Zn^{2+} signal (Figure 4. 13B and D). Similar results were obtained in PC-3 cells showing significant cytosolic Zn^{2+} increase induced by Zn-PTO that was quenched by TPEN (Figure 4. 13E).

Taken together, these results indicate that FluoZin3-AM and TPEN are specific for Zn^{2+}, and that Zn-PTO can be used to selectively increase cytosolic Zn^{2+} to examine the role of Zn^{2+} in actin remodelling. The results also confirm the non-selective ability of BAPTA-AM to chelate Zn^{2+}.
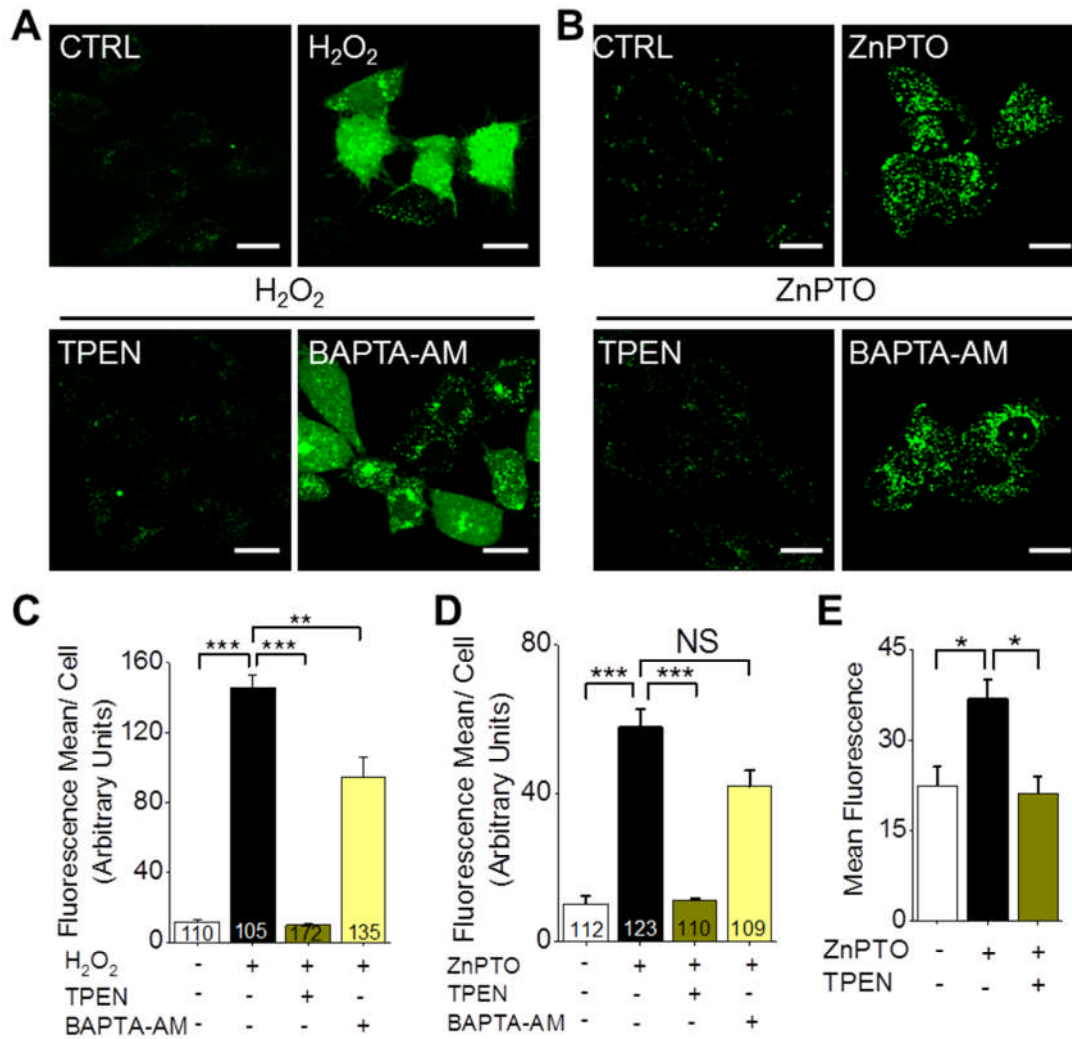
Figure 4. 13 Zn-pyrithione can be used to selectively elevate cytosolic Zn²⁺ levels. (**A**) H₂O₂ induced increase in FluoZin3 signal can be fully inhibited by TPEN, and partially by BAPTA-AM; HeLa cells were treated without (CTRL) or with H₂O₂ (200 µM) minus or plus TPEN (5 µM) and BAPTA-AM (10 µM); representative confocal images are shown; scale bars = 20 µm. (**B**) Zn-PTO raises cytosolic Zn²⁺, but not Ca²⁺; Cells were either not treated (CTRL) or treated with Zn-PTO (3 µM) minus or plus TPEN (5 µM) and BAPTA-AM (10 µM); representative confocal images are shown; scale bars = 20 µm. (**C-D**) Mean ± SEM of average FluoZin3 fluorescence per cell (cell numbers are indicated in the bar chart) from three independent experiments performed as in (A) or (B); *** indicates $p < 0.001$; ** indicates $p < 0.01$; NS, not significant; one-way Anova with post-hoc Tukey test. (**E**) PC-3 cells were labelled with FluoZin3-AM for 1 hour at 37°C followed by incubation with different compounds (CTRL; Zn-PTO minus or plus TPEN) for 2 hours at 37°C. Cytosolic Zn²⁺ was then measured by FlexStation II. Mean ± SEM of fluorescence was shown from at least three independent experiments. * indicates $p < 0.05$; one-way Anova with post-hoc Tukey test.

4. 2. 13 Opposite effects of Ca^{2+} and Zn^{2+} on actin remodelling

Previous studies have reported that Ca^{2+} plays a key role in the actin cytoskeleton remodelling. Given the above findings, it is reasonable to assume that Zn^{2+} also contributes to actin remodelling. Chelation of Zn^{2+} with TPEN indeed showed a striking effect on the actin cytoskeleton: it suppressed H_2O_2 induced filopodia formation and loss of stress fibres (Figure 4.14A and C). Interestingly, however, chelation of Ca^{2+} with BAPTA-AM has little effect on H_2O_2 induced changes in the actin cytoskeleton (Figure 4.14A and C).

Since H_2O_2 can affect a number of other signalling pathways that could confound the interpretation of the data here, A23187 and Zn-PTO were used to raise the cytosolic concentrations of Ca^{2+} and Zn^{2+} respectively and thus examine the individual roles of these two ions on actin remodelling in the absence of H_2O_2. The results (Figure 4.14B and D) show that delivery of Zn^{2+} through PTO suppresses stress fibres and increases filopodia formation. Co-application of TPEN was able to antagonise the effect of Zn-PTO. Together with the results presented in Figure 4.14A and C, these data confirm that Zn^{2+} promotes filopodia formation and disassembly of stress fibres. Increasing the Ca^{2+} entry via A23187 had no major effect on actin cytoskeleton, but, interestingly, co-treatment with BAPTA-AM attenuated stress fibres and induced filopodia formation (Figure 4.14B and D). These results indicate that basal levels of Ca^{2+} are required to maintain stress fibres, and to suppress filopodia formation.

Similar results were obtained with PC-3 cells (Figure 4. 15). Taken together, these results indicate that Ca^{2+} and Zn^{2+} have distinct, but opposite, effects on stress fibres and filopodia formation. Interestingly, the effects of Zn-PTO are very similar to those of H_2O_2 indicating that Zn^{2+}, rather than Ca^{2+}, plays a dominant role in H_2O_2 induced remodelling of the actin cytoskeleton.
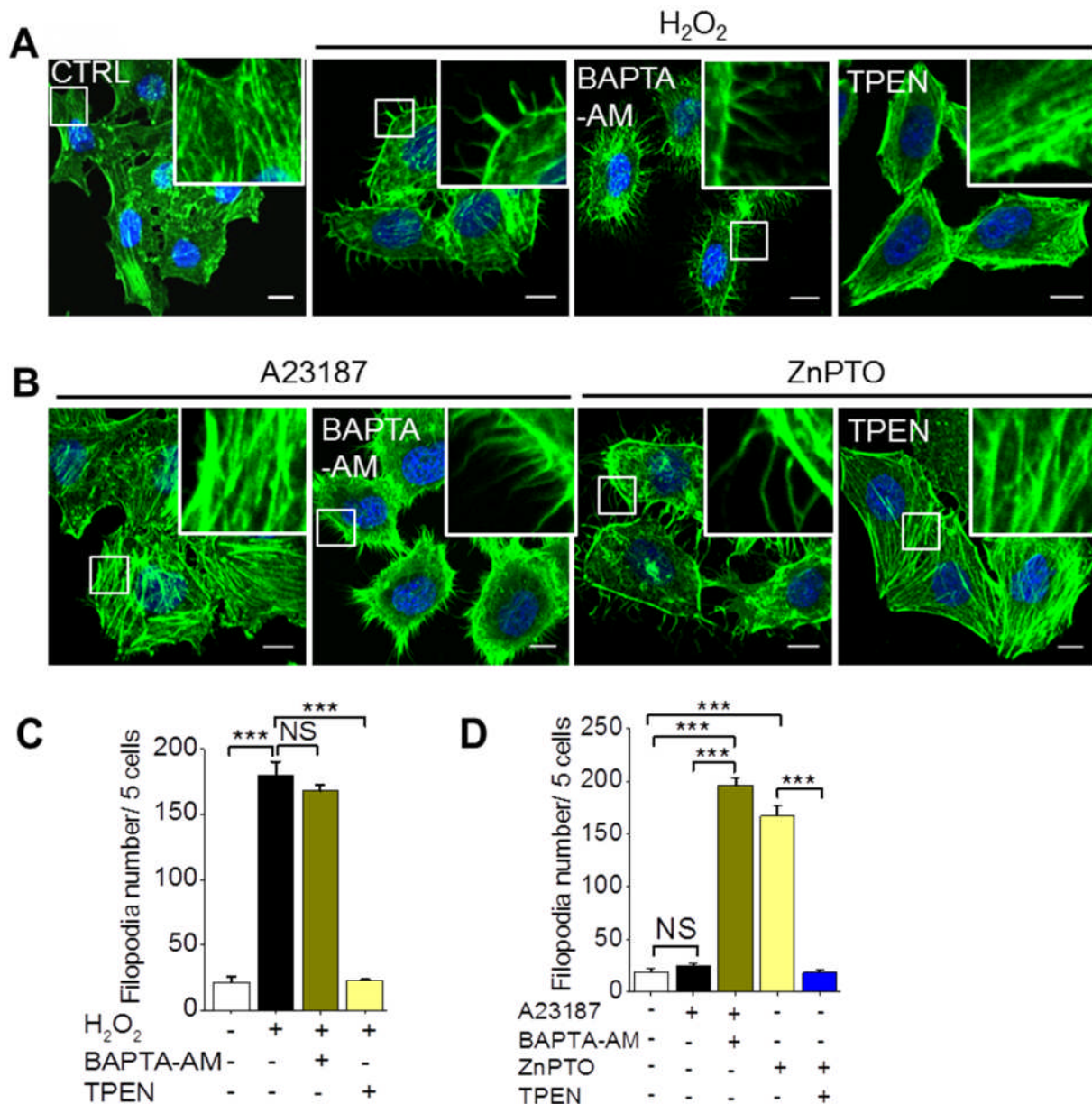
Figure 4. 14 Opposite effects of Ca^{2+} and Zn^{2+} on H$_2$O$_2$ mediated actin remodelling (**A**) HeLa cells were either not treated (CTRL) or treated with H$_2$O$_2$ (200 µM) plus or minus BAPTA-AM (10 µM) and TPEN (5 µM) and then stained for F-actin. Representative images are shown; scale bars = 20 µm. (**B**) F-actin was stained in HeLa cells following buffer (CTRL), A23187 (3 µM) minus or plus BAPTA-AM (10 µM) and Zn-PTO (3 µM) minus or plus TPEN (5 µM) treatments. Representative images are shown; scale bars = 20 µm. (**C**) Mean ± SEM of filopodia number (5 cells) from three independent experiments performed as in (A); *** indicates $p < 0.001$; NS, not significant; one-way Anova with post-hoc Tukey test. (**D**) Mean ± SEM of filopodia number (5 cells) from three independent experiments performed as in (B); *** indicates $p < 0.001$; Student's t test.
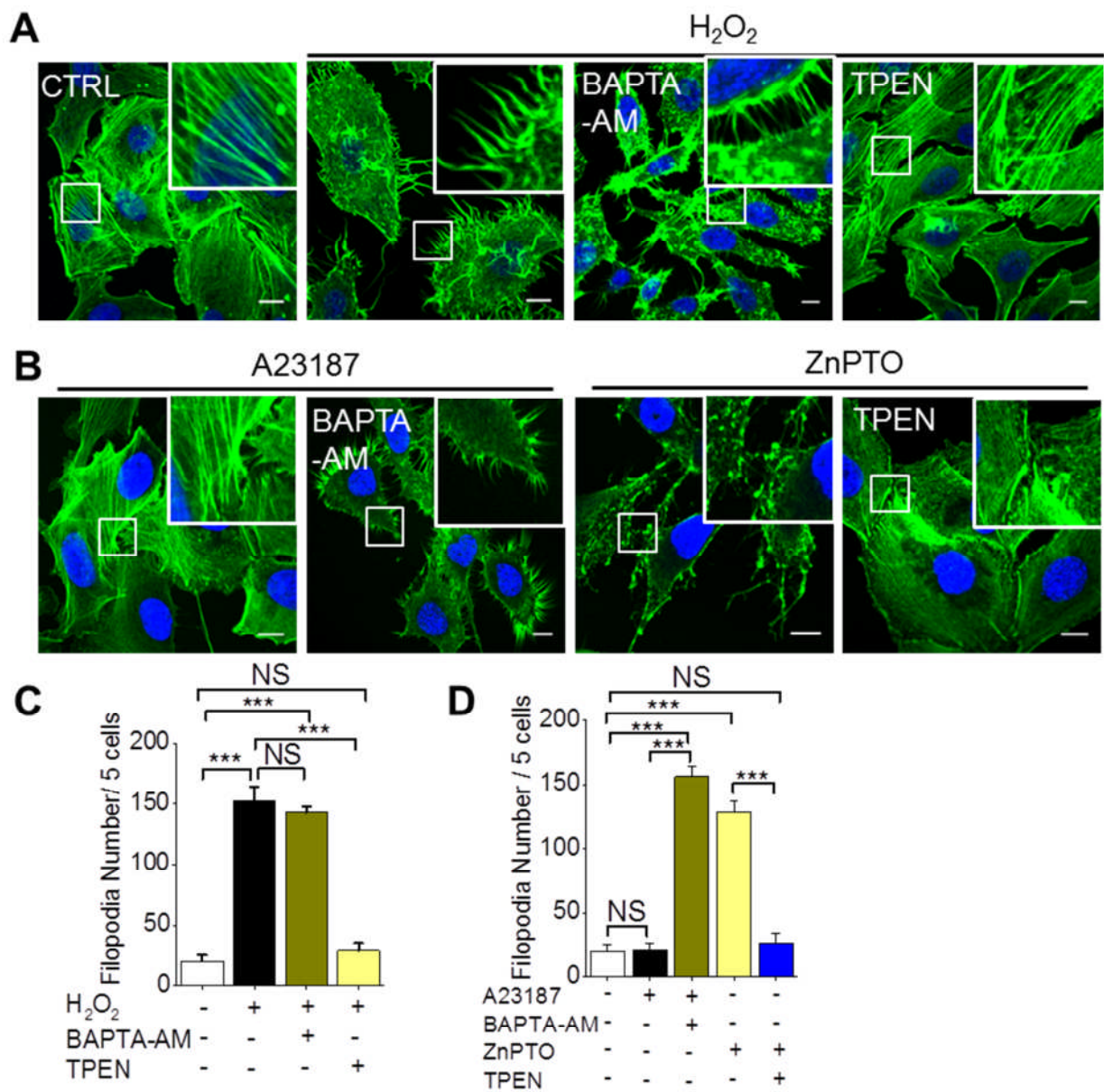
Figure 4. 15 Opposite effects of Ca^{2+} and Zn^{2+} on actin remodelling in PC-3 cells.
Experiments were performed and analysed as in Figure 4. 14.

4. 2. 14 Cdc42 and Rif are not involved in H_2O_2 induced filopodia formation

Previous studies have demonstrated that Cdc42 is the main regulator of filopodia formation in mammalian cells (Nobes and Hall, 1995). Cdc42 belongs to the Rho GTPase family (Nobes and Hall, 1995). In its GTP-bound form, Cdc42 is active and induces filopodia; while in the GDP-bound form, Cdc42 is inactive and incapable of inducing filopodia formation. To examine whether Cdc42 is involved in H_2O_2 induced filopodia formation, constitutively-active (QL-Cdc42) and dominant-negative (TN-Cdc42) Cdc42 mutant constructs were used. If H_2O_2 induced filopodia formation is dependent on Cdc42, one would expect heterologous expression of QL-Cdc42 to have no major effect, but TN-Cdc42 to inhibit H_2O_2 induced filopodia formation. After transfection with EGFP-tagged QL-Cdc42, the transfected cells generated filopodia but not as significant as H_2O_2 (Figure 4. 17A); cells transfected with the TN-Cdc42 construct failed to suppress H_2O_2 induced filopodia formation treatment (Figure 4. 17A). These data indicate that Cdc42 does not appear to mediate H_2O_2 induced filopodia formation. One previous study reported that active Cdc42 accumulates at the leading edge of migrating astrocytes and contributes to the cell polarity required for directional migration (Osmani et al., 2010). Interestingly, H_2O_2 caused translocation of constitutively-active Cdc42 from the cytoplasm to cell periphery was also observed (Figure 4.17A). Whether this translocation plays a role in HeLa cell migration needs further investigation.

Apart from the classical Rho GTPase, non-classical Rho GTPases were also demonstrated to play roles in actin regulation, among which, Rif is an important one. It has been reported that Rif functions as a regulator of filopodia formation in HeLa cells (Pellegrin and Mellor, 2005). Therefore, the role of Rif in H_2O_2 induced filopodia formation was examined. Effect of two Rif mutants was tested: Myc-tagged constitutively-active Rif (QL-Rif) and dominant-negative Rif (TN-Rif). QL-Rif transfection failed to induce filopodia formation; however, as reported before (Fan et al., 2010), constitutively active Rif strengthened stress fibres (Figure 4. 17B). TN-Rif, failed to suppress H_2O_2 induced filopodia formation. Therefore, Rif does not appear to be essential for H_2O_2 induced filopodia formation.

Taken together, these results demonstrate that H_2O_2 induced filopodia formation in HeLa cells does not appear to be dependent on Cdc42 and Rif.
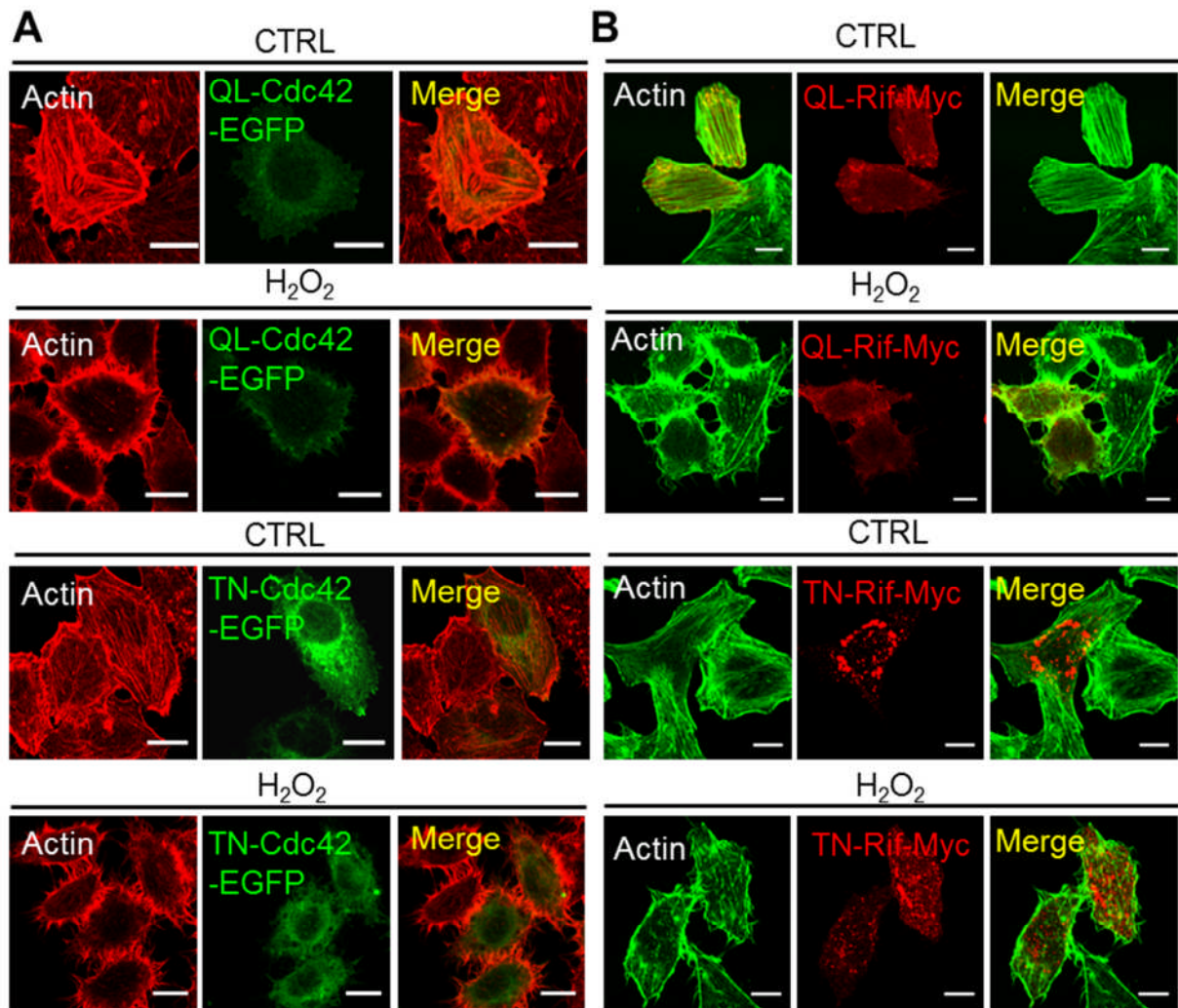
Figure 4. 16 Cdc42 and Rif are not involved in H_2O_2 induced filopodia formation. (**A**) HeLa cells were transfected with EGFP-tagged QL-Cdc42 or TN-Cdc42 plasmids for 48 hours and then exposed to medium alone (CTRL) or medium containing H_2O_2 for 2 hours at 37°C. Then cells were fixed, permeabilized and stained for F-actin. Representative confocal images are shown. Scale bars = 20 μm. (**B**) HeLa cells were transfected with Myc-tagged QL-Rif or TN-Rif for 48 hours and then exposed to medium alone (CTRL) or medium containing H_2O_2 for 2 hours at 37°C. Cells were then fixed, permeabilized and stained for Myc tag and F-actin. Representative confocal images were shown. Scale bars = 20 μm.

4. 2. 15 PI-3K and MAPK are not involved in H_2O_2 induced filopodia formation

PI3-K has been previously been shown to play a role in actin remodelling. Overexpression of PI3-K has been shown to cause an increase in lamellipodia and filopodia formation in chicken embryo fibroblast cells as well as a decrease of actin stress fibers (Qian et al., 2004). Besides, the activation of Akt/PI3-K signaling pathway by H_2O_2 has been reported previously (Lee et al., 2002). Thus, the effect of PI3-K inhibitor, LY294002, on H_2O_2 induced filopodia formation and loss of stress fibres was tested. However, inhibition of PI3-K had no effect on H_2O_2 induced filopodia formation and disassembly of stress fibres (Figure 4.17). These data, indicate that H_2O_2 induced actin remodelling is independent of PI3-K signalling.

Another signaling pathway that can be activated by H_2O_2 is MAPK signalling pathway (Pennanen et al., 2014). A role for MAPK signalling pathway in actin remodelling has been reported previously (Li et al., 2006; Wang and Doerschuk, 2001). For example, activation of MAPK is critical for the formation of filopodia in hippocampal neurons (Wu et al., 2001). In aortic vascular smooth muscle cells, MAPK pathway inhibition significantly reduced filopodia formation (Campbell and Trimble, 2005). To address the role of MAPK in H_2O_2 induced filopodia formation, a MAPK inhibitor, SB203580, was used. MAPK inhibition by SB203580 failed to inhibit H_2O_2 induced filopodia formation (Figure 4.17). These data indicate that MAPK signalling pathway is not involved in H_2O_2 induced actin cytoskeleton reorganization.

Taken together, these results show that neither PI3-K nor MAPK signalling pathway plays important part in H_2O_2 induced actin remodelling in HeLa cells.
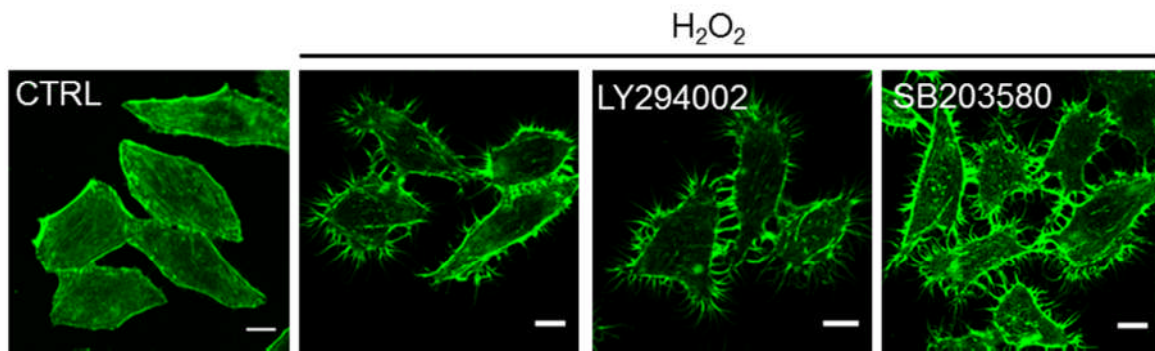
Figure 4. 17 PI3-K and MAPK are not essential for H_2O_2-induced actin remodelling in HeLa cells. HeLa cells were either not treated (CTRL) or treated with H_2O_2 in the absence and presence of PI3-K inhibitor (LY294002, 20 µM) or MAPK inhibitor (SB203580, 10 µM) for 2 hours at 37 °C. Cells were then fixed, permeabilized and stained for F-actin. Representative confocal images are shown; Scale bars = 10 µm.

4. 2. 16 TRPM2 channels are involved in H_2O_2 induced focal adhesions disassembly

Focal adhesions are protein complexes that link the cytoplasmic stress fibres to ECM and play a crucial role in cell migration (Nagano et al., 2012). By undergoing assembly and disassembly, focal adhesions regulate the speed of directional cell migration. It has been demonstrated that loss of stress fibres is accompanied by the simultaneous loss of focal adhesions (Chrzanowska-Wodnicka and Burridge, 1996; Ridley and Hall, 1992). Therefore the effect of H_2O_2 on the size and number of focal adhesions was examined by immunostaining for paxillin. Paxillin is an adaptor protein involved in focal adhesion organization and is widely used as a focal adhesion marker.

Consistent with the expectation, H_2O_2 treatment caused a marked loss of focal adhesions, as well as a decrease in their size (Figure 4. 18A-C). To investigate whether TRPM2 channels are involved in H_2O_2 induced focal adhesions reorganization, PJ34 and 2-APB were used. PJ34 failed to rescue the loss of focal adhesions, which is consistent with the above results where PJ34 failed to fully prevent H_2O_2 induced stress fibres loss (Figure 4. 3). These data are consistent with the view that there is a close relationship between focal adhesion dynamics and stress fibre dynamics. On the other hand, 2-APB was able to prevent H_2O_2 induced loss of focal adhesions (Figure 4. 18A-C). Knock-down of TRPM2 channels with siRNA significantly rescued focal adhesion density, but not the size of focal adhesions (Figure 4.18D-F), indicating that there may be other pathways responsible for H_2O_2 induced focal adhesion reorganization. The role of TRPM2 channels in focal adhesion dynamics was also examined in PC-3 cells. As expected, H_2O_2 reduced both the size and number of focal adhesions; the effect was fully rescued by 2-APB (Figure 4.18 G-I).

Taken together, these data indicate that H_2O_2 treatment induces disassembly of focal adhesions, and that the disassembly of focal adhesions is partially dependent on TRPM2 channels. Previous studies have indicated that the number and size of focal adhesions are related to the speed of cell migration with smaller focal adhesions contributing to fast migration and large focal adhesions leading to slow migration (Huang et al., 2003). Therefore, the smaller and fewer focal adhesions induced by H_2O_2 might promote rapid migration of HeLa cells.
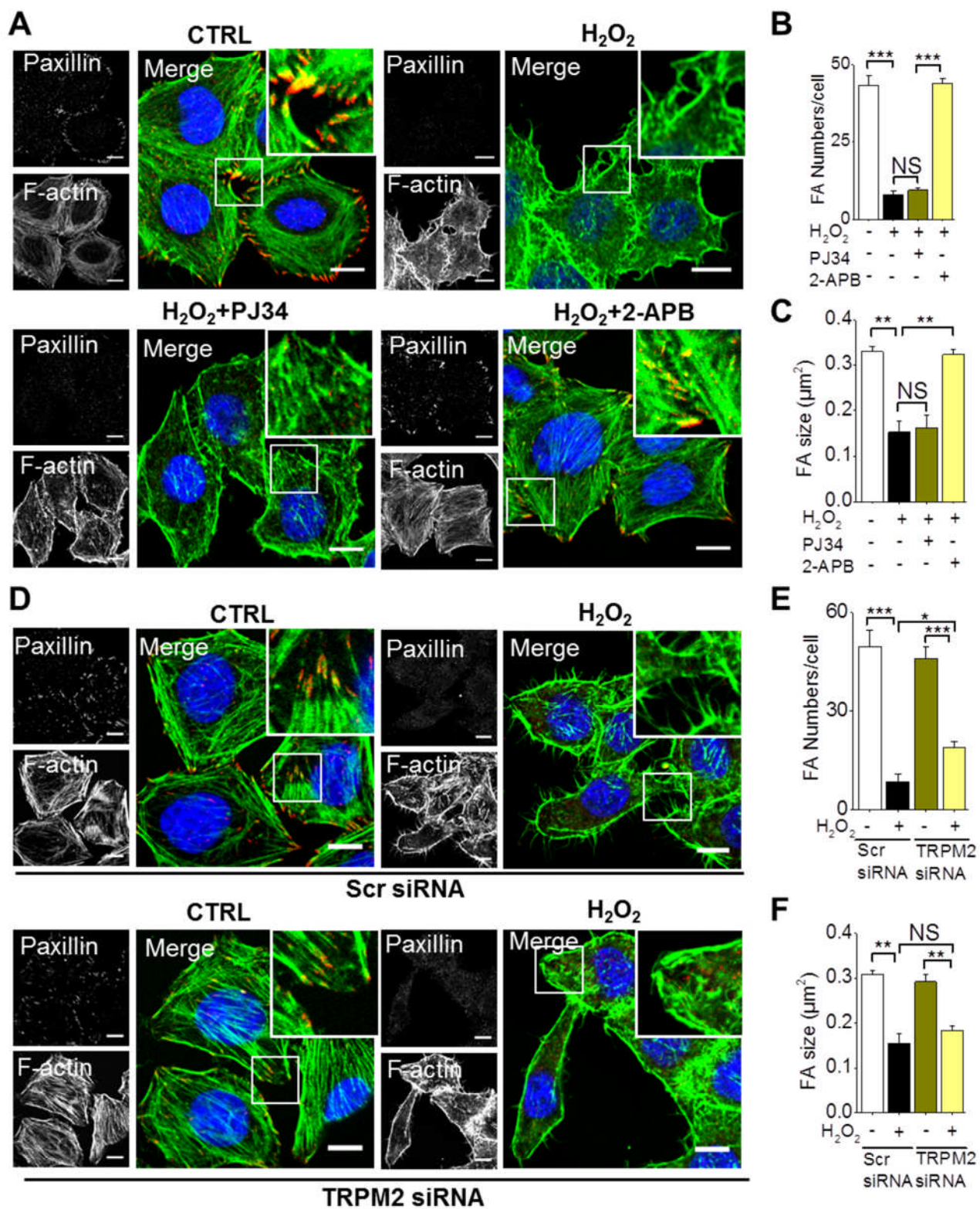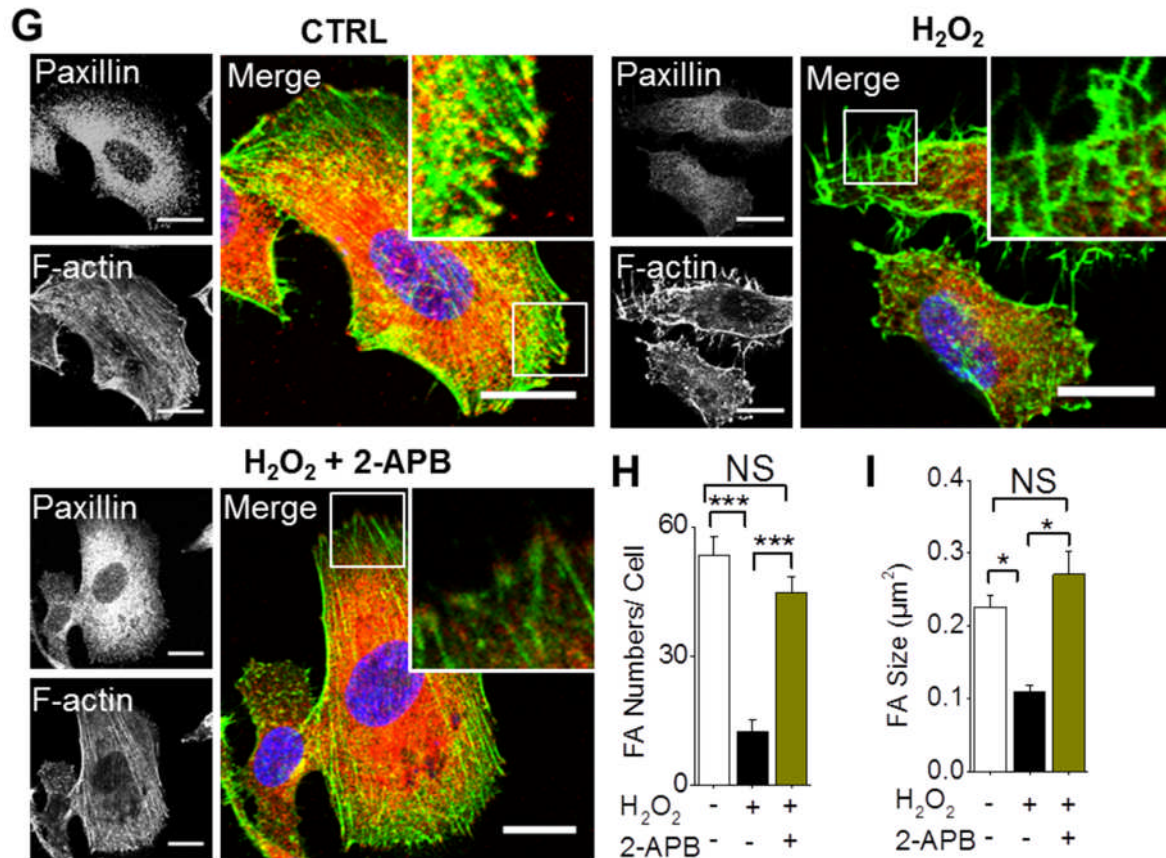
Figure 4. 18 TRPM2 channels contribute to H_2O_2 induced focal adhesion disassembly.
(**A**) Staining of F-actin (green) and paxillin (red) in HeLa cells following buffer (CTRL) or H_2O_2 (200 µM) treatment in the absence and presence of PJ34 (10 µM) or 2-APB (150 µM); Representative confocal images were shown; scale bars = 20 µm. (**B-C**) Mean ± SEM of average paxillin number (B) and size (C) per cell from three independent experiments performed as in (A). *** indicates $p < 0.001$; ** indicates $p < 0.01$; NS, not significant; one-way Anova with post-hoc Tukey test. (**D**) HeLa cells transfected with scrambled siRNA or siRNA against TRPM2 were treated with buffer (CTRL) or H_2O_2 (200 µM) and were then stained for F-actin and paxillin; Representative confocal images were shown; scale bars = 20 µm. (**E-F**) Mean ± SEM of average paxillin number and size from three independent experiments performed as in (D). *** indicates $p < 0.001$; ** indicates $p < 0.01$; * indicates $p < 0.05$; NS, not significant; one-way Anova with post-hoc Tukey test; (**G**) PC-3 cells were stained for F-actin (green) and paxillin (red) following buffer (CTRL) or H_2O_2 treatment (100 µM) in the absence and presence of 2-APB (150 µM); scale bars = 20 µm. (**H-I**) Mean ± SEM of average paxillin number (H) and size (I) per cell from three independent experiments performed as in (G). *** indicates $p < 0.001$; ** indicates $p < 0.01$; NS, not significant; one-way Anova with post-hoc Tukey test.

164

4. 2. 17 Opposite effects of Ca^{2+} and Zn^{2+} on focal adhesions

A role for Ca^{2+} in dynamics of focal adhesions has been reported previously (Giannone et al., 2004), but the effect appears to be cell type dependent. In breast cancer cells, decrease in cytosolic Ca^{2+} induces large mature focal adhesions (Yang et al., 2009a). However, in NIE-115 neuroblastoma cells, rise in cytosolic Ca^{2+} increases the number of large focal adhesions (Clark et al., 2006). A role for Zn^{2+} in focal adhesion dynamics, on the other hand, has not been reported previously. However, a previous study has reported that influx of Zn^{2+} via PTO induces translocation and activation of PKC (Yang et al., 1993), which is a signalling protein important for focal adhesion formation (Kamata et al., 2002). This suggests that elevated cytosolic Zn^{2+} is related to changes in focal adhesions. Since H_2O_2 induced increase in cytosolic Ca^{2+} and Zn^{2+} affects focal adhesions disassembly (Figure 4.5, 4.7, 4.8 and 4.9), the individual roles of Ca^{2+} and Zn^{2+} in H_2O_2 induced reorganization of focal adhesions were examined.

Raising the intracellular Ca^{2+} with A23187 had no effect on either the size or the number of focal adhesions while chelation of Ca^{2+} with BAPTA-AM significantly reduced the size and number of focal adhesions (Figure 4.19A-C for HeLa cells and D-F for PC-3 cells). By contrast, elevation of cytosolic Zn^{2+} with Zn-PTO led to a significant decrease in the number and size of focal adhesions (Figure 4.19A-C for HeLa cells and D-F for PC-3 cells). These effects of Zn-PTO were reversed by the co-application of TPEN. Thus Ca^{2+} and Zn^{2+} have contrasting effects on the dynamics of focal adhesions: Ca^{2+} promotes, whereas Zn^{2+} attenuates focal adhesion formation. However, depletion of intracellular Ca^{2+} appears to be more effective on the disassembly of focal adhesions than the elevation of Zn^{2+}.

Collectively, these data suggest that Ca^{2+} is required for the assembly of focal adhesions while Zn^{2+} promotes focal adhesions disassembly. These two ions thus have opposite effects on focal adhesion reorganization induced by H_2O_2.
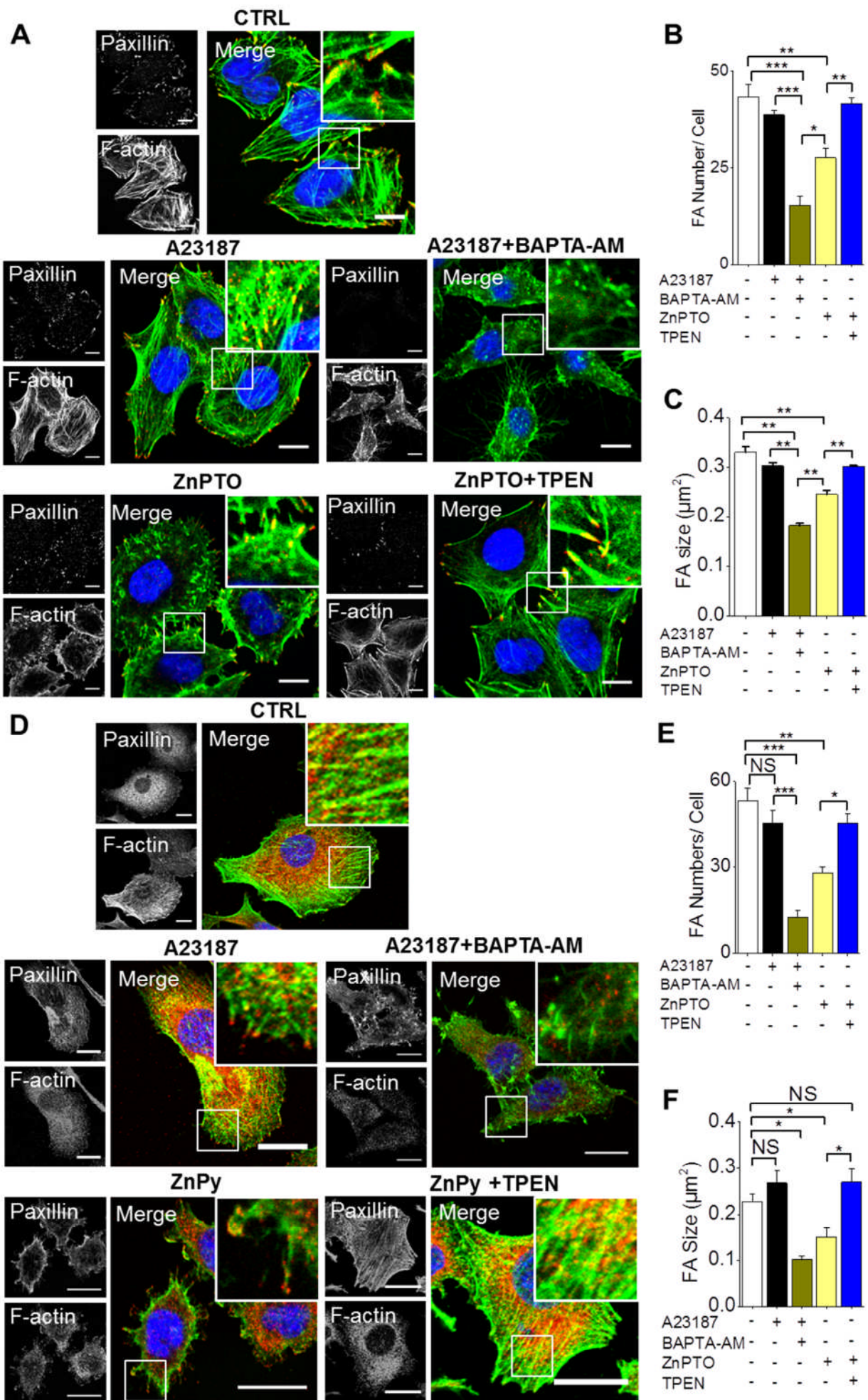
Figure 4. 19 Opposite effects of Ca^{2+} and Zn^{2+} on focal adhesions (**A**) HeLa cells were stained for F-actin and paxillin following buffer (CTRL), A23187 (3 µM) minus or plus BAPTA-AM (10 µM) and Zn-PTO (3 µM) minus or plus TPEN (5 µM) treatments; Scale bars: 20 µm. (**B-C**) Mean ± SEM of average paxillin number and size per cell from three independent experiments performed as in (A); *** indicates $p < 0.001$; ** indicates $p < 0.01$; * indicates $p < 0.05$; one-way Anova with post-hoc Tukey test. (**D-F**) Effects of Ca^{2+} and Zn^{2+} on focal adhesions of PC-3 cells. Experiments and data analysis were performed as for HeLa cells. Representative images (D) and mean ± SEM of average paxillin number and size per cell from three independent experiments are shown. Scale bars = 20 µm.

4. 2. 18 TRPM2 channels mediate palmitate induced actin remodelling in PC-3 cells

Above data have shown that excess ROS induces actin remodelling in PC-3 cells. ROS is involved in the aetiology of many pathophysiological conditions such as diabetes (Kaneto et al., 2010). As explained in the previous chapter, in diabetes, both glucose and free fatty acid levels are elevated. The results of the previous chapter have shown that high levels of fatty acids induce apoptosis of β-cells by elevating ROS levels. Whether palmitate induced ROS production triggers actin remodelling is unknown, but given palmitate induces ROS production, one would expect palmitate to produce effects similar to H_2O_2.

To address this question, the tdTomato-F-actin-P construct was transfected into PC-3 cells. After 10 hours of palmitate treatment, the actin cytoskeleton in transfected live PC-3 cells was recorded using confocal microscopy. The transfected cells showed numerous filopodia as well as distinct lamellipodia (Figure 4.20 A-B).This finding is interesting as H_2O_2 induces filopodia alone in PC-3 cells without any apparent lamellipodia formation (Figure 4.1B). To test whether the palmitate induced actin remodelling is mediated by ROS, antioxidant NAC was used. To test the role of TRPM2 channels, 2-APB was used. The results show that 2-APB and NAC fully prevented palmitate induced filopodia formation (Figure 4. 20A-B). Thus the data indicate that palmitate induced changes in actin cytoskeleton are mediated by ROS and TRPM2 channels.

Taken together, these data suggest that H_2O_2 induced actin remodelling reported in this chapter can occur in pathological conditions where free fatty acid levels of the surrounding medium are elevated; such conditions include diabetes.
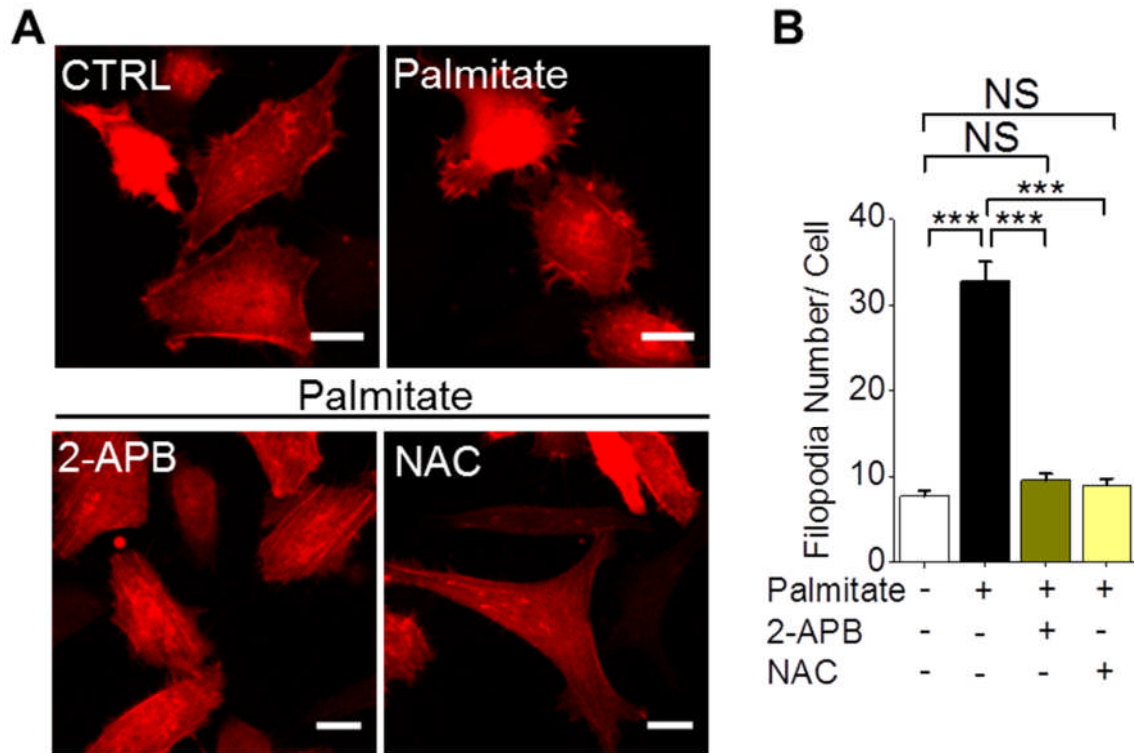
Figure 4. 20 ROS and TRPM2 channels are involved in palmitate induced actin remodelling in PC-3 cells. (**A**) PC-3 cells transfected with tdTomato-F-actin-P (ITPKA-9-52) were exposed to medium alone (CTRL), or medium containing palmitate (500 μM) in the absence or presence of 2-APB (30 μM) or NAC (10 mM) for 10 hours and imaged under a confocal microscope. Representative confocal images were shown; scale bars = 20 μm. (**B**) Mean ± SEM of filopodia number per cell from three independent experiments performed as in (A); *** indicates $p < 0.001$; NS, not significant; one-way Anova with Tukey post-hoc test.

4. 3 Discussion

The aim of the current chapter was to investigate the mechanisms by which H_2O_2, a known chemo-tactic agent, regulates actin cytoskeleton and focal adhesions of cancer cells. Using two cancer cell lines, one derived from cervical cancer (HeLa) and the other from prostate cancer (PC-3), four main observations were made: (i) H_2O_2 induces changes in the actin cytoskeleton and focal adhesions by activating the TRPM2 channels; (ii) the effects are mediated by TRPM2 mediated changes in cytosolic Ca^{2+} and Zn^{2+}; (iii) intriguingly, Ca^{2+} stabilises actin stress fibres and focal adhesions, while Zn^{2+} disrupts stress fibres and focal adhesions; (iv) Zn^{2+} strongly promotes filopodia formation. Thus this chapter reveals a previously unrecognised role for TRPM2 channels in the actin cytoskeleton and focal adhesion dynamics.

4. 3. 1 TRPM2 channels mediate H_2O_2 induced remodelling of actin and focal adhesions in cancer cells

It has previously been reported that activation of some TRP channels induces remodelling of the actin cytoskeleton and focal adhesions in cancer cells (Clark et al., 2008; Meng et al., 2013; Middelbeek et al., 2012; Pla et al., 2011). In NIE-115 neuroblastoma cells, activation of TRPM7 channels by bradykinin increases the size and number of focal adhesion complexes, and actin-rich podosomes at the cell periphery. In this report, the authors demonstrated that TRPM7 channels affect podosome assembly through a direct association with cytoskeletal proteins: β-actin and myosinIIA (Clark et al., 2006). However, in breast tumour cells, silencing of TRPM7 channels induces F-actin redistribution from cytoplasmic stress fibres to cell cortex and a strong increase in the number of focal adhesions (Middelbeek et al., 2012). In human breast carcinoma derived endothelial cells, activation of TRPV4 channels causes disappearance of actin stress fibres and formation of cortical actin (Pla et al., 2011). Whilst there is growing evidence implicating TRP channels in the regulation of actin cytoskeleton and focal adhesion dynamics in cancer cells, the underlying mechanisms are not fully understood. In particular, it is not clear how different TRP channels produce different effects, although they all permeate Ca^{2+}.

Previous studies have shown that ROS induce actin and focal adhesion remodelling (Cinq-Frais et al., 2015; Mahdi et al., 2000; Taulet et al., 2012). One of the most important targets of ROS is TRPM2 channels (Hara et al., 2002). However, whether TRPM2 channels affect the dynamics of actin cytoskeleton and focal adhesions is unknown. To address this question, two approaches were used, firstly pharmacological inhibition of TRPM2 channels and secondly siRNA targeted to TRPM2 channels (Figure 4.3, 4.18A-C, 4.18G-I and Figure

4.4, 4.18D-F respectively). These data demonstrated that inhibition of TRPM2 channels was sufficient to block H_2O_2 induced actin remodelling in both HeLa and PC-3 cells; the rescue of focal adhesions, however, was partial. There are no previous reports implicating TRPM2 channels in the regulation of actin and focal adhesions dynamics. Thus, the data presented here for the first time reveal the importance of TRPM2 channels in remodelling of actin cytoskeleton and focal adhesions in cancer cells.

4. 3. 2 TRPM2 channels mediate intracellular Ca^{2+} increase and Zn^{2+} release in cancer cells

As a non-selective ion channel, TRPM2 channels have been reported to mediate extracellular Ca^{2+} entry into cytosol in a variety of cells, including pancreatic β-cells (Bari et al., 2009), endothelial cells (Hecquet et al., 2008) and neuronal cells (Nazıroğlu et al., 2014). In addition to its role in mediating Ca^{2+} influx into cells, TRPM2 channels can also function as a lysosomal Ca^{2+} release channel (Lange et al., 2009; Sumoza-Toledo et al., 2011). However, there are little published data showing TRPM2-mediated Ca^{2+} influx in tumour cells (Ishii et al., 2007). To investigate TRPM2 regulation of actin and focal adhesion dynamics, the cytosolic Ca^{2+} dynamics in cancer cells was investigated. The results presented in the current chapter (Figure 4. 5, 4. 7 and 4. 11) suggest that TRPM2 channels in lysosomes of cancer cells could function as Ca^{2+} release channels, as with pancreatic β-cells (Lange et al., 2009). Depletion of extracellular Ca^{2+} had no discernible effect on H_2O_2 induced actin remodelling (Figure 4. 6), suggesting that Ca^{2+} entry is not essential for H_2O_2 induced actin remodelling. These findings therefore suggest a role for intracellular Ca^{2+} release in cytoskeletal remodelling.

In addition to mediating Ca^{2+} influx and release, activation of TRPM2 channels has also been reported to cause a rise in the cytosolic levels of Zn^{2+} in pancreatic and HEK293 cells (Manna et al., 2015; Yu et al., 2012). In the current chapter, TRPM2 mediated cytosolic Zn^{2+} elevation has been observed in cancer cells (Figure 4. 8 and 4. 9), indicating TRPM2-mediated Zn^{2+} increase may be a conserved phenomenon in mammalian cells. As the H_2O_2 induced cytosolic Zn^{2+} increase was observed in the absence of extracellular Zn^{2+}, it is assumed that the elevated Zn^{2+} is from an intracellular source. Using intracellular organelle indicators and Zn^{2+} reporter, it was demonstrated that Zn^{2+} is enriched in lysosomes, not in mitochondria or ER (Figure 4. 10); in combination with the results showing the expression of TRPM2 channels in lysosomes (Figure 4. 11), the data suggest that lysosomal TRPM2 channels may function as a Zn^{2+} release channel in cancer cells. This observation is consistent with a recent suggestion that H_2O_2 activation of TRPM2 channels induces Zn^{2+} release likely from lysosomes in pancreatic β-cells (Manna et al., 2015). However, Zn^{2+}

release via lysosomal TRPM2 channels has yet to be directly demonstrated. The induction of multiple pathways by Zn^{2+}, such as ERK (Azriel-Tamir et al., 2004) and PI3-K in cancer cells (Dubi et al., 2008), well-known regulators of cytoskeleton organization (Kalwat and Thurmond, 2013; Qian et al., 2004), suggest a possible role for these Zn^{2+} induced signalling pathways in cytoskeletal remodelling of cancer cells.

4. 3. 3 Opposite roles of Ca^{2+} and Zn^{2+} in actin remodelling and focal adhesion reorganization in cancer cells

Ca^{2+} has been reported to play an important part in the regulation of actin and focal adhesion dynamics. However, there are conflicting reports on the effects of Ca^{2+} in these events. For example, inhibition of Ca^{2+} entry via STIM1/Orai1 reduced the turnover of focal adhesions (Schafer et al., 2012) whereas inhibition of Ca^{2+} entry via TRPC5 appears to have an opposite effect (Tian et al., 2010). Studies on receptor-activated TRPC5 and TRPC6 channels showed contrasting effects of Ca^{2+} on the actin cytoskeleton: TRPC6 mediated Ca^{2+} rise increased stress fibres, whereas TRPC5 mediated Ca^{2+} reduced stress fibres (Tian et al., 2010). These differences in the effects of Ca^{2+} might be attributed to differences in coupling to different signalling mechanisms regulating the actin cytoskeleton and focal adhesion and the adherent properties of the cells.

The data presented in the current chapter showed that the rise in cytosolic Ca^{2+} has little effect on the reorganization of actin cytoskeleton and focal adhesions. By contrast, BAPTA-AM led to the opposite effects (Figure 4. 14, 4.15 and 4. 19). These data suggested that basal Ca^{2+} is required for the stability of stress fibres and focal adhesions and that decrease in basal Ca^{2+} leads to remodelling of actin cytoskeleton and focal adhesions. Similar findings were reported by Tsai et al who demonstrated that reducing the basal Ca^{2+} in endothelial cells decreases focal adhesions (Tsai et al., 2014). Rehder and Kater reported that in neuronal cells, there is a range of Ca^{2+} concentration where filopodia is not seen, but outside this range, Ca^{2+} induces filopodia formation (Rehder and Kater, 1992). Thus both an increase and decrease in cytosolic Ca^{2+} levels appear to be able to induce filopodia formation.

Studies have reported that Ca^{2+} gradients induce differential remodelling of the actin cytoskeleton and focal adhesions (Tsai et al., 2015; Tsai and Meyer, 2012). In a migrating cell, Ca^{2+} levels are higher at the rear of the cell where stress fibres tend to be prominent, but low at the front of the cell where lamellipodia and filopodia develop. It has been suggested that Ca^{2+} levels fall below basal levels by the removal of Ca^{2+} by plasma membrane Ca^{2+} ATPase at the front of the cell (Tsai et al., 2014). While this is a possibility,

the finding that the disassembly of actin stress fibres and focal adhesions is accompanied by the appearance of filopodia following cytosolic Zn^{2+} increase (Figure 4. 14, 4. 15 and 4. 19) suggests an alternative mechanism whereby rise in Zn^{2+} can antagonise the actions of Ca^{2+}. This may indicate that Zn^{2+} can override the effects of Ca^{2+}, even when levels of the latter exceed basal levels. Taken together with the observation that removal of Zn^{2+} alone was sufficient to abolish H_2O_2-induced remodelling of the actin cytoskeleton (Figure 4. 14A and 4. 15A), these results argue that Zn^{2+} is capable of overriding Ca^{2+}-induced cytoskeletal changes and that the ratio of Ca^{2+}/Zn^{2+} determines the actin cytoskeleton phenotype. The ability of Zn^{2+} to counter the effects of Ca^{2+} may explain some of the conflicting reports on the role of Ca^{2+} in actin cytoskeleton. Thus, when examining the roles of ion channels, in particular TRP channels, it is important to take into account their ability to affect Zn^{2+} homeostasis.

4. 3. 4 Cdc42, RIF, PI3-K and MAPK do not appear to be essential for H_2O_2 induced filopodia formation

Actin cytoskeleton dynamics is essential for a wide range of cellular processes, including cytokinesis (Riggs et al., 2003) and migration (Lamalice et al., 2007). In an attempt to gain further mechanistic insight into the regulation of the actin cytoskeleton by H_2O_2, Ca^{2+} and Zn^{2+}, experiments were carried out to assess the involvement of three potential candidate proteins. Cdc42 is a well-known regulator of the filopodia formation (Krugmann et al., 2001). Although expression of constitutive-active Cdc42 induced some filopodia formation, dominant-negative inhibition of Cdc42 was unable to block H_2O_2 induced filopodia formation (Figure 4. 16A). These data suggest that the effect of H_2O_2 is not mediated by Cdc42. In HeLa cells, a non-classical Rho GTPase RIF has been implicated in the generation of filopodia (Pellegrin and Mellor, 2005). Interestingly, RIF induced filopodia appear more similar to those observed in the current study following H_2O_2 or Zn-PTO treatment ((Pellegrin and Mellor, 2005) (Figure 4. 1A, Figure 4. 14B and Figure 4. 15B). However, expression of dominant negative mutant of RIF in HeLa cells failed to inhibit H_2O_2 induced filopodia formation (Figure 4. 16B) implying lack of a role for RIF in H_2O_2 induced filopodia generation. The PI3-K and MAPK pathways regulate many cellular processes, including cytoskeletal rearrangement (Hoffman et al., 2012; Qian et al., 2004; Wu et al., 2001). Besides, activities of PI3-K and MAPK are regulated by H_2O_2 (Gough and Cotter, 2011; Suzaki et al., 2002) and Zn^{2+} (Malaiyandi et al., 2005; Seo et al., 2001). However, lack of inhibitory effect by the broad spectrum PI3-K inhibitor LY294002 and MAPK inhibitor SB203580 excludes roles for PI-3K and MAPK pathways in H_2O_2-induced actin remodelling (Figure 4. 17).

4. 3. 5 Potential targets of Ca^{2+} and Zn^{2+} for actin remodelling

As shown above, Cdc42, RIF, PI-3K and MAPK do not appear to be involved in H_2O_2-induced actin remodelling (Figure 4. 16 and 4. 17). The mechanism by which H_2O_2 regulates reorganization of actin cytoskeleton must be much complex because it increases the cytosolic levels of both Ca^{2+} and Zn^{2+}. The following sections speculate on potential downstream effectors of Ca^{2+} and Zn^{2+} in the regulation of actin remodelling.

In current study, elevation of Ca^{2+} by A23187 has no distinct effect on stress fibres, while chelation of Ca^{2+} by BAPTA-AM disrupted stress fibres (Figure 4. 6C-D, 4. 14 and 4. 15). It has been reported that cytosolic Ca^{2+} elevation can increase RhoA protein synthesis and thereby induce stress fibre formation (Rao et al., 2001). Whether BAPTA-AM induced stress fibre loss involves alteration of RhoA expression or activity requires further investigation. Another candidate for BAPTA-AM induced filopodia formation might be Ca^{2+}-dependent actin-depolymerizing factor cofilin. It has been demonstrated that Ca^{2+}, by activating cofilin (Wang et al., 2005), mediates filopodia disassembly (Breitsprecher et al., 2011). Whether BAPTA-AM, by inhibiting cofilin, induces filopodia formation needs further investigation.

The data showed in the current chapter indicate a role for Zn^{2+} in the regulation of actin cytoskeleton (Figure 4. 14 and 4. 15). However, the downstream effectors for Zn^{2+}-induced filopodia formation are still unclear. Previous studies have shown that Zn^{2+} can function as an important second messenger (Murakami and Hirano, 2008; Yamasaki et al., 2007). The authors of these studies demonstrated that Zn^{2+} can inhibit PTPs (Yamasaki et al., 2007) although no specific PTP was identified. However, a previous study reported that Zn^{2+} can inhibit the activity of PTP-PEST (Yang et al., 1993), which is an important regulator of actin cytoskeletal dynamics (Sastry et al., 2002; Sastry et al., 2006). It has been reported that loss of PTP-PEST can enhance the activity of Rac1 and protrusion formation (Sastry et al., 2006). Whether Zn^{2+} induced filopodia formation is mediated by PTP-PEST needs further investigation.

4. 3. 6 Potential effectors of Ca^{2+} and Zn^{2+} for focal adhesions

In addition to the effects on actin remodelling, Ca^{2+} also modulates focal adhesion reorganization (Franco et al., 2004; Giannone et al., 2004; Yang et al., 2009a). Among these pathways, calpain is a key target for Ca^{2+}. Although calpain-mediated proteolysis of talin1 is reported to induce focal adhesion disassembly (Franco et al., 2004), Cortesio reported that calpain-generated proteolytic fragment of paxillin maintains intact focal adhesions (Cortesio et al., 2011). Consistent with the latter study, the current chapter demonstrated that elevation of cytosolic Ca^{2+} by A23187 had no effect on focal adhesion dynamics while decreasing Ca^{2+}

with BAPTA-AM caused disassembly of focal adhesions (Figure 4. 19). Whether the BAPTA-AM induced focal adhesion decrease is dependent on the alteration of calpain activity needs further investigation.

As for Zn^{2+}-induced focal adhesion disassembly, PTP-PEST is a potential downstream effector. In addition to regulating actin cytoskeleton dynamics, PTP-PEST has been reported to regulate focal adhesion formation (Souza et al., 2012). The authors of this study reported that cells lacking PTP-PEST had reduced focal adhesions. Whether Zn^{2+}-induced focal adhesion disassembly is mediated by PTP-PEST remains to be investigated.

4. 4 Summary

The present study demonstrates a novel role for TRPM2 channels in remodelling of actin cytoskeleton and focal adhesions, and a role for Zn^{2+} in the regulation of actin and focal adhesion dynamics. The results presented in this chapter indicate that it is the balance between Ca^{2+} and Zn^{2+}, rather than Ca^{2+} alone, which regulates the actin cytoskeleton and focal adhesion dynamics of some cancer cells. Interestingly, the two ions elicited opposite effect on the dynamics of the actin cytoskeleton and focal adhesions, resulting in reciprocal regulation. Thus these results suggest that any future studies on the ionic regulation of actin cytoskeleton and focal adhesions should examine the role of both the ions, rather than one ion alone.

Since reorganization of actin cytoskeleton and focal adhesions plays an important part in many other processes, such as wound healing, phagocytosis and angiogenesis, it would be interesting to see if TRPM2 channels, and the ions they conduct, play a role in other pathophysiological processes.

Chapter 5 TRPM2 channels regulate directional migration of cancer cells: Role of calcium, zinc and lysosomes

5. 1 Introduction

Cell migration plays an essential role in multiple processes, such as angiogenesis (Lamalice et al., 2007), tumour invasion (Friedl and Wolf, 2003) and immune response (Luster et al., 2005). In response to motogenic signals or chemo-attractants, cells exhibit directional cell migration called chemotaxis. Previous studies have reported that H_2O_2 plays an important role in chemotaxis (Wang et al., 2015; Yoo et al., 2011). To undergo efficient directional cell migration, two components need to be spatiotemporally regulated: actin cytoskeleton and focal adhesions. Data presented in Chapter 4 have demonstrated that H_2O_2 exposure induces actin remodelling and focal adhesion reorganization in HeLa and PC-3 cells. As such, it is conceivable that H_2O_2 induces cell migration by modulating the dynamics of actin cytoskeleton and focal adhesions. The overall aim of this chapter is therefore to examine the effect of H_2O_2 on cancer cell migration and the underlying mechanisms.

The role of TRP channels in cell migration has been extensively studied. Activation of TRPC1 channels enhances migration of pancreatic cancer cells and glioma cells (Bomben et al., 2011; Dong et al., 2010a). TRPM8 and TRPV2 channels increase cell migration of DBTRG glioblastoma cells (Wondergem et al., 2008) and PC-3 cells (Monet et al., 2009) respectively. Although TRPM2 mediated dendritic chemotaxis has been reported, the role of TRPM2 channels in cancer cell migration has not been previously reported. Given the importance of TRPM2 channels in regulation of actin remodelling and focal adhesion rearrangement (Chapter 4), it is hypothesized that TRPM2 channels mediate H_2O_2 induced migration in cancer cells.

TRP channels regulate cancer cell migration by generating Ca^{2+} signals (Prevarskaya et al., 2011). However, there are contrasting reports regarding the effect of Ca^{2+} on cell migration. In breast cancer cells, elevation of cytosolic Ca^{2+} promotes cell migration (Yang et al., 2009a), while Ca^{2+} influx in PC-3 cells decreases cell migration (Yang et al., 2009b). Moreover, recent studies proposed that Ca^{2+} gradient exists during cell migration and perturbation of Ca^{2+} gradient, or lack of Ca^{2+} gradient, decreases cell migration (Mrkonjić et al., 2015; Tsai et al., 2014). These contrasting results imply that there might be other factors modulating Ca^{2+} signals during cell migration. Among these factors, Zn^{2+} is a noteworthy one. Compared to Ca^{2+} signals, there is little information regarding the role of Zn^{2+} in cancer cell migration so far. It has been reported that rise in extracellular Zn^{2+} concentration increases the migration of breast cancer cells (Kagara et al., 2007), and this effect is mediated by Zn^{2+}

transporters. Whether this effect represents a general effect of Zn^{2+} upon cell migration is unclear. Moreover, as an ion channel capable of modulating cytosolic Zn^{2+} levels (Manna et al., 2015; Yu et al., 2012), whether TRPM2 channel is involved in Zn^{2+}-induced cell migration remains unknown. The results of Chapter 4 demonstrated that Zn^{2+} induces actin remodelling and focal adhesion, thereby suggesting the possibility that Zn^{2+} could play an important role in cancer cell migration.

This chapter therefore has two specific aims: firstly, to explore the role of TRPM2 channels and secondly, to examine the role of Ca^{2+} and Zn^{2+} in cancer cell migration.

5. 2 Results

5. 2. 1 H_2O_2 induced cell migration is inhibited by 2-APB in HeLa and PC-3 cells

As shown in Chapter 4, H_2O_2 induced both actin remodelling and focal adhesion reorganization. To investigate the relevance of these changes to cell migration, an agarose spot cell migration assay was used where H_2O_2 was included in the agarose spot and the migration of surrounding cells into the spot was examined (Figure 5. 1). To exclude the effect of proliferation and serum on cell migration, medium containing 0.1% serum was used in migration assays. Effect of H_2O_2 on the migration of HeLa and PC-3 cells was examined.

The results show that inclusion of H_2O_2 in the agarose spot promoted migration of surrounding cells into the spot; there was no such migration in the PBS controls (Figure 5. 1A-D). 2-APB was able to prevent H_2O_2 stimulated cell migration (Figure 5. 1B-E). These results suggest that the directional migration of HeLa and PC-3 cells in response to H_2O_2 may be dependent on the activation of TRPM2 channels. However, PJ34 failed to inhibit H_2O_2 induced cell migration. Upon further investigation, PJ34 was found to stimulate cell migration even in the absence of H_2O_2 (Figure 5. 1F-I), explaining the anomalous, TRPM2 independent effect of PJ34 on cell migration. This finding may be of clinical relevance because PARP inhibitors are currently being evaluated for cancer therapy.

These data suggest that TRPM2 might play a role in H_2O_2 induced directional cell migration.
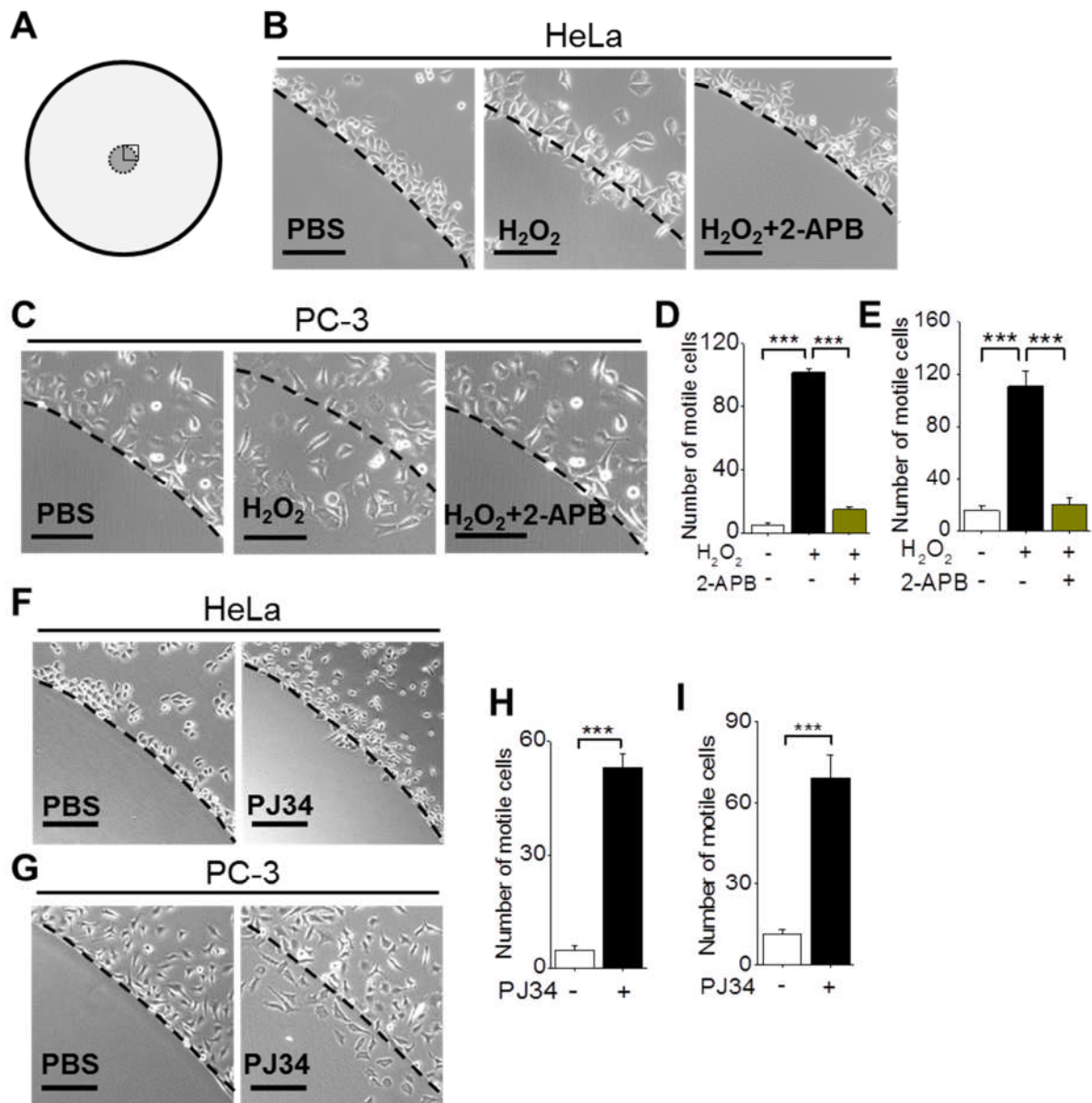
Figure 5. 1 Effect of 2-APB and PJ34 on H_2O_2 induced migration of HeLa and PC-3 cells (**A**) Schematic illustrating an agarose bead (broken circle) in the centre of a petri-dish plated with cells; the square box represents the section imaged. (**B-C**) Agarose spots containing PBS, 1 mM H_2O_2 or H_2O_2 plus 2-APB were plated onto 6-well plates and then HeLa (B) or PC-3 (C) cells were plated around the agarose spots followed by incubation for 16 hours at 37ºC. (**D-E**) Mean ± SEM of number of motile cells per spot from three independent experiments performed as in (B) and (C) respectively. (**F-G**) HeLa (F) or PC-3 (G) cells were plated around agarose spots containing PBS or PBS containing 10 µM PJ34 and incubated for 16 hr at 37ºC. (**H-I**) Mean ± SEM of number of motile cells per spot from three independent experiments performed as in (F) and (G) respectively. In all cases, representative images of a section of the spot and surrounding area are shown, broken line indicates agarose boundary; *** indicates $p < 0.001$; one-way Anova with post-hoc Tukey test. Scale bars: 200 µm.

5. 2. 2 Silencing of TRPM2 channels inhibits H_2O_2 induced cell migration

Above results have shown that 2-APB significantly inhibits H_2O_2 induced cell migration in HeLa and PC-3 cells. However, 2-APB is a compound that targets several other channels, and is not specific for TRPM2 channels (Togashi et al., 2008). Therefore, the inhibition of 2-APB in H_2O_2 induced cell migration might be unrelated TRPM2 channels.

To address this, siRNA specifically targeted to TRPM2 channels was used. Transfection of cells with scrambled siRNA failed to prevent H_2O_2 induced migration of both HeLa (Figure 5. 2A-B) and PC-3 cells (Figure 5. 2C). However, silencing of TRPM2 channels with TRPM2 targeted siRNA significantly prevented H_2O_2 induced cell migration of HeLa (Figure 5. 2A-B) and PC-3 cells (Figure 5. 2C).

To further confirm the role of TRPM2 channels in H_2O_2 induced directional cell migration, a recombinant approach was used. HEK-MSR cells which do not express TRPM2 channels (HEK-MSR) failed to migrate after stimulation with H_2O_2 (Figure 5. 2G, left panel). However, over-expression of TRPM2 channels (TRPM2-HEK-MSR) led to a significant increase in H_2O_2 induced migration when compared to HEK-MSR cells (Figure 5. 2G-H).

Collectively, these data demonstrate that TRPM2 channels play an essential role in H_2O_2 induced directional cell migration.
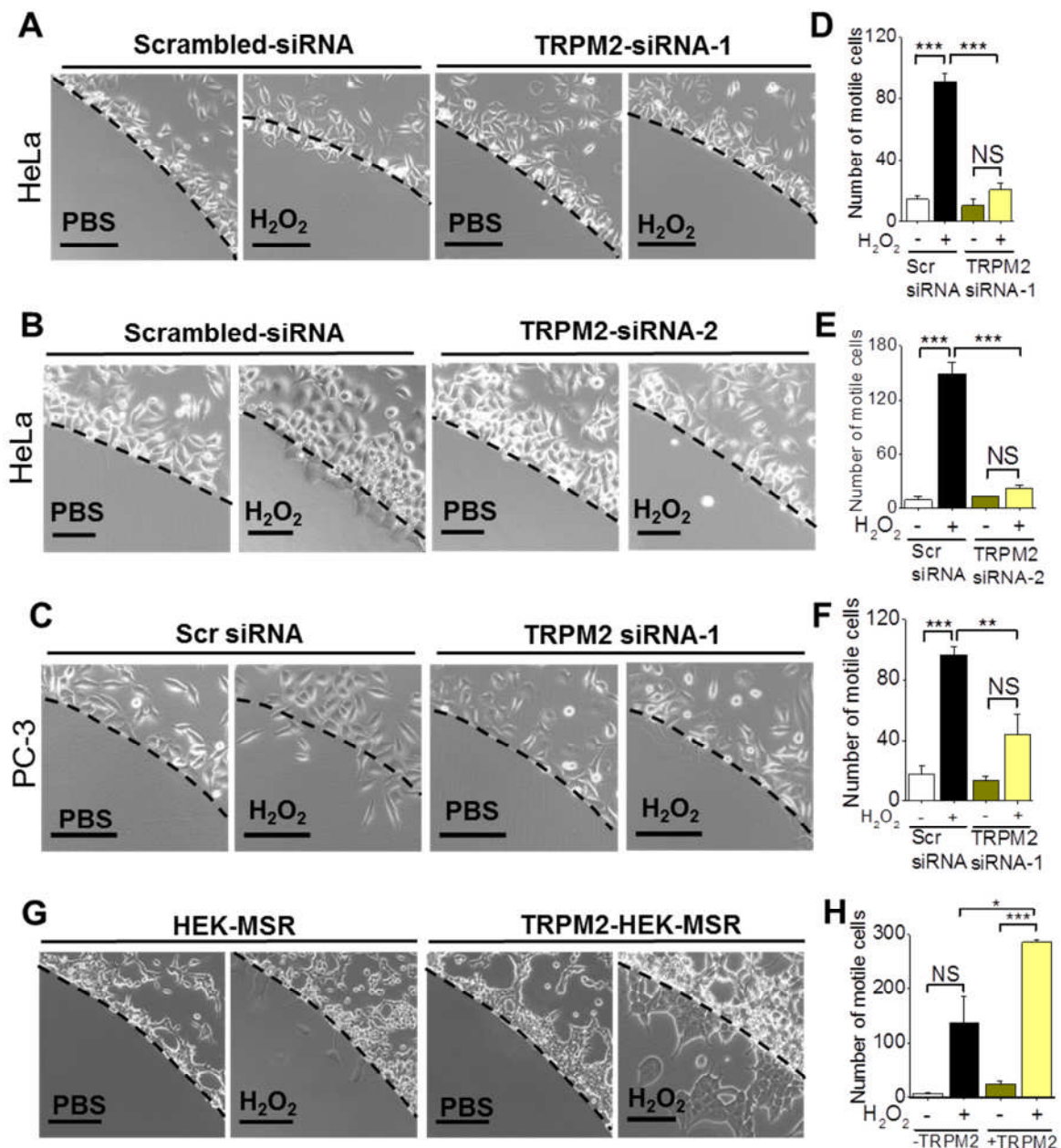
Figure 5. 2 Silencing of TRPM2 channels inhibits H_2O_2 induced cell migration. (**A-C**) HeLa cells transfected with scrambled siRNA or siRNA against TRPM2 (A for siRNA-1 and C for siRNA-2) and PC-3 cells transfected with scrambled siRNA or siRNA-1 (C) were plated onto a 6-well plate containing PBS (CTRL) or 1 mM H_2O_2-containing agarose spots. (**D-F**) Mean ± SEM of number of motile cells per spot; three independent experiments were performed as in (A), (B) and (C) respectively. (**G**) Agarose spots containing PBS or 400 µM H_2O_2 were loaded into 6-well plates and then HEK-MSR or TRPM2-HEK-MSR cells were plated around the agarose spots. (**H**) Data was analysed as in (D-F). In all cases, representative images of a section of spot and surrounding area are shown, broken line indicates agarose boundary; *** indicates $p < 0.001$; ** indicates $p < 0.01$; NS, not significant; one-way Anova with post-hoc Tukey test. Scale bars: 200 µm.

5. 2. 3 Opposite effects of Ca^{2+} and Zn^{2+} on migration of HeLa cells

Studies presented in Chapter 4 have shown that TRPM2 channels regulate actin remodelling and focal adhesion reorganization by affecting intracellular dynamics of Ca^{2+} and Zn^{2+}. Effect of Ca^{2+} on cell migration has been studied in cancer cells previously (Prevarskaya et al., 2011); however, little is known about the role of Zn^{2+}. It was demonstrated in last chapter that raising cytosolic Zn^{2+} induces filopodia formation and focal adhesion disassembly and Ca^{2+} has reciprocal effects. To investigate the individual roles of Ca^{2+} and Zn^{2+} in cell migration, Ca^{2+} and Zn^{2+} ionophores and metal chelators were used. Cytosolic levels of Ca^{2+} and Zn^{2+} were elevated using ionophores and their effect on cell migration was examined in the absence of H_2O_2.

A23187 showed no effect on migration while inclusion of BAPTA-AM caused a modest, but significant, increase in the migration of HeLa cells (Figure 5. 3). Thapsigargin is an inhibitor of sarco/endoplasmic reticulum Ca^{2+} ATPase (SERCA). Therefore, it can elevate cytosolic Ca^{2+} level by preventing Ca^{2+} entry into sarcoplasmic and endoplasmic reticula (Lytton et al., 1991). Raising the cytosolic Ca^{2+} using thapsigargin produced effects similar to A23187 (Figure 5. 3). This finding is interesting but is consistent with the findings of Chapter 4, where A23187 had no effect while BAPTA-AM induced both actin remodelling and focal adhesion disassembly. Zn-PTO, on the other hand, strongly promoted cell migration that was suppressed by TPEN (Figure 5. 3).

These data suggest that Ca^{2+} and Zn^{2+} play distinct, but contrasting roles in HeLa cell migration.
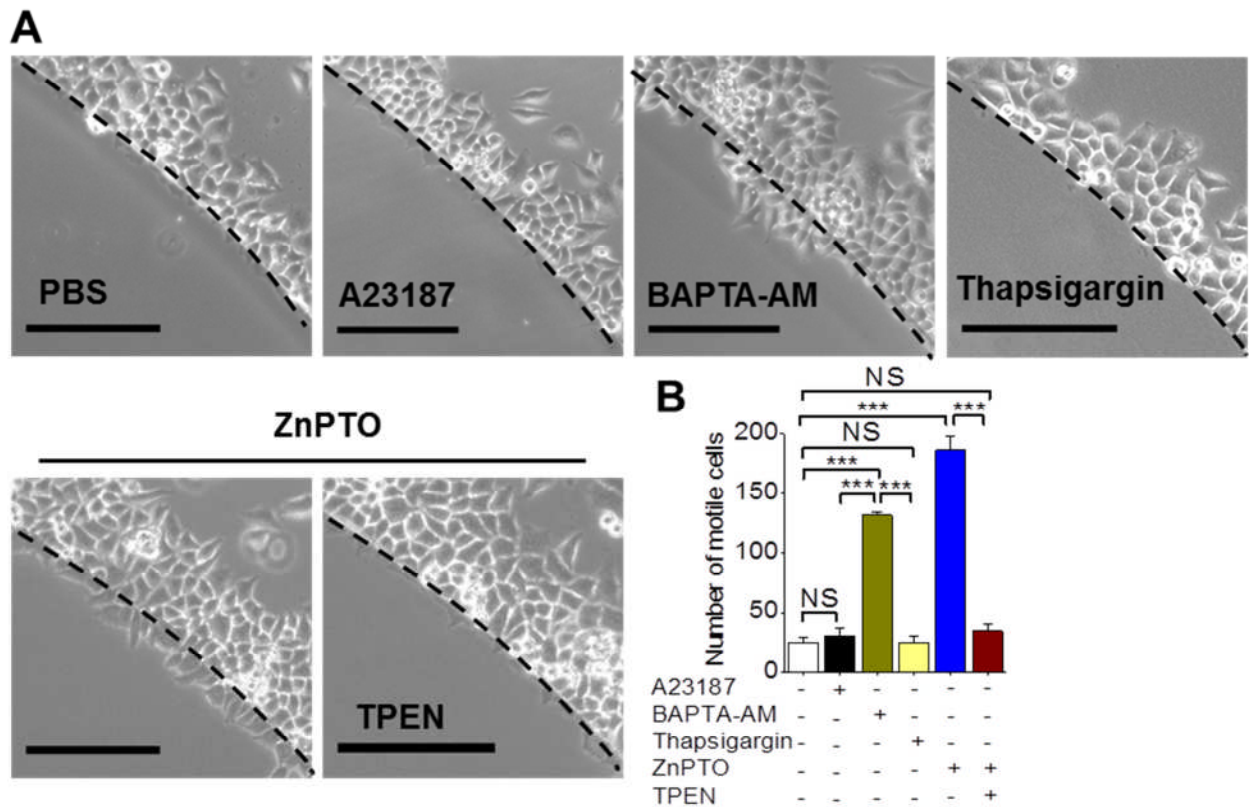
Figure 5. 3 Opposite effects of Ca^{2+} and Zn^{2+} on migration of HeLa cells (**A**) Agarose spots containing PBS, A23187 (5 µM), BAPTA-AM (15 µM), thapsigargin (1.5 µM), or Zn-PTO (5 µM) with and without TPEN (10 µM) were plated onto 6-well plate. HeLa cells were then plated around the spots. (**B**) Mean ± SEM of number of cells that crossed the agarose boundary from three independent experiments performed as in (A). In all cases, representative images of a section of the spot and the surrounding area are shown; broken line indicates agarose boundary; *** $p < 0.001$; NS, not significant; one-way Anova with post-hoc Tukey test. Scale bars: 200 µm.

5. 2. 4 Both Ca^{2+} and Zn^{2+} induce cell migration in PC-3 cells

The distinctive roles of Ca^{2+} and Zn^{2+} on directional cell migration in HeLa cells have been demonstrated above (Figure 5. 3). Since the effects of Ca^{2+} and Zn^{2+} on actin cytoskeleton and focal adhesions in PC-3 cells are similar to HeLa cells, it is expected that Ca^{2+} and Zn^{2+} ionophores and metal chelators will have similar effects on PC-3 cells as with HeLa cells. However, A23187 induced significant cell migration that was inhibited by BAPTA-AM (Figure 5. 4). This finding is opposite to that seen in HeLa cells. Published studies suggest that the effect of Ca^{2+} on cell migration could be cell type dependent. For example, in breast cancer cells, elevating the cytosolic Ca^{2+} level increases cell migration (Yang et al., 2009a), while Ca^{2+} has an inhibitory effect on endothelial cell migration (Chaudhuri et al., 2003). Zn-PTO induced significant cell migration which was inhibited by TPEN. Thus the effect of Zn^{2+} is similar in HeLa and PC-3 cells (Figure 5. 3 and Figure 5. 4).

Thus while both Ca^{2+} and Zn^{2+} contribute to H$_2$O$_2$ induced directional cell migration, the effects of individual ions might be cell-type dependent.
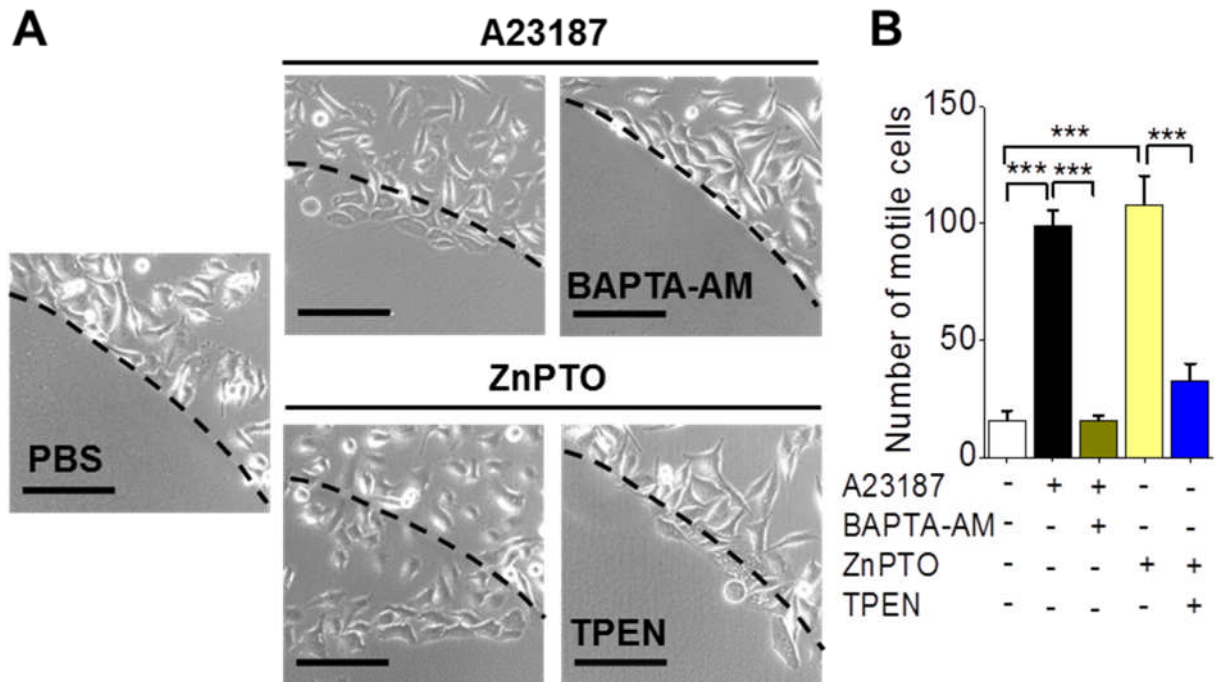
Figure 5. 4 Both Ca^{2+} and Zn^{2+} induce cell migration of PC-3 cells. (**A**) Agarose spots containing PBS, A23187 (5 µM), A23187 (5 µM) plus BAPTA-AM (15 µM), or Zn-PTO (5 µM) with or without TPEN (10 µM) were loaded into 6-well plates and then PC-3 cells were plated around the agarose spots. (**B**) Mean ± SEM of number of motile cells per spot; data were from three independent experiments performed as in (A). In all cases, representative images of a section of the spot and surrounding area are shown, broken line indicates agarose boundary; *** indicates $p < 0.001$; one-way Anova with post-hoc Tukey test. Scale bars: 200 µm.

5. 2. 5 H$_2$O$_2$ and TRPM2 channels mediate trafficking of lysosomes to the leading edge of migrating HeLa cells

Since filopodia are formed at the leading edge of migrating cells, and rise in Zn^{2+} triggers filopodia formation, it was expected preferential Zn^{2+} release would occur at the leading edge of the cell (resulting in more Zn^{2+} at the front of the cell relative to the rear). Given the evidence that lysosomes are the major source of intracellular free Zn^{2+} (Figure 4. 10), it was predicted that lysosomes move towards the leading edge of the cell.

To test this idea, HeLa cells were transfected with tdTomato-F-actin-P (ITPKA-9-52) and LAMP1-GFP (labels lysosomes) and plated around agarose spots containing PBS (control) or H$_2$O$_2$. Live cell imaging of migrating cells showed marked accumulation of lysosomes at the leading edge of cells migrating into H$_2$O$_2$ containing agarose spot (Figure 5. 5A-C). Furthermore, these cells showed numerous actin stained filopodia at the leading edge of migrating cells. By contrast, in control experiments, neither lysosomal trafficking nor filopodia formation was observed (Figure 5. 5A-C).

These data have thus shown that lysosomes migrate to the leading edge of migrating cells in response to H$_2$O$_2$ (Figure 5. 5A). Since TRPM2 channels are activated by H$_2$O$_2$, it was hypothesized that activation of TRPM2 channels might be involved in the polarisation of lysosomes. To test this, HeLa cells were co-transfected with TRPM2-siRNA (or scrambled siRNA) and LAMP1-GFP and migration of lysosomes in migrating cells was recorded by live cell imaging as in Figure 5. 5D. As shown in Figure 5. 5D, TRPM2 siRNA, but not scrambled siRNA, prevented H$_2$O$_2$ induced polarization of lysosomes.

These data indicate that lysosomes migrate towards the leading edge of cells in response to H$_2$O$_2$ stimulus, presumably to increase the local concentration of Zn^{2+}. Besides, TRPM2 channels appear to play a role in mediating lysosome trafficking.
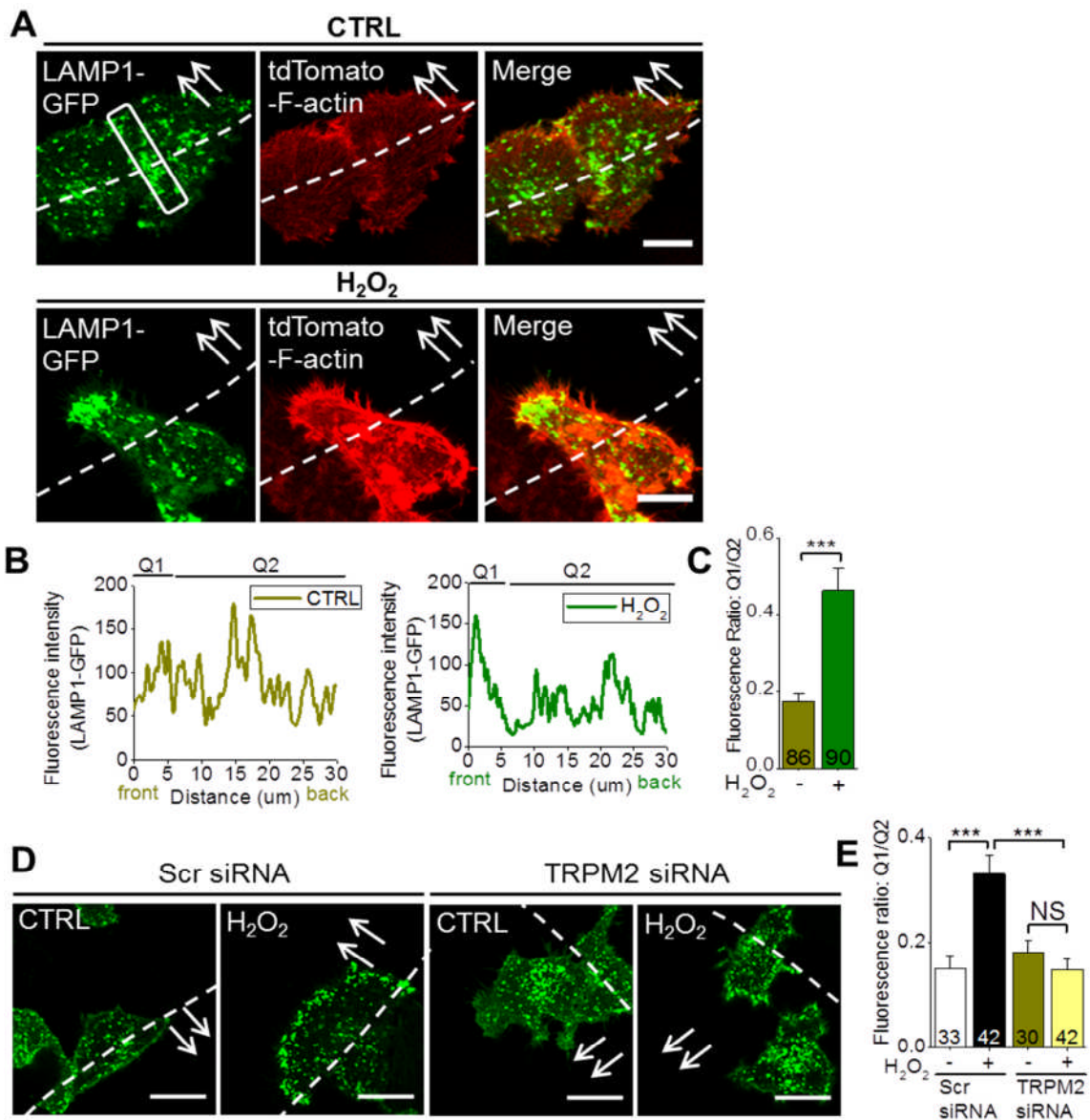
Figure 5. 5 H$_2$O$_2$ induces trafficking of lysosomes to the leading edge of migrating HeLa cells. (**A**) HeLa cells were transfected with LAMP1-GFP and tdTomato-F-actin-P and plated onto glass-bottomed dishes with agarose spots containing PBS (CTRL) or H$_2$O$_2$ (1 mM) followed by 16 hours incubation at 37°C. (**B**) Plot of fluorescence intensity of LAMP1-GFP-positive puncta along the migrational axis of a single cell (indicated as a rectangle in A). (**C and E**) LAMP1-GFP fluorescence at the leading edge (Q1) of the cell relative to the rest of the cell (Q2), where Q1 is fluorescence intensity at the leading edge (0-5 μm, arbitrary) of the cell and Q2, fluorescence intensity behind the leading edge (5-30 μm). Data are expressed as mean ± SEM; number of cells analysed from three independent experiments are shown within the bars; *** represents $p < 0.001$; NS, not significant, determined using one-way Anova with post-hoc Tukey test. (**D**) HeLa cells were transfected with scrambled or TRPM2 siRNA and LAMP1-GFP and plated onto glass-bottomed dishes with agarose spots containing PBS (CTRL) or H$_2$O$_2$ (1 mM). In all cases, representative images are shown; Scale bars: 20 μm; the white arrows indicate direction of migration across the boundary of the agarose bead shown as dashed curve.

5. 2. 6 EGF induced cell migration is dependent on ROS production and TRPM2 channel in PC-3 cells

EGF-mediated signalling pathway plays an important role in triggering cancer cell migration (Price et al., 1999) and angiogenesis (van Cruijsen et al., 2005). Recent studies reported that EGF can exert its function by elevating cytosolic ROS level (Binker et al., 2009; Huo et al., 2009). For example, in ovarian cancer cells, EGF-mediated down-regulation of E-cadherin and induction of cell invasion is dependent on H_2O_2 production (Cheng et al., 2010). These studies indicate the crosstalk between EGF-driven pathways and ROS-mediated signal transduction. Since ROS activates TRPM2 channels, it is reasonable to speculate that TRPM2 might be involved in EGF-triggered cancer cell migration. To address this question, effect of EGF on cell migration of PC-3 cells and the role of TRPM2 channels in this process was investigated.

Inclusion of EGF (300 ng/ml) in agarose spot induced marked migration of PC-3 cells while addition of 2-APB significantly suppressed it (Figure 5. 6A-B), indicating that EGF-induced cell migration might involve activation of TRPM2 channels. Since activation of TRPM2 channels requires ROS, effect of EGF on ROS levels was examined in PC-3 cells. In accordance with the previous studies (Bae et al., 1997; Cheng et al., 2010), cytosolic ROS levels were substantially elevated in cells exposed to EGF (300 ng/ml) (Figure 5. 6C, right panel) compared to medium alone (Figure 5. 6C, left panel).

Taken together, these data suggest a role for TRPM2 channels and ROS in EGF-induced cell migration.
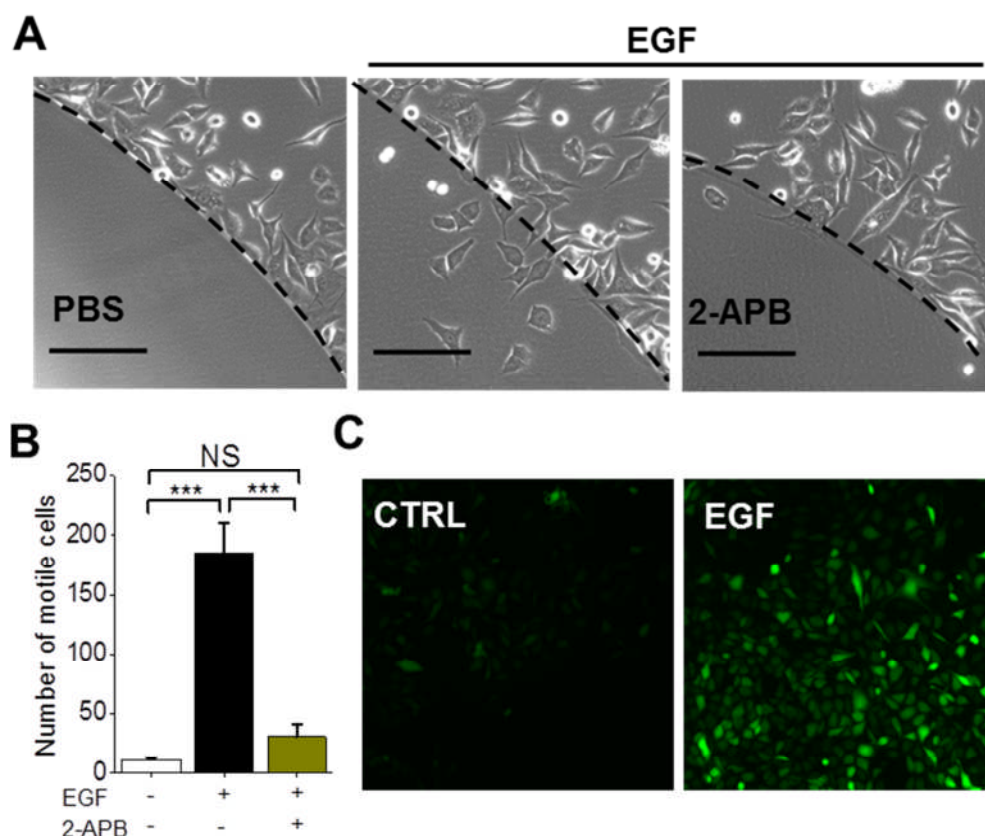
Figure 5. 6 EGF induced cell migration is dependent on ROS production and TRPM2 activation in PC-3 cells. (**A**) PC-3 cells were plated onto 6-well plate containing agarose spots including PBS or EGF (300 ng/ml) with and without 2-APB (150 µM) for 16 hours before recording under a microscope. Scale bars: 200 µm. (**B**) Mean ± SEM of number of cells that crossed the agarose boundary from three independent experiments performed as in (A). Scale bars: 200 µm. *** $p < 0.001$; NS, not significant; one-way Anova with post-hoc Tukey test. (**C**) Live cell fluorescent images of PC-3 cells exposed to medium (CTRL) or medium containing EGF (300 ng/ml) for 30 min; cells were stained for cytosolic ROS level using H2DCF-DA. Representative images are shown. Scale bars: 10 µm.

5. 3 Discussion

The data presented in this chapter demonstrate that H_2O_2 induces directional migration of HeLa and PC-3 cells. This phenomenon is TRPM2 channel (Figure 5. 1A-E and 5. 2) and Zn^{2+} dependent (Figure 5. 3 and 5. 4). However, elevation of Ca^{2+} appears to have no effect on the migration of HeLa cells (Figure 5. 3) but promotes migration of PC-3 cells (Figure 5. 4). Importantly, directional migration of HeLa cells is associated with the mobilisation of lysosomes towards the leading edge of migrating HeLa cells (Figure 5. 5), suggesting a role for lysosomal dynamics in H_2O_2 induced cell migration.

5. 3. 1 Ion channels in cell migration

A number of ion channels from the TRP family and the STIM-1/Orai1 store operated ion channels have been reported to play roles in cell migration, but the effects appear to be cell type dependent. For example, in NIE-115 neuroblastoma cells, silencing of TRPM7 channels promotes cell migration (Clark et al., 2006). In H1299 cells, silencing STIM1 promotes directional cell migration (Tsai et al., 2014), while activation of TRPM8 channels in DBTRG glioblastoma cells and TRPV1 channels in hepatoblastoma cells increase cell migration (Waning et al., 2007; Wondergem et al., 2008).

Sumoza-Toledo et al reported that TRPM2 channels mediate dendritic cell chemotaxis in response to CXCL12 and CCL19 chemokines (Sumoza-Toledo et al., 2011). However, there are no previous reports on the potential role of TRPM2 channels in cancer cell migration, despite the fact that H_2O_2 induces migration of cancer cells, including breast cancer cells (Payne et al., 2005) and H_2O_2 is a potent activator of TRPM2 channels. In the previous chapter, a role for TRPM2 channels in actin remodelling and focal adhesion dynamics has been demonstrated. As these events are intimately associated with cell migration, the role of TRPM2 channels in cell migration was investigated. An agarose spot-based cell migration assay (Wiggins and Rappoport, 2010) was performed using two cancer cell lines: HeLa and PC-3 cells. The results (Figure 5. 1 and 5. 2) provide evidence that TRPM2 channels play a key role in H_2O_2-induced cell migration.

5. 3. 2 Ca^{2+} in cell migration

Previous studies have reported that cell migration mediated by TRP channels and STIM-1/Orai1 involves Ca^{2+} signals (Fabian et al., 2008; Pla et al., 2011; Yang et al., 2009a). However, the impact of Ca^{2+} signals on cell migration is more complex and seems to depend on the cell type. For example, while a decrease in Ca^{2+} promoted endothelial cell migration (Tsai et al., 2014), a rise in Ca^{2+} was found to increase migration of certain cancer cells

(Chen et al., 2011; Meng et al., 2013). Moreover, in fibroblasts and renal epithelial cells, elevation of cytosolic Ca^{2+} with ionomycin had no effect on cell migration (Fabian et al., 2008; Yang and Huang, 2005). In consistent with the latter report, the results indicate the lack of effect of A23187 on migration of HeLa cells which is also consistent with the effects on actin cytoskeleton and focal adhesions described in the Chapter 4.

The effect of A23187 and BAPTA-AM on migration of PC-3 cells (Figure 5. 4) is, however, different from HeLa cells, despite the fact that these agents have similar effects on the actin cytoskeleton and focal adhesions in both the cell lines. The reasons for this difference are unclear, but previous studies showed inconsistent responses of PC-3 cells to Ca^{2+}. Ca^{2+} influx mediated by TRPV2 channels induced migration of PC-3 cells (Monet et al., 2010) while elevation of cytosolic Ca^{2+} by overexpression of TRPM8 channels caused an inhibition of PC-3 cell migration (Yang et al., 2009b). Therefore, in PC-3 cells, the Ca^{2+} signal mediated cell migration requires further studies. It is possible that different channels generate different spatio-temporally regulated Ca^{2+} micro-domains that could have opposite effects on cell migration.

Several previous studies have shown that migrating cells have a Ca^{2+} gradient and that this Ca^{2+} gradient is essential for triggering directional cell migration (Fabian et al., 2008; Tsai et al., 2014). Regarding to the pattern of the Ca^{2+} gradient, there is some discrepancy in the published reports. In renal epithelial cells, there is high level of Ca^{2+} at the leading edge compared to the rear (Fabian et al., 2008) while Ca^{2+} gradient in endothelial cells shows lower levels at the leading edge and higher levels at the rear (Tsai et al., 2014). Attempts to demonstrate a Ca^{2+} gradient in migrating HeLa cells were unsuccessful. Thus a role for Ca^{2+} gradient in H_2O_2 induced directional migration of HeLa cells could not be established unambiguously.

5. 3. 3 Zn^{2+} in cell migration

While a role for calcium channels in cellular processes has been widely accepted, in some situations, there is a concern that the effects seen might be due to permeable ions other than Ca^{2+} alone. Activation of TRPM2 channels results in the elevation of not only Ca^{2+}, but also Zn^{2+} as demonstrated in Chapter 4 and in the previous reports (Manna et al., 2015; Yu et al., 2012). Zinc plays a crucial role in many cellular processes, including endocytosis (Kim et al., 2004), apoptosis (Manna et al., 2015) and cancer progression (Jin et al., 2015; Takatani-Nakase et al., 2014). Studies have shown that Zn^{2+} can inhibit multiple phosphatases thereby supporting the active states of several tyrosine kinases, such as the EGF receptor, which is responsible for the aggressive behaviour of cancer cells (Normanno et al., 2006). In breast cancer cells, elevation of cytosolic Zn^{2+} has been shown to increase

their invasive potential (Taylor et al., 2008). Results presented in this chapter demonstrate that elevation of cytosolic Zn^{2+} with Zn-PTO can significantly increase directional migration of both HeLa and PC-3 cells and that the effect can be fully prevented by TPEN (Figure 5. 3 and 5. 4). These findings are consistent with the marked effect that Zn^{2+} has on filopodia formation and focal adhesion disassembly in Chapter 4.

Thus these results suggest that there is strong association between Zn^{2+} induced filopodia formation and focal adhesion disassembly and cell migration.

5. 3. 4 Intracellular organelles in cell migration

Results presented in Chapter 4 (Figure 4. 14 and Figure 4. 10A) suggested that Zn^{2+} is responsible for filopodia formation in HeLa cells and that the likely source of Zn^{2+} is lysosomes. Since filopodia are formed at the leading edge of migrating cells (Mattila and Lappalainen, 2008), it was surmised that Zn^{2+}-enriched lysosomes might migrate towards the leading edge of a migrating cell to provide free Zn^{2+} required for filopodia formation. Consistent with this idea, H_2O_2 caused significant accumulation of lysosomes at the leading edge of migrating cells, where filopodia were formed (Figure 5. 5A-C). These observations suggest lysosomes migrate to the leading edge of the cell presumably to release free Zn^{2+}. Furthermore, the results shown in Figure 5. 5 indicate a role for activation of TRPM2 channels in lysosomal polarisation. Attempts to demonstrate higher Zn^{2+} levels at the leading edge of the cell were unsuccessful. Further studies are required to understand how TRPM2 channels regulate polarization of lysosomes to drive cell migration.

Although polarisation of lysosomes in migrating cells has not been previously reported, polarisation of other organelles has been reported. For example, Nabi and colleagues have reported mobilisation of Golgi apparatus towards the leading edge of migrating cells (Nabi, 1999). It was suggested that polarization of the Golgi apparatus plays an important role in supplying membrane components to the leading edge (Magdalena et al., 2003; Uetrecht and Bear, 2009). However, recent studies argue that the polarization of the Golgi has little effect on membrane protrusion formation (Pu and Zhao, 2005) as it occurs concomitantly with cell polarization which occurs after the protrusion formation (Pu and Zhao, 2005).

Mitochondrion is another organelle reported to undergo redistribution in a migrating cell (Zhao et al., 2013). Redistribution of mitochondria to the leading edge has been observed in breast cancer cells and prostate cancer cells (Desai et al., 2013; Zhao et al., 2013). It has been reported that during directional migration, redistribution of mitochondria to the leading edge is required to induce cancer cell migration and this translocation is dependent on mitochondrial fission (Zhao et al., 2013). Furthermore, redistribution of fragmented

mitochondria has been shown to enhance lamellipodia formation in response to chemo-attractant (Zhao et al., 2013). The induction of mitochondrial fission and lamellipodia formation by ROS and regulation of these events by TRPM2 channels has been shown in Chapters 3 and 4 respectively. It would be interesting to examine whether ROS induced mitochondrial fragmentation would be accompanied by their redistribution to the leading edge of migrating cell.

Taken together, organelle redistribution might play an important role in cell migration and is an area that requires further studies.

5. 4 Summary

Collectively, current Chapter demonstrates that H_2O_2 induces directional migration of HeLa and PC-3 cells and this directional cell migration is dependent on the activation of TRPM2 channels. Furthermore, the role of Ca^{2+} and Zn^{2+}, the cytosolic levels of which increase by TRPM2 activation, in directional cell migration was investigated. Zn^{2+} induces migration of both HeLa and PC-3 cells. Ca^{2+}, on the other hand, exerts opposite effect. Decrease of cytosolic Ca^{2+} promotes migration of HeLa cells while elevation of cytosolic Ca^{2+} promotes migration of PC-3 cells. An interesting finding is that TRPM2 channels mediate cell migration by promoting trafficking of Zn^{2+}-enriched lysosomes to the leading edge of cells, presumably to provide Zn^{2+} required for filopodia formation. Taken together with the results of the previous Chapter, these findings support a role for TRPM2 channels and Zn^{2+} in cancer cell migration.

Chapter 6 Conclusions and further experiments

6. 1 Summary of key findings

Diabetic conditions including hyperglycaemia and hyperlipidaemia are thought to increase the risk of pancreatic β-cell death (Breitsprecher et al., 2011; Wang et al., 2005). Recent evidence has also implicated diabetes in increasing the risk of cancer (Nomura et al., 2010; Takatani-Nakase et al., 2014). The effects of hyperglycaemia and hyperlipidaemia are generally attributed to their ability to exert oxidative stress on these cells. In this thesis, it was hypothesised that oxidative stress sensitive TRPM2 channels play a central role in these two pathological processes. To test this hypothesis, a combination of immunofluorescence staining, flow cytometry, gene silencing and biochemical techniques were used.

Data presented in Chapter 3 investigated the role of TRPM2 channels in palmitate induced apoptosis in INS1 cells and pancreatic islets. Since mitochondria play a role in apoptosis, effect of palmitate on mitochondrial morphology (mitochondrial dynamics) and function and the role that TRPM2 channels play was examined. In agreement with previous findings (Molina et al., 2009; Wiederkehr and Wollheim, 2009), mitochondria were found to undergo fragmentation during exposure to high levels of palmitate, which was accompanied by significant cell death. Along with mitochondrial fragmentation, there was a marked loss of ΔΨm. Mitochondrial fragmentation was found to be due to palmitate induced increase in the recruitment of fission protein, Drp1, to mitochondria. Inhibition of TRPM2 channels with pharmacological inhibitors and siRNA significantly prevented the effects of palmitate on mitochondria and apoptosis, indicating a role for TRPM2 channels in palmitate induced apoptosis. Further investigation into the mechanism via which TRPM2 channels exert this function revealed that TRPM2 mediated changes in intracellular Zn^{2+} dynamics are responsible for the palmitate effects on mitochondria and cell viability.

The data also demonstrate that ROS required for TRPM2 activation are generated through activation of NOX2 by palmitate. Interestingly, activation of TRPM2 channels and changes in intracellular Zn^{2+} dynamics regulate mitochondrial ROS production via a mechanism that is yet to be investigated. A phenomenon termed "RIRS" has been suggested in cardio-myocytes (Zorov et al., 2006). It is suggested that mitochondrial ROS can be released into cytosol to trigger ROS production in neighbouring mitochondria. And this mitochondrion-to-mitochondrion ROS signalling constitutes a positive feedback mechanism for enhanced ROS production leading to deleterious impact on cells. Since rise in mitochondrial Zn^{2+} is known

to inhibit the electron transport chain (Dineley et al., 2003), it seems possible that the TRPM2 mediated rise in mitochondria Zn^{2+} is responsible for mitochondrial ROS production.

The cell death assay with mouse islets further demonstrated that TRPM2 channels mediate palmitate induced apoptosis as $TRPM2^{-/-}$ islets were resistant to apoptosis. Compared with the murine islets, human islets appear to be resistant to palmitate induced cell death. However, when palmitate was used in combination with cytokines (IL-1β and IFN-γ), the levels of which are increased in diabetes (Geraldes and King, 2010), significant increase in apoptosis was observed in human islets. Apoptosis of human islet cells was prevented by TRPM2 inhibition, further indicating the essential role of TRPM2 channels in oxidative stress induced apoptosis. The findings of this part are illustrated in Figure 6. 1A.

Data presented in Chapter 4 revealed a mechanism by which H_2O_2 induces actin and focal adhesion remodelling in HeLa and PC-3 carcinoma cells. H_2O_2 induced actin reorganization has been reported previously, however, the underlying mechanism is less well understood (Zhu et al., 2005). The current study, for the first time, revealed a role for TRPM2 channels in actin and focal adhesion dynamics. It was found that H_2O_2 induced remodelling of actin stress fibres and focal adhesions- required for cell migration- are dependent on the activation of TRPM2 channels. Further investigation revealed that TRPM2 channels mediate these changes by increasing cytosolic Ca^{2+} and Zn^{2+}. Interestingly, the effects of Ca^{2+} and Zn^{2+} on actin and focal adhesion remodelling were reciprocal in nature: Ca^{2+} maintained stress fibres, focal adhesions and prevented filopodia formation while Zn^{2+} displayed opposite effects. Further investigation led to the finding that Zn^{2+} is released from lysosomes and Zn^{2+} release is TRPM2 dependent. Although TRPM2 channels were found in the lysosomes, as in pancreatic β-cells (Lange et al., 2009) and dendritic cells (Sumoza-Toledo et al., 2011), there is no evidence that they mediate Zn^{2+} release. Based on the findings that palmitate could induce ROS production (Chapter 3), the effect of palmitate on actin remodelling in PC-3 cells was examined. Interestingly, in contrast to H_2O_2, palmitate treatment not only induced filopodia formation, but also induced fan-like lamellipodia formation. The effects of palmitate on actin remodelling were reversed by the antioxidant, NAC, indicating the involvement of ROS. These findings may explain the relationship between hyperlipidaemia seen in diabetes and the increased risk of cancer as actin remodelling plays an important role in cancer progression.

Data presented in Chapter 5 investigated the effect of actin cytoskeleton and focal adhesion remodelling on cancer cell migration based on the findings of Chapter 4. More importantly, the role of TRPM2 channels in cancer cell migration was examined. The involvement of TRPM2 channels in chemo-attractant-induced dendritic cell migration has been reported

previously (Sumoza-Toledo et al., 2011), however, neither the involvement of actin cytoskeleton nor the role of focal adhesions in this process was reported in that study. Using agarose spot cell migration assay, H_2O_2 induced cell migration in both HeLa and PC-3 cells was demonstrated. Further investigation indicated that TRPM2 channels mediate this effect as inhibition of TRPM2 channels by pharmacological inhibitors or siRNA prevented the cell migration. Heterologous expression of TRPM2 channels in HEK-MSR (+TRPM2) cells induced significant cell migration compared to HEK-MSR (-TRPM2) cells, further confirming the essential role of TRPM2 channels in H_2O_2 induced cell migration. In agreement with the reciprocal role of Ca^{2+} and Zn^{2+} in actin and focal adhesion remodelling in Chapter 4, Ca^{2+} and Zn^{2+} also had opposite effects on cell migration. Decrease of Ca^{2+} and increase of Zn^{2+} induced cell migration in HeLa cells. As Zn^{2+} is required for filopodia formation which is generally formed at the leading edge of a migrating cell, the intracellular distribution of Zn^{2+}-enriched lysosomes was investigated. Interestingly, filopodia formation at the leading edge of the migrating cell was accompanied by the movement of lysosomes to the leading edge. Although the mechanism is still unclear from current study, loss of lysosome migration in TRPM2-siRNA treated cells indicated a role of TRPM2 channels. The essential role of Ca^{2+} gradient in migrating cells has been reported previously in many types of cells (Fabian et al., 2008; Kuras et al., 2012; Tsai et al., 2014), however, in current study, such Ca^{2+} gradients could not be demonstrated. Finally, EGF induced migration of PC-3 cells was found to be dependent on ROS production and consequent activation of TRPM2 channels. Thus TRPM2 channels may play a role in growth factor stimulated cancer cell migration. The findings of the chapter 4 and chapter 5 are shown in Figure 6. 1B.
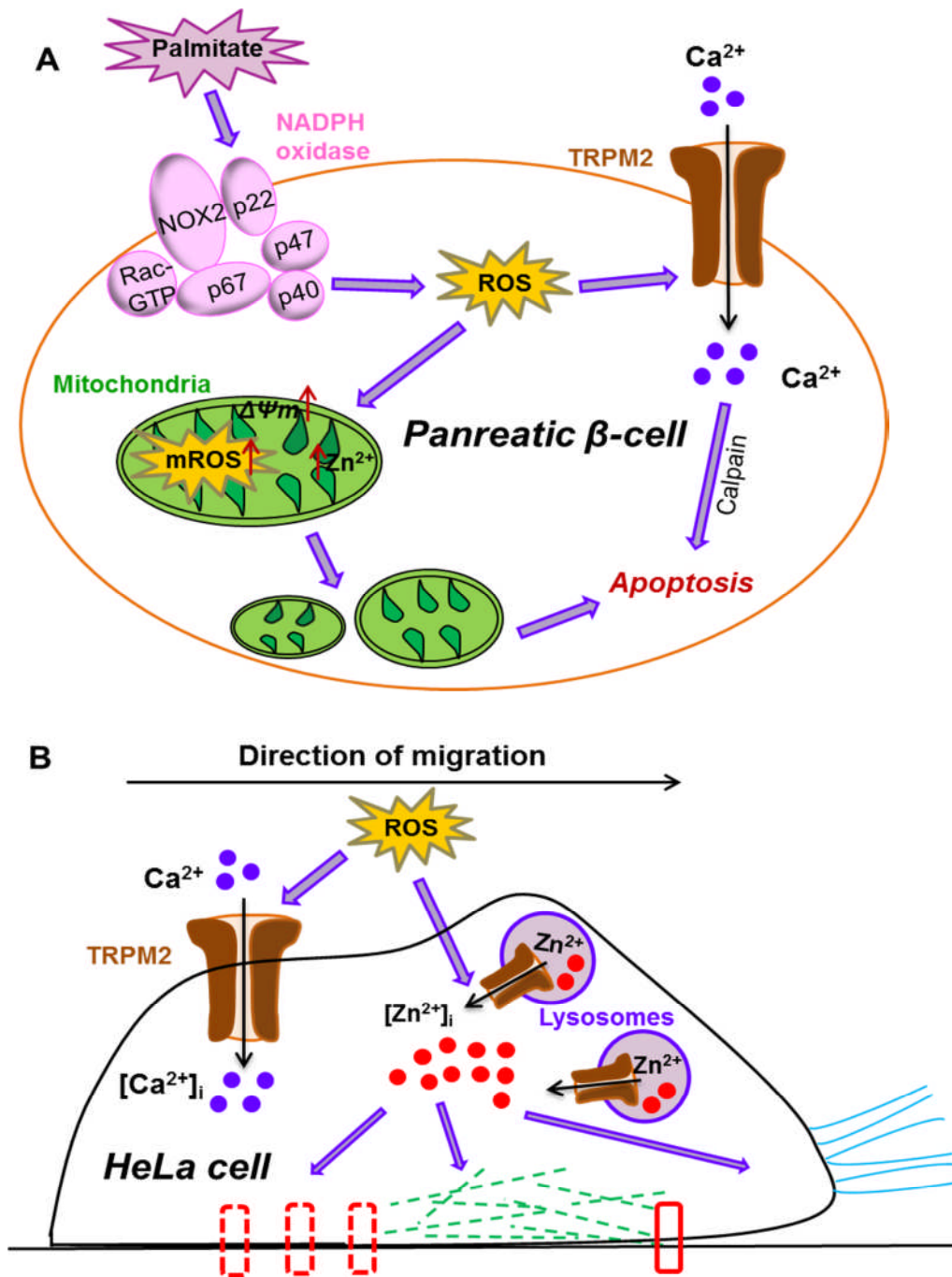
Figure 6. 1 Schematic overview of TRPM2 functions in palmitate-induced pancreatic β-cell death and ROS-induced Hela cell migration. (**A**) In pancreatic β-cells, palmitate induces NOX2-dependent ROS production followed by TRPM2-dependent mitochondrial Zn^{2+} increase, mitochondrial ROS production, loss of $\Delta\Psi m$, mitochondrial fragmentation and finally apoptosis. Ca^{2+} elevation through ROS-activated TRPM2 channels induces calpain-dependent, mitochondria-independent apoptosis. (**B**) In HeLa cells, ROS activation of TRPM2 channels mediates cytosolic Zn^{2+} elevation, potentially due to the release of the ion from lysosomes. Elevated Zn^{2+} induces stress fibre and focal adhesion remodelling, filopodia formation and cell migration. TRPM2-mediated Ca^{2+}, on the other hand, plays reciprocal role in these events (see text for details).

197

6. 2 Further experiments to examine the mechanism of NOX activation by palmitate

In Chapter 3, palmitate was found to induce cytosolic ROS production by activating NOX2 and mitochondrial ROS by affecting Zn^{2+} redistribution to mitochondria. Palmitate induced mitochondrial ROS production was found to be due to TRPM2 mediated changes in Zn^{2+} redistribution in the cell. However, how plasma membrane NOX2 is activated by palmitate is unclear. TRPM2 could be a potential mediator. Consistent with this idea, a recent study has shown that knock-out of TRPM2 in mice decreased NOX activity (Gao et al., 2014). Besides, the authors of this study reported that TRPM2 channels interact directly with Rac1, a cytosol-localised component of NOX, and that Rac1-TRPM2 interaction promotes NOX-dependent ROS production. Whether this is the case in palmitate treated β-cells remains be tested using biochemical approaches and dominant negative constructs of Rac1.

6. 3 Further experiments to investigate the effect of palmitate on ROS level in PC-3 cells

In Chapter 4, palmitate was found to stimulate lamellipodia and filopodia formation and that this was dependent on ROS generation as the antioxidant, NAC, was able to prevent the palmitate effect. Whether palmitate generates ROS in PC-3 cells in the same way as in INS1 cells need to be examined. Based on the effects of palmitate in INS1 cells, it is conceivable that palmitate might also induce ROS production in mitochondria. These possibilities need to be tested to see if β-cell apoptosis and cancer cell migration share ROS generating signalling events.

6. 4 Further experiments to reveal the role of TRPM2 channels in palmitate induced actin and focal adhesion remodelling

The finding that palmitate can induce actin remodelling is interesting. The effect of palmitate on actin arrangement has recently been reported in mouse podocytes (Xu et al., 2015). Besides, the authors of this study also observed that palmitate induces disassembly of focal adhesions. Whether this is the same for PC-3 cells will need to be investigated with further experiments. In their paper, the authors related palmitate-induced actin remodelling to proteinuria in chronic kidney disease (Xu et al., 2015). As one of the most important roles of actin remodelling is to mediate cell migration, the impact of palmitate-induced protrusion formation on PC-3 cell migration will need to be investigated. Whether the mechanism

underlying palmitate induced cell migration is similar to that of H_2O_2 remains to be investigated.

The data from Chapter 6 demonstrate that EGF induces ROS production in PC-3 cells, and that EGF induced cell migration can be inhibited by 2-APB. This observation could provide the basis for the investigation of the potential roles of ROS and 2-APB sensitive effectors in EGF induced cell migration, of which TRPM2 might be a potential candidate.

References

Abramov, A. Y., Jacobson, J., Wientjes, F., Hothersall, J., Canevari, L. and Duchen, M. R. (2005). Expression and modulation of an NADPH oxidase in mammalian astrocytes. *The Journal of neuroscience* **25**, 9176-9184.

Abreu-Blanco, M. T., Watts, J. J., Verboon, J. M. and Parkhurst, S. M. (2012). Cytoskeleton responses in wound repair. *Cellular and Molecular Life Sciences* **69**, 2469-2483.

Ackermann, M. and Matus, A. (2003). Activity-induced targeting of profilin and stabilization of dendritic spine morphology. *Nature neuroscience* **6**, 1194-1200.

Aldieri, E., Riganti, C., Polimeni, M., Gazzano, E., Lussiana, C., Campia, I. and Ghigo, D. (2008). Classical inhibitors of NOX NADPH oxidases are not specific. *Current drug metabolism* **9**, 686-696.

Angers-Loustau, A., Côté, J.-F., Charest, A., Dowbenko, D., Spencer, S., Lasky, L. A. and Tremblay, M. L. (1999). Protein tyrosine phosphatase-PEST regulates focal adhesion disassembly, migration, and cytokinesis in fibroblasts. *The Journal of cell biology* **144**, 1019-1031.

Arjonen, A., Kaukonen, R. and Ivaska, J. (2011). Filopodia and adhesion in cancer cell motility. *Cell adhesion & migration* **5**, 421-430.

Arkan, M. C., Hevener, A. L., Greten, F. R., Maeda, S., Li, Z.-W., Long, J. M., Wynshaw-Boris, A., Poli, G., Olefsky, J. and Karin, M. (2005). IKK-β links inflammation to obesity-induced insulin resistance. *Nature medicine* **11**, 191-198.

Arnoult, D. (2007). Mitochondrial fragmentation in apoptosis. *Trends in cell biology* **17**, 6-12.

Ashktorab, H., Frank, S., Khaled, A., Durum, S., Kifle, B. and Smoot, D. (2004). Bax translocation and mitochondrial fragmentation induced by Helicobacter pylori. *Gut* **53**, 805-813.

Atlante, A., Calissano, P., Bobba, A., Azzariti, A., Marra, E. and Passarella, S. (2000). Cytochrome c is released from mitochondria in a reactive oxygen species (ROS)-dependent fashion and can operate as a ROS scavenger and as a respiratory substrate in cerebellar neurons undergoing excitotoxic death. *Journal of Biological Chemistry* **275**, 37159-37166.

Azriel-Tamir, H., Sharir, H., Schwartz, B. and Hershfinkel, M. (2004). Extracellular zinc triggers ERK-dependent activation of Na^+/H^+ exchange in colonocytes mediated by the zinc-sensing receptor. *Journal of Biological Chemistry* **279**, 51804-51816.

Bach, D., Naon, D., Pich, S., Soriano, F. X., Vega, N., Rieusset, J., Laville, M., Guillet, C., Boirie, Y. and Wallberg-Henriksson, H. (2005). Expression of Mfn2, the Charcot-Marie-Tooth neuropathy type 2A gene, in human skeletal muscle effects of type 2 diabetes, obesity, weight loss, and the regulatory role of tumor necrosis factor α and interleukin-6. *Diabetes* **54**, 2685-2693.

Bach, D., Pich, S., Soriano, F. X., Vega, N., Baumgartner, B., Oriola, J., Daugaard, J. R., Lloberas, J., Camps, M. and Zierath, J. R. (2003). Mitofusin-2 determines mitochondrial network architecture and mitochondrial metabolism A novel regulatory mechanism altered in obesity. *Journal of Biological Chemistry* **278**, 17190-17197.

Bae, Y. S., Kang, S. W., Seo, M. S., Baines, I. C., Tekle, E., Chock, P. B. and Rhee, S. G. (1997). Epidermal growth factor (EGF)-induced generation of hydrogen peroxide role in EGF receptor-mediated tyrosine phosphorylation. *Journal of Biological Chemistry* **272**, 217-221.

Balteau, M., Tajeddine, N., de Meester, C., Ginion, A., Des Rosiers, C., Brady, N. R., Sommereyns, C., Horman, S., Vanoverschelde, J.-L. and Gailly, P. (2011). NADPH oxidase activation

by hyperglycaemia in cardiomyocytes is independent of glucose metabolism but requires SGLT1. *Cardiovascular Research* **92**, 237-246.

Bao, Q. and Shi, Y. (2007). Apoptosome: a platform for the activation of initiator caspases. *Cell Death & Differentiation* **14**, 56-65.

Barbu, A., Welsh, N. and Saldeen, J. (2002). Cytokine-induced apoptosis and necrosis are preceded by disruption of the mitochondrial membrane potential (Δψm) in pancreatic RINm5F cells: prevention by Bcl-2. *Molecular and cellular endocrinology* **190**, 75-82.

Bari, M. R., Akbar, S., Eweida, M., Kühn, F. J., Gustafsson, A. J., Lückhoff, A. and Islam, M. (2009). H_2O_2-induced Ca^{2+} influx and its inhibition by N(p-amylcinnamoyl) anthranilic acid in the β-cells: involvement of TRPM2 channels. *Journal of cellular and molecular medicine* **13**, 3260-3267.

Barnham, K. J., Masters, C. L. and Bush, A. I. (2004). Neurodegenerative diseases and oxidative stress. *Nature Reviews Drug Discovery* **3**, 205-214.

Basso, E., Fante, L., Fowlkes, J., Petronilli, V., Forte, M. A. and Bernardi, P. (2005). Properties of the permeability transition pore in mitochondria devoid of Cyclophilin D. *Journal of Biological Chemistry* **280**, 18558-18561.

Baumgartner, H. K., Gerasimenko, J. V., Thorne, C., Ferdek, P., Pozzan, T., Tepikin, A. V., Petersen, O. H., Sutton, R., Watson, A. J. and Gerasimenko, O. V. (2009). Calcium elevation in mitochondria is the main Ca^{2+} requirement for mitochondrial permeability transition pore (mPTP) opening. *Journal of Biological Chemistry* **284**, 20796-20803.

Beal, M. F. (2004). Mitochondrial dysfunction and oxidative damage in Alzheimer's and Parkinson's diseases and coenzyme Q10 as a potential treatment. *Journal of bioenergetics and biomembranes* **36**, 381-386.

Bedard, K. and Krause, K.-H. (2007). The NOX family of ROS-generating NADPH oxidases: physiology and pathophysiology. *Physiological reviews* **87**, 245-313.

Benard, G., Bellance, N., James, D., Parrone, P., Fernandez, H., Letellier, T. and Rossignol, R. (2007). Mitochondrial bioenergetics and structural network organization. *Journal of Cell Science* **120**, 838-848.

Bessac, B. F., Sivula, M., Von Hehn, C. A., Escalera, J., Cohn, L. and Jordt, S.-E. (2008). TRPA1 is a major oxidant sensor in murine airway sensory neurons. *The Journal of clinical investigation* **118**, 1899.

Bhatt, A., Kaverina, I., Otey, C. and Huttenlocher, A. (2002). Regulation of focal complex composition and disassembly by the calcium-dependent protease calpain. *Journal of Cell Science* **115**, 3415-3425.

Bindokas, V. P., Kuznetsov, A., Sreenan, S., Polonsky, K. S., Roe, M. W. and Philipson, L. H. (2003). Visualizing superoxide production in normal and diabetic rat islets of Langerhans. *Journal of Biological Chemistry* **278**, 9796-9801.

Binker, M. G., Binker-Cosen, A. A., Richards, D., Oliver, B. and Cosen-Binker, L. I. (2009). EGF promotes invasion by PANC-1 cells through Rac1/ROS-dependent secretion and activation of MMP-2. *Biochemical and Biophysical Research Communications* **379**, 445-450.

Bogeski, I., Kappl, R., Kummerow, C., Gulaboski, R., Hoth, M. and Niemeyer, B. A. (2011). Redox regulation of calcium ion channels: chemical and physiological aspects. *Cell Calcium* **50**, 407-423.

Bohil, A. B., Robertson, B. W. and Cheney, R. E. (2006). Myosin-X is a molecular motor that functions in filopodia formation. *Proceedings of the National Academy of Sciences* **103**, 12411-6.

Bomben, V. C., Turner, K. L., Barclay, T. T. C. and Sontheimer, H. (2011). Transient receptor potential canonical channels are essential for chemotactic migration of human malignant gliomas. *Journal of Cell Physiology* **226**, 1879-1888.

Bos, J. L., Rehmann, H. and Wittinghofer, A. (2007). GEFs and GAPs: critical elements in the control of small G proteins. *Cell* **129**, 865-877.

Bose, T., Cieślar-Pobuda, A. and Wiechec, E. (2015). Role of ion channels in regulating Ca^{2+}; homeostasis during the interplay between immune and cancer cells. *Cell death & disease* **6**, e1648.

Bossy-Wetzel, E., Talantova, M. V., Lee, W. D., Schölzke, M. N., Harrop, A., Mathews, E., Götz, T., Han, J., Ellisman, M. H. and Perkins, G. A. (2004). Crosstalk between nitric oxide and zinc pathways to neuronal cell death involving mitochondrial dysfunction and p38-activated K^+ channels. *Neuron* **41**, 351-365.

Bouron, A., Kiselyov, K. and Oberwinkler, J. (2014). Permeation, regulation and control of expression of TRP channels by trace metal ions. *Pflügers Archiv-European Journal of Physiology* **467**, 1143-1164.

Brandt, D., Gimona, M., Hillmann, M., Haller, H. and Mischak, H. (2002). Protein kinase C induces actin reorganization via a Src-and Rho-dependent pathway. *Journal of Biological Chemistry* **277**, 20903-20910.

Braun, R. J. (2012). Mitochondrion-mediated cell death: dissecting yeast apoptosis for a better understanding of neurodegeneration. *Frontiers in oncology* **2**. 182.

Breckenridge, D. G., Stojanovic, M., Marcellus, R. C. and Shore, G. C. (2003). Caspase cleavage product of BAP31 induces mitochondrial fission through endoplasmic reticulum calcium signals, enhancing cytochrome c release to the cytosol. *The Journal of cell biology* **160**, 1115-1127.

Breitsprecher, D., Koestler, S. A., Chizhov, I., Nemethova, M., Mueller, J., Goode, B. L., Small, J. V., Rottner, K. and Faix, J. (2011). Cofilin cooperates with fascin to disassemble filopodial actin filaments. *Journal of Cell Science* **124**, 3305-3318.

Brini, M. and Carafoli, E. (2009). Calcium pumps in health and disease. *Physiological reviews* **89**, 1341-1378.

Brooks, C., Wei, Q., Feng, L., Dong, G., Tao, Y., Mei, L., Xie, Z.-J. and Dong, Z. (2007). Bak regulates mitochondrial morphology and pathology during apoptosis by interacting with mitofusins. *Proceedings of the National Academy of Sciences* **104**, 11649-11654.

Brustovetsky, N. and Dubinsky, J. M. (2000). Dual responses of CNS mitochondria to elevated calcium. *The Journal of neuroscience* **20**, 103-113.

Busik, J. V., Mohr, S. and Grant, M. B. (2008). Hyperglycemia-induced reactive oxygen species toxicity to endothelial cells is dependent on paracrine mediators. *Diabetes* **57**, 1952-1965.

Cai, D., Yuan, M., Frantz, D. F., Melendez, P. A., Hansen, L., Lee, J. and Shoelson, S. E. (2005). Local and systemic insulin resistance resulting from hepatic activation of IKK-β and NF-κB. *Nature medicine* **11**, 183-190.

Caltagarone, J., Jing, Z. and Bowser, R. (2007). Focal adhesions regulate Aβ signaling and cell death in Alzheimer's disease. *Biochimica et Biophysica Acta (BBA)-Molecular Basis of Disease* **1772**, 438-445.

Campbell, M. and Trimble, E. R. (2005). Modification of PI3K-and MAPK-dependent chemotaxis in aortic vascular smooth muscle cells by protein kinase CβII. *Circulation Research* **96**, 197-206.

Cao, G., pil Lee, K., van der Wijst, J., de Graaf, M., van der Kemp, A., Bindels, R. J. and Hoenderop, J. G. (2010). Methionine sulfoxide reductase B1 (MsrB1) recovers TRPM6 channel activity during oxidative stress. *Journal of Biological Chemistry* **285**, 26081-26087.

Capano, M. and Crompton, M. (2002). Biphasic translocation of Bax to mitochondria. *Biochemical Journal* **367**, 169-178.

Carlsson, C., Hakan Borg, L. and Welsh, N. (1999). Sodium Palmitate Induces Partial Mitochondrial Uncoupling and Reactive Oxygen Species in Rat Pancreatic Islets in Vitro 1. *Endocrinology* **140**, 3422-3428.

Caterina, M. J., Schumacher, M. A., Tominaga, M., Rosen, T. A., Levine, J. D. and Julius, D. (1997). The capsaicin receptor: a heat-activated ion channel in the pain pathway. *Nature* **389**, 816-824.

Cereghetti, G., Costa, V. and Scorrano, L. (2010). Inhibition of Drp1-dependent mitochondrial fragmentation and apoptosis by a polypeptide antagonist of calcineurin. *Cell Death & Differentiation* **17**, 1785-1794.

Cereghetti, G., Stangherlin, A., De Brito, O. M., Chang, C., Blackstone, C., Bernardi, P. and Scorrano, L. (2008). Dephosphorylation by calcineurin regulates translocation of Drp1 to mitochondria. *Proceedings of the National Academy of Sciences* **105**, 15803-15808.

Chalmers, S. and McCarron, J. G. (2008). The mitochondrial membrane potential and Ca^{2+} oscillations in smooth muscle. *Journal of Cell Science* **121**, 75-85.

Chan, K. T., Bennin, D. A. and Huttenlocher, A. (2010). Regulation of adhesion dynamics by calpain-mediated proteolysis of focal adhesion kinase (FAK). *Journal of Biological Chemistry* **285**, 11418-11426.

Chaudhuri, P., Colles, S. M., Bhat, M., Van Wagoner, D. R., Birnbaumer, L. and Graham, L. M. (2008). Elucidation of a TRPC6-TRPC5 channel cascade that restricts endothelial cell movement. *Molecular Biology of the Cell* **19**, 3203-3211.

Chaudhuri, P., Colles, S. M., Damron, D. S. and Graham, L. M. (2003). Lysophosphatidylcholine inhibits endothelial cell migration by increasing intracellular calcium and activating calpain. *Arteriosclerosis, Thrombosis and Vascular Biology* **23**, 218-223.

Chen, H. and Chan, D. C. (2009). Mitochondrial dynamics–fusion, fission, movement, and mitophagy–in neurodegenerative diseases. *Human molecular genetics* **18**, R169-R176.

Chen, X., Zhang, X., Kubo, H., Harris, D. M., Mills, G. D., Moyer, J., Berretta, R., Potts, S. T., Marsh, J. D. and Houser, S. R. (2005). Ca^{2+} Influx–Induced Sarcoplasmic Reticulum Ca^{2+} Overload Causes Mitochondrial-Dependent Apoptosis in Ventricular Myocytes. *Circulation Research* **97**, 1009-1017.

Chen, Y.-F., Chiu, W.-T., Chen, Y.-T., Lin, P.-Y., Huang, H.-J., Chou, C.-Y., Chang, H.-C., Tang, M.-J. and Shen, M.-R. (2011). Calcium store sensor stromal-interaction molecule 1-dependent signaling plays an important role in cervical cancer growth, migration, and angiogenesis. *Proceedings of the National Academy of Sciences* **108**, 15225-15230.

Cheng, J.-C., Klausen, C. and Leung, P. C. (2010). Hydrogen peroxide mediates EGF-induced down-regulation of E-cadherin expression via p38 MAPK and snail in human ovarian cancer cells. *Molecular Endocrinology* **24**, 1569-1580.

Chiarugi, P. and Fiaschi, T. (2007). Redox signalling in anchorage-dependent cell growth. *Cellular signalling* **19**, 672-682.

Chiarugi, P., Pani, G., Giannoni, E., Taddei, L., Colavitti, R., Raugei, G., Symons, M., Borrello, S., Galeotti, T. and Ramponi, G. (2003). Reactive oxygen species as essential mediators of cell

adhesion the oxidative inhibition of a FAK tyrosine phosphatase is required for cell adhesion. *The Journal of cell biology* **161**, 933-944.

Chien, C.-B., Rosenthal, D. E., Harris, W. A. and Holt, C. E. (1993). Navigational errors made by growth cones without filopodia in the embryonic Xenopus brain. *Neuron* **11**, 237-251.

Cho, K. H., Choi, M. J., Jeong, K. J., Kim, J. J., Hwang, M. H., Shin, S. C., Park, C. G. and Lee, H. Y. (2014). A ROS/STAT3/HIF-1α signaling cascade mediates EGF-induced TWIST1 expression and prostate cancer cell invasion. *The prostate* **74**, 528-536.

Christensen, K. A., Myers, J. T. and Swanson, J. A. (2002). pH-dependent regulation of lysosomal calcium in macrophages. *Journal of Cell Science* **115**, 599-607.

Chrzanowska-Wodnicka, M. and Burridge, K. (1996). Rho-stimulated contractility drives the formation of stress fibers and focal adhesions. *The Journal of cell biology* **133**, 1403-1415.

Cingolani, L. A. and Goda, Y. (2008). Actin in action: the interplay between the actin cytoskeleton and synaptic efficacy. *Nature reviews neuroscience* **9**, 344-356.

Cinq-Frais, C., Coatrieux, C., Savary, A., D'Angelo, R., Bernis, C., Salvayre, R., Nègre-Salvayre, A. and Augé, N. (2015). Annexin II-dependent actin remodelling evoked by hydrogen peroxide requires the metalloproteinase/sphingolipid pathway. *Redox biology* **4**, 169-179.

Cipolat, S., de Brito, O. M., Dal Zilio, B. and Scorrano, L. (2004). OPA1 requires mitofusin 1 to promote mitochondrial fusion. *Proceedings of the National Academy of Sciences* **101**, 15927-15932.

Clapham, D. E. (2003). TRP channels as cellular sensors. *Nature* **426**, 517-524.

Clapham, D. E. (2007). Calcium signaling. *Cell* **131**, 1047-1058.

Clark, K., Langeslag, M., Van Leeuwen, B., Ran, L., Ryazanov, A. G., Figdor, C. G., Moolenaar, W. H., Jalink, K. and Van Leeuwen, F. N. (2006). TRPM7, a novel regulator of actomyosin contractility and cell adhesion. *EMBO Journal* **25**, 290-301.

Clark, K., Middelbeek, J. and van Leeuwen, F. N. (2008). Interplay between TRP channels and the cytoskeleton in health and disease. *European Journal of Cell Biology* **87**, 631-640.

Cnop, M., Welsh, N., Jonas, J.-C., Jörns, A., Lenzen, S. and Eizirik, D. L. (2005). Mechanisms of pancreatic β-cell death in Type 1 and Type 2 diabetes many differences, few similarities. *Diabetes* **54**, S97-S107.

Collins, T. J., Lipp, P., Berridge, M. J. and Bootman, M. D. (2001). Mitochondrial Ca^{2+} uptake depends on the spatial and temporal profile of cytosolic Ca^{2+} signals. *Journal of Biological Chemistry* **276**, 26411-26420.

Colvin, R. A., Fontaine, C. P., Laskowski, M. and Thomas, D. (2003). Zn^{2+} transporters and Zn^{2+} homeostasis in neurons. *European journal of pharmacology* **479**, 171-185.

Cooper, L. L., Li, W., Lu, Y., Centracchio, J., Terentyeva, R., Koren, G. and Terentyev, D. (2013). Redox modification of ryanodine receptors by mitochondria-derived reactive oxygen species contributes to aberrant Ca^{2+} handling in ageing rabbit hearts. *The Journal of Physiology* **591**, 5895-5911.

Correia, S. C., Santos, R. X., Perry, G., Zhu, X., Moreira, P. I. and Smith, M. A. (2012). Mitochondrial importance in Alzheimer's, Huntington's and Parkinson's diseases. *Advances in Experimental Medicine and Biology* **724**, 205-221.

Corson, L. B., Yamanaka, Y., Lai, K.-M. V. and Rossant, J. (2003). Spatial and temporal patterns of ERK signaling during mouse embryogenesis. *Development* **130**, 4527-4537.

Cortesio, C. L., Boateng, L. R., Piazza, T. M., Bennin, D. A. and Huttenlocher, A. (2011). Calpain-mediated proteolysis of paxillin negatively regulates focal adhesion dynamics and cell migration. *Journal of Biological Chemistry* **286**, 9998-10006.

Costello, L. C., Guan, Z., Kukoyi, B., Feng, P. and Franklin, R. B. (2004). Terminal oxidation and the effects of zinc in prostate versus liver mitochondria. *Mitochondrion* **4**, 331-338.

Côté, J.-F., Turner, C. E. and Tremblay, M. L. (1999). Intact LIM 3 and LIM 4 domains of paxillin are required for the association to a novel polyproline region (Pro2) of protein-tyrosine phosphatase-PEST. *Journal of Biological Chemistry* **274**, 20550-20560.

Csanády, L. and Törőcsik, B. (2009). Four Ca^{2+} ions activate TRPM2 channels by binding in deep crevices near the pore but intracellularly of the gate. *The Journal of general physiology* **133**, 189-203.

Cui, Y. and Yamada, S. (2013). N-cadherin dependent collective cell invasion of prostate cancer cells is regulated by the N-terminus of α-catenin. *PLoS One* **8**, e55069.

Cukierman, E., Pankov, R., Stevens, D. R. and Yamada, K. M. (2001). Taking cell-matrix adhesions to the third dimension. *Science* **294**, 1708-1712.

D'Autréaux, B. and Toledano, M. B. (2007). ROS as signalling molecules: mechanisms that generate specificity in ROS homeostasis. *Nature Reviews Molecular Cell Biology* **8**, 813-824.

Danciu, T. E., Adam, R. M., Naruse, K., Freeman, M. R. and Hauschka, P. V. (2003). Calcium regulates the PI3K-Akt pathway in stretched osteoblasts. *FEBS letters* **536**, 193-197.

De Giorgi, F., Lartigue, L., Bauer, M. K., Schubert, A., Grimm, S., Hanson, G. T., Remington, S. J., Youle, R. J. and Ichas, F. (2002). The permeability transition pore signals apoptosis by directing Bax translocation and multimerization. *FASEB Journal* **16**, 607-609.

De Smet, F., Segura, I., De Bock, K., Hohensinner, P. J. and Carmeliet, P. (2009). Mechanisms of vessel branching filopodia on endothelial tip cells lead the way. *Arteriosclerosis, Thrombosis, and Vascular Biology* **29**, 639-649.

Defilippi, P., Olivo, C., Venturino, M., Dolce, L., Silengo, L. and Tarone, G. (1999). Actin cytoskeleton organization in response to integrin-mediated adhesion. *Microscopy research and technique* **47**, 67-78.

Degli Esposti, M., Erler, J. T., Hickman, J. A. and Dive, C. (2001). Bid, a widely expressed proapoptotic protein of the Bcl-2 family, displays lipid transfer activity. *Molecular and cellular biology* **21**, 7268-7276.

DeHaven, W. I., Smyth, J. T., Boyles, R. R. and Putney, J. W. (2007). Calcium inhibition and calcium potentiation of Orai1, Orai2, and Orai3 calcium release-activated calcium channels. *Journal of Biological Chemistry* **282**, 17548-17556.

Dent, E. W., Kwiatkowski, A. V., Mebane, L. M., Philippar, U., Barzik, M., Rubinson, D. A., Gupton, S., Van Veen, J. E., Furman, C. and Zhang, J. (2007). Filopodia are required for cortical neurite initiation. *Nature Cell Biology* **9**, 1347-1359.

Denu, J. M. and Tanner, K. G. (1998). Specific and reversible inactivation of protein tyrosine phosphatases by hydrogen peroxide: evidence for a sulfenic acid intermediate and implications for redox regulation. *Biochemistry* **37**, 5633-5642.

Desai, S. P., Bhatia, S. N., Toner, M. and Irimia, D. (2013). Mitochondrial localization and the persistent migration of epithelial cancer cells. *Biophysical Journal* **104**, 2077-2088.

Devinney, M. J., Malaiyandi, L. M., Vergun, O., DeFranco, D. B., Hastings, T. G. and Dineley, K. E. (2009). A comparison of Zn^{2+}-and Ca^{2+}-triggered depolarization of liver mitochondria reveals no evidence of Zn^{2+}-induced permeability transition. *Cell Calcium* **45**, 447-455.

Di Lisa, F. and Ziegler, M. (2001). Pathophysiological relevance of mitochondria in NAD+ metabolism. *FEBS letters* **492**, 4-8.

Diaz, B., Shani, G., Pass, I., Anderson, D., Quintavalle, M. and Courtneidge, S. A. (2009). Tks5-dependent, nox-mediated generation of reactive oxygen species is necessary for invadopodia formation. *Science signaling* **2**, ra53.

Dinauer, M. C., Orkin, S. H., Brown, R., Jesaitis, A. J. and Parkos, C. A. (1987). The glycoprotein encoded by the X-linked chronic granulomatous disease locus is a component of the neutrophil cytochrome b complex. *Nature* **327**, 717-720.

Dineley, K. E., Votyakova, T. V. and Reynolds, I. J. (2003). Zinc inhibition of cellular energy production: implications for mitochondria and neurodegeneration. *Journal of neurochemistry* **85**, 563-570.

Djordjevic, T., Pogrebniak, A., BelAiba, R. S., Bonello, S., Wotzlaw, C., Acker, H., Hess, J. and Görlach, A. (2005). The expression of the NADPH oxidase subunit p22phox is regulated by a redox-sensitive pathway in endothelial cells. *Free Radical Biology and Medicine* **38**, 616-630.

Dong, H., Shim, K.-N., Li, J. M., Estrema, C., Ornelas, T. A., Nguyen, F., Liu, S., Ramamoorthy, S. L., Ho, S. and Carethers, J. M. (2010a). Molecular mechanisms underlying Ca^{2+}-mediated motility of human pancreatic duct cells. *American Journal of Physiology-Cell Physiology* **299**, C1493-C1503.

Dong, X. P., Wang, X. and Xu, H. (2010b). TRP channels of intracellular membranes. *Journal of neurochemistry* **113**, 313-328.

Dourdin, N., Bhatt, A. K., Dutt, P., Greer, P. A., Arthur, J. S. C., Elce, J. S. and Huttenlocher, A. (2001). Reduced cell migration and disruption of the actin cytoskeleton in calpain-deficient embryonic fibroblasts. *Journal of Biological Chemistry* **276**, 48382-48388.

Du, X., Matsumura, T., Edelstein, D., Rossetti, L., Zsengellér, Z., Szabó, C. and Brownlee, M. (2003). Inhibition of GAPDH activity by poly (ADP-ribose) polymerase activates three major pathways of hyperglycemic damage in endothelial cells. *Journal of Clinical Investigation* **112**, 1049.

Dubi, N., Gheber, L., Fishman, D., Sekler, I. and Hershfinkel, M. (2008). Extracellular zinc and zinc-citrate, acting through a putative zinc-sensing receptor, regulate growth and survival of prostate cancer cells. *Carcinogenesis* **29**, 1692-1700.

Dumont, M. and Beal, M. F. (2011). Neuroprotective strategies involving ROS in Alzheimer disease. *Free Radical Biology and Medicine* **51**, 1014-1026.

Duncan, C., Greenaway, H. C., Publicover, S., Rudge, M. F. and Smith, J. (1980). Experimental production of "septa" and apparent subdivision of muscle mitochondria. *Journal of bioenergetics and biomembranes* **12**, 13-33.

Earnshaw, W. C., Martins, L. M. and Kaufmann, S. H. (1999). Mammalian caspases: structure, activation, substrates, and functions during apoptosis. *Annual review of biochemistry* **68**, 383-424.

Eckert, A., Keil, U., Marques, C. A., Bonert, A., Frey, C., Schüssel, K. and Müller, W. E. (2003). Mitochondrial dysfunction, apoptotic cell death, and Alzheimer's disease. *Biochemical pharmacology* **66**, 1627-1634.

Elmore, S. (2007). Apoptosis: a review of programmed cell death. *Toxicologic pathology* **35**, 495-516.

Evan, G. I. and Vousden, K. H. (2001). Proliferation, cell cycle and apoptosis in cancer. *Nature* **411**, 342-348.

Fabian, A., Fortmann, T., Dieterich, P., Riethmüller, C., Schön, P., Mally, S., Nilius, B. and Schwab, A. (2008). TRPC1 channels regulate directionality of migrating cells. *Pflügers Archiv-European Journal of Physiology* **457**, 475-484.

Falcón-Pérez, J. M. and Dell'Angelica, E. C. (2007). Zinc transporter 2 (SLC30A2) can suppress the vesicular zinc defect of adaptor protein 3-depleted fibroblasts by promoting zinc accumulation in lysosomes. *Experimental Cell Research* **313**, 1473-1483.

Fan, L., Pellegrin, S., Scott, A. and Mellor, H. (2010). The small GTPase Rif is an alternative trigger for the formation of actin stress fibers in epithelial cells. *Journal of Cell Science* **123**, 1247-1252.

Fauzee, N. J. S., Pan, J. and Wang, Y.-l. (2010). PARP and PARG inhibitors—new therapeutic targets in cancer treatment. *Pathology & Oncology Research* **16**, 469-478.

Favaloro, B., Allocati, N., Graziano, V., Di Ilio, C. and De Laurenzi, V. (2012). Role of apoptosis in disease. *Aging* **4**, 330.

Finkel, T. (2012). Signal transduction by mitochondrial oxidants. *Journal of Biological Chemistry* **287**, 4434-4440.

Fleig, A. and Penner, R. (2004). The TRPM ion channel subfamily: molecular, biophysical and functional features. *Trends in pharmacological sciences* **25**, 633-639.

Florea, S. M. and Blatter, L. A. (2008). The effect of oxidative stress on Ca^{2+} release and capacitative Ca^{2+} entry in vascular endothelial cells. *Cell Calcium* **43**, 405-415.

Folkman, J. (1995). Angiogenesis in cancer, vascular, rheumatoid and other disease. *Nature medicine* **1**, 27-30.

Fonfria, E., Marshall, I. C., Benham, C. D., Boyfield, I., Brown, J. D., Hill, K., Hughes, J. P., Skaper, S. D. and McNulty, S. (2004). TRPM2 channel opening in response to oxidative stress is dependent on activation of poly (ADP-ribose) polymerase. *British Journal of Pharmacology* **143**, 186-192.

Frame, M. C., Fincham, V. J., Carragher, N. O. and Wyke, J. A. (2002). v-Src's hold over actin and cell adhesions. *Nature Reviews Molecular Cell Biology* **3**, 233-245.

Franco, S. J., Rodgers, M. A., Perrin, B. J., Han, J., Bennin, D. A., Critchley, D. R. and Huttenlocher, A. (2004). Calpain-mediated proteolysis of talin regulates adhesion dynamics. *Nature Cell Biology* **6**, 977-983.

Friedl, P. and Gilmour, D. (2009). Collective cell migration in morphogenesis, regeneration and cancer. *Nature Reviews Molecular Cell Biology* **10**, 445-457.

Friedl, P. and Wolf, K. (2003). Tumour-cell invasion and migration: diversity and escape mechanisms. *Nature Reviews Cancer* **3**, 362-374.

Friedman, J. R., Lackner, L. L., West, M., DiBenedetto, J. R., Nunnari, J. and Voeltz, G. K. (2011). ER tubules mark sites of mitochondrial division. *Science* **334**, 358-362.

Fukawa, T., Kajiya, H., Ozeki, S., Ikebe, T. and Okabe, K. (2012). Reactive oxygen species stimulates epithelial mesenchymal transition in normal human epidermal keratinocytes via TGF-beta secretion. *Experimental Cell Research* **318**, 1926-1932.

Gallo, G. and Letourneau, P. C. (2004). Regulation of growth cone actin filaments by guidance cues. *Journal of neurobiology* **58**, 92-102.

Gao, G., Wang, W., Tadagavadi, R. K., Briley, N. E., Love, M. I., Miller, B. A. and Reeves, W. B. (2014). TRPM2 mediates ischemic kidney injury and oxidant stress through RAC1. *The Journal of clinical investigation* **124**, 4989.

Gazaryan, I. G., Krasinskaya, I. P., Kristal, B. S. and Brown, A. M. (2007). Zinc irreversibly damages major enzymes of energy production and antioxidant defense prior to mitochondrial permeability transition. *Journal of Biological Chemistry* **282**, 24373-24380.

Geiger, B., Bershadsky, A., Pankov, R. and Yamada, K. M. (2001). Transmembrane crosstalk between the extracellular matrix and the cytoskeleton. *Nature Reviews Molecular Cell Biology* **2**, 793-805.

Gencer, S., Cebeci, A. and Irmak-Yazicioglu, M. B. (2013). Matrix metalloproteinase gene expressions might be oxidative stress targets in gastric cancer cell lines. *Chinese Journal of Cancer Research* **25**, 322.

Geraldes, P. and King, G. L. (2010). Activation of protein kinase C isoforms and its impact on diabetic complications. *Circulation Research* **106**, 1319-1331.

Giannone, G., Rondé, P., Gaire, M., Beaudouin, J., Haiech, J., Ellenberg, J. and Takeda, K. (2004). Calcium rises locally trigger focal adhesion disassembly and enhance residency of focal adhesion kinase at focal adhesions. *Journal of Biological Chemistry* **279**, 28715-28723.

Gough, D. and Cotter, T. (2011). Hydrogen peroxide: a Jekyll and Hyde signalling molecule. *Cell death & disease* **2**, e213.

Green, K., Brand, M. D. and Murphy, M. P. (2004). Prevention of mitochondrial oxidative damage as a therapeutic strategy in diabetes. *Diabetes* **53**, S110-S118.

Greka, A., Navarro, B., Oancea, E., Duggan, A. and Clapham, D. E. (2003). TRPC5 is a regulator of hippocampal neurite length and growth cone morphology. *Nature neuroscience* **6**, 837-845.

Grijalba, M. T., Vercesi, A. E. and Schreier, S. (1999). Ca^{2+}-induced increased lipid packing and domain formation in submitochondrial particles. A possible early step in the mechanism of Ca^{2+}-stimulated generation of reactive oxygen species by the respiratory chain. *Biochemistry* **38**, 13279-13287.

Grupe, M., Myers, G., Penner, R. and Fleig, A. (2010). Activation of store-operated I CRAC by hydrogen peroxide. *Cell Calcium* **48**, 1-9.

Guilherme, A., Virbasius, J. V., Puri, V. and Czech, M. P. (2008). Adipocyte dysfunctions linking obesity to insulin resistance and type 2 diabetes. *Nature Reviews Molecular Cell Biology* **9**, 367-377.

Gupta, G. P. and Massagué, J. (2006). Cancer metastasis: building a framework. *Cell* **127**, 679-695.

Gurzov, E. N., Stanley, W. J., Brodnicki, T. C. and Thomas, H. E. (2015). Protein tyrosine phosphatases: molecular switches in metabolism and diabetes. *Trends in Endocrinology & Metabolism* **26**, 30-39.

Guvakova, M. A. and Surmacz, E. (1999). The activated insulin-like growth factor I receptor induces depolarization in breast epithelial cells characterized by actin filament disassembly and tyrosine dephosphorylation of FAK, Cas, and paxillin. *Experimental Cell Research* **251**, 244-255.

Gwiazda, K. S., Yang, T.-L. B., Lin, Y. and Johnson, J. D. (2009). Effects of palmitate on ER and cytosolic Ca^{2+} homeostasis in β-cells. *American Journal of Physiology-Endocrinology and Metabolism* **296**, E690-E701.

Gyulkhandanyan, A. V., Lee, S. C., Bikopoulos, G., Dai, F. and Wheeler, M. B. (2006). The Zn^{2+}-transporting Pathways in Pancreatic β-Cells: a role of the L-type voltage-gated Ca^{2+} channel. *Journal of Biological Chemistry* **281**, 9361-9372.

Hajnóczky, G., Csordás, G., Das, S., Garcia-Perez, C., Saotome, M., Roy, S. S. and Yi, M. (2006). Mitochondrial calcium signalling and cell death: approaches for assessing the role of mitochondrial Ca^{2+} uptake in apoptosis. *Cell Calcium* **40**, 553-560.

Hall, A. (1998). Rho GTPases and the actin cytoskeleton. *Science* **279**, 509-514.

Haller, T., Dietl, P., Deetjen, P. and Völkl, H. (1996). The lysosomal compartment as intracellular calcium store in MDCK cells: a possible involvement in InsP3-mediated Ca^{2+} release. *Cell Calcium* **19**, 157-165.

Han, K. S., Kang, H. J., Kim, E. Y., Yoon, W. J., Sohn, S., Kwon, H. J. and Gwag, B. J. (2001). 1, 2-bis (2-Aminophenoxy) ethane-N, N, N', N'-tetraacetic acid induces caspase-mediated apoptosis and reactive oxygen species-mediated necrosis in cultured cortical neurons. *Journal of neurochemistry* **78**, 230-239.

Hanahan, D. and Weinberg, R. A. (2011). Hallmarks of cancer: the next generation. *Cell* **144**, 646-674.

Hansen, L. L., Ikeda, Y., Olsen, G. S., Busch, A. K. and Mosthaf, L. (1999). Insulin Signaling Is Inhibited by Micromolar Concentrations of H_2O_2 EVIDENCE FOR A ROLE OF H_2O_2 IN TUMOR NECROSIS FACTOR α-MEDIATED INSULIN RESISTANCE. *Journal of Biological Chemistry* **274**, 25078-25084.

Hara, Y., Wakamori, M., Ishii, M., Maeno, E., Nishida, M., Yoshida, T., Yamada, H., Shimizu, S., Mori, E. and Kudoh, J. (2002). LTRPC2 Ca^{2+}-permeable channel activated by changes in redox status confers susceptibility to cell death. *Molecular cell* **9**, 163-173.

Hashimoto, Y., Tsuji, O., Niikura, T., Yamagishi, Y., Ishizaka, M., Kawasumi, M., Chiba, T., Kanekura, K., Yamada, M. and Tsukamoto, E. (2003). Involvement of c-Jun N-terminal kinase in amyloid precursor protein-mediated neuronal cell death. *Journal of neurochemistry* **84**, 864-877.

Hawkins, B. J., Irrinki, K. M., Mallilankaraman, K., Lien, Y.-C., Wang, Y., Bhanumathy, C. D., Subbiah, R., Ritchie, M. F., Soboloff, J. and Baba, Y. (2010). S-glutathionylation activates STIM1 and alters mitochondrial homeostasis. *The Journal of cell biology* **190**, 391-405.

Hecquet, C. M., Ahmmed, G. U., Vogel, S. M. and Malik, A. B. (2008). Role of TRPM2 channel in mediating H_2O_2-induced Ca^{2+} entry and endothelial hyperpermeability. *Circulation Research* **102**, 347-355.

Hecquet, C. M. and Malik, A. B. (2009). Role of H_2O_2-activated TRPM2 calcium channel in oxidant-induced endothelial injury. *Thrombosis and Haemostasis* **101**, 619-625.

Hemmings, B. A. and Restuccia, D. F. (2012). PI3K-PKB/Akt Pathway. *Cold Spring Harbor perspectives in biology* **4**, a011189.

Herreros, L., Rodríguez-Fernández, J. L., Brown, M. C., Alonso-Lebrero, J. L., Cabañas, C., Sánchez-Madrid, F., Longo, N., Turner, C. E. and Sánchez-Mateos, P. (2000). Paxillin localizes to the lymphocyte microtubule organizing center and associates with the microtubule cytoskeleton. *Journal of Biological Chemistry* **275**, 26436-26440.

Hill, K., Benham, C., McNulty, S. and Randall, A. (2004). Flufenamic acid is a pH-dependent antagonist of TRPM2 channels. *Neuropharmacology* **47**, 450-460.

Hiraga, R., Kato, M., Miyagawa, S. and Kamata, T. (2013). Nox4-derived ROS signaling contributes to TGF-β-induced epithelial-mesenchymal transition in pancreatic cancer cells. *Anticancer research* **33**, 4431-4438.

Hitchler, M. J., Oberley, L. W. and Domann, F. E. (2008). Epigenetic silencing of SOD2 by histone modifications in human breast cancer cells. *Free Radical Biology and Medicine* **45**, 1573-1580.

Hoffman, L. M., Jensen, C. C., Chaturvedi, A., Yoshigi, M. and Beckerle, M. C. (2012). Stretch-induced actin remodeling requires targeting of zyxin to stress fibers and recruitment of actin regulators. *Molecular Biology of the Cell* **23**, 1846-59.

Hölttä-Vuori, M., Vainio, S., Kauppi, M., Van Eck, M., Jokitalo, E. and Ikonen, E. (2012). Endosomal Actin Remodeling by Coronin-1A Controls Lipoprotein Uptake and Degradation in MacrophagesNovelty and Significance. *Circulation Research* **110**, 450-455.

Houstis, N., Rosen, E. D. and Lander, E. S. (2006). Reactive oxygen species have a causal role in multiple forms of insulin resistance. *Nature* **440**, 944-948.

Hu, T., RamachandraRao, S. P., Siva, S., Valancius, C., Zhu, Y., Mahadev, K., Toh, I., Goldstein, B. J., Woolkalis, M. and Sharma, K. (2005). Reactive oxygen species production via NADPH oxidase mediates TGF-β-induced cytoskeletal alterations in endothelial cells. *American Journal of Physiology-Renal Physiology* **289**, F816-F825.

Huang, C., Rajfur, Z., Borchers, C., Schaller, M. D. and Jacobson, K. (2003). JNK phosphorylates paxillin and regulates cell migration. *Nature* **424**, 219-223.

Huang, T. Y., DerMardirossian, C. and Bokoch, G. M. (2006). Cofilin phosphatases and regulation of actin dynamics. *Current opinion in cell biology* **18**, 26-31.

Huang, Y., Li, X., Wang, Y., Wang, H., Huang, C. and Li, J. (2014). Endoplasmic reticulum stress-induced hepatic stellate cell apoptosis through calcium-mediated JNK/P38 MAPK and Calpain/Caspase-12 pathways. *Molecular and cellular biochemistry* **394**, 1-12.

Huber, A. B., Kolodkin, A. L., Ginty, D. D. and Cloutier, J. F. (2003). Signaling at the growth cone: ligand-receptor complexes and the control of axon growth and guidance. *Annual review of neuroscience* **26**, 509-563.

Hudasek, K., Brown, S. T. and Fearon, I. M. (2004). H_2O_2 regulates recombinant Ca^{2+} channel α1C subunits but does not mediate their sensitivity to acute hypoxia. *Biochemical and Biophysical Research Communications* **318**, 135-141.

Huo, Y., Qiu, W.-Y., Pan, Q., Yao, Y.-F., Xing, K. and Lou, M. F. (2009). Reactive oxygen species (ROS) are essential mediators in epidermal growth factor (EGF)-stimulated corneal epithelial cell proliferation, adhesion, migration, and wound healing. *Experimental eye research* **89**, 876-886.

Hurd, T. R., DeGennaro, M. and Lehmann, R. (2012). Redox regulation of cell migration and adhesion. *Trends in cell biology* **22**, 107-115.

Hüttemann, M., Helling, S., Sanderson, T. H., Sinkler, C., Samavati, L., Mahapatra, G., Varughese, A., Lu, G., Liu, J. and Ramzan, R. (2012). Regulation of mitochondrial respiration and apoptosis through cell signaling: cytochrome c oxidase and cytochrome c in ischemia/reperfusion injury and inflammation. *Biochimica et Biophysica Acta (BBA)-Bioenergetics* **1817**, 598-609.

Hwang, N., Yim, S., Kim, Y., Jeong, J., Song, E., Lee, Y., Lee, J., Choi, S. and Lee, K. (2009). Oxidative modifications of glyceraldehyde-3-phosphate dehydrogenase play a key role in its multiple cellular functions. *Biochemical Journal* **423**, 253-264.

Iden, S. and Collard, J. G. (2008). Crosstalk between small GTPases and polarity proteins in cell polarization. *Nature Reviews Molecular Cell Biology* **9**, 846-859.

Inoguchi, T., Li, P., Umeda, F., Yu, H. Y., Kakimoto, M., Imamura, M., Aoki, T., Etoh, T., Hashimoto, T. and Naruse, M. (2000). High glucose level and free fatty acid stimulate reactive oxygen species production through protein kinase C--dependent activation of NADPH oxidase in cultured vascular cells. *Diabetes* **49**, 1939-1945.

Inoue, R., Jensen, L. J., Shi, J., Morita, H., Nishida, M., Honda, A. and Ito, Y. (2006). Transient receptor potential channels in cardiovascular function and disease. *Circulation Research* **99**, 119-131.

Ira, K., Jeffrey, K. L., Jessica, C., Shannon, L. K. and Kirill, K. (2013). Zinc-dependent lysosomal enlargement in TRPML1-deficient cells involves MTF-1 transcription factor and ZnT4 (Slc30a4) transporter. *Biochemical Journal* **451**, 155-163.

Ishihara, N., Jofuku, A., Eura, Y. and Mihara, K. (2003). Regulation of mitochondrial morphology by membrane potential, and DRP1-dependent division and FZO1-dependent fusion reaction in mammalian cells. *Biochemical and Biophysical Research Communications* **301**, 891-898.

Ishii, M., Oyama, A., Hagiwara, T., Miyazaki, A., Mori, Y., Kiuchi, Y. and Shimizu, S. (2007). Facilitation of H_2O_2-induced A172 human glioblastoma cell death by insertion of oxidative stress-sensitive TRPM2 channels. *Anticancer research* **27**, 3987-3992.

Jacinto, A., Wood, W., Balayo, T., Turmaine, M., Martinez-Arias, A. and Martin, P. (2000). Dynamic actin-based epithelial adhesion and cell matching during Drosophila dorsal closure. *Current Biology* **10**, 1420-1426.

Jang, Y., Lee, M. H., Lee, J., Jung, J., Lee, S. H., Yang, D.-J., Kim, B. W., Son, H., Lee, B. and Chang, S. (2014). TRPM2 mediates the lysophosphatidic acid-induced neurite retraction in the developing brain. *Pflügers Archiv-European Journal of Physiology* **466**, 1987-1998.

Jendrach, M., Mai, S., Pohl, S., Vöth, M. and Bereiter-Hahn, J. (2008). Short-and long-term alterations of mitochondrial morphology, dynamics and mtDNA after transient oxidative stress. *Mitochondrion* **8**, 293-304.

Jeong, J. C., Shin, W. Y., Kim, T. H., Kwon, C. H., Kim, J. H., Kim, Y. K. and Kim, K. H. (2011). Silibinin induces apoptosis via calpain-dependent AIF nuclear translocation in U87MG human glioma cell death. *Journal of Experimental & Clinical Cancer Research* **30**, 44.

Jeyaraju, D. V., Cisbani, G. and Pellegrini, L. (2009). Calcium regulation of mitochondria motility and morphology. *Biochimica et Biophysica Acta (BBA)-Bioenergetics* **1787**, 1363-1373.

Jheng, H.-F., Tsai, P.-J., Guo, S.-M., Kuo, L.-H., Chang, C.-S., Su, I.-J., Chang, C.-R. and Tsai, Y.-S. (2012). Mitochondrial fission contributes to mitochondrial dysfunction and insulin resistance in skeletal muscle. *Molecular and cellular biology* **32**, 309-319.

Jiang, D., Sullivan, P. G., Sensi, S. L., Steward, O. and Weiss, J. H. (2001). Zn^{2+} induces permeability transition pore opening and release of pro-apoptotic peptides from neuronal mitochondria. *Journal of Biological Chemistry* **276**, 47524-47529.

Jiang, L. (2007). Subunit interaction in channel assembly and functional regulation of transient receptor potential melastatin (TRPM) channels. *Biochemical Society Transactions* **35**, 86.

Jin, J., Li, Z., Liu, J., Wu, Y., Gao, X. and He, Y. (2015). Knockdown of zinc transporter ZIP5 (SLC39A5) expression significantly inhibits human esophageal cancer progression. *Oncology reports* **34**, 1431-1439.

Johnson, J. L., Monfregola, J., Napolitano, G., Kiosses, W. B. and Catz, S. D. (2012). Vesicular trafficking through cortical actin during exocytosis is regulated by the Rab27a effector JFC1/Slp1 and the RhoA-GTPase-activating protein Gem-interacting protein. *Molecular Biology of the Cell* **23**, 1902-16.

Jones, G. E. (2000). Cellular signaling in macrophage migration and chemotaxis. *Journal of leukocyte biology* **68**, 593-602.

Jontes, J. D., Buchanan, J. and Smith, S. J. (2000). Growth cone and dendrite dynamics in zebrafish embryos: early events in synaptogenesis imaged in vivo. *Nature neuroscience* **3**, 231-237.

Kaddour-Djebbar, I., Choudhary, V., Brooks, C., Ghazaly, T., Lakshmikanthan, V., Dong, Z. and Kumar, M. V. (2010). Specific mitochondrial calcium overload induces mitochondrial fission in prostate cancer cells. *International journal of oncology* **36**, 1437-1444.

Kagara, N., Tanaka, N., Noguchi, S. and Hirano, T. (2007). Zinc and its transporter ZIP10 are involved in invasive behavior of breast cancer cells. *Cancer science* **98**, 692-697.

Kahn, S. E., Hull, R. L. and Utzschneider, K. M. (2006). Mechanisms linking obesity to insulin resistance and type 2 diabetes. *Nature* **444**, 840-846.

Kalwat, M. A. and Thurmond, D. C. (2013). Signaling mechanisms of glucose-induced F-actin remodeling in pancreatic islet β cells. *Experimental & molecular medicine* **45**, e37.

Kamata, H., Manabe, T., Oka, S.-i., Kamata, K. and Hirata, H. (2002). Hydrogen peroxide activates IκB kinases through phosphorylation of serine residues in the activation loops. *FEBS letters* **519**, 231-237.

Kambe, T., Yamaguchi-Iwai, Y., Sasaki, R. and Nagao, M. (2004). Overview of mammalian zinc transporters. *Cellular and molecular life sciences* **61**, 49-68.

Kaneko, S., Kawakami, S., Hara, Y., Wakamori, M., Itoh, E., Minami, T., Takada, Y., Kume, T., Katsuki, H. and Mori, Y. (2006). A critical role of TRPM2 in neuronal cell death by hydrogen peroxide. *Journal of pharmacological sciences* **101**, 66-76.

Kaneto, H., Katakami, N., Matsuhisa, M. and Matsuoka, T.-a. (2010). Role of reactive oxygen species in the progression of type 2 diabetes and atherosclerosis. *Mediators of inflammation* **2010**, 453892.

Kanji, G. K. (2006). 100 statistical tests: Sage.

Kanta, J. (2011). The role of hydrogen peroxide and other reactive oxygen species in wound healing. *Acta Medica (Hradec Kralove)* **54**, 97-101.

Karbowski, M., Lee, Y.-J., Gaume, B., Jeong, S.-Y., Frank, S., Nechushtan, A., Santel, A., Fuller, M., Smith, C. L. and Youle, R. J. (2002). Spatial and temporal association of Bax with mitochondrial fission sites, Drp1, and Mfn2 during apoptosis. *The Journal of cell biology* **159**, 931-938.

Karbowski, M. and Youle, R. (2003). Dynamics of mitochondrial morphology in healthy cells and during apoptosis. *Cell Death & Differentiation* **10**, 870-880.

Kim, B.-E., Wang, F., Dufner-Beattie, J., Andrews, G. K., Eide, D. J. and Petris, M. J. (2004). Zn^{2+}-stimulated endocytosis of the mZIP4 zinc transporter regulates its location at the plasma membrane. *Journal of Biological Chemistry* **279**, 4523-4530.

Kim, E. Y., Koh, J. Y., Kim, Y. H., Sohn, S., Joe, E. and Gwag, B. J. (1999). Zn^{2+} entry produces oxidative neuronal necrosis in cortical cell cultures. *European Journal of Neuroscience* **11**, 327-334.

Kim, H. J., Soyombo, A. A., Tjon‑Kon‑Sang, S., So, I. and Muallem, S. (2009a). The Ca^{2+} channel TRPML3 regulates membrane trafficking and autophagy. *Traffick* **10**, 1157-1167.

Kim, J.-S., Huang, T. Y. and Bokoch, G. M. (2009b). Reactive oxygen species regulate a slingshot-cofilin activation pathway. *Molecular Biology of the Cell* **20**, 2650-2660.

Kim, Y. M. and Cho, M. (2014). Activation of NADPH oxidase subunit NCF4 induces ROS-mediated EMT signaling in HeLa cells. *Cellular signalling* **26**, 784-796.

Kimura, S., Zhang, G.-X., Nishiyama, A., Shokoji, T., Yao, L., Fan, Y.-Y., Rahman, M., Suzuki, T., Maeta, H. and Abe, Y. (2005). Role of NADPH oxidase-and mitochondria-derived reactive oxygen species in cardioprotection of ischemic reperfusion injury by angiotensin II. *Hypertension* **45**, 860-866.

Knott, A. B., Perkins, G., Schwarzenbacher, R. and Bossy-Wetzel, E. (2008). Mitochondrial fragmentation in neurodegeneration. *Nature reviews neuroscience* **9**, 505-518.

Kokoszka, J. E., Waymire, K. G., Levy, S. E., Sligh, J. E., Cai, J., Jones, D. P., MacGregor, G. R. and Wallace, D. C. (2004). The ADP/ATP translocator is not essential for the mitochondrial permeability transition pore. *Nature* **427**, 461-465.

Korge, P. and Weiss, J. N. (1999). Thapsigargin directly induces the mitochondrial permeability transition. *European Journal of Biochemistry* **265**, 273-280.

Korobova, F., Ramabhadran, V. and Higgs, H. N. (2013). An actin-dependent step in mitochondrial fission mediated by the ER-associated formin INF2. *Science* **339**, 464-467.

Korshunov, S. S., Skulachev, V. P. and Starkov, A. A. (1997). High protonic potential actuates a mechanism of production of reactive oxygen species in mitochondria. *FEBS letters* **416**, 15-18.

Korsmeyer, S., Wei, M., Saito, M., Weiler, S., Oh, K. and Schlesinger, P. (2000). Pro-apoptotic cascade activates BID, which oligomerizes BAK or BAX into pores that result in the release of cytochrome c. *Cell death and differentiation* **7**, 1166-1173.

Koshkin, V., Dai, F. F., Robson-Doucette, C. A., Chan, C. B. and Wheeler, M. B. (2008). Limited mitochondrial permeabilization is an early manifestation of palmitate-induced lipotoxicity in pancreatic β-cells. *Journal of Biological Chemistry* **283**, 7936-7948.

Kraft, R., Grimm, C., Frenzel, H. and Harteneck, C. (2006). Inhibition of TRPM2 cation channels by N-(p-amylcinnamoyl) anthranilic acid. *British Journal of Pharmacology* **148**, 264-273.

Kraft, R., Grimm, C., Grosse, K., Hoffmann, A., Sauerbruch, S., Kettenmann, H., Schultz, G. and Harteneck, C. (2004). Hydrogen peroxide and ADP-ribose induce TRPM2-mediated calcium influx and cation currents in microglia. *American Journal of Physiology-Cell Physiology* **286**, C129-C137.

Kroemer, G. and Reed, J. C. (2000). Mitochondrial control of cell death. *Nature medicine* **6**. 513-519.

Krugmann, S., Jordens, I., Gevaert, K., Driessens, M., Vandekerckhove, J. and Hall, A. (2001). Cdc42 induces filopodia by promoting the formation of an IRSp53: Mena complex. *Current Biology* **11**, 1645-1655.

Kruman, I. I. and Mattson, M. P. (1999). Pivotal role of mitochondrial calcium uptake in neural cell apoptosis and necrosis. *Journal of neurochemistry* **72**, 529-540.

Kühn, F. J. and Lückhoff, A. (2004). Sites of the NUDT9-H domain critical for ADP-ribose activation of the cation channel TRPM2. *Journal of Biological Chemistry* **279**, 46431-46437.

Kukic, I., Kelleher, S. L. and Kiselyov, K. (2014). Zn^{2+} efflux through lysosomal exocytosis prevents Zn^{2+}-induced toxicity. *Journal of Cell Science* **127**, 3094-3103.

Kumar, B., Koul, S., Khandrika, L., Meacham, R. B. and Koul, H. K. (2008). Oxidative stress is inherent in prostate cancer cells and is required for aggressive phenotype. *Cancer research* **68**, 1777-1785.

Kundu, N., Zhang, S. and Fulton, A. M. (1995). Sublethal oxidative stress inhibits tumor cell adhesion and enhances experimental metastasis of murine mammary carcinoma. *Clinical & experimental metastasis* **13**, 16-22.

Kuras, Z., Yun, Y.-H., Chimote, A. A., Neumeier, L. and Conforti, L. (2012). KCa3. 1 and TRPM7 channels at the uropod regulate migration of activated human T cells. *PLoS One* **7**, e43859.

Kuwana, T., Smith, J. J., Muzio, M., Dixit, V., Newmeyer, D. D. and Kornbluth, S. (1998). Apoptosis induction by caspase-8 is amplified through the mitochondrial release of cytochrome c. *Journal of Biological Chemistry* **273**, 16589-16594.

Lacinova, L. (2005). Voltage-dependent calcium channels. *General physiology and biophysics* **24**. Suppl 1: 1-78.

Lakhani, S. A., Masud, A., Kuida, K., Porter, G. A., Booth, C. J., Mehal, W. Z., Inayat, I. and Flavell, R. A. (2006). Caspases 3 and 7: key mediators of mitochondrial events of apoptosis. *Science* **311**, 847-851.

Lamalice, L., Le Boeuf, F. and Huot, J. (2007). Endothelial cell migration during angiogenesis. *Circulation Research* **100**, 782-794.

Lambert, A. and Brand, M. (2004). Superoxide production by NADH: ubiquinone oxidoreductase (complex I) depends on the pH gradient across the mitochondrial inner membrane. *Biochemical Journal* **382**, 511-517.

Lambeth, J. D. (2004). NOX enzymes and the biology of reactive oxygen. *Nature Reviews Immunology* **4**, 181-189.

Lamorte, L., Rodrigues, S., Sangwan, V., Turner, C. E. and Park, M. (2003). Crk associates with a multimolecular Paxillin/GIT2/β-PIX complex and promotes Rac-dependent relocalization of Paxillin to focal contacts. *Molecular Biology of the Cell* **14**, 2818-2831.

Landes, T., Emorine, L. J., Courilleau, D., Rojo, M., Belenguer, P. and Arnauné‐Pelloquin, L. (2010). The BH3-only Bnip3 binds to the dynamin Opa1 to promote mitochondrial fragmentation and apoptosis by distinct mechanisms. *EMBO reports* **11**, 459-465.

Lange, I., Yamamoto, S., Partida-Sanchez, S., Mori, Y., Fleig, A. and Penner, R. (2009). TRPM2 Functions as a Lysosomal Ca^{2+}-Release Channel in beta Cells. *Science signaling* **2**, ra23.

Lassegue, B. and Clempus, R. E. (2003). Vascular NADPH oxidases: specific features, expression, and regulation. *American Journal of Physiology-Regulatory, Integrative and Comparative Physiology* **285**, R277-R297.

Launay, P., Fleig, A., Perraud, A.-L., Scharenberg, A. M., Penner, R. and Kinet, J.-P. (2002). TRPM4 is a Ca^{2+}-activated nonselective cation channel mediating cell membrane depolarization. *Cell* **109**, 397-407.

Lee, J.-Y., Kapur, M., Li, M., Choi, M.-C., Choi, S., Kim, H.-J., Kim, I., Lee, E., Taylor, J. P. and Yao, T.-P. (2014). MFN1 deacetylation activates adaptive mitochondrial fusion and protects metabolically challenged mitochondria. *Journal of Cell Science* **127**, 4954-4963.

Lee, K. and Esselman, W. J. (2002). Inhibition of PTPs by H_2O_2 regulates the activation of distinct MAPK pathways. *Free Radical Biology and Medicine* **33**, 1121-1132.

Lee, S.-R., Yang, K.-S., Kwon, J., Lee, C., Jeong, W. and Rhee, S. G. (2002). Reversible inactivation of the tumor suppressor PTEN by H_2O_2. *Journal of Biological Chemistry* **277**, 20336-20342.

Lee, S. B., Bae, I. H., Bae, Y. S. and Um, H.-D. (2006). Link between mitochondria and NADPH oxidase 1 isozyme for the sustained production of reactive oxygen species and cell death. *Journal of Biological Chemistry* **281**, 36228-36235.

Legros, F., Lombes, A., Frachon, P. and Rojo, M. (2002). Mitochondrial fusion in human cells is efficient, requires the inner membrane potential, and is mediated by mitofusins. *Molecular Biology of the Cell* **13**, 4343-4354.

Lemasters, J. and Nieminen, A. (1997). Mitochondrial oxygen radical formation during reductive and oxidative stress to intact hepatocytes. *Bioscience reports* **17**, 281-291.

Lemasters, J. J., Nieminen, A.-L., Qian, T., Trost, L. C., Elmore, S. P., Nishimura, Y., Crowe, R. A., Cascio, W. E., Bradham, C. A. and Brenner, D. A. (1998). The mitochondrial permeability transition in cell death: a common mechanism in necrosis, apoptosis and autophagy. *Biochimica et Biophysica Acta (BBA)-Bioenergetics* **1366**, 177-196.

Lenzen, S., Drinkgern, J. and Tiedge, M. (1996). Low antioxidant enzyme gene expression in pancreatic islets compared with various other mouse tissues. *Free Radical Biology and Medicine* **20**, 463-466.

Leslie, N. R., Bennett, D., Lindsay, Y. E., Stewart, H., Gray, A. and Downes, C. P. (2003). Redox regulation of PI3-kinase signalling via inactivation of PTEN. *EMBO Journal* **22**, 5501-5510.

Lewis, A., Du, J., Liu, J., Ritchie, J. M., Oberley, L. W. and Cullen, J. J. (2005). Metastatic progression of pancreatic cancer: changes in antioxidant enzymes and cell growth. *Clinical & experimental metastasis* **22**, 523-532.

Lewis, A. K. and Bridgman, P. C. (1992). Nerve growth cone lamellipodia contain two populations of actin filaments that differ in organization and polarity. *The Journal of cell biology* **119**, 1219-1243.

Li, H., Zhu, H., Xu, C.-j. and Yuan, J. (1998). Cleavage of BID by caspase 8 mediates the mitochondrial damage in the Fas pathway of apoptosis. *Cell* **94**, 491-501.

Li, M., Lai, P., Chou, Y., Chi, A., Mi, Y., Khoo, K., Chang, G., Wu, C., Meng, T. and Chen, G. (2014). Protein tyrosine phosphatase PTPN3 inhibits lung cancer cell proliferation and migration by promoting EGFR endocytic degradation. *Oncogene* **34**, 3791-3803.

Li, N., Frigerio, F. and Maechler, P. (2008). The sensitivity of pancreatic beta-cells to mitochondrial injuries triggered by lipotoxicity and oxidative stress. *Biochemical Society Transactions* **36**, 930-934.

Li, N., Li, B., Brun, T., Deffert-Delbouille, C., Mahiout, Z., Daali, Y., Ma, X.-J., Krause, K.-H. and Maechler, P. (2012). NADPH oxidase NOX2 defines a new antagonistic role for reactive oxygen species and cAMP/PKA in the regulation of insulin secretion. *Diabetes* **61**, 2842-2850.

Li, S., Tanaka, H., Wang, H. H., Yoshiyama, S., Kumagai, H., Nakamura, A., Brown, D. L., Thatcher, S. E., Wright, G. L. and Kohama, K. (2006). Intracellular signal transduction for migration and actin remodeling in vascular smooth muscle cells after sphingosylphosphorylcholine stimulation. *American Journal of Physiology-Heart and Circulatory Physiology* **291**, H1262-H1272.

Li, Y. V. (2014). Zinc and insulin in pancreatic beta-cells. *Endocrine* **45**, 178-189.

Liao, M., Cao, E., Julius, D. and Cheng, Y. (2013). Structure of the TRPV1 ion channel determined by electron cryo-microscopy. *Nature* **504**, 107-112.

Lin, M. T. and Beal, M. F. (2006). Mitochondrial dysfunction and oxidative stress in neurodegenerative diseases. *Nature* **443**, 787-795.

Liot, G., Bossy, B., Lubitz, S., Kushnareva, Y., Sejbuk, N. and Bossy-Wetzel, E. (2009). Complex II inhibition by 3-NP causes mitochondrial fragmentation and neuronal cell death via an NMDA-and ROS-dependent pathway. *Cell Death & Differentiation* **16**, 899-909.

Liou, G.-Y. and Storz, P. (2010). Reactive oxygen species in cancer. *Free Radical Research* **44**, 479-496.

Lohmann, C., Finski, A. and Bonhoeffer, T. (2005). Local calcium transients regulate the spontaneous motility of dendritic filopodia. *Nature neuroscience* **8**, 305-312.

López-Lázaro, M. (2007). Dual role of hydrogen peroxide in cancer: possible relevance to cancer chemoprevention and therapy. *Cancer letters* **252**, 1-8.

López-Sanjurjo, C. I., Tovey, S. C., Prole, D. L. and Taylor, C. W. (2013). Lysosomes shape Ins (1, 4, 5) P3-evoked Ca^{2+} signals by selectively sequestering Ca^{2+} released from the endoplasmic reticulum. *Journal of Cell Science* **126**, 289-300.

Lou, W., Ni, Z., Dyer, K., Tweardy, D. J. and Gao, A. C. (2000). Interleukin-6 induces prostate cancer cell growth accompanied by activation of Stat3 signaling pathway. *The prostate* **42**, 239-242.

Lovell, M. A., Xiong, S., Xie, C., Davies, P. and Markesbery, W. R. (2004). Induction of hyperphosphorylated tau in primary rat cortical neuron cultures mediated by oxidative stress and glycogen synthase kinase-3. *Journal of Alzheimer's disease* **6**, 659-71; discussion 673-81.

Luster, A. D., Alon, R. and von Andrian, U. H. (2005). Immune cell migration in inflammation: present and future therapeutic targets. *Nature Immunology* **6**, 1182-1190.

Ly, J. D., Grubb, D. and Lawen, A. (2003). The mitochondrial membrane potential (Δψm) in apoptosis; an update. *Apoptosis* **8**, 115-128.

Lytton, J., Westlin, M. and Hanley, M. R. (1991). Thapsigargin inhibits the sarcoplasmic or endoplasmic reticulum Ca-ATPase family of calcium pumps. *Journal of Biological Chemistry* **266**, 17067-17071.

Machesky, L. M. (2008). Lamellipodia and filopodia in metastasis and invasion. *FEBS letters* **582**, 2102-2111.

Maechler, P. and Wollheim, C. B. (2001). Mitochondrial function in normal and diabetic β-cells. *Nature* **414**, 807-812.

Maestre, I., Jordán, J., Calvo, S., Reig, J. A., Ceña, V., Soria, B., Prentki, M. and Roche, E. (2003). Mitochondrial dysfunction is involved in apoptosis induced by serum withdrawal and fatty acids in the β-cell line INS-1. *Endocrinology* **144**, 335-345.

Magdalena, J., Millard, T. H. and Machesky, L. M. (2003). Microtubule involvement in NIH 3T3 Golgi and MTOC polarity establishment. *Journal of Cell Science* **116**, 743-756.

Mahdi, M. H. B., Andrieu, V. and Pasquier, C. (2000). Focal adhesion kinase regulation by oxidative stress in different cell types. *IUBMB Life* **50**, 291-299.

Malaiyandi, L. M., Honick, A. S., Rintoul, G. L., Wang, Q. J. and Reynolds, I. J. (2005). Zn^{2+} inhibits mitochondrial movement in neurons by phosphatidylinositol 3-kinase activation. *The Journal of neuroscience* **25**, 9507-9514.

Mandemakers, W., Morais, V. A. and De Strooper, B. (2007). A cell biological perspective on mitochondrial dysfunction in Parkinson disease and other neurodegenerative diseases. *Journal of Cell Science* **120**, 1707-1716.

Mandic, A., Viktorsson, K., Strandberg, L., Heiden, T., Hansson, J., Linder, S. and Shoshan, M. C. (2002). Calpain-mediated Bid cleavage and calpain-independent Bak modulation: two separate pathways in cisplatin-induced apoptosis. *Molecular and cellular biology* **22**, 3003-3013.

Manna, Paul T., Munsey, Tim S., Abuarab, N., Li, F., Asipu, A., Howell, G., Sedo, A., Yang, W., Naylor, J., Beech, David J. et al. (2015). TRPM2-mediated intracellular Zn^{2+} release triggers pancreatic β-cell death. *Biochemical Journal* **466**, 537-546.

Marble, A. (1934). Diabetes and cancer. *New England Journal of Medicine* **211**, 339-349.

Marín, J., Encabo, A., Briones, A., García-Cohen, E.-C. and Alonso, M. J. (1998). Mechanisms involved in the cellular calcium homeostasis in vascular smooth muscle: calcium pumps. *Life sciences* **64**, 279-303.

Martin, B., Warram, J., Krolewski, A., Soeldner, J., Kahn, C. and Bergman, R. (1992). Role of glucose and insulin resistance in development of type 2 diabetes mellitus: results of a 25-year follow-up study. *The Lancet* **340**, 925-929.

Martinez, J. A., Zhang, Z., Svetlov, S. I., Hayes, R. L., Wang, K. K. and Larner, S. F. (2010). Calpain and caspase processing of caspase-12 contribute to the ER stress-induced cell death pathway in differentiated PC12 cells. *Apoptosis* **15**, 1480-1493.

Mattila, P. K. and Lappalainen, P. (2008). Filopodia: molecular architecture and cellular functions. *Nature Reviews Molecular Cell Biology* **9**, 446-454.

May, J. M. and Contoreggi, C. (1982). The mechanism of the insulin-like effects of ionic zinc. *Journal of Biological Chemistry* **257**, 4362-4368.

McCormick, N. H. and Kelleher, S. L. (2012). ZnT4 provides zinc to zinc-dependent proteins in the trans-Golgi network critical for cell function and Zn export in mammary epithelial cells. *American Journal of Physiology-Cell Physiology* **303**, C291-C297.

McGuinness, L., Bardo, S. J. and Emptage, N. J. (2007). The lysosome or lysosome-related organelle may serve as a Ca^{2+} store in the boutons of hippocampal pyramidal cells. *Neuropharmacology* **52**, 126-135.

McIlwain, D. R., Berger, T. and Mak, T. W. (2013). Caspase functions in cell death and disease. *Cold Spring Harbor perspectives in biology* **5**, a008656.

Medvedeva, Y. V., Lin, B., Shuttleworth, C. W. and Weiss, J. H. (2009). Intracellular Zn^{2+} accumulation contributes to synaptic failure, mitochondrial depolarization, and cell death in an acute slice oxygen–glucose deprivation model of ischemia. *The Journal of neuroscience* **29**, 1105-1114.

Mehlen, P. and Puisieux, A. (2006). Metastasis: a question of life or death. *Nature Reviews Cancer* **6**, 449-458.

Mehta, S., Aye-Han, N.-N., Ganesan, A., Oldach, L., Gorshkov, K. and Zhang, J. (2014). Calmodulin-controlled spatial decoding of oscillatory Ca^{2+} signals by calcineurin. *eLife* **3**, e03765.

Mei, Z.-Z., Xia, R., Beech, D. J. and Jiang, L.-H. (2006). Intracellular coiled-coil domain engaged in subunit interaction and assembly of melastatin-related transient receptor potential channel 2. *Journal of Biological Chemistry* **281**, 38748-38756.

Meng, X., Cai, C., Wu, J., Cai, S., Ye, C., Chen, H., Yang, Z., Zeng, H., Shen, Q. and Zou, F. (2013). TRPM7 mediates breast cancer cell migration and invasion through the MAPK pathway. *Cancer letters* **333**, 96-102.

Middelbeek, J., Kuipers, A. J., Henneman, L., Visser, D., Eidhof, I., van Horssen, R., Wieringa, B., Canisius, S. V., Zwart, W. and Wessels, L. F. (2012). TRPM7 is required for breast tumor cell metastasis. *Cancer research* **72**, 4250-4261.

Miller, B. (2006). The role of TRP channels in oxidative stress-induced cell death. *The Journal of membrane biology* **209**, 31-41.

Mills, J. W., Zhou, J.-H., Cardoza, L. and Ferm, V. H. (1992). Zinc alters actin filaments in Madin-Darby canine kidney cells. *Toxicology and applied pharmacology* **116**, 92-100.

Minamikawa, T., Williams, D. A., Bowser, D. N. and Nagley, P. (1999). Mitochondrial permeability transition and swelling can occur reversibly without inducing cell death in intact human cells. *Experimental Cell Research* **246**, 26-37.

Minton, K. (2014). Cell migration: Coordinating calcium signalling. *Nature Reviews Molecular Cell Biology* **15**, 152-152.

Mishra, P. and Chan, D. C. (2014). Mitochondrial dynamics and inheritance during cell division, development and disease. *Nature Reviews Molecular Cell Biology* **15**, 634-646.

Mitra, S. K., Hanson, D. A. and Schlaepfer, D. D. (2005). Focal adhesion kinase: in command and control of cell motility. *Nature Reviews Molecular Cell Biology* **6**, 56-68.

Mize, C. E. and Langdon, R. G. (1962). Hepatic glutathione reductase I. Purification and general kinetic properties. *Journal of Biological Chemistry* **237**, 1589-1595.

Moldovan, L., Moldovan, N. I., Sohn, R. H., Parikh, S. A. and Goldschmidt-Clermont, P. J. (2000). Redox changes of cultured endothelial cells and actin dynamics. *Circulation Research* **86**, 549-557.

Molina, A. J., Wikstrom, J. D., Stiles, L., Las, G., Mohamed, H., Elorza, A., Walzer, G., Twig, G., Katz, S. and Corkey, B. E. (2009). Mitochondrial networking protects β-cells from nutrient-induced apoptosis. *Diabetes* **58**, 2303-2315.

Monet, M., Gkika, D., Lehen'kyi, V. y., Pourtier, A., Abeele, F. V., Bidaux, G., Juvin, V., Rassendren, F., Humez, S. and Prevarsakaya, N. (2009). Lysophospholipids stimulate prostate cancer cell migration via TRPV2 channel activation. *Biochimica et Biophysica Acta (BBA)-Molecular Cell Research* **1793**, 528-539.

Monet, M., Lehen'kyi, V. y., Gackiere, F., Firlej, V., Vandenberghe, M., Roudbaraki, M., Gkika, D., Pourtier, A., Bidaux, G. and Slomianny, C. (2010). Role of cationic channel TRPV2 in promoting prostate cancer migration and progression to androgen resistance. *Cancer research* **70**, 1225-1235.

Montell, C. and Rubin, G. M. (1989). Molecular characterization of the Drosophila trp locus: a putative integral membrane protein required for phototransduction. *Neuron* **2**, 1313-1323.

Morgan, D., Oliveira-Emilio, H., Keane, D., Hirata, A., da Rocha, M. S., Bordin, S., Curi, R., Newsholme, P. and Carpinelli, A. (2007). Glucose, palmitate and pro-inflammatory cytokines modulate production and activity of a phagocyte-like NADPH oxidase in rat pancreatic islets and a clonal beta cell line. *Diabetologia* **50**, 359-369.

Morgan, M. J. and Liu, Z.-g. (2011). Crosstalk of reactive oxygen species and NF-κB signaling. *Cell research* **21**, 103-115.

Mrkonjić, S., Garcia-Elias, A., Pardo-Pastor, C., Bazellières, E., Trepat, X., Vriens, J., Ghosh, D., Voets, T., Vicente, R. and Valverde, M. A. (2015). TRPV4 participates in the establishment of trailing adhesions and directional persistence of migrating cells. *Pflügers Archiv-European Journal of Physiology* **467** (10), 2107-2119.

Multhaup, G., Ruppert, T., Schlicksupp, A., Hesse, L., Beher, D., Masters, C. L. and Beyreuther, K. (1997). Reactive oxygen species and Alzheimer's disease. *Biochemical pharmacology* **54**, 533-539.

Murakami, M. and Hirano, T. (2008). Intracellular zinc homeostasis and zinc signaling. *Cancer science* **99**, 1515-1522.

Murphy, M. (2009). How mitochondria produce reactive oxygen species. *Biochemical Journal* **417**, 1-13.

Nabeshima, K., Inoue, T., Shimao, Y. and Sameshima, T. (2002). Matrix metalloproteinases in tumor invasion: role for cell migration. *Pathology international* **52**, 255-264.

Nabi, I. R. (1999). The polarization of the motile cell. *Journal of Cell Science* **112**, 1803-1811.

Nagano, M., Hoshino, D., Koshikawa, N., Akizawa, T. and Seiki, M. (2012). Turnover of focal adhesions and cancer cell migration. *International Journal of Cell Biology* **2012**, 310616, 10 pages.

Naito, Y., Yamada, T., Ui-Tei, K., Morishita, S. and Saigo, K. (2004). siDirect: highly effective, target-specific siRNA design software for mammalian RNA interference. *Nucleic acids research* **32**, W124-W129.

Nakagawa, T., Zhu, H., Morishima, N., Li, E., Xu, J., Yankner, B. A. and Yuan, J. (2000). Caspase-12 mediates endoplasmic-reticulum-specific apoptosis and cytotoxicity by amyloid-β. *Nature* **403**, 98-103.

NakagawaT, Y. (2000). Cross-talk between two cysteine protease families. Activation of caspase-12 by calpain in apoptosis. *The Journal of cell biology* **150** (4), 887-894.

Nakamura, S., Takamura, T., Matsuzawa-Nagata, N., Takayama, H., Misu, H., Noda, H., Nabemoto, S., Kurita, S., Ota, T. and Ando, H. (2009). Palmitate induces insulin resistance in H4IIEC3 hepatocytes through reactive oxygen species produced by mitochondria. *Journal of Biological Chemistry* **284**, 14809-14818.

Nakanishi, A., Wada, Y., Kitagishi, Y. and Matsuda, S. (2014). Link between PI3K/AKT/PTEN pathway and NOX proteinin diseases. *Aging and disease* **5**, 203.

Nazıroğlu, M. (2011). TRPM2 cation channels, oxidative stress and neurological diseases: where are we now? *Neurochemical research* **36**, 355-366.

Nazıroğlu, M., Çiğ, B. and Özgül, C. (2014). Modulation of oxidative stress and Ca^{2+} mobilization through TRPM2 channels in rat dorsal root ganglion neuron by Hypericum perforatum. *Neuroscience* **263**, 27-35.

Nechushtan, A., Smith, C. L., Lamensdorf, I., Yoon, S.-H. and Youle, R. J. (2001). Bax and Bak coalesce into novel mitochondria-associated clusters during apoptosis. *The Journal of cell biology* **153**, 1265-1276.

Newsholme, P., Haber, E., Hirabara, S., Rebelato, E., Procopio, J., Morgan, D., Oliveira‐Emilio, H., Carpinelli, A. and Curi, R. (2007). Diabetes associated cell stress and dysfunction: role of mitochondrial and non-mitochondrial ROS production and activity. *The Journal of Physiology* **583**, 9-24.

Newsholme, P., Morgan, D., Rebelato, E., Oliveira-Emilio, H., Procopio, J., Curi, R. and Carpinelli, A. (2009). Insights into the critical role of NADPH oxidases in the normal and dysregulated pancreatic beta cell. *Diabetologia* **52**, 2489-2498.

Niedergang, F. and Chavrier, P. (2004). Signaling and membrane dynamics during phagocytosis: many roads lead to the phagosome. *Current opinion in cell biology* **16**, 422-428.

Nilius, B. (2006). Transient receptor potential (TRP) cation channels: rewarding unique proteins. *Bulletin et memoires de l'Academie royale de medecine de Belgique* **162**, 244-253.

Nilius, B. and Szallasi, A. (2014). Transient receptor potential channels as drug targets: from the science of basic research to the art of medicine. *Pharmacological reviews* **66**, 676-814.

Nishikawa, M. (2008). Reactive oxygen species in tumor metastasis. *Cancer letters* **266**, 53-59.

Niswender, K. D., Morrison, C. D., Clegg, D. J., Olson, R., Baskin, D. G., Myers, M. G., Seeley, R. J. and Schwartz, M. W. (2003). Insulin activation of phosphatidylinositol 3-kinase in the hypothalamic arcuate nucleus a key mediator of insulin-induced anorexia. *Diabetes* **52**, 227-231.

Nobes, C. D. and Hall, A. (1995). Rho, rac, and cdc42 GTPases regulate the assembly of multimolecular focal complexes associated with actin stress fibers, lamellipodia, and filopodia. *Cell* **81**, 53-62.

Noh, K.-M. and Koh, J.-Y. (2000). Induction and activation by zinc of NADPH oxidase in cultured cortical neurons and astrocytes. *The Journal of neuroscience: the official journal of the Society for Neuroscience* **20**, RC111-RC111.

Nomura, D. K., Long, J. Z., Niessen, S., Hoover, H. S., Ng, S.-W. and Cravatt, B. F. (2010). Monoacylglycerol lipase regulates a fatty acid network that promotes cancer pathogenesis. *Cell* **140**, 49-61.

Normanno, N., De Luca, A., Bianco, C., Strizzi, L., Mancino, M., Maiello, M. R., Carotenuto, A., De Feo, G., Caponigro, F. and Salomon, D. S. (2006). Epidermal growth factor receptor (EGFR) signaling in cancer. *Gene* **366**, 2-16.

Obata, N. H., Tamakoshi, K., Shibata, K., Kikkawa, F. and Tomoda, Y. (1996). Effects of interleukin-6 on in vitro cell attachment, migration and invasion of human ovarian carcinoma. *Anticancer research* **17**, 337-342.

Oertner, T. G. and Matus, A. (2005). Calcium regulation of actin dynamics in dendritic spines. *Cell Calcium* **37**, 477-482.

Olichon, A., Baricault, L., Gas, N., Guillou, E., Valette, A., Belenguer, P. and Lenaers, G. (2003). Loss of OPA1 perturbates the mitochondrial inner membrane structure and integrity, leading to cytochrome c release and apoptosis. *Journal of Biological Chemistry* **278**, 7743-7746.

Onyango, I. G. (2008). Mitochondrial dysfunction and oxidative stress in Parkinson's disease. *Neurochemical research* **33**, 589-597.

Orrenius, S. (2007). Reactive oxygen species in mitochondria-mediated cell death. *Drug metabolism reviews* **39**, 443-455.

Orrenius, S., Zhivotovsky, B. and Nicotera, P. (2003). Regulation of cell death: the calcium–apoptosis link. *Nature Reviews Molecular Cell Biology* **4**, 552-565.

Osmani, N., Peglion, F., Chavrier, P. and Etienne-Manneville, S. (2010). Cdc42 localization and cell polarity depend on membrane traffic. *The Journal of cell biology* **191**, 1261-1269.

Östman, A., Frijhoff, J., Sandin, Å. and Böhmer, F.-D. (2011). Regulation of protein tyrosine phosphatases by reversible oxidation. *Journal of biochemistry* **150**, 345-356.

Palmer, C. S., Osellame, L. D., Laine, D., Koutsopoulos, O. S., Frazier, A. E. and Ryan, M. T. (2011). MiD49 and MiD51, new components of the mitochondrial fission machinery. *EMBO reports* **12**, 565-573.

Paltauf-Doburzynska, J., Malli, R. and Graier, W. F. (2004). Hyperglycemic conditions affect shape and Ca^{2+} homeostasis of mitochondria in endothelial cells. *Journal of cardiovascular pharmacology* **44**, 423-436.

Pardo, J., Pérez-Galán, P., Gamen, S., Marzo, I., Monleón, I., Kaspar, A. A., Susín, S. A., Kroemer, G., Krensky, A. M. and Naval, J. (2001). A role of the mitochondrial apoptosis-inducing factor in granulysin-induced apoptosis. *The Journal of Immunology* **167**, 1222-1229.

Park, C. Y., Hoover, P. J., Mullins, F. M., Bachhawat, P., Covington, E. D., Raunser, S., Walz, T., Garcia, K. C., Dolmetsch, R. E. and Lewis, R. S. (2009a). STIM1 clusters and activates CRAC channels via direct binding of a cytosolic domain to Orai1. *Cell* **136**, 876-890.

Park, J.-S., Koentjoro, B., Veivers, D., Mackay-Sim, A. and Sue, C. M. (2014). Parkinson's disease-associated human ATP13A2 (PARK9) deficiency causes zinc dyshomeostasis and mitochondrial dysfunction. *Human molecular genetics* **23**, 2802-2815.

Park, S.-A., Na, H.-K., Kim, E.-H., Cha, Y.-N. and Surh, Y.-J. (2009b). 4-Hydroxyestradiol induces anchorage-independent growth of human mammary epithelial cells via activation of IκB kinase: Potential role of reactive oxygen species. *Cancer research* **69**, 2416-2424.

Patel, S. and Santani, D. (2009). Role of NF-κB in the pathogenesis of diabetes and its associated complications. *Pharmacological Reports* **61**, 595-603.

Paulsen, C. E., Armache, J.-P., Gao, Y., Cheng, Y. and Julius, D. (2015). Structure of the TRPA1 ion channel suggests regulatory mechanisms. *Nature* **520**, 511-517.

Payne, S. L., Fogelgren, B., Hess, A. R., Seftor, E. A., Wiley, E. L., Fong, S. F., Csiszar, K., Hendrix, M. J. and Kirschmann, D. A. (2005). Lysyl oxidase regulates breast cancer cell migration and adhesion through a hydrogen peroxide–mediated mechanism. *Cancer research* **65**, 11429-11436.

Peier, A. M., Moqrich, A., Hergarden, A. C., Reeve, A. J., Andersson, D. A., Story, G. M., Earley, T. J., Dragoni, I., McIntyre, P. and Bevan, S. (2002). A TRP channel that senses cold stimuli and menthol. *Cell* **108**, 705-715.

Pellegrin, S. and Mellor, H. (2005). The Rho family GTPase Rif induces filopodia through mDia2. *Current Biology* **15**, 129-133.

Peng, L., Men, X., Zhang, W., Wang, H., Xu, S., Fang, Q., Liu, H., Yang, W. and Lou, J. (2012). Involvement of dynamin-related protein 1 in free fatty acid-induced INS-1-derived cell apoptosis. *PloS One* **7**, e49258.

Pennanen, C., Parra, V., López-Crisosto, C., Morales, P. E., del Campo, A., Gutierrez, T., Rivera-Mejías, P., Kuzmicic, J., Chiong, M. and Zorzano, A. (2014). Mitochondrial fission is required for cardiomyocyte hypertrophy mediated by a Ca^{2+}-calcineurin signaling pathway. *Journal of Cell Science* **127**, 2659-2671.

Perraud, A.-L., Fleig, A., Dunn, C. A., Bagley, L. A., Launay, P., Schmitz, C., Stokes, A. J., Zhu, Q., Bessman, M. J. and Penner, R. (2001). ADP-ribose gating of the calcium-permeable LTRPC2 channel revealed by Nudix motif homology. *Nature* **411**, 595-599.

Perraud, A.-L., Schmitz, C. and Scharenberg, A. M. (2003a). TRPM2 Ca^{2+} permeable cation channels: from gene to biological function. *Cell Calcium* **33**, 519-531.

Perraud, A.-L., Shen, B., Dunn, C. A., Rippe, K., Smith, M. K., Bessman, M. J., Stoddard, B. L. and Scharenberg, A. M. (2003b). NUDT9, a member of the Nudix hydrolase family, is an evolutionarily conserved mitochondrial ADP-ribose pyrophosphatase. *Journal of Biological Chemistry* **278**, 1794-1801.

Petronilli, V., Penzo, D., Scorrano, L., Bernardi, P. and Di Lisa, F. (2001). The mitochondrial permeability transition, release of cytochrome c and cell death correlation with the duration of pore openings in situ. *Journal of Biological Chemistry* **276**, 12030-12034.

Pickup, J. C., Chusney, G. D., Thomas, S. M. and Burt, D. (2000). Plasma interleukin-6, tumour necrosis factor α and blood cytokine production in type 2 diabetes. *Life sciences* **67**, 291-300.

Piconi, L., Quagliaro, L., Assaloni, R., Da Ros, R., Maier, A., Zuodar, G. and Ceriello, A. (2006). Constant and intermittent high glucose enhances endothelial cell apoptosis through mitochondrial superoxide overproduction. *Diabetes/metabolism research and reviews* **22**, 198-203.

Pinton, P., Giorgi, C., Siviero, R., Zecchini, E. and Rizzuto, R. (2008). Calcium and apoptosis: ER-mitochondria Ca^{2+}; transfer in the control of apoptosis. *Oncogene* **27**, 6407-6418.

Piro, S., Anello, M., Di Pietro, C., Lizzio, M. N., Patan, G., Rabuazzo, A. M., Vigneri, R., Purrello, M. and Purrello, F. (2002). Chronic exposure to free fatty acids or high glucose induces apoptosis in rat pancreatic islets: possible role of oxidative stress. *Metabolism* **51**, 1340-1347.

Pitts, K., Yoon, Y., Krueger, E. and McNiven, M. (1999). The dynamin-like protein DLP1 is essential for normal distribution and morphology of the endoplasmic reticulum and mitochondria in mammalian cells. *Molecular Biology of the Cell* **10**, 4403-4417.

Pla, A. F. and Gkika, D. (2013). Emerging role of TRP channels in cell migration: from tumor vascularization to metastasis. *Frontiers in physiology* **4**. 311.

Pla, A. F., Ong, H., Cheng, K., Brossa, A., Bussolati, B., Lockwich, T., Paria, B., Munaron, L. and Ambudkar, I. (2011). TRPV4 mediates tumor-derived endothelial cell migration via arachidonic acid-activated actin remodeling. *Oncogene* **31**, 200-212.

Pletjushkina, O. Y., Lyamzaev, K., Popova, E., Nepryakhina, O., Ivanova, O. Y., Domnina, L., Chernyak, B. and Skulachev, V. (2006). Effect of oxidative stress on dynamics of mitochondrial reticulum. *Biochimica et Biophysica Acta (BBA)-Bioenergetics* **1757**, 518-524.

Pollard, T. D. and Borisy, G. G. (2003). Cellular motility driven by assembly and disassembly of actin filaments. *Cell* **112**, 453-465.

Prakriya, M., Feske, S., Gwack, Y., Srikanth, S., Rao, A. and Hogan, P. G. (2006). Orai1 is an essential pore subunit of the CRAC channel. *Nature* **443**, 230-233.

Prevarskaya, N., Skryma, R. and Shuba, Y. (2011). Calcium in tumour metastasis: new roles for known actors. *Nature Reviews Cancer* **11**, 609-618.

Préville, X., Gaestel, M. and Arrigo, A.-P. (1998). Phosphorylation is not essential for protection of L929 cells by Hsp25 against H_2O_2-mediated disruption actin cytoskeleton, a protection which appears related to the redox change mediated by Hsp25. *Cell stress & chaperones* **3**, 177.

Price, J. T., Tiganis, T., Agarwal, A., Djakiew, D. and Thompson, E. W. (1999). Epidermal growth factor promotes MDA-MB-231 breast cancer cell migration through a phosphatidylinositol 3'-kinase and phospholipase C-dependent mechanism. *Cancer research* **59**, 5475-5478.

Price, K. L. and Lummis, S. C. (2005). FlexStation examination of 5-HT3 receptor function using Ca^{2+}-and membrane potential-sensitive dyes: advantages and potential problems. *Journal of neuroscience methods* **149**, 172-177.

Price, L. S., Leng, J., Schwartz, M. A. and Bokoch, G. M. (1998). Activation of Rac and Cdc42 by integrins mediates cell spreading. *Molecular Biology of the Cell* **9**, 1863-1871.

Provenzano, P. P. and Keely, P. J. (2011). Mechanical signaling through the cytoskeleton regulates cell proliferation by coordinated focal adhesion and Rho GTPase signaling. *Journal of Cell Science* **124**, 1195-1205.

Pu, J. and Zhao, M. (2005). Golgi polarization in a strong electric field. *Journal of Cell Science* **118**, 1117-1128.

Qian, Y., Corum, L., Meng, Q., Blenis, J., Zheng, J. Z., Shi, X., Flynn, D. C. and Jiang, B.-H. (2004). PI3K induced actin filament remodeling through Akt and p70S6K1: implication of essential role in cell migration. *American Journal of Physiology-Cell Physiology* **286**, C153-C163.

Raftopoulou, M. and Hall, A. (2004). Cell migration: Rho GTPases lead the way. *Developmental Biology* **265**, 23-32.

Rahman, K. W., Aranha, O., Glazyrin, A., Chinni, S. R. and Sarkar, F. H. (2000). Translocation of Bax to mitochondria induces apoptotic cell death in indole-3-carbinol (I3C) treated breast cancer cells. *Oncogene* **19**, 5764-5771.

Rao, J. N., Li, L., Golovina, V. A., Platoshyn, O., Strauch, E. D., Yuan, J. X.-J. and Wang, J.-Y. (2001). Ca^{2+}-RhoA signaling pathway required for polyamine-dependent intestinal epithelial cell migration. *American Journal of Physiology-Cell Physiology* **280**, C993-C1007.

Rao, J. Y. and Li, N. (2004). Microfilament actin remodeling as a potential target for cancer drug development. *Current cancer drug targets* **4**, 345-354.

Rapizzi, E., Pinton, P., Szabadkai, G., Wieckowski, M. R., Vandecasteele, G., Baird, G., Tuft, R. A., Fogarty, K. E. and Rizzuto, R. (2002). Recombinant expression of the voltage-dependent anion channel enhances the transfer of Ca^{2+} microdomains to mitochondria. *The Journal of cell biology* **159**, 613-624.

Rathore, R., Zheng, Y.-M., Niu, C.-F., Liu, Q.-H., Korde, A., Ho, Y.-S. and Wang, Y.-X. (2008). Hypoxia activates NADPH oxidase to increase $[ROS]_i$ and $[Ca^{2+}]_i$ through the mitochondrial ROS-PKCε signaling axis in pulmonary artery smooth muscle cells. *Free Radical Biology and Medicine* **45**, 1223-1231.

Ray, P. D., Huang, B.-W. and Tsuji, Y. (2012). Reactive oxygen species (ROS) homeostasis and redox regulation in cellular signaling. *Cellular signalling* **24**, 981-990.

Redd, M. J., Cooper, L., Wood, W., Stramer, B. and Martin, P. (2004). Wound healing and inflammation: embryos reveal the way to perfect repair. *Philosophical Transactions of the Royal Society of London. Series B, Biological Sciences* **359**, 777-784.

Reddy, K. B. and Glaros, S. (2007). Inhibition of the MAP kinase activity suppresses estrogen-induced breast tumor growth both in vitro and in vivo. *International journal of oncology* **30**, 971-975.

Rehder, V. and Kater, S. (1992). Regulation of neuronal growth cone filopodia by intracellular calcium. *The Journal of neuroscience* **12**, 3175-3186.

Ren, L., Hong, S., Cassavaugh, J., Osborne, T., Chou, A., Kim, S., Gorlick, R., Hewitt, S. and Khanna, C. (2009). The actin-cytoskeleton linker protein ezrin is regulated during osteosarcoma metastasis by PKC. *Oncogene* **28**, 792-802.

Rey, F., Cifuentes, M., Kiarash, A., Quinn, M. and Pagano, P. (2001). Novel competitive inhibitor of NADPH oxidase assembly attenuates vascular O_2- and systolic blood pressure in mice. *Circulation Research* **89**, 408-414.

Reymond, N., d'Água, B. B. and Ridley, A. J. (2013). Crossing the endothelial barrier during metastasis. *Nature Reviews Cancer* **13**, 858-870.

Ridley, A. J. (2001). Rho GTPases and cell migration. *Journal of Cell Science* **114**, 2713-2722.

Ridley, A. J. (2006). Rho GTPases and actin dynamics in membrane protrusions and vesicle trafficking. *Trends in cell biology* **16**, 522-529.

Ridley, A. J. and Hall, A. (1992). The small GTP-binding protein rho regulates the assembly of focal adhesions and actin stress fibers in response to growth factors. *Cell* **70**, 389-399.

Ridley, A. J., Schwartz, M. A., Burridge, K., Firtel, R. A., Ginsberg, M. H., Borisy, G., Parsons, J. T. and Horwitz, A. R. (2003). Cell migration: integrating signals from front to back. *Science* **302**, 1704-1709.

Riggs, B., Rothwell, W., Mische, S., Hickson, G. R., Matheson, J., Hays, T. S., Gould, G. W. and Sullivan, W. (2003). Actin cytoskeleton remodeling during early Drosophila furrow formation requires recycling endosomal components Nuclear-fallout and Rab11. *The Journal of cell biology* **163**, 143-154.

Rintoul, G. L., Filiano, A. J., Brocard, J. B., Kress, G. J. and Reynolds, I. J. (2003). Glutamate decreases mitochondrial size and movement in primary forebrain neurons. *The Journal of neuroscience* **23**, 7881-7888.

Rizzuto, R., Marchi, S., Bonora, M., Aguiari, P., Bononi, A., De Stefani, D., Giorgi, C., Leo, S., Rimessi, A. and Siviero, R. (2009). Ca^{2+} transfer from the ER to mitochondria: when, how and why. *Biochimica et Biophysica Acta (BBA)-Bioenergetics* **1787**, 1342-1351.

Robertson, R. P. (2004). Chronic oxidative stress as a central mechanism for glucose toxicity in pancreatic islet beta cells in diabetes. *Journal of Biological Chemistry* **279**, 42351-42354.

Robertson, R. P., Harmon, J., Tran, P. O. T. and Poitout, V. (2004). β-cell glucose toxicity, lipotoxicity, and chronic oxidative stress in type 2 diabetes. *Diabetes* **53**, S119-S124.

Robinson, K. A., Stewart, C. A., Pye, Q. N., Nguyen, X., Kenney, L., Salzman, S., Floyd, R. A. and Hensley, K. (1999). Redox-sensitive protein phosphatase activity regulates the phosphorylation state of p38 protein kinase in primary astrocyte culture. *Journal of neuroscience research* **55**, 724-732.

Rohatgi, R., Ma, L., Miki, H., Lopez, M., Kirchhausen, T., Takenawa, T. and Kirschner, M. W. (1999). The interaction between N-WASP and the Arp2/3 complex links Cdc42-dependent signals to actin assembly. *Cell* **97**, 221-231.

Romagnoli, A., Aguiari, P., De Stefani, D., Leo, S., Marchi, S., Rimessi, A., Zecchini, E., Pinton, P. and Rizzuto, R. (2007). Endoplasmic reticulum/mitochondria calcium cross-talk. In *Novartis Foundation symposium*, vol. 287, pp. 122: Chichester; New York; John Wiley; 1999.

Roos, G. and Messens, J. (2011). Protein sulfenic acid formation: from cellular damage to redox regulation. *Free Radical Biology and Medicine* **51**, 314-326.

Rousseau, S., Houle, F. and Huot, J. (2000). Integrating the VEGF signals leading to actin-based motility in vascular endothelial cells. *Trends in cardiovascular medicine* **10**, 321-327.

Saeki, M., Irie, Y., Ni, L., Itsuki, Y., Terao, Y., Kawabata, S. and Kamisaki, Y. (2007). Calcineurin potentiates the activation of procaspase-3 by accelerating its proteolytic maturation. *Journal of Biological Chemistry* **282**, 11786-11794.

Salmeen, A. and Barford, D. (2005). Functions and mechanisms of redox regulation of cysteine-based phosphatases. *Antioxidants & redox signaling* **7**, 560-577.

Saltiel, A. R. and Kahn, C. R. (2001). Insulin signalling and the regulation of glucose and lipid metabolism. *Nature* **414**, 799-806.

Salvesen, G. S. and Riedl, S. J. (2008). Caspase mechanisms. *Advances in Experimental Medicine and Biology* **615**, 13-23.

Samie, M., Wang, X., Zhang, X., Goschka, A., Li, X., Cheng, X., Gregg, E., Azar, M., Zhuo, Y. and Garrity, A. G. (2013). A TRP channel in the lysosome regulates large particle phagocytosis via focal exocytosis. *Developmental Cell* **26**, 511-524.

Sander, E. E., Jean, P., Van Delft, S., Van Der Kammen, R. A. and Collard, J. G. (1999). Rac Downregulates Rho Activity Reciprocal Balance between Both Gtpases Determines Cellular Morphology and Migratory Behavior. *The Journal of cell biology* **147**, 1009-1022.

Sano, M., Ernesto, C., Thomas, R. G., Klauber, M. R., Schafer, K., Grundman, M., Woodbury, P., Growdon, J., Cotman, C. W. and Pfeiffer, E. (1997). A controlled trial of selegiline, alpha-tocopherol, or both as treatment for Alzheimer's disease. *New England Journal of Medicine* **336**, 1216-1222.

Sano, Y., Inamura, K., Miyake, A., Mochizuki, S., Yokoi, H., Matsushime, H. and Furuichi, K. (2001). Immunocyte Ca^{2+} influx system mediated by LTRPC2. *Science* **293**, 1327-1330.

Santin, I., Moore, F., Colli, M. L., Gurzov, E. N., Marselli, L., Marchetti, P. and Eizirik, D. L. (2011). PTPN2, a candidate gene for type 1 diabetes, modulates pancreatic β-cell apoptosis via regulation of the BH3-only protein Bim. *Diabetes* **60**, 3279-3288.

Sastry, S. K., Lyons, P. D., Schaller, M. D. and Burridge, K. (2002). PTP-PEST controls motility through regulation of Rac1. *Journal of Cell Science* **115**, 4305-4316.

Sastry, S. K., Rajfur, Z., Liu, B. P., Cote, J.-F., Tremblay, M. L. and Burridge, K. (2006). PTP-PEST couples membrane protrusion and tail retraction via VAV2 and p190RhoGAP. *Journal of Biological Chemistry* **281**, 11627-11636.

Sato, Y., Fujimoto, S., Mukai, E., Sato, H., Tahara, Y., Ogura, K., Yamano, G., Ogura, M., Nagashima, K. and Inagaki, N. (2014). Palmitate induces reactive oxygen species production and β-cell dysfunction by activating nicotinamide adenine dinucleotide phosphate oxidase through Src signaling. *Journal of diabetes investigation* **5**, 19-26.

Schafer, C., Rymarczyk, G., Ding, L., Kirber, M. T. and Bolotina, V. M. (2012). Role of molecular determinants of store-operated Ca^{2+} entry (Orai1, phospholipase A2 group 6 and STIM1) in focal adhesion formation and cell migration. *Journal of Biological Chemistry* **287**. 40745-40757.

Schaller, M. D. and Parsons, J. T. (1995). pp125FAK-dependent tyrosine phosphorylation of paxillin creates a high-affinity binding site for Crk. *Molecular and cellular biology* **15**, 2635-2645.

Schmidt, H., Gelhaus, C., Lucius, R., Nebendahl, M., Leippe, M. and Janssen, O. (2009). Enrichment and analysis of secretory lysosomes from lymphocyte populations. *BMC immunology* **10**, 41.

Schneeberger, M., Dietrich, M. O., Sebastián, D., Imbernón, M., Castaño, C., Garcia, A., Esteban, Y., Gonzalez-Franquesa, A., Rodríguez, I. C. and Bortolozzi, A. (2013). Mitofusin 2 in POMC neurons connects ER stress with leptin resistance and energy imbalance. *Cell* **155**, 172-187.

Schumacher, M. A. (2010). Transient receptor potential channels in pain and inflammation: therapeutic opportunities. *Pain Practice* **10**, 185-200.

Segal, A. W. and JONES, O. T. (1978). Novel cytochrome *b* system in phagocytic vacuoles of human granulocytes. *Nature* **276**, 515-517.

Sensi, S. L., Paoletti, P., Bush, A. I. and Sekler, I. (2009). Zinc in the physiology and pathology of the CNS. *Nature reviews neuroscience* **10**, 780-791.

Sensi, S. L., Ton-That, D., Sullivan, P. G., Jonas, E. A., Gee, K. R., Kaczmarek, L. K. and Weiss, J. H. (2003). Modulation of mitochondrial function by endogenous Zn^{2+} pools. *Proceedings of the National Academy of Sciences* **100**, 6157-6162.

Sensi, S. L., Yin, H. Z. and Weiss, J. H. (2000). AMPA/kainate receptor-triggered Zn^{2+} entry into cortical neurons induces mitochondrial Zn^{2+} uptake and persistent mitochondrial dysfunction. *European Journal of Neuroscience* **12**, 3813-3818.

Seo, S. R., Chong, S. A., Lee, S. I., Sung, J. Y., Ahn, Y. S., Chung, K. C. and Seo, J. T. (2001). Zn^{2+}-induced ERK activation mediated by reactive oxygen species causes cell death in differentiated PC12 cells. *Journal of neurochemistry* **78**, 600-610.

Settembre, C., Fraldi, A., Medina, D. L. and Ballabio, A. (2013). Signals from the lysosome: a control centre for cellular clearance and energy metabolism. *Nature Reviews Molecular Cell Biology* **14**, 283-296.

Shah, B. H., Neithardt, A., Chu, D. B., Shah, F. B. and Catt, K. J. (2006). Role of EGF receptor transactivation in phosphoinositide 3-kinase-dependent activation of MAP kinase by GPCRs. *Journal of Cell Physiology* **206**, 47-57.

Sharpley, M. S. and Hirst, J. (2006). The inhibition of mitochondrial complex I (NADH: ubiquinone oxidoreductase) by Zn^{2+}. *Journal of Biological Chemistry* **281**, 34803-34809.

Sheetz, M. P., Felsenfeld, D., Galbraith, C. and Choquet, D. (1998). Cell migration as a five-step cycle. In *Biochemical Society symposium*, vol. 65, pp. 233-243.

Shimabukuro, M., Zhou, Y.-T., Levi, M. and Unger, R. H. (1998). Fatty acid-induced β cell apoptosis: a link between obesity and diabetes. *Proceedings of the National Academy of Sciences* **95**, 2498-2502.

Shin, H.-W., Shinotsuka, C., Torii, S., Murakami, K. and Nakayama, K. (1997). Identification and subcellular localization of a novel mammalian dynamin-related protein homologous to yeast Vps1p and Dnm1p. *Journal of biochemistry* **122**, 525-530.

Simon, F., Leiva-Salcedo, E., Armisén, R., Riveros, A., Cerda, O., Varela, D., Eguiguren, A. L., Olivero, P. and Stutzin, A. (2010). Hydrogen peroxide removes TRPM4 current desensitization conferring increased vulnerability to necrotic cell death. *Journal of Biological Chemistry* **285**, 37150-37158.

Sivitz, W. I. and Yorek, M. A. (2010). Mitochondrial dysfunction in diabetes: from molecular mechanisms to functional significance and therapeutic opportunities. *Antioxidants & redox signaling* **12**, 537-577.

Smirnova, E., Griparic, L., Shurland, D.-L. and Van Der Bliek, A. M. (2001). Dynamin-related protein Drp1 is required for mitochondrial division in mammalian cells. *Molecular Biology of the Cell* **12**, 2245-2256.

Smyth, J. T., Hwang, S. Y., Tomita, T., DeHaven, W. I., Mercer, J. C. and Putney, J. W. (2010). Activation and regulation of store-operated calcium entry. *Journal of cellular and molecular medicine* **14**, 2337-2349.

Souza, C. M., Davidson, D., Rhee, I., Gratton, J.-P., Davis, E. C. and Veillette, A. (2012). The phosphatase PTP-PEST/PTPN12 regulates endothelial cell migration and adhesion, but not permeability, and controls vascular development and embryonic viability. *Journal of Biological Chemistry* **287**, 43180-43190.

Stambolic, V., Suzuki, A., De La Pompa, J. L., Brothers, G. M., Mirtsos, C., Sasaki, T., Ruland, J., Penninger, J. M., Siderovski, D. P. and Mak, T. W. (1998). Negative regulation of PKB/Akt-dependent cell survival by the tumor suppressor PTEN. *Cell* **95**, 29-39.

Starkov, A. A., Chinopoulos, C. and Fiskum, G. (2004). Mitochondrial calcium and oxidative stress as mediators of ischemic brain injury. *Cell Calcium* **36**, 257-264.

Sugioka, R., Shimizu, S. and Tsujimoto, Y. (2004). Fzo1, a protein involved in mitochondrial fusion, inhibits apoptosis. *Journal of Biological Chemistry* **279**, 52726-52734.

Sumoza-Toledo, A., Lange, I., Cortado, H., Bhagat, H., Mori, Y., Fleig, A., Penner, R. and Partida-Sánchez, S. (2011). Dendritic cell maturation and chemotaxis is regulated by TRPM2-mediated lysosomal Ca^{2+} release. *FASEB Journal* **25**, 3529-3542.

Sumoza‑Toledo, A. and Penner, R. (2011). TRPM2: a multifunctional ion channel for calcium signalling. *The Journal of Physiology* **589**, 1515-1525.

Sun, L., Yau, H.-Y., Wong, W.-Y., Li, R. A., Huang, Y. and Yao, X. (2012). Role of TRPM2 in H_2O_2-induced cell apoptosis in endothelial cells. *PLoS One* **7**, e43186-e43186.

Susin, S. A., Lorenzo, H. K., Zamzami, N., Marzo, I., Snow, B. E., Brothers, G. M., Mangion, J., Jacotot, E., Costantini, P. and Loeffler, M. (1999). Molecular characterization of mitochondrial apoptosis-inducing factor. *Nature* **397**, 441-446.

Susztak, K., Raff, A. C., Schiffer, M. and Böttinger, E. P. (2006). Glucose-induced reactive oxygen species cause apoptosis of podocytes and podocyte depletion at the onset of diabetic nephropathy. *Diabetes* **55**, 225-233.

Suzaki, Y., Yoshizumi, M., Kagami, S., Koyama, A. H., Taketani, Y., Houchi, H., Tsuchiya, K., Takeda, E. and Tamaki, T. (2002). Hydrogen peroxide stimulates c-src-mediated big mitogen-activated protein kinase 1 (BMK1) and the MEF2C signaling pathway in PC12 cells potential role in cell survival following oxidative insults. *Journal of Biological Chemistry* **277**, 9614-9621.

Svitkina, T. M., Bulanova, E. A., Chaga, O. Y., Vignjevic, D. M., Kojima, S.-i., Vasiliev, J. M. and Borisy, G. G. (2003). Mechanism of filopodia initiation by reorganization of a dendritic network. *The Journal of cell biology* **160**, 409-421.

Syed, I., Kyathanahalli, C. N., Jayaram, B., Govind, S., Rhodes, C. J., Kowluru, R. A. and Kowluru, A. (2011). Increased Phagocyte-Like NADPH Oxidase and ROS Generation in Type 2 Diabetic ZDF Rat and Human Islets Role of Rac1–JNK1/2 Signaling Pathway in Mitochondrial Dysregulation in the Diabetic Islet. *Diabetes* **60**, 2843-2852.

Symons, M. and Rusk, N. (2003). Control of vesicular trafficking by Rho GTPases. *Current Biology* **13**, R409-R418.

Szalai, G., Krishnamurthy, R. and Hajnόczky, G. (1999). Apoptosis driven by IP3-linked mitochondrial calcium signals. *EMBO Journal* **18**, 6349-6361.

Takatani-Nakase, T., Matsui, C., Maeda, S., Kawahara, S. and Takahashi, K. (2014). High glucose level promotes migration behavior of breast cancer cells through zinc and its transporters. *PLoS One* **9**. E90136.

Tamagno, E., Parola, M., Bardini, P., Piccini, A., Borghi, R., Guglielmotto, M., Santoro, G., Davit, A., Danni, O. and Smith, M. (2005). β-Site APP cleaving enzyme up-regulation induced by 4-hydroxynonenal is mediated by stress-activated protein kinases pathways. *Journal of neurochemistry* **92**, 628-636.

Tamariz, E. and Grinnell, F. (2002). Modulation of fibroblast morphology and adhesion during collagen matrix remodeling. *Molecular Biology of the Cell* **13**, 3915-3929.

Taulet, N., Delorme-Walker, V. D. and DerMardirossian, C. (2012). Reactive oxygen species regulate protrusion efficiency by controlling actin dynamics. *PLoS One* **7**, e41342-e41342.

Taylor, D. A., Bowman, B. and Stull, J. (1989). Cytoplasmic Ca^{2+} is a primary determinant for myosin phosphorylation in smooth muscle cells. *Journal of Biological Chemistry* **264**, 6207-6213.

Taylor, K. M., Vichova, P., Jordan, N., Hiscox, S., Hendley, R. and Nicholson, R. I. (2008). ZIP7-mediated intracellular zinc transport contributes to aberrant growth factor signaling in antihormone-resistant breast cancer Cells. *Endocrinology* **149**, 4912-4920.

Thebault, S., Lemonnier, L., Bidaux, G., Flourakis, M., Bavencoffe, A., Gordienko, D., Roudbaraki, M., Delcourt, P., Panchin, Y. and Shuba, Y. (2005). Novel role of cold/menthol-sensitive transient receptor potential melastatine family member 8 (TRPM8) in the activation of store-operated channels in LNCaP human prostate cancer epithelial cells. *Journal of Biological Chemistry* **280**, 39423-39435.

Thiery, J. P. (2002). Epithelial–mesenchymal transitions in tumour progression. *Nature Reviews Cancer* **2**, 442-454.

Tian, D., Jacobo, S. M. P., Billing, D., Rozkalne, A., Gage, S. D., Anagnostou, T., Pavenstadt, H., Hsu, H. H., Schlondorff, J. and Ramos, A. (2010). Antagonistic regulation of actin dynamics and cell motility by TRPC5 and TRPC6 channels. *Science Signalling* **3**, ra77.

Tiedge, M., Lortz, S., Drinkgern, J. and Lenzen, S. (1997). Relation between antioxidant enzyme gene expression and antioxidative defense status of insulin-producing cells. *Diabetes* **46**, 1733-1742.

Tieu, K., Ischiropoulos, H. and Przedborski, S. (2003). Nitric oxide and reactive oxygen species in Parkinson's disease. *IUBMB Life* **55**, 329-335.

Tintinger, G. R., Theron, A. J., Potjo, M. and Anderson, R. (2007). Reactive oxidants regulate membrane repolarization and store-operated uptake of calcium by formyl peptide-activated human neutrophils. *Free Radical Biology and Medicine* **42**, 1851-1857.

Todorovic, S. M. and Jevtovic-Todorovic, V. (2014). Redox regulation of neuronal voltage-gated calcium channels. *Antioxidants & redox signaling* **21**, 880-891.

Togashi, K., Inada, H. and Tominaga, M. (2008). Inhibition of the transient receptor potential cation channel TRPM2 by 2-aminoethoxydiphenyl borate (2-APB). *British Journal of Pharmacology* **153**, 1324-1330.

Tondera, D., Czauderna, F., Paulick, K., Schwarzer, R., Kaufmann, J. and Santel, A. (2005). The mitochondrial protein MTP18 contributes to mitochondrial fission in mammalian cells. *Journal of Cell Science* **118**, 3049-3059.

Tondera, D., Santel, A., Schwarzer, R., Dames, S., Giese, K., Klippel, A. and Kaufmann, J. (2004). Knockdown of MTP18, a novel phosphatidylinositol 3-kinase-dependent protein, affects mitochondrial morphology and induces apoptosis. *Journal of Biological Chemistry* **279**, 31544-31555.

Tong, Q., Zhang, W., Conrad, K., Mostoller, K., Cheung, J. Y., Peterson, B. Z. and Miller, B. A. (2006). Regulation of the transient receptor potential channel TRPM2 by the Ca^{2+} sensor calmodulin. *Journal of Biological Chemistry* **281**, 9076-9085.

Tsai, F.-C., Kuo, G.-H., Chang, S.-W. and Tsai, P.-J. (2015). Ca^{2+} Signaling in Cytoskeletal Reorganization, Cell Migration, and Cancer Metastasis. *BioMed research international* **2015**, 409245.

Tsai, F.-C. and Meyer, T. (2012). Ca^{2+} Pulses Control Local Cycles of Lamellipodia Retraction and Adhesion along the Front of Migrating Cells. *Current Biology* **22**, 837-842.

Tsai, F.-C., Seki, A., Yang, H. W., Hayer, A., Carrasco, S., Malmersjö, S. and Meyer, T. (2014). A polarized Ca^{2+}, diacylglycerol and STIM1 signalling system regulates directed cell migration. *Nature Cell Biology* **16**, 133-144.

Tsushima, K., Bugger, H., Wende, A. R., Schaffer, J. E. and Abel, E. D. (2012). Lipid Overload in Cardiomyocytes Impairs Mitochondrial Energetics by Altering Mitochondrial Dynamics. *Circulation* **126**, A14154.

Tsutsumi, S., Gupta, S. K., Hogan, V., Collard, J. G. and Raz, A. (2002). Activation of small GTPase Rho is required for autocrine motility factor signaling. *Cancer research* **62**, 4484-4490.

Turner, H., Fleig, A., Stokes, A., Kinet, J. and Penner, R. (2003). Discrimination of intracellular calcium store subcompartments using TRPV1 (transient receptor potential channel, vanilloid subfamily member 1) release channel activity. *Biochemical Journal* **371**, 341-350.

Twig, G., Elorza, A., Molina, A. J., Mohamed, H., Wikstrom, J. D., Walzer, G., Stiles, L., Haigh, S. E., Katz, S. and Las, G. (2008). Fission and selective fusion govern mitochondrial segregation and elimination by autophagy. *EMBO Journal* **27**, 433-446.

Uchida, K., Dezaki, K., Damdindorj, B., Inada, H., Shiuchi, T., Mori, Y., Yada, T., Minokoshi, Y. and Tominaga, M. (2011). Lack of TRPM2 impaired insulin secretion and glucose metabolisms in mice. *Diabetes* **60**, 119-126.

Uchida, K. and Tominaga, M. (2011). The role of thermosensitive TRP (transient receptor potential) channels in insulin secretion. *Endocrine journal* **58**, 1021-1028.

Uchida, K. and Tominaga, M. (2014). The role of TRPM2 in pancreatic β-cells and the development of diabetes. *Cell Calcium* **56**, 332-339.

Uetrecht, A. C. and Bear, J. E. (2009). Golgi polarity does not correlate with speed or persistence of freely migrating fibroblasts. *European Journal of Cell Biology* **88**, 711-717.

Ushio-Fukai, M. and Alexander, R. W. (2004). Reactive oxygen species as mediators of angiogenesis signaling. Role of NADPH oxidase. *Molecular and cellular biochemistry* **264**, 85-97.

Ushio-Fukai, M. and Nakamura, Y. (2008). Reactive oxygen species and angiogenesis: NADPH oxidase as target for cancer therapy. *Cancer letters* **266**, 37-52.

Uttara, B., Singh, A. V., Zamboni, P. and Mahajan, R. (2009). Oxidative stress and neurodegenerative diseases: a review of upstream and downstream antioxidant therapeutic options. *Current neuropharmacology* **7**, 65.

van Cruijsen, H., Giaccone, G. and Hoekman, K. (2005). Epidermal growth factor receptor and angiogenesis: opportunities for combined anticancer strategies. *International journal of cancer* **117**, 883-888.

Vander Heiden, M. G., Cantley, L. C. and Thompson, C. B. (2009). Understanding the Warburg effect: the metabolic requirements of cell proliferation. *Science* **324**, 1029-1033.

Vander Heiden, M. G., Chandel, N. S., Williamson, E. K., Schumacker, P. T. and Thompson, C. B. (1997). Bcl-x L regulates the membrane potential and volume homeostasis of mitochondria. *Cell* **91**, 627-637.

Venkatachalam, K. and Montell, C. (2007). TRP channels. *Annual review of biochemistry* **76**, 387.

Vignjevic, D., Schoumacher, M., Gavert, N., Janssen, K.-P., Jih, G., Laé, M., Louvard, D., Ben-Ze'ev, A. and Robine, S. (2007). Fascin, a novel target of β-catenin-TCF signaling, is expressed at the invasive front of human colon cancer. *Cancer research* **67**, 6844-6853.

Vonna, L., Wiedemann, A., Aepfelbacher, M. and Sackmann, E. (2007). Micromechanics of filopodia mediated capture of pathogens by macrophages. *European Biophysics Journal* **36**, 145-151.

Wada, T. and Penninger, J. M. (2004). Mitogen-activated protein kinases in apoptosis regulation. *Oncogene* **23**, 2838-2849.

Walker, S., Galbreath, T., Chen, Q., Barsotti, R. J., Patel, H., Chau, W. and Young, L. H. (2014). Gp91ds-tat, a Selective NADPH Oxidase Peptide Inhibitor, Increases Blood Nitric Oxide (NO) Bioavailability in Bind Limb Ischemia and Reperfusion (I/R).

Wang, C. and Youle, R. J. (2009). The role of mitochondria in apoptosis. *Annual review of genetics* **43**, 95-118.

Wang, Q. and Doerschuk, C. M. (2001). The p38 mitogen-activated protein kinase mediates cytoskeletal remodeling in pulmonary microvascular endothelial cells upon intracellular adhesion molecule-1 ligation. *The Journal of Immunology* **166**, 6877-6884.

Wang, Q., Symes, A. J., Kane, C. A., Freeman, A., Nariculam, J., Munson, P., Thrasivoulou, C., Masters, J. R. and Ahmed, A. (2010). A novel role for Wnt/Ca^{2+} signaling in actin cytoskeleton remodeling and cell motility in prostate cancer. *PLoS One* **5**, e10456.

Wang, S.-J., Saadi, W., Lin, F., Nguyen, C. M.-C. and Jeon, N. L. (2004). Differential effects of EGF gradient profiles on MDA-MB-231 breast cancer cell chemotaxis. *Experimental Cell Research* **300**, 180-189.

Wang, S., Chu, C.-H., Stewart, T., Ginghina, C., Wang, Y., Nie, H., Guo, M., Wilson, B., Hong, J.-S. and Zhang, J. (2015). α-Synuclein, a chemoattractant, directs microglial migration via H_2O_2-dependent Lyn phosphorylation. *Proceedings of the National Academy of Sciences* **112**, E1926-E1935.

Wang, Y., Shibasaki, F. and Mizuno, K. (2005). Calcium signal-induced cofilin dephosphorylation is mediated by Slingshot via calcineurin. *Journal of Biological Chemistry* **280**, 12683-12689.

Waning, J., Vriens, J., Owsianik, G., Stüwe, L., Mally, S., Fabian, A., Frippiat, C., Nilius, B. and Schwab, A. (2007). A novel function of capsaicin-sensitive TRPV1 channels: involvement in cell migration. *Cell Calcium* **42**, 17-25.

Webb, D. J., Parsons, J. T. and Horwitz, A. F. (2002). Adhesion assembly, disassembly and turnover in migrating cells–over and over and over again. *Nature Cell Biology* **4**, E97-E100.

Webster, K. A. (2012). Mitochondrial membrane permeabilization and cell death during myocardial infarction: roles of calcium and reactive oxygen species. *Future cardiology* **8**, 863-884.

Wehrhahn, J., Kraft, R., Harteneck, C. and Hauschildt, S. (2010). Transient receptor potential melastatin 2 is required for lipopolysaccharide-induced cytokine production in human monocytes. *The Journal of Immunology* **184**, 2386-2393.

Wei, C., Wang, X., Chen, M., Ouyang, K., Song, L.-S. and Cheng, H. (2009). Calcium flickers steer cell migration. *Nature* **457**, 901-905.

Wei, M. C., Zong, W.-X., Cheng, E. H.-Y., Lindsten, T., Panoutsakopoulou, V., Ross, A. J., Roth, K. A., MacGregor, G. R., Thompson, C. B. and Korsmeyer, S. J. (2001). Proapoptotic BAX and BAK: a requisite gateway to mitochondrial dysfunction and death. *Science* **292**, 727-730.

Wen, Z., Han, L., Bamburg, J. R., Shim, S., Ming, G. and Zheng, J. Q. (2007). BMP gradients steer nerve growth cones by a balancing act of LIM kinase and Slingshot phosphatase on ADF/cofilin. *Science Signalling* **178**, 107.

Westermann, B. (2010). Mitochondrial fusion and fission in cell life and death. *Nature Reviews Molecular Cell Biology* **11**, 872-884.

Westermann, B. (2012). Bioenergetic role of mitochondrial fusion and fission. *Biochimica et Biophysica Acta (BBA)-Bioenergetics* **1817**, 1833-1838.

Wiederkehr, A. and Wollheim, C. B. (2009). Linking fatty acid stress to β-cell mitochondrial dynamics. *Diabetes* **58**, 2185-2186.

Wiggins, H. and Rappoport, J. (2010). An agarose spot assay for chemotactic invasion. *Biotechniques* **48**, 121-124.

Wollman, R. and Meyer, T. (2012). Coordinated oscillations in cortical actin and Ca^{2+} correlate with cycles of vesicle secretion. *Nature Cell Biology* **14**, 1261-1269.

Wolter, K. G., Hsu, Y.-T., Smith, C. L., Nechushtan, A., Xi, X.-G. and Youle, R. J. (1997). Movement of Bax from the cytosol to mitochondria during apoptosis. *The Journal of cell biology* **139**, 1281-1292.

Wondergem, R., Ecay, T. W., Mahieu, F., Owsianik, G. and Nilius, B. (2008). HGF/SF and menthol increase human glioblastoma cell calcium and migration. *Biochemical and Biophysical Research Communications* **372**, 210-215.

Wozniak, M. A., Desai, R., Solski, P. A., Der, C. J. and Keely, P. J. (2003). ROCK-generated contractility regulates breast epithelial cell differentiation in response to the physical properties of a three-dimensional collagen matrix. *The Journal of cell biology* **163**, 583-595.

Wozniak, M. A., Modzelewska, K., Kwong, L. and Keely, P. J. (2004). Focal adhesion regulation of cell behavior. *Biochimica et Biophysica Acta (BBA)-Molecular Cell Research* **1692**, 103-119.

Wu, G.-Y., Deisseroth, K. and Tsien, R. W. (2001). Spaced stimuli stabilize MAPK pathway activation and its effects on dendritic morphology. *Nature neuroscience* **4**, 151-158.

Wu, R. F., Xu, Y. C., Ma, Z., Nwariaku, F. E., Sarosi, G. A. and Terada, L. S. (2005). Subcellular targeting of oxidants during endothelial cell migration. *The Journal of cell biology* **171**, 893-904.

Wu, W.-S., Tsai, R. K., Chang, C. H., Wang, S., Wu, J.-R. and Chang, Y.-X. (2006). Reactive oxygen species mediated sustained activation of protein kinase Cα and extracellular signal-regulated kinase for migration of human hepatoma cell Hepg2. *Molecular Cancer Research* **4**, 747-758.

Wudarczyk, J., Dębska, G. and Lenartowicz, E. (1999). Zinc as an inducer of the membrane permeability transition in rat liver mitochondria. *Archives of biochemistry and biophysics* **363**, 1-8.

Xia, C., Meng, Q., Liu, L.-Z., Rojanasakul, Y., Wang, X.-R. and Jiang, B.-H. (2007). Reactive oxygen species regulate angiogenesis and tumor growth through vascular endothelial growth factor. *Cancer research* **67**, 10823-10830.

Xiang, F.-L., Lu, X., Strutt, B., Hill, D. J. and Feng, Q. (2010). NOX2 deficiency protects against streptozotocin-induced β-cell destruction and development of diabetes in mice. *Diabetes* **59**, 2603-2611.

Xu, S., Nam, S., Kim, J., Das, R., Choi, S., Nguyen, T., Quan, X., Choi, S., Chung, C. and Lee, E. (2015). Palmitate induces ER calcium depletion and apoptosis in mouse podocytes subsequent to mitochondrial oxidative stress. *Cell death & disease* **6**, e1976.

Xu, S., Pi, H., Chen, Y., Zhang, N., Guo, P., Lu, Y., He, M., Xie, J., Zhong, M. and Zhang, Y. (2013). Cadmium induced Drp1-dependent mitochondrial fragmentation by disturbing calcium homeostasis in its hepatotoxicity. *Cell death & disease* **4**, e540.

Xu, X., Wang, Y., Chen, Z., Sternlicht, M. D., Hidalgo, M. and Steffensen, B. (2005). Matrix metalloproteinase-2 contributes to cancer cell migration on collagen. *Cancer research* **65**, 130-136.

Yamaguchi, H. and Condeelis, J. (2007). Regulation of the actin cytoskeleton in cancer cell migration and invasion. *Biochimica et Biophysica Acta (BBA)-Molecular Cell Research* **1773**, 642-652.

Yamamoto, S., Takahashi, N. and Mori, Y. (2010). Chemical physiology of oxidative stress-activated TRPM2 and TRPC5 channels. *Progress in biophysics and molecular biology* **103**, 18-27.

Yamasaki, S., Sakata-Sogawa, K., Hasegawa, A., Suzuki, T., Kabu, K., Sato, E., Kurosaki, T., Yamashita, S., Tokunaga, M. and Nishida, K. (2007). Zinc is a novel intracellular second messenger. *The Journal of cell biology* **177**, 637-645.

Yang, D., Elner, S. G., Bian, Z.-M., Till, G. O., Petty, H. R. and Elner, V. M. (2007). Pro-inflammatory cytokines increase reactive oxygen species through mitochondria and NADPH oxidase in cultured RPE cells. *Experimental eye research* **85**, 462-472.

Yang, Q., Sommercorn, J. and Tonks, N. (1993). Cloning and expression of PTP-PEST. A novel, human, nontransmembrane protein tyrosine phosphatase. *Journal of Biological Chemistry* **268**, 6622-6628.

Yang, S. and Huang, X.-Y. (2005). Ca^{2+} influx through L-type Ca^{2+} channels controls the trailing tail contraction in growth factor-induced fibroblast cell migration. *Journal of Biological Chemistry* **280**, 27130-27137.

Yang, S., Yip, R., Polena, S., Sharma, M., Rao, S., Griciene, P., Gintautas, J. and Jerome, H. (2003). Reactive oxygen species increased focal adhesion kinase production in pulmonary

microvascular endothelial cells. In *Proceedings of the Western Pharmacology Society*, vol. **47**, pp. 54-56.

Yang, S., Zhang, J. J. and Huang, X.-Y. (2009a). Orai1 and STIM1 are critical for breast tumor cell migration and metastasis. *Cancer cell* **15**, 124-134.

Yang, Z.-H., Wang, X.-H., Wang, H.-P. and Hu, L.-Q. (2009b). Effects of TRPM8 on the proliferation and motility of prostate cancer PC-3 cells. *Asian Journal of Andrology* **11**, 157-165.

Yokoyama, K., Kaji, H., He, J., Tanaka, C., Hazama, R., Kamigaki, T., Ku, Y., Tohyama, K. and Tohyama, Y. (2011). Rab27a negatively regulates phagocytosis by prolongation of the actin-coating stage around phagosomes. *Journal of Biological Chemistry* **286**, 5375-5382.

Yoo, S. K., Starnes, T. W., Deng, Q. and Huttenlocher, A. (2011). Lyn is a redox sensor that mediates leukocyte wound attraction in vivo. *Nature* **480**, 109-112.

Yoon, Y., Galloway, C. A., Jhun, B. S. and Yu, T. (2011). Mitochondrial dynamics in diabetes. *Antioxidants & redox signaling* **14**, 439-457.

Yoon, Y., Krueger, E. W., Oswald, B. J. and McNiven, M. A. (2003). The mitochondrial protein hFis1 regulates mitochondrial fission in mammalian cells through an interaction with the dynamin-like protein DLP1. *Molecular and cellular biology* **23**, 5409-5420.

Yu, P., Wang, Q., Zhang, L.-H., Lee, H.-C., Zhang, L. and Yue, J. (2012). A cell permeable NPE caged ADP-ribose for studying TRPM2. *PLoS One* **7**, e51028.

Yu, T., Robotham, J. L. and Yoon, Y. (2006). Increased production of reactive oxygen species in hyperglycemic conditions requires dynamic change of mitochondrial morphology. *Proceedings of the National Academy of Sciences* **103**, 2653-2658.

Yu, T., Sheu, S.-S., Robotham, J. L. and Yoon, Y. (2008). Mitochondrial fission mediates high glucose-induced cell death through elevated production of reactive oxygen species. *Cardiovascular Research* **79**, 341-351.

Yuan, H., Zhang, X., Huang, X., Lu, Y., Tang, W., Man, Y., Wang, S., Xi, J. and Li, J. (2010). NADPH oxidase 2-derived reactive oxygen species mediate FFAs-induced dysfunction and apoptosis of β-cells via JNK, p38 MAPK and p53 pathways. *PLoS One* **5**, e15726.

Yuzefovych, L., Wilson, G. and Rachek, L. (2010). Different effects of oleate vs. palmitate on mitochondrial function, apoptosis, and insulin signaling in L6 skeletal muscle cells: role of oxidative stress. *American Journal of Physiology-Endocrinology and Metabolism* **299**, E1096-E1105.

Zalewski, P., Forbes, I., Giannakis, C. and Betts, W. (1991). Regulation of protein kinase C by Zn^{2+}-dependent interaction with actin. *Biochemistry international* **24**, 1103-1110.

Zamir, E. and Geiger, B. (2001). Molecular complexity and dynamics of cell-matrix adhesions. *Journal of Cell Science* **114**, 3583-3590.

Zeng, X., Sikka, S. C., Huang, L., Sun, C., Xu, C., Jia, D., Abdel-Mageed, A. B., Pottle, J. E., Taylor, J. T. and Li, M. (2010). Novel role for the transient receptor potential channel TRPM2 in prostate cancer cell proliferation. *Prostate Cancer Prostatic Disease* **13**, 195-201.

Zhang, H., Wang, Z.-Q., Zhao, D.-Y., Zheng, D.-M., Feng, J., Song, L.-C. and Luo, Y. (2011a). AIF-mediated mitochondrial pathway is critical for the protective effect of diazoxide against SH-SY5Y cell apoptosis. *Brain research* **1370**, 89-98.

Zhang, H. J., Zhao, W., Venkataraman, S., Robbins, M. E., Buettner, G. R., Kregel, K. C. and Oberley, L. W. (2002). Activation of matrix metalloproteinase-2 by overexpression of manganese superoxide dismutase in human breast cancer MCF-7 cells involves reactive oxygen species. *Journal of Biological Chemistry* **277**, 20919-20926.

Zhang, W., Hirschler-Laszkiewicz, I., Tong, Q., Conrad, K., Sun, S.-C., Penn, L., Barber, D. L., Stahl, R., Carey, D. J. and Cheung, J. Y. (2006). TRPM2 is an ion channel that modulates hematopoietic cell death through activation of caspases and PARP cleavage. *American Journal of Physiology-Cell Physiology* **290**, C1146-C1159.

Zhang, W. and Liu, H. T. (2002). MAPK signal pathways in the regulation of cell proliferation in mammalian cells. *Cell research* **12**, 9-18.

Zhang, Z., Wakabayashi, N., Wakabayashi, J., Tamura, Y., Song, W.-J., Sereda, S., Clerc, P., Polster, B. M., Aja, S. M. and Pletnikov, M. V. (2011b). The dynamin-related GTPase Opa1 is required for glucose-stimulated ATP production in pancreatic beta cells. *Molecular Biology of the Cell* **22**, 2235-2245.

Zhao, J., Zhang, J., Yu, M., Xie, Y., Huang, Y., Wolff, D. W., Abel, P. W. and Tu, Y. (2013). Mitochondrial dynamics regulates migration and invasion of breast cancer cells. *Oncogene* **32**, 4814-4824.

Zheng, J. Q., Wan, J. and Poo, M. (1996). Essential role of filopodia in chemotropic turning of nerve growth cone induced by a glutamate gradient. *The Journal of neuroscience* **16**, 1140-1149.

Zheng, Y. and Lu, Z. (2013). Regulation of tumor cell migration by protein tyrosine phosphatase (PTP)-proline-, glutamate-, serine-, and threonine-rich sequence (PEST). *Chinese journal of cancer* **32**, 75.

Zhu, D., Tan, K. S., Zhang, X., Sun, A. Y., Sun, G. Y. and Lee, J. C.-M. (2005). Hydrogen peroxide alters membrane and cytoskeleton properties and increases intercellular connections in astrocytes. *Journal of Cell Science* **118**, 3695-3703.

Zhu, X., Lee, H.-G., Raina, A. K., Perry, G. and Smith, M. A. (2002). The role of mitogen-activated protein kinase pathways in Alzheimer's disease. *Neurosignals* **11**, 270-281.

Zorov, D. B., Juhaszova, M. and Sollott, S. J. (2006). Mitochondrial ROS-induced ROS release: an update and review. *Biochimica et Biophysica Acta (BBA)-Bioenergetics* **1757**, 509-517.

Zorov, D. B., Juhaszova, M. and Sollott, S. J. (2014). Mitochondrial reactive oxygen species (ROS) and ROS-induced ROS release. *Physiological reviews* **94**, 909-950.

Zuo, L. and Motherwell, M. S. (2013). The impact of reactive oxygen species and genetic mitochondrial mutations in Parkinson's disease. *Gene* **532**, 18-23.